# MONASH University

# Interactions between urban heat islands, heatwaves, and synoptic patterns in southern Australian cities

Cassandra Denise Wilks Rogers

BSc, Monash University (2011)

BSc (Hons), Monash University (2012)

A thesis submitted for the degree of Doctor of Philosophy at

Monash University in 2019

School of Earth, Atmosphere and Environment

## Copyright notice

# Abstract

Most cities are affected by urban heat islands (UHIs), whereby urban areas are warmer than surrounding rural areas, with the strongest UHIs usually occurring at night. While much research on the UHI has focused on the influence of the land surface, there has been little attention paid to the role that atmospheric mechanisms play in modulating UHIs, particularly in the Southern Hemisphere and Australia. This thesis aims to address this gap by examining the relationship between UHIs, heatwaves, and synoptic weather patterns in three southern Australian cities, Melbourne, Adelaide, and Perth.

This thesis investigates the relationship between the UHI and warm-season heatwaves (November to March) in observations spanning January 1995 to March 2014. It compares UHIs during heatwave periods to those during non-heatwave periods to determine if and how the strength of the UHI changes. The thesis finds UHIs to be exacerbated (warmer than normal) during heatwaves in Melbourne and Adelaide at night. Conversely, Perth shows a diminished (cooler than normal) UHI at night during heatwaves. Findings show that the characteristic differences between heatwave and non-heatwave periods cannot be explained by variability in wind speed, wind direction, or station location.

Next, self-organising maps (SOMs) are employed to determine if there are any relationships between the strength of the UHI in each city and the overlying synoptic patterns, and whether this can help to explain why there are exacerbated (diminished) UHIs in Melbourne and Adelaide (Perth) during heatwaves. This thesis finds that heatwaves are a stronger predictor of UHI strength than synoptic patterns in Melbourne and Adelaide, showing that synoptic patterns do not explain why the UHI is exacerbated

during heatwaves there. In Perth, findings show that synoptic patterns have some influence on UHI strength during heatwaves and play some role in diminishing the UHI during these events. However, the relationship is weak so it is likely that there are additional processes at play, but these remain unknown.

Outside heatwaves, the SOM analysis shows a strong relationship with the strength of the UHI and particular Synoptic Types. In every city, there is a clear preference toward one or more Types being more closely associated with exacerbated or diminished UHIs, beyond what is expected from random chance. Thus, the results show that synoptic conditions predispose the overlying atmosphere to UHIs of particular strengths. Different synoptic environments are important for different cities.

Lastly, this thesis uses CMIP5 model data to examine how those synoptic environments associated with strongly exacerbated or diminished UHIs in the present day are likely to change with anthropogenic warming. Three models are used, ACCESS1-3, MPI-ESM-LR, and MRI-CGCM3, and two representative concentration pathways (RCPs), a moderate radiative forcing pathway (RCP4.5), and a high forcing pathway (RCP8.5), to examine a range of potential future scenarios centred on the 20 years from 2065 to 2084. While results between the models and cities varied, the models tended to show that synoptic patterns that are presently associated with strongly exacerbated UHIs are unlikely to become more frequent in the future.

## Declaration

I hereby declare that this thesis contains no material which has been accepted for the award of any other degree or diploma at any university or equivalent institution and that, to the best of my knowledge and belief, this thesis contains no material previously published or written by another person, except where due reference is made in the text of the thesis.

This thesis includes one original paper published in a peer reviewed journal. The core theme of the thesis is the relationship between the urban heat island, heatwaves, and synoptic patterns in southern Australian cities. The ideas, development and writing up of all the papers in the thesis were the principal responsibility of myself, the student, working within the School of Earth, Atmosphere and Environment under the supervision of Dr Ailie Gallant and Prof Nigel Tapper. In the case of Chapter 4 my contribution to the work involved the following:

| Thesis Chapter | Publication Title | Status | Nature and % of student contribution | Co-author names Nature and % of Co-authors' contribution | Co-author(s), Monash student Y/N |
|---|---|---|---|---|---|
| 4 | Is the urban heat island exacerbated during heatwaves in southern Australian cities? | In press | Methodology, analysis, and writing 90 % | Ailie Gallant, methodology and writing 5 %<br><br>Nigel Tapper, methodology and writing 5 % | No<br><br><br><br>No |

The original paper constitutes the majority of Chapter 4. However, minor modifications have been made in order to generate a consistent presentation within the thesis.

**Student signature:**                                                                **Date:**

The undersigned hereby certify that the above declaration correctly reflects the nature and extent of the student's and co-authors' contributions to this work.

**Main Supervisor signature:**                                                    **Date:**

# Acknowledgements

# Table of contents

# 1. Introduction

The majority of Australians live in the country's capital cities (66 % as of 2013, Australian Bureau of Statistics 2014). For a number of reasons, urban populations experience vulnerabilities associated with climate. One of these is higher urban temperatures due to the urban heat island effect (UHI). The UHI is the phenomenon whereby the urban fabric stores heat during the day and releases it at night (e.g. Oke 1982; Morris and Simmonds 2000), resulting in warmer night-time temperatures within cities when compared to the surrounding countryside. UHIs are known to affect temperatures in many Australian cities and towns (e.g. Morris and Simmonds 2000; Morris et al. 2001; Torok et al. 2001; Erell and Williamson 2007; Guan et al. 2013; Soltani and Sharifi 2017).

Both abnormally warm and cold temperatures have an effect on urban populations. Some demographics are at particular risk including the elderly and the very young. For example, Nicholls et al. (2008) and Loughnan et al. (2010a) have shown that mortality rates for elderly people (over 64 years old) increased significantly under extremely hot temperatures in southeast Australia. Similarly, Loughnan et al. (2010b) showed that socioeconomic inequality and age affected the number of people admitted to hospital with acute myocardial infarctions during hot weather in Melbourne, Australia.

Further, urban populations are expected to become more vulnerable to extreme heat in the future. Not only are Australian heatwaves expected to become hotter, longer, and more frequent due to anthropogenic climate change (Perkins et al. 2012; Perkins and Alexander 2013; Cowan et al. 2014a; Cowan et al. 2014b), but increasing urban populations (Australian Bureau of Statistics 2014), along with an increasing proportion

of elderly people (Australian Bureau of Statistics 2013a), will make future urban populations even more vulnerable to extreme heat.

Given the risk to urban populations, understanding the underlying mechanisms that are conducive to an UHI is imperative. Further, changes to both climate and the urban form into the future will have direct and indirect effects on the UHI, which must be quantified if we are to understand future risks to urban populations from extreme temperatures.

While there are a number of ways to define the UHI, i.e. surface UHI, boundary layer UHI, etc., as this research examines only the canopy layer UHI, that is, the UHI calculated using temperature sensors at screen height, the literature review provided in this chapter is largely limited to research examining the canopy layer UHI.

## 1.1 Modulation of the urban heat island by the urban form

The UHI effect is the phenomenon whereby urban areas are warmer than surrounding rural areas (Oke 1973; Oke 1982). The strength of the UHI is proportional to population (Oke 1973; Torok et al. 2001). One of the major causes of the UHI is the alteration of energy partitioning by urban surfaces. The main inputs of energy into urban areas are incoming shortwave and longwave radiation. When this incoming radiation comes into contact with the land surface, a portion of it is reflected back into the atmosphere, with the remainder partitioned into three types of energy: sensible energy, which corresponds to increases in air temperature, stored energy, which is stored in surfaces such as soil, buildings, etc., and latent energy, which occurs when liquid water is converted to a gas, thus removing energy from the land surface via evaporation (Broadbent et al. 2018a; Broadbent et al. 2018b) or evapotranspiration (Broadbent et al. 2018a; Smithers et al. 2018; Moss et al. 2019).

Urban areas generally consist of a small fraction of vegetated and/or undeveloped land, with the majority of the land surface covered by built surfaces, including buildings and roads. These built surfaces typically have larger heat capacities than vegetation and natural landscapes. Thus, heat is able to be stored in urban surfaces (Oke 1973; Morris and Simmonds 2000). The stored energy is released into the urban atmosphere at night (Oke et al. 1991; Coutts et al. 2010), preventing the city from cooling down to the same extent as the surrounding rural areas. As a result, UHIs are typically most evident at night (Oke et al. 1991; Coutts et al. 2010; Loughnan et al. 2013).

The removal of water (for example via storm water systems) and vegetation from urban areas alters the energy balance. As water evaporates it absorbs energy, resulting in latent heat loss. Similarly, as vegetation transpires, water is released into the atmosphere where it evaporates. This process is known as evapotranspiration. Decreases in water and vegetation fraction affect energy transformation within the city by decreasing the amount of latent energy and increasing sensible and stored energy, thus reducing the amount of longwave radiation lost to the atmosphere and increasing urban temperatures. The removal of vegetation can further increase urban temperatures by increasing the amount of radiation absorbed by the urban fabric, as trees have the ability to shade surfaces with higher heat capacities, such as concrete (Smithers et al. 2018).

While the removal of water from urban areas can have a direct effect on urban temperatures through a reduction of latent heat loss (Broadbent et al. 2018a; Broadbent et al. 2018b), vegetation can also be affected. The removal of stormwater from cities can cause urban areas to be drier than they otherwise would be (Coutts et al. 2013), significantly reducing the evapotranspiration rates of plants (Reichstein et al. 2013),

and thus causing an increase in sensible heat (Alexander 2011) and less heat to be removed from the city through latent cooling. A lack of water in urban areas can be due to natural causes, such as drought, but is often largely due to urban planning decisions. Similarly, soil moisture has been shown to affect the strength of the UHI (Jacobs et al. 2017; Ramamurthy and Bou-Zeid 2017), further emphasising the susceptibility of the UHI to water within the urban landscape.

Canyon geometry and sky view factor can affect urban temperatures by reducing the amount of longwave radiation that is emitted to the overlying atmosphere. Cities with lower sky view fractions, such as highly urbanised areas with tall buildings, have a reduced ability to cool overnight and thus the UHI is warmer (Oke et al. 1991). The structure of the city can further affect the amount of energy exchanged between the urban fabric and the overlying atmosphere by altering the surface area of urban areas (Oke 1982).

As well as absorbing and storing incoming radiation, cities often produce additional anthropogenic heat through cars, heating systems, and air conditioners, amongst other sources. This additional heat can further amplify the effect of the city on air temperatures. Using the meteorological Weather Research and Forecasting model (WRF), Ma et al. (2017) found that additional anthropogenic heat comprises 20 % of the UHI at night in Sydney in the summer, and 90 % of the night-time UHI in winter. The study covered the period 2007 to 2009. Similarly, Earl et al. (2016) found evidence of a contribution of anthropogenic heat to the UHI in Melbourne from 1973 to 2013. The authors found that due to population behaviour, anthropogenic heat exhibits a weekly cycle, thus the UHI in Melbourne also shows a weekly cycle. Given the populations of Melbourne, Adelaide, and Perth are all expected to increase in the future (Australian Bureau of Statistics 2013b), this suggests that the amount of anthropogenic

heat released into urban areas will also increase. This additional anthropogenic heat therefore has the potential to lead to a strengthening of the cyclical behaviour of the UHI.

In some cases, the opposite of an UHI can occur, known as an urban cool island (UCI), where urban areas are cooler than rural areas (e.g. Unwin 1980; Morris and Simmonds 2000; Erell and Williamson 2007; Rasul et al. 2015; Haashemi et al. 2016). UCIs have been reported as lasting for a few hours in the morning in cities that typically experience an UHI at night (Lai et al. 2018). Lai et al. (2018) found that more than 50 % of urban areas in China experience an UCI, with cities within cooler climate zones more likely to experience UCIs.

This temporary UCI is due to differing heating rates between urban and rural areas (Oke 1982). Runnalls and Oke (2000) also noted that minimums in the UHI are due to urban/rural heating rate differences. After sunrise, rural surfaces heat quickly due to low thermal inertia, whereas urban areas heat more slowly as incoming radiation is stored within building materials rather than being partitioned into sensible heat. This can cause the city to experience an UCI until temperatures in urban and rural areas equalise later in the day (Oke 1982). Other causes of UCIs include canyon geometry, which Oke (1982) noted causes shading of urban canyons by buildings when the sun angle is low. In semi-arid landscapes, increased vegetation cover (Haashemi et al. 2016; Lai et al. 2018) and water availability (Rasul et al. 2015) in urban areas, relative to rural areas, can also lead to the development of an UCI.

In summary, there are a number of internal mechanisms that control the UHI. Energy storage and emission, reduced longwave radiation loss, additional anthropogenic heat, and a lack of latent cooling interact to create cities that are generally warmer than surrounding, less built up areas.

## 1.2 Atmospheric modulation of the urban heat island

The surface characteristics, composition materials, population size and industrialisation of a city are not the only factors that affect the strength of the UHI. The strength of the UHI is also dependent on meso- and synoptic scale weather features.

A number of studies have identified calm or low wind speeds as being associated with warmer UHIs (e.g. Oke 1973; Unger 1996; Runnalls and Oke 2000; Morris et al. 2001; Bejarán and Camilloni 2003; Arnds et al. 2017). This is because on days with high wind speeds, heat is effectively removed from the city via turbulent transport and the emission of longwave radiation (Morris et al. 2001). On days with low wind speeds, the effect of advection and turbulence is reduced and a larger portion of heat is removed via longwave radiation emission. In Melbourne, Morris et al. (2001) noted a seasonal influence whereby the wind had the strongest influence on the UHI in summer, and the weakest influence in winter.

A lack of cloud cover is also conducive to warm UHIs (e.g. Oke et al. 1991; Unger 1996; Runnalls and Oke 2000; Morris et al. 2001; Bejarán and Camilloni 2003; Arnds et al. 2017). Morris et al. (2001) suggested that this relationship is due to cloud cover preventing the emission of longwave radiation at night, thus the temperature differences between urban and rural areas diminishes on cloudy nights. A lack of precipitation has also been related to the presence of a warmer UHI (Lee and Baik 2010). The authors suggested that increased rainfall is associated with a cooler UHI as rainfall and the associated clouds reduce incoming solar radiation while increasing the amount of heat lost through evaporation.

Some studies have further determined relationships between the synoptic environment and the strength of UHIs. The relatively stable conditions that are often associated with anticyclonic conditions, including weak winds, reduced cloudiness, and

reduced precipitation, are conducive to warm UHIs (Yagüe et al. 1991; Unger 1996).

Numerous studies have identified such relationships between anticyclonic conditions

and warmer UHIs. Morris and Simmonds (2000), in the only such study for Australia,

found that high-pressure systems located along the southeast coast of Australia were

associated with the warmest UHIs in Melbourne, that is UHIs greater than or equal to

2°C, see Figure 1.1. Other studies that have found a relationship between anticyclonic

synoptic patterns and UHIs include Unwin (1980) and Zhang et al. (2014b) in

Birmingham, UK, Yagüe et al. (1991) in Madrid, Spain, Unger (1996) in Szeged,

Hungary, Bejarán and Camilloni (2003) in Buenos Aires, Argentina, Beranová and

Huth (2003) in Prague, Czech Republic, He et al. (2013) in Changsha, China, and

Targino et al. (2014) in Londrina, Brazil. He et al. (2013) noted that anticyclonic

systems in Changsha, China, resulted in a stable surface layer with low wind speeds, a

low mixed layer height, and a strong inversion layer.
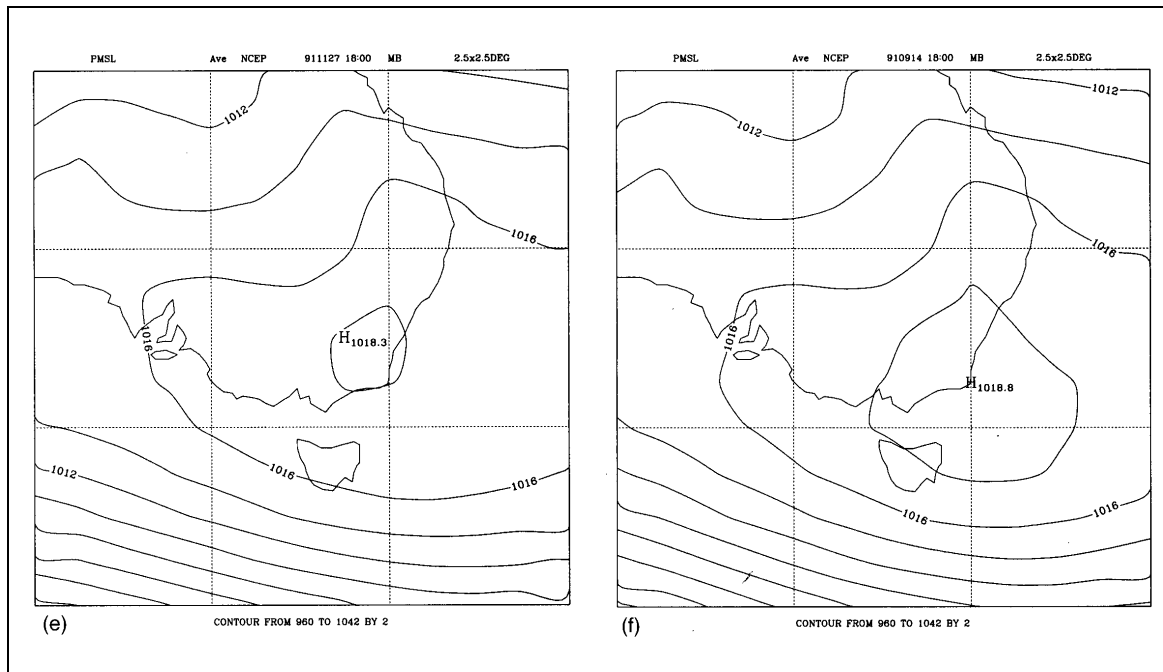


Figure 1.1: Mean MSLP (hPa) plots for UHI groups: e) $2 \leq UHI < 3°C$, and f) $UHI \geq 3°C$. Figure and caption adapted from Morris and Simmonds (2000).

While Morris and Simmonds (2000) examined MSLP composites on days where the UHI was a certain strength, most studies used predetermined weather types and calculated the strength of the UHI for each of these types (e.g. Unwin 1980; Yagüe et al. 1991; Unger 1996; Zhang et al. 2014b). Using a third method, He et al. (2013) examined synoptic patterns for the 6 warmest UHIs during December 2008 and concluded that the warmest UHIs are associated with anticyclonic synoptic patterns. Since the three different methods for determining the synoptic patterns associated with warm UHIs produced similar results, this suggests that the results are robust.

Rather than using MSLP to examine the relationship between circulation and the strength of the UHI, using a number of cities in the USA, Scott et al. (2018) compared UHIs under moist weather types to those with dry weather types. The authors found that the strength of the UHI was reduced for moist weather conditions.

While atmospheric conditions can affect urban temperatures, the structure of the city can also influence heating. Using a case study in Melbourne, Morris and Simmonds (2000) found that a northwesterly on 11 January 1987 was associated with the formation of an UCI. The urban structure prevented warm air advection throughout the city, resulting in cool temperatures compared to the surrounding rural stations, which increased in temperature due to the northwesterly wind.

The strength of the UHI on a given day can also be dependent on the UHI one day earlier (Yagüe et al. 1991). Yagüe et al. (1991) found that UHIs in the top (bottom) 25 % of events were more likely than not to be followed by UHIs also in the top (bottom) 25 % of events. However, the authors did not examine UHI persistence within weather types which might help elucidate whether UHI persistence is due to the persistence of weather types, or whether heat stored in the urban fabric might take

longer than one day to dissipate, thus causing the UHI on day $i$ to affect that on day $j$, where day $j$ follows day $i$.

A seasonal cycle in the strength of the UHI has been identified in many cities and depends on the city in question. A number of studies have found the UHI in summer to be warmer on average (e.g. Morris et al. 2001; Wilby 2003; Arnds et al. 2017; Lai et al. 2018) and last longer (Lai et al. 2018). Wilby (2003), who found that the UHI at night in London is typically strongest in summer, noted that this difference is often due to differences in the radiative forcing between the seasons. That is, more solar radiation is absorbed by the city surface in summer than in winter, thus more heat is released at night, leading to a stronger nocturnal UHI.

However, this finding is not universal, with some cities showing stronger UHIs in seasons other than summer. Zhou and Shepherd (2010) found the UHI in Atlanta, USA, to be warmest in spring and coolest in summer due to differences in cloud cover, while some studies found the UHI to be greatest in winter (e.g. Hinkel et al. 2003; Da Silva 2018).

On extremely hot days, Sun et al. (2017) showed that urban landscapes are able to store more heat, thus releasing more stored energy into urban areas at night. Given that warmer background temperatures and high levels of radiative heating have been found to be conducive to warmer UHIs, the occurrence of extreme heat events, including heatwaves, may also affect the strength of the UHI.

## 1.2.1 The urban heat island effect during heatwaves

Heatwaves, which are broadly defined as extreme heat events that last for multiple days (Perkins et al. 2012), can significantly increase urban temperatures. Heatwaves and extreme heat can cause a large number of deaths (Chestnut et al. 1998;

De Bono et al. 2004; Nicholls et al. 2008; Loughnan et al. 2010a; Queensland University of Technology 2010; Williams et al. 2012a; Williams et al. 2012b; Met Office 2016), with small increases in extreme temperatures associated with disproportionately large increases in mortality rates (Nicholls et al. 2008). The negative health impacts of extreme heat are often associated with warm nights (Chestnut et al. 1998; Nicholls et al. 2008; Loughnan et al. 2010a), when any UHI effect is most prevalent (Coutts et al. 2010). Thus relatively small increases in urban temperatures during heatwaves due to the UHI pose a great threat to the health of urban populations. It is therefore imperative that any relationship between the UHI and heatwaves be investigated and understood.

Past research has found that the strength of the UHI is generally exacerbated during heatwaves, for example Zhou and Shepherd (2010) in Altanta, USA, Li and Bou-Zeid (2013) in Baltimore, USA, Heaviside et al. (2015) in Birmingham, UK, Li et al. (2015) in Beijing, China, Ortiz et al. (2018) in New York, USA, and Ramamurthy and Bou-Zeid (2017) for multiple cities in the USA. Similarly, Fenner et al. (2014) found that the UHI at night in Berlin was exacerbated on hot days compared to the rest of the year.

The mechanisms behind any potential relationship between heatwaves and the strength of the UHI are not certain. Li et al. (2015) found that radiative energy budgets at urban and rural stations vary between heatwave and non-heatwave conditions. The authors note that urban areas are typically cloudier than rural areas during non-heatwave conditions, but this difference is not evident during heatwaves. Thus, the difference in cloud cover means that the urban stations receive relatively more incoming solar radiation than the rural stations during heatwaves, thus resulting in hotter UHIs during heatwaves. Similarly, Fenner et al. (2014) found that both

vegetation fraction and sky view factor, both of which affect the amount of solar radiation absorbed by a given surface, have linear relationships with UHI strength on hot days. Ramamurthy and Bou-Zeid (2017) also found that soil moisture deficits lead to an increase in the UHI in Washington and Baltimore in their simulation.

Using WRF, Heaviside et al. (2015) calculated the strength of the UHI during heatwaves by replacing the city of Birmingham, UK, with a different land surface type. Their research found that the exacerbation of the UHI is due to the difference in land surface types between the urban and rural areas. Li and Bou-Zeid (2013) also used modelling to attribute UHI strength to differences in the urban and rural forms, with their model implementing differing surface energy budgets over urban and rural areas.

Ramamurthy and Bou-Zeid (2017) examined some potential mechanisms behind the UHI-heatwave relationship through modelling in various cities in the northeastern USA. The authors found that a change in wind direction was responsible for increases in the UHI during heatwaves in simulations over New York City as the absense of a southerly sea breeze prevented the city from cooling down in the mid-afternoon. This implies that the proximity of a city to the coast may affect the mechanisms behind any exacerbation of the UHI during heatwaves.

A number of studies have shown that the relationship between UHIs and heatwaves may be dependent on the choice of stations for UHI calculations (Zhou and Shepherd 2010), and city size (Ramamurthy and Bou-Zeid 2017; Herbel et al. 2018). Zhou and Shepherd (2010) found that by using a hybrid (non-rural) station rather than a rural station for their calculation of the UHI, there was no significant difference between the strength of the UHI during heatwave and non-heatwave periods. They also calculated the UHI using more traditional urban and rural stations in the same city and found that this produced an exacerbated UHI during heatwaves. This suggests that

suitable station choice is crucial when quantifying the contribution of heatwaves to the strength of the UHI.

Ramamurthy and Bou-Zeid (2017) found no significant difference in UHIs during heatwave and non-heatwave periods for a number of cities with populations of less than 200,000 people, thus suggesting that population and city size have an influence on the relationship between UHIs and heatwaves. Similarly, when examining a city with a population of approximately 320,000 inhabitants in Romania, Herbel et al. (2018) found that the most extreme heatwaves caused an exacerbation of the UHI, but the same was not true for less severe heatwaves. However, the authors noted that due to small sample sizes, their results should be treated as preliminary findings. Having said that, the findings of Ramamurthy and Bou-Zeid (2017) and Herbel et al. (2018) suggest that the response of the UHI to heatwaves may be dependent on city size.

In contrast to the above results, Scott et al. (2018) examined the strength of the UHI on single hot days in multiple cities in the USA and found the UHI to be typically cooler on hot days than on the days prior to the heat event; where hot days consist of the 15 hottest days for each city. Figure 1.2 illustrates the average strength of the UHI on the day of the heat event minus that four days earlier. From this figure we see that cities with cool UHIs during the heat events (relative to those prior to the event) are located all over the country. However, the majority of the coolest UHIs occur in California, in the southwest of the USA. The authors further noted that one third of the cities showed an UCI during heat extremes.
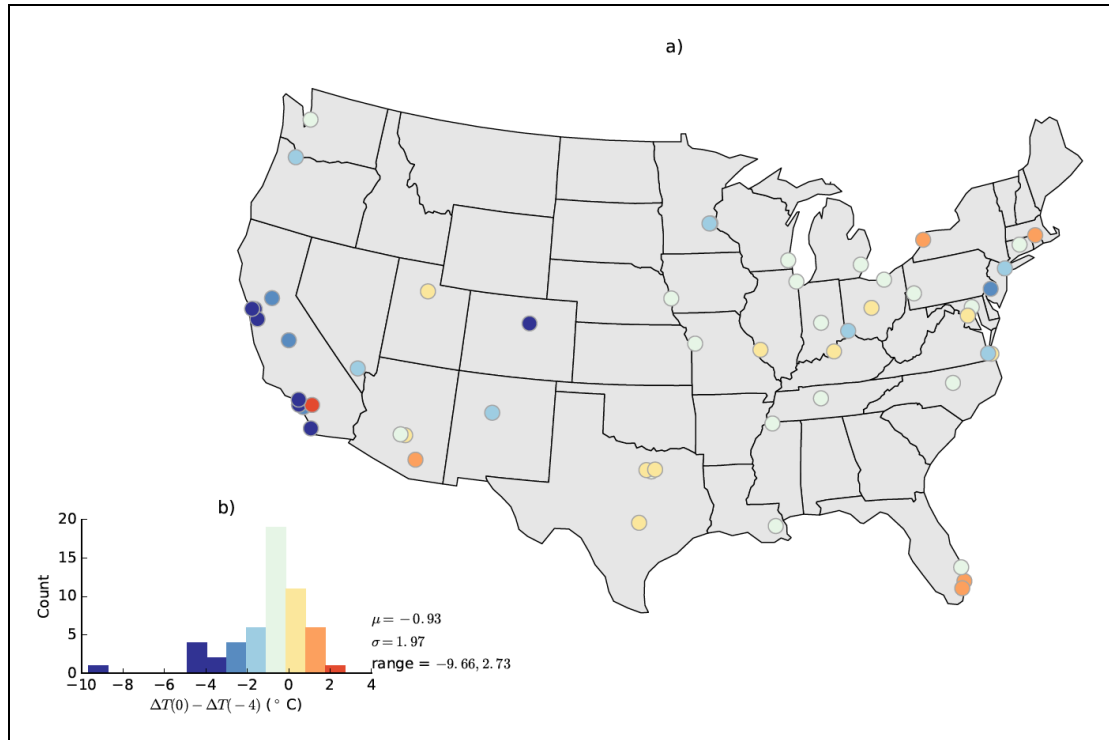
Figure 1.2: The temperature change of the UHI during heat events (UHI on heat event day zero minus UHI four days prior) is plotted for each city as a (a) map and (b) as a histogram. The color scale is as indicated by the histogram. The mean μ, standard deviation σ, and range are listed. Figure and caption from Scott et al. (2018) supplementary section.

While Scott et al. (2018) did not specifically examine heatwaves, they argued that their results were inconsistent with many other papers that found UHIs to be warmer during heatwave events than during non-heatwave periods (e.g. Li and Bou-Zeid 2013). Scott et al. (2018) showed that UHIs decrease with increasing temperatures due to larger temperature increases in rural areas than in urban areas. Therefore, despite many studies finding that UHIs are exacerbated during heat events, as discussed so far throughout this section (e.g. Zhou and Shepherd 2010; Li and Bou-Zeid 2013; Heaviside et al. 2015; Li et al. 2015; Ramamurthy and Bou-Zeid 2017), the contrasting results of Scott et al. (2018) suggest that the relationship between extreme heat and UHIs is not simply due to increased heat storage and emission by the urban fabric during extreme heat events.

While many studies have found that synoptic patterns have an influence on the strength of the UHI, only one study has examined extreme heat, UHIs, and circulation

in combination. Scott et al. (2018) examined UHI strength on hot days for moist and dry synoptic conditions in multiple cities in the USA. They found that UHIs are warmer when air masses are drier and noted that rural areas responded more to differing weather types than urban areas. While the authors did not examine heatwaves, this research shows that synoptic weather conditions may affect the strength of the UHI during heatwaves.

Section 1.2 has shown that there have been numerous investigations into the effect of synoptic conditions on UHIs, particularly in the northern hemisphere, while other studies have examined the effect of heatwaves on UHIs. However, there is a clear lack of research into the relationships between synoptic environments and the UHI in Australia, with the exception of Melbourne. Furthermore, Scott et al. (2018) suggests that the heatwave-UHI relationship is potentially more complicated than a simple urban form-heat relationship. Therefore, investigations into the overlying synoptic conditions and the strength of the UHI is warranted for Australian cities, particularly during heatwave conditions.

## 1.3 Urban heat islands and heatwaves in southern Australia

The studies described so far in this chapter highlight the lack of research on external influences of UHIs in the southern hemisphere, and in particular in Australia. While Morris and Simmonds (2000) examined the relationship between synoptic patterns and UHIs in Melbourne, this relationship has not been examined in other Australian cities. Furthermore, to our knowledge, no studies have examined the relationship between the UHI and heatwaves in Australia or elsewhere in the southern hemisphere.

This thesis focuses on three large coastal cities in southern Australia, Melbourne, Adelaide, and Perth, the locations of which are shown in Figure 1.3. These cities were selected as they are particularly susceptible to summer heatwaves. Combined, the three cities account for approximately 33% of the Australian population (as of June 2016, Australian Bureau of Statistics 2017). Melbourne is the second largest city in Australia, with a population of 4.9 million people (as of June 2017, Australian Bureau of Statistics 2018). Adelaide and Perth, while amongst the most populous cities in the country, are less than half the size of Melbourne. Adelaide and Perth have populations of 1.3 and 2.0 million people respectively (as of June 2017, Australian Bureau of Statistics 2018).
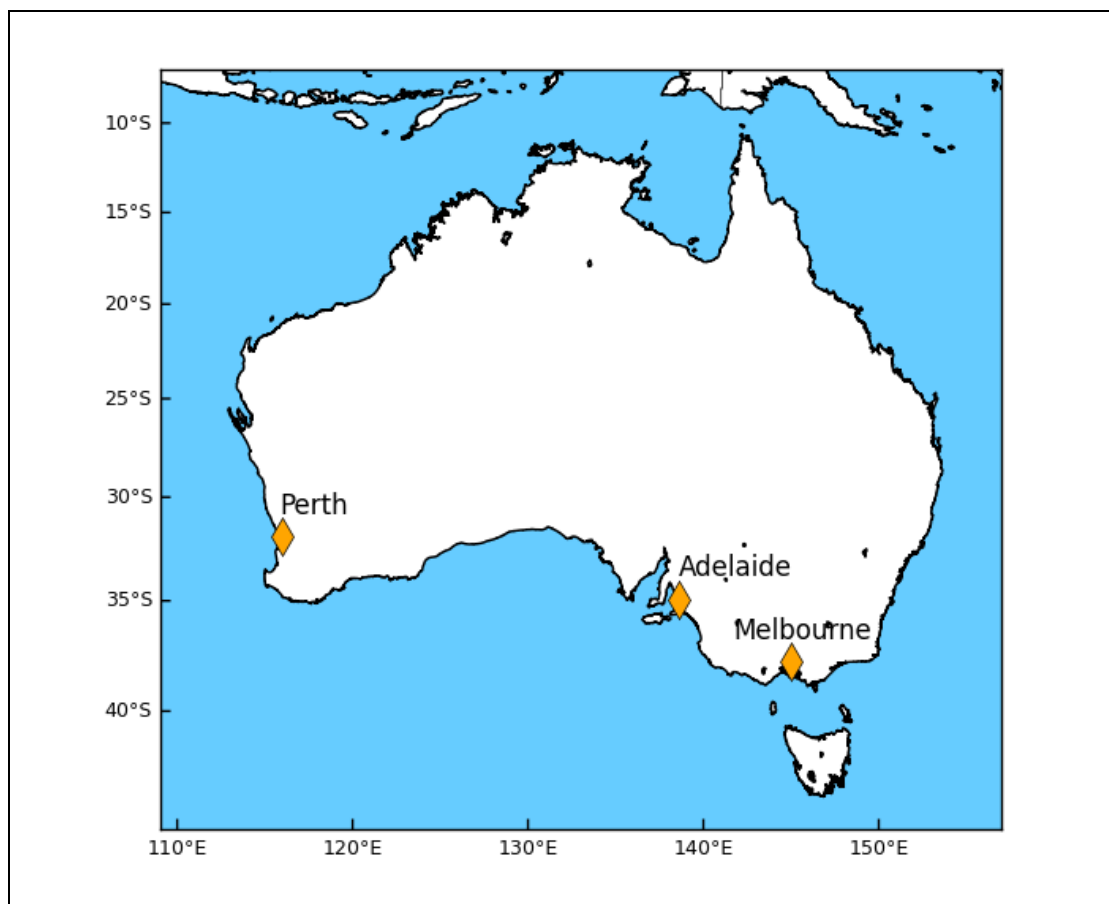


Figure 1.3: Locations of the cities of Melbourne, Adelaide, and Perth.

Population densities in Melbourne, 1,500 people per km$^2$, Adelaide, 1,300 people per km$^2$, and Perth, 1,000 people per km$^2$ are quite low compared to other cities around the world (Demographia 2017). For comparison, these urban densities are much smaller than those for London, 5,600 people per km$^2$, and Los Angeles, 2,300 people per km$^2$, which are the most densely populated cities in the UK and USA respectively.

Figure 1.4 illustrates the UHI effect in Melbourne on March 23, 2006 at 01:00 (Coutts et al. 2010). This figure shows that the UHI is strongest near the most urbanised parts of Melbourne (i.e. the CBD), where the UHI is approximately 4˚C, and less intense in areas away from the city centre. This indicates that the strength of the UHI varies within the city.
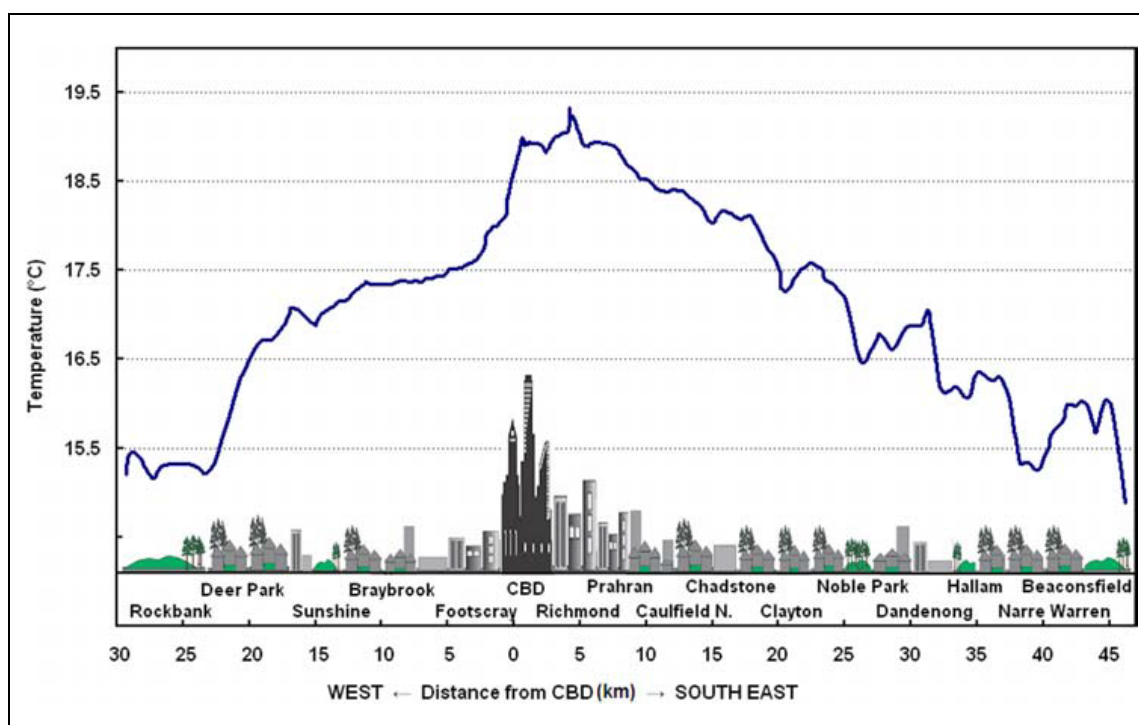


Figure 1.4: Spatial variability of the Melbourne urban heat island at 0100, 23 March 2006. Maximum urban heat island intensity of around 4˚C with peak warming in the CBD and high density commercial and residential development to the east of the CBD. Recorded weather at the Melbourne Regional Office at midnight was 19.4˚C with a westerly wind of 3 knots. The previous day's maximum temperature was 27.0˚C. Figure and caption from Coutts et al. (2010).

Several other studies have quantified the strength of the UHI in Melbourne. Morris and Simmonds (2000) found that the city of Melbourne has a typical UHI of

between -3.2°C and 6.0°C. When examining the UHI depending on season, Morris et al. (2001) found the strength of the UHI at 06:00 to be greatest in summer (1.29˚C) and coolest in winter (0.98˚C), with a yearly average of 1.13˚C. A transect study in August 1992 under calm conditions resulted in an UHI of 7.1˚C (Torok et al. 2001).

Soltani and Sharifi (2017) found that Adelaide has a median UHI of 5.41˚C at midnight in winter using a transect study. No research has yet determined the strength of the UHI in Adelaide or Perth using fixed weather stations, but intra-urban heat islands of 3.1˚C (Erell and Williamson 2007) and 1.5˚C (Guan et al. 2013) have been calculated in Adelaide.

Due to Melbourne, Adelaide, and Perth's geographical locations in the lower mid-latitudes, they experience extreme heatwaves (Cowan et al. 2014b) that are associated with synoptic patterns that have their origins in the mid-latitudes (Tryhorn and Risbey 2006; Pezza et al. 2012; Boschat et al. 2015; Gibson et al. 2017b). Research has also found that air parcels originating in tropical regions near northern Australia (Parker et al. 2013), and subtropical and mid-latitude regions over the south Indian Ocean (Quinting and Reeder 2017), are associated with heatwaves in southeast Australia. Heatwaves in southern Australia tend to be predominantly associated with dry conditions (Boschat et al. 2015) and are known to have an inverse relationship with soil moisture, that is, drier soil conditions exacerbate warming in the lower atmosphere (Herold et al. 2016).

Pezza et al. (2012) showed that synoptic patterns have a well-established relationship with heatwaves in Melbourne, Adelaide, and Perth, as shown in Figure 1.5. This figure shows that heatwaves in all three cities are generally associated with high-pressure systems to the east or southeast of the city; that is, high-pressure systems are located over the Tasman Sea for heatwaves in Melbourne and Adelaide (Figure 1.5a),

and over the Great Australian Bight for heatwaves in Perth (Figure 1.5b). Other observational studies identifed similar patterns for heatwaves in Melbourne (Boschat et al. 2015; Gibson et al. 2017b), Adelaide, and Perth (Gibson et al. 2017b).

Given the adverse impacts of extreme heat on health in Australian cities (Nicholls et al. 2008; Department of Human Services 2009; Loughnan et al. 2010a; Queensland University of Technology 2010; Williams et al. 2012a; Williams et al. 2012b), it is imperative that any potential additive effect of the UHI on heatwaves is quantified. As shown in Figure 1.5, all three cities experience similar anticyclonic synoptic patterns during heatwave events (Pezza et al. 2012; Gibson et al. 2017b). In Melbourne, these synoptic patterns are similar to those for strong UHI events, as is shown in Figure 1.1 (Morris and Simmonds 2000), leading us to hypothesise that heatwaves might have the potential to exacerbate the UHI due to the co-occurrence of similar synoptic patterns. Further, if UHIs in Australian cities add to urban temperatures during heatwaves, there exists the potential to partially ameliorate any associated health impacts through UHI mitigation approaches including urban design strategies such as white roofs (Oleson et al. 2010; Fallmann et al. 2013), the inclusion of green spaces (Fallmann et al. 2013; Zhang et al. 2014a), or the implementation of water sensitive urban design (Broadbent et al. 2018b) in the urban landscape.
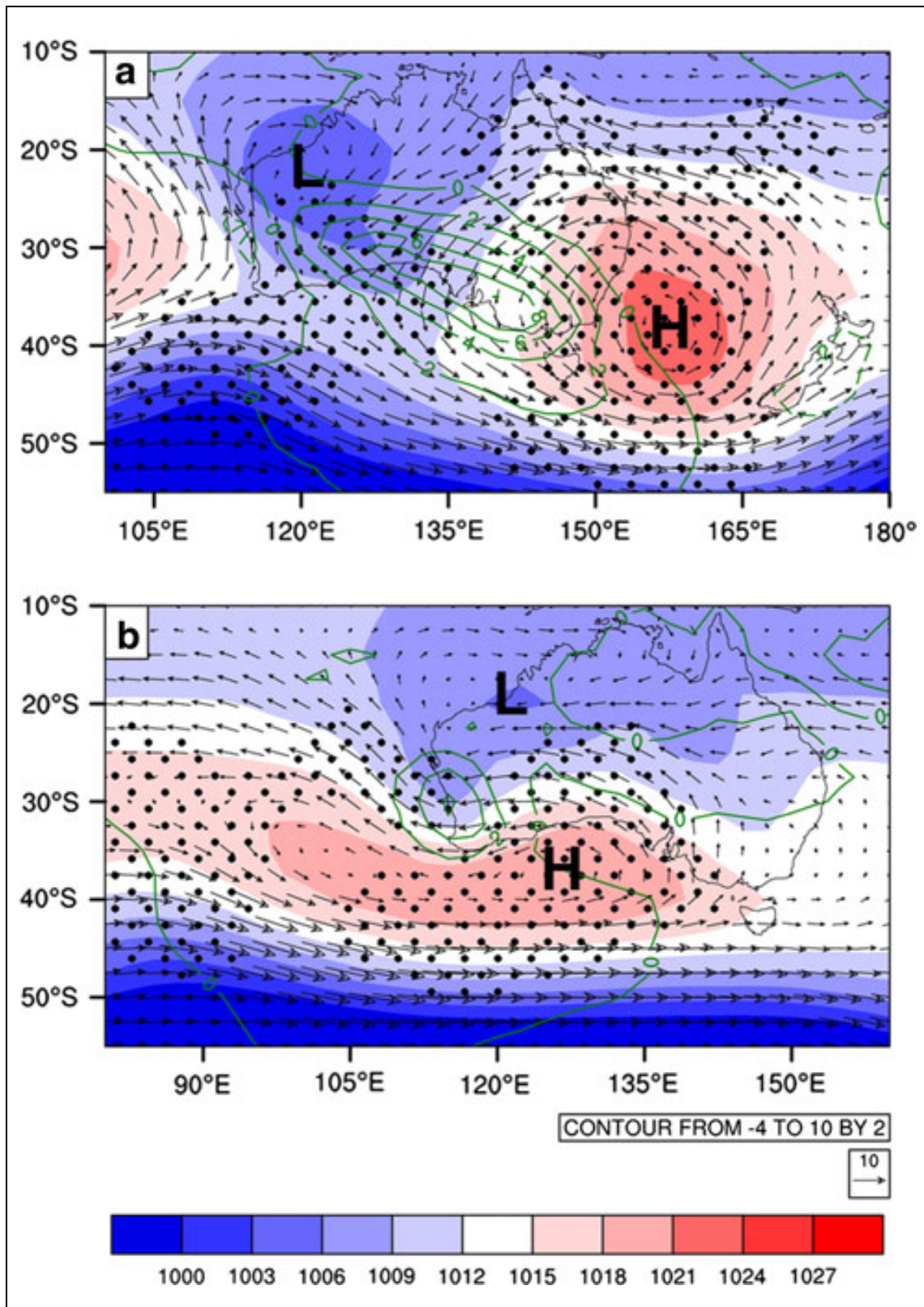
Figure 1.5: DJF composite of MSLP (*shading*) and surface temperature anomalies (*contours*) on the first day of HWs in a) Melbourne and b) Perth overlaid with 925 hPa winds. Units are in hPa (*colour scheme*), K (*contours*) and wind magnitude in m/s given by vector size. Number of events is 13 for Melbourne and 19 for Perth. Statistically significant MSLP areas above the 95% confidence level are given by stippling. The circulation associated with HWs in Adelaide is very similar to that of Melbourne just slightly shifted to the southwest, and is omitted in the interest of space. Figure and caption from Pezza et al. (2012).

## 1.4 Future change

Urban populations have increased globally from 30 % in 1950 to 55 % in 2018 (United Nations 2018). Since urban populations are affected by UHIs it is important to understand how UHIs may change in the future due to anthropogenic climate change, and how increasing urban populations may affect the future strength of the UHI.

### 1.4.1 Future urban heat islands

Urban areas will be subjected to ongoing changing conditions due to urbanisation and city planning decisions, as well as the effects of anthropogenic climate change. This subsection discusses factors that are likely to affect future urban temperatures, with a focus on cities in southern Australia.

UHIs are generally expected to increase in magnitude and/or spatial extent in the future due to increases in urban populations and urbanisation. An observational study in Melbourne (Coutts et al. 2007) and a study modelling Sydney's future UHI (Argüeso et al. 2014) both found that increasing urbanisation leads to increased night-time temperatures in the respective cities. Both studies found that temperatures increased due to increased heat storage in urban materials, while Argüeso et al. (2014) also found that reduced evaporation in the city contributes to increased urban temperatures. The above-mentioned studies found that increasing urbanisation is likely to cause a warmer UHI at night, corresponding to when UHIs are typically strongest (Oke et al. 1991; Coutts et al. 2010). If this warmer future UHI is superimposed on an exacerbated UHI due to the presence of a heatwave, urban populations are likely to be more vulnerable to extreme heat in the future, regardless of any increases in heatwave magnitude.

On the other hand, using modelling Coutts et al. (2008) showed that while the maximum strength of the nocturnal UHI is not expected to increase in Melbourne in the near future (2030), the spatial extent of the UHI is likely to increase. This coincides with a decrease in UHI variability across the city at night, thus increasing night-time temperatures in the city's growth areas. Their study was based on an urban planning scenario in the Victorian Government's "Melbourne 2030" planning strategy and therefore shows that planning decisions have the potential to impact future UHIs.

Melbourne, Adelaide, and Perth are expected to increase their populations from 4.9, 1.3, and 2.0 million people respectively as of 30 June 2017 (Australian Bureau of Statistics 2018) to 8.6, 1.9, and 5.5 million people in 2061 (Australian Bureau of Statistics 2013b). Given that increased levels of urbanisation are associated with increases in UHI magnitude and/or extent (Coutts et al. 2007; Coutts et al. 2008; Argüeso et al. 2014), we can expect the UHI to have a stronger influence on temperatures in Melbourne, Adelaide, and Perth in the future.

Anthropogenic climate change is also expected to affect future UHIs. Zhang and Ayyub (2018) found that the future UHI in Washington D.C., USA, is expected to be stronger on hot days for a high radiative forcing pathway (RCP8.5), but not for a low pathway (RCP2.6). Similarly, in Montreal, Canada, Roberge and Sushama (2018) noted a slight increase in UHI temperatures on top of a larger increase in both urban and rural temperatures due to climate change using RCP8.5.

Sachindra et al. (2016) used a downscaled general circulation model with a high emissions scenario (the IPCC's A2 emissions scenario) to show that nocturnal UHIs in Melbourne are expected to be warmer in the future (2000 to 2099) due to climate change, whereas Argüeso et al. (2014) used WRF to show a similar trend is likely to

occur in Sydney. Sachindra et al. (2016) suggested that the effect of climate change in Melbourne will be amplified by the UHI.

Conversely, using observational data Scott et al. (2018) argued that warmer temperatures are not associated with an increase in the strength of the UHI, and that recent climate change (between 2000 and 2015) has not amplified the UHI. The inconsistencies between these studies show that there are many uncertainties surrounding how the UHI will change with increasing greenhouse gas emissions. Alcoforado and Andrade (2008) identified some of these uncertainties, such as the representation of urban areas in models, planning decisions surrounding urban sprawl and/or increased urban density, and potential changes to synoptic patterns associated with UHIs.

Synoptic patterns are known to affect the strength of the UHI. In Prague, Czech Republic, Beranová and Huth (2005) identified an association between trends in the strength of the UHI in the past (1961 to 1990) and various synoptic patterns. The authors found that trends in the strength of the UHI under anticyclonic conditions were greater than those under cyclonic conditions. Synoptic patterns are expected to change in a warmer world in Australia (e.g. Gibson et al. 2017c) and in other countries (e.g. Demuzere et al. 2009). However, no studies have examined the potential role of changing synoptic conditions and how this might affect UHI strength with anthropogenic climate change.

## 1.4.2 Future heatwaves

Heatwaves have increased in number, duration, and intensity since the middle of the 20th century in Australia (Alexander and Arblaster 2009; Perkins and Alexander 2013) and around the world (Perkins et al. 2012), with these trends expected to continue

in the future in Australia (Perkins et al. 2012; Perkins and Alexander 2013; Cowan et al. 2014a; Cowan et al. 2014b) and around the world (e.g. Meehl and Tebaldi 2004; Fallmann et al. 2017) due to anthropogenic climate change.

Further, Mishra et al. (2015) identified an increase in the number of heatwaves in various urban areas in Europe, North and South America, Africa, and Asia over the recent past (1973 to 2012). They also found that hot days have increased more in urban areas than in nearby non-urban areas over the same period. Similarly, Sachindra et al. (2016) found that the number of hot days in the Melbourne CBD is expected to increase with climate change. If these trends continue as expected, urban populations will be more vulnerable to future heatwaves.

As mentioned earlier, heatwaves in southern Australian cities are most frequently associated with anticyclonic systems to the east or southeast of the city (Pezza et al. 2012; Boschat et al. 2015; Gibson et al. 2017b). Gibson et al. (2017c) noted an increase in the frequency of synoptic patterns associated with heatwaves in regions of Australia including Melbourne, Adelaide, and Perth, suggesting that these areas may see more heatwaves in the future. However, Purich et al. (2014) noted a weakening and/or shift of the pressure systems associated with future southern Australian heatwaves, suggesting that an increase in synoptic patterns associated with heatwaves may not lead to a proportional increase in the number of heatwaves.

Similarly, research in other countries has also identified changes in the relationship between synoptic patterns and heatwaves or hot days over time. Kim et al. (2018) found a weakening of pressure anomalies associated with future (2006 to 2100) hot days in Finland under RCP4.5. They found that higher background temperatures, which made heatwave thresholds easier to exceed, were responsible for the weakening of the weather systems. Similarly, Huth et al. (2000) noted that as the number of

heatwaves the Czech Republic increased, the relationship between heatwaves and synoptic patterns decreased.

While the above-mentioned studies have shown that the relationship between synoptic patterns and heatwaves is projected to weaken, in the northern hemisphere Horton et al. (2015) noted that changes in the frequency of temperature extremes can be partially explained by changes in synoptic patterns over the recent past. Zittis et al. (2016) found that a strengthening of anticyclonic synoptic patterns in summer will contribute to higher maximum heatwave temperatures in the eastern Mediterranean and the Middle East. These findings suggest that synoptic patterns will remain a crucial driver of heatwaves in the future.

### 1.4.3 Future urban heat islands during heatwaves

While research has found that heatwaves and UHIs are expected to change in the future, and that there is a relationship between the two, few studies have examined the future relationship between heatwaves and the strength of the UHI. This leaves a clear lack of understanding of how these events will affect future populations, particularly in Australia where research into the relationship between heatwaves and the UHI in the past has not been undertaken.

Zhao et al. (2018) noted the importance of investigating whether relationships between heatwaves and the UHI will persist into the future. The authors found that the relationship between the strength of the UHI and heatwaves intensifies in the future. Their study examined a number of cities in the USA in the last 30 years of the $21^{st}$ century and found that increased heat release at night is one of the main drivers of the intensification. If Melbourne, Adelaide, and Perth see a similar intensification of the relationship between heatwaves and the UHI in the future, in conjunction with hotter

heatwaves and a warmer UHI due to climate change and increased urbanisation, the cities' residents are likely to be more vulnerable to future heatwaves.

The importance of understanding the link between UHIs and heatwaves becomes more important in the future given that future heatwaves in urban areas have a greater potential to adversely affect the population than current heatwaves for three major reasons. First, heatwave number, duration, and intensity are likely to increase with anthropogenic climate change in Australia (Alexander and Perkins 2013; Cowan et al. 2014a; Cowan et al. 2014b), and around the world (Meehl and Tebaldi 2004; Fallmann et al. 2017). Second, projections from the Australian Bureau of Statistics (2014) show that the proportion of Australians living in capital cities is expected to increase from 66 % in 2013 to 72 % in 2053. And third, elderly Australians (over 64 years old) who are particularly vulnerable to extreme temperatures (Nicholls et al. 2008; Loughnan et al. 2010a) are expected to make up a larger proportion of the Australian population in the future (Australian Bureau of Statistics 2013a). The combined risk of future increases in Australia's urban population and changes in demographic, as well as increasing number, duration, and intensity of heatwaves has the potential to increase the number of heat related deaths in urban areas in Australia.

## 1.5 Thesis aims and structure

While past studies have shown that synoptic patterns are an important modulator of UHIs, there is a notable lack of studies focusing on Australia. The little work that there is highlights that overlying synoptic conditions likely play an important role in modulating the strength of the UHI. Quantifying these relationships will form a key part of this thesis. Furthermore, while there is an increasing body of work investigating changes to UHIs with anthropogenic climate change, no studies have

examined the possibility of the influence of changes in synoptic conditions on the UHI into the future. The presence of heatwaves is another factor that is known to affect the strength of the UHI in a number of cities around the world, yet no research has identified a link (or lack thereof) between UHIs and heatwaves in Australian cities. This thesis aims to address the above-mentioned gaps in the literature by focusing on the aims first summarised and then described below.

The main aims of this thesis are to:

1. Examine the relationship between heatwaves and the strength of the UHI in southern Australian cities.

2. Determine the relationship between synoptic patterns and the strength of the UHI during heatwaves and the extended summer season.

3. Examine future changes related to those atmospheric mechanisms identified in 1 and 2 that are important for the UHI.

    a. Future changes in synoptic patterns from 2 to determine the potential change to those synoptic environments most closely associated with anomalous UHIs.

    b. Future changes in heatwaves.

The first aim of this thesis is to examine whether there is a relationship between heatwaves and the strength of the UHI, and if so, is the UHI exacerbated or diminished during heatwaves. This is undertaken using observational data from the Bureau of Meteorology for the southern Australian cities of Melbourne, Adelaide, and Perth. We examine different environmental factors that have the potential to affect the UHI,

including wind speed and direction, geography, and station placement, to determine any effect they may have on the strength of the UHI during heatwaves.

Our second aim is to investigate which synoptic patterns are associated with strong UHIs and with UHIs during heatwave events. We examine the strength of the UHI for synoptic patterns typical to each of the cities. We also determine synoptic patterns that are typical during heatwaves and investigate whether the occurrence of certain synoptic patterns can explain any potential relationship between UHIs and heatwaves. If synoptic patterns that occur during heatwaves also happen to be prevalent during strong UHI events, this could explain any potential exacerbation of the UHI. Alternatively, variability in the relationships between synoptic patterns, UHIs, and heatwaves, between cities, may indicate why some cities show stronger relationships between heatwaves and UHIs than others.

The last aim of this thesis is to examine future, anthropogenically-driven changes in those synoptic patterns that are related to the strength of the UHI. That is, are those synoptic patterns that are associated with strong UHIs expected to increase or decrease in frequency with anthropogenic climate change? We also examine how the relationship between heatwaves and synoptic patterns is likely to change in a warmer world.

Chapter 2 of this thesis details the data used for this research and Chapter 3 describes the majority of the methods used throughout this thesis, although some methods are described within results chapters. The results addressing the aforementioned aims are discussed in Chapters 4 through 6. Chapter 4 examines the existence of a relationship between heatwaves and the UHI and investigates some potential causes of this relationship, other than urban-rural land cover differences. These causes include wind speed and wind direction. Chapter 5 investigates whether

synoptic meteorology influences the potential relationships between heatwaves and the UHI in all three cities, and determines which synoptic patterns are associated with strong UHIs and heatwaves. Lastly, Chapter 6 examines how heatwaves and synoptic patterns are likely to change in the future with anthropogenic climate change and discusses the implications this might have on the UHI given the findings in previous chapters. Our findings are summarised and overarching conclusions are provided in Chapter 7.

# 2. Data

This thesis uses observational and modelled data from various sources to identify heatwaves, calculate the strength of the UHI, and examine synoptic patterns. This chapter describes the data and data sources used for this work and will also detail the quality control undertaken for some data. We limit our investigation to the extended summer season, which we define as November to March. This is because it is the warmest time of the year, when additional heat from the UHI is most likely to be detrimental to human health. Moreover, some of our investigation is limited to heatwaves and those heatwaves that occur during this November to March period represent the hottest heatwaves during the year.

## 2.1 Automatic weather station data

The identification and analysis of the UHI are performed using the Bureau of Meteorology three-hourly, Automatic Weather Station (AWS) data from January 1995 to March 2014 for the extended summer season. The station classification methods, defined as urban, urban fringe, and rural, are described in detail in Chapter 3. Station names, numbers, latitudes, longitudes, elevations, and classifications are listed in Table 2.1, and station locations are shown in Figure 2.1. The Bureau of Meteorology AWSs are required to be placed in cleared areas with surrounding vegetation no taller than 50 mm (Bureau of Meteorology 2014). These standards can have implications for temperatures measured at weather stations as the effects of the surrounding areas, urban or rural, are dampened.

| City | Station name | Station number | Lat (˚S) | Lon (˚E) | Station classification | Elevation (m) |
|---|---|---|---|---|---|---|
| Melbourne | Avalon Airport *Avalon* | 87113 | 38.03 | 144.48 | Rural | 10.6 |
| | Coldstream | 86383 | 37.72 | 145.41 | Rural | 83.0 |
| | Melbourne Airport | 86282 | 37.67 | 144.83 | Rural | 113.4 |
| | Melbourne Regional Office *MRO*\* | 86071 | 37.81 | 144.97 | Urban | 31.2 |
| | Moorabbin Airport *Moorabbin* | 86077 | 37.98 | 145.10 | Urban | 12.1 |
| | Scoresby Research Institute *Scoresby* | 86104 | 37.87 | 145.26 | Urban | 80.0 |
| | Sheoaks | 87168 | 37.91 | 144.13 | Rural | 236.7 |
| Adelaide | Adelaide (Kent Town)\* | 23090 | 34.92 | 138.62 | Urban | 48.0 |
| | Adelaide Airport | 23034 | 34.95 | 138.52 | Urban fringe | 2.0 |
| | Edinburgh RAAF | 23083 | 34.71 | 138.62 | Rural | 16.5 |
| | Parafield Airport | 23013 | 34.80 | 138.63 | Urban fringe | 9.5 |
| | Roseworthy AWS | 23122 | 34.51 | 138.68 | Rural | 65.0 |
| | Strathalbyn Racecourse | 24580 | 35.28 | 138.89 | Rural | 58.0 |
| Perth | Gingin Aero | 9178 | 31.46 | 115.86 | Rural | 73.0 |
| | Gooseberry Hill | 9204 | 31.94 | 116.05 | Rural | 220.0 |
| | Jandakot | 9172 | 32.10 | 115.88 | Urban fringe | 30.0 |
| | Pearce RAAF | 9053 | 31.67 | 116.02 | Rural | 40.0 |
| | Perth Airport\* | 9021 | 31.93 | 115.98 | Urban fringe | 15.4 |
| | Perth Metro | 9225 | 31.92 | 115.87 | Urban | 24.9 |

Table 2.1: Bureau of Meteorology Automatic Weather Station names, identification numbers, latitudes, longitudes, urban/rural classifications, and elevations for Melbourne, Adelaide, and Perth. Elevation is height in metres above mean sea level. If a station has an abbreviated name, it is indicated in italics. The ACORN-SAT stations are marked with an asterisk. Note that the high quality controlled ACORN-SAT data at these sites are used for heatwave identification only and not for calculation of the UHI.

Prior to 1995, a lack of data availability means that the calculation of the UHI becomes difficult when using multiple stations as urban and rural references. Therefore, we limit our examination to data from January 1995 onward. The magnitude of the UHI is determined using three-hourly dry-bulb screen temperature data. Three-hourly data are the highest time resolution for which data are available but are sufficiently frequent to capture the diurnal cycle in the magnitude of the UHI. Dry-bulb temperature data are recorded using resistance temperature detectors housed within a Stevenson Screen (Bureau of Meteorology 2018).
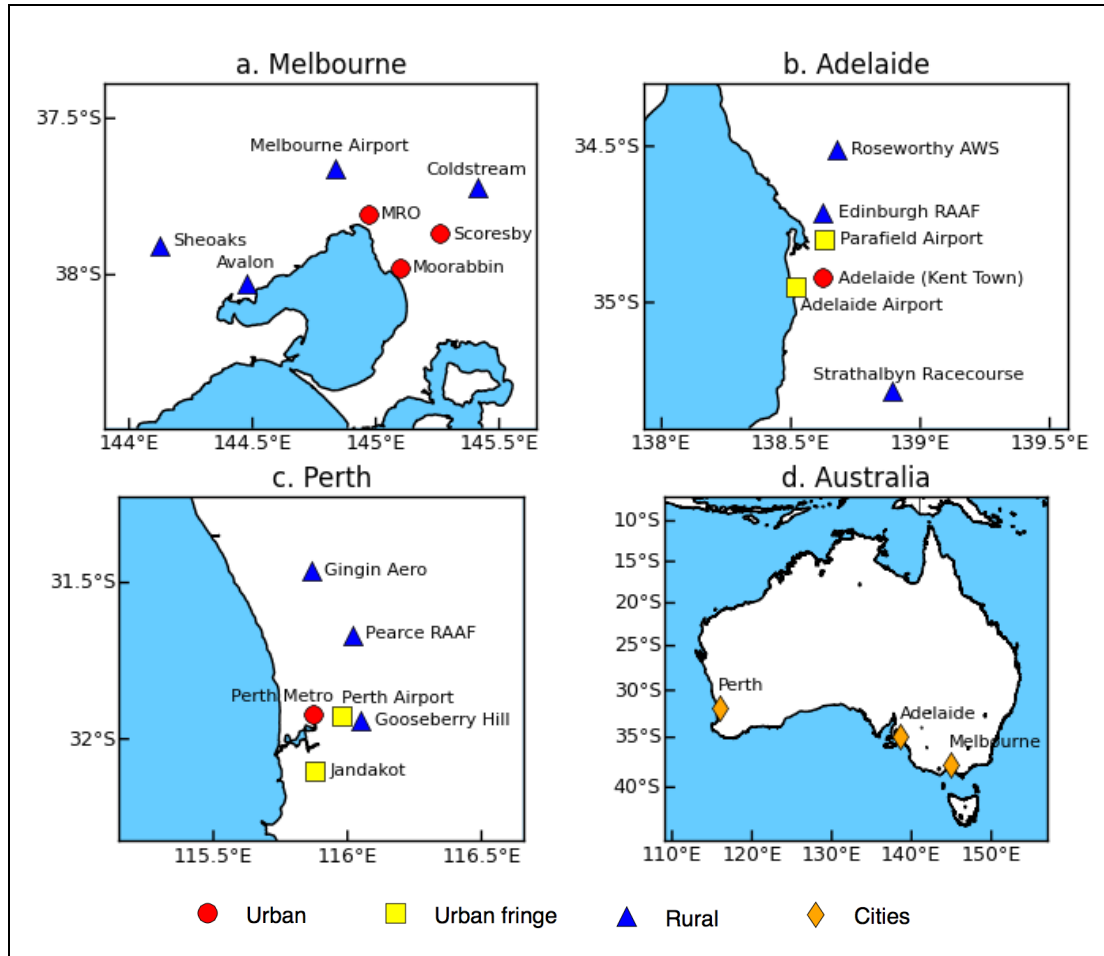
Figure 2.1: Station locations in a) Melbourne, b) Adelaide, and c) Perth. d) shows locations of Melbourne, Adelaide, and Perth (orange diamonds). Red circles represent urban stations, yellow squares represent urban fringe stations, and blue triangles represent rural stations. Abbreviated names are used for clarity, see Table 2.1.

The Bureau of Meteorology AWS dry-bulb temperature data can be susceptible to artificial temperature spikes (i.e. a sharp increase in temperature followed by a sudden decrease) on hot days due to instrumentation error (B. Trewin, pers. comm. August 7 2014). These erroneous spikes can spuriously increase the magnitude of heatwave temperatures at a single station and hence affect the strength of the UHI. Therefore, we perform quality control on the AWS temperature data and unexplained temperature spikes are removed from the analysis.

Artificial temperature spikes are identified as periods when an anomalously large increase in temperature is followed by an anomalously large decrease in temperature. To identify temperature spikes, we create two time-series:

1. $T_a$: The current temperature ($T_0$) minus the temperature three hours earlier ($T_{-3}$), i.e. $T_a = T_0 - T_{-3}$

2. $T_b$: The temperature three hours later ($T_{+3}$) minus the current temperature ($T_0$), i.e. $T_b = T_{+3} - T_0$

The 90th and 10th percentiles are found for each of these time series and temperature spikes are defined as time periods where $T_a$ is greater than the 90th percentile and $T_b$ is less than the 10th percentile.

If a spike is detected at station $i$, the data at neighbouring stations are compared to station $i$ to determine whether or not temperature spikes are likely to be artificial or the result of real world temperature change (e.g. the rapid onset and decay of a sea breeze). The temperature spikes are considered to be a real reflection of diurnal temperature progression if a neighbouring station experiences a similar temperature spike at the same time, or three hours earlier or later. Neighbouring stations are those located geographically closest to the station in question. For example, Avalon is the neighbouring station for Sheoaks and is located approximately 33 km southeast of the Sheoaks AWS (see Figure 2.1a). Temperature spikes are also deemed to be real if the temperature of a neighbouring station is within 2˚C of the current temperature, $T_0$.

Of the remaining temperature spikes, AWS wind direction data are assessed to determine if each temperature spike can be explained by changes in wind direction (e.g. a sea breeze). Overall, the quality control process resulted in the removal of four

temperature records from the Melbourne stations, two from the Adelaide stations, and two from the Perth stations, none of which occurred during a heatwave.

Alongside temperature, we examine three-hourly wind speed and direction data from these same AWSs in order to examine possible causes of the relationship between heatwaves and the UHI in Chapter 4. These data are used to examine the likelihood that signals in the above-mentioned relationship are due to factors other than urbanisation, for example, proximity to the coast. Wind data are measured using cup and vane anemometers mounted to wind masts. Information about wind instruments is available online from individual station metadata files, for example, information for the Melbourne Regional Office AWS station is available from http://www.bom.gov.au/clim_data/cdio/metadata/pdf/siteinfo/IDCJMD0040.086071.SiteInfo.pdf.

## 2.2 ACORN-SAT data

Heatwave identification is performed using the Australian Bureau of Meteorology's Australian Climate Observations Reference Network – Surface Air Temperature (ACORN-SAT) dataset. As spurious data are often manifest as the extremes in temperature distributions, high quality data are necessary to ensure the correct identification of extreme weather events such as heatwaves (Coumou and Rahmstorf 2012). The ACORN-SAT dataset contains maximum and minimum daily temperature data at Australian meteorological stations. Maximum and minimum temperatures are determined using a 9 am to 9 am window. These data are freely available from http://www.bom.gov.au/climate/change/acorn-sat/#tabs=Data-and-networks.

The ACORN-SAT dataset consists of high quality, homogenised data (Trewin 2013; Bureau of Meteorology 2015) that has undergone quality control to ensure the data are reliable. The data are examined for short-term issues, such as instrument faults, and longer-term issues, which can create inhomogeneities (Trewin 2013). These inhomogeneities can be caused by Bureau actions, such as instrument changes and site relocations, or external changes, such as changes to the area surrounding a weather station, e.g. increased urbanisation. The quality control process aims to ensure the historical data undergo a similar level of quality control to newly acquired data (Trewin 2013).

Heatwaves whose entirety occurs between January 1995 and March 2014 during the extended summer season (November to March) are identified using the heatwave definition described in Chapter 3. We investigate heatwaves from 1995 to 2014 in order to be consistent with the period over which AWS data are available. The ACORN-SAT stations used to identify heatwaves for each city are those stations that are closest to the centre of that city. These are Melbourne Regional Office (#86071), Adelaide (Kent Town) (#23090), and Perth Airport (#9021), see Table 2.1 and Figure 2.1.

## 2.3 ERA-Interim data

The ERA-Interim data are a gridded global atmospheric reanalysis data produced by the European Centre for Medium-Range Weather Forecasts (ECMWF) (Dee et al. 2011). The data are available from 1979 onwards and are updated continuously (ECMWF 2018). The ERA-Interim data are on a grid with latitude and longitude spacing of approximately 79 km (approximately 0.75˚ latitude by 0.75˚ longitude). See Dee et al. (2011) for details about the dataset. We choose to use ERA-Interim data as

this dataset was found to be suitable for use with self-organising maps (SOMs), a clustering method used throughout this thesis and explained in Chapter 3, when researching Australian heatwaves (Gibson et al. 2017b). Gibson et al. (2017b) performed their research using both ERA-Interim and the Modern-Era Retrospective analysis for Research and Applications, Version 2 (MERRA-2) dataset, and found that the choice of reanalysis dataset did not alter the outcomes of their research. While the ERA-Interim dataset is a reanalysis product, we refer to it as observational data throughout this thesis as we use it in conjunction with observational ACORN-SAT and AWS temperature data.

Synoptic patterns over Melbourne, Adelaide, and Perth are examined using six-hourly ERA-Interim MSLP data over the same period of time for which the AWS data are available, January 1995 to March 2014. The methods by which the Synoptic Types are created from the ERA-Interim MSLP data are described in Chapter 3.

We examine synoptic patterns over a domain of size 35˚ latitude by 40˚ longitude, roughly centred over the ACORN-SAT station in each of the three cities (Table 2.2 and Figure 2.1). We choose this domain size as it is large enough to include synoptic scale features that influence the weather in each of the cities, such as high-pressure systems, but small enough to exclude features that may confuse the analysis, for example, tropical features such as tropical cyclones. This choice of domain size is consistent with Jiang et al. (2017) who examine air pollution events over Sydney using SOMs.

Since the UHI tends to be strongest at night (Oke et al. 1991; Coutts et al. 2010; Loughnan et al. 2013) our analysis of synoptic patterns is restricted to the middle of the night, around midnight. The ERA-Interim data are available at a frequency of six-hours but are consistently shown for the same UTC time. Thus, data are unavailable at the

same time for all three cities. We therefore select the data that are closest to the local time of midnight; these times are: 23:00 for Melbourne, 22:30 for Adelaide, and 02:00 for Perth. Given the time and space scales on which synoptic systems operate, we posit that there will be no significant changes in MSLP patterns between the time used and midnight.

| City | ACORN-SAT station locations | | SOM domain | |
|---|---|---|---|---|
| | Latitude (˚S) | Longitude (˚E) | Latitudes (˚S) | Longitudes (˚E) |
| Melbourne | 37.81 | 144.97 | 20.00 - 55.00 | 125.00 - 165.00 |
| Adelaide | 34.92 | 138.62 | 17.50 - 52.50 | 120.00 - 160.00 |
| Perth | 31.93 | 115.98 | 15.00 - 50.00 | 95.00 - 135.00 |

Table 2.2: ACORN-SAT station locations for Melbourne, Adelaide, and Perth, and the latitude and longitude bounds used in the SOMs.

## 2.4 CMIP5 data

Throughout Chapter 6 we compare historical synoptic patterns and heatwave metrics to those simulated for a future climate that includes a signal of anthropogenic climate change. To do this we use model data from the Coupled Model Intercomparison Project Phase 5 (CMIP5). CMIP5 provides a common set of model simulations for modelling groups worldwide. CMIP5 models have skill in reproducing MSLP patterns during heatwave periods (Purich et al. 2014; Gibson et al. 2017a) and over the entire calendar year (Gibson et al. 2016) over Australia. However, there is a lot of variability between models.

We use three CMIP5 models throughout this work: ACCESS1-3 (Australian Community Climate and Earth-System Simulator, version 1.3), MPI-ESM-LR (Max Planck Institute Earth System Model, low resolution), and MRI-CGCM3 (Meteorological Research Institute Coupled Atmosphere-Ocean General Circulation Model, version 3). We choose these models based on past research as detailed later in this section.

ACCESS1-3 is a coupled model and incorporates the following model components: NOAA/GFDL MOM4pl for the ocean, LANL CICE4.1 for sea-ice, the atmosphere component is from the UK Meteorological Office's unified model (UM7.3), and CABLE v1.8 is used for the land-biosphere (Collier and Uhe 2012; Bi et al. 2013). The OASIS3.25 coupler is used to couple MOM4p1, CICE4.1, and UM7.3 (Bi et al. 2013). Atmospheric data are on a 1.25˚ latitude by 1.875˚ longitude grid with 38 vertical levels (Collier and Uhe 2012).

MPI-ESM-LR consists of the following coupled general circulation models: ECHAM6 and MPIOM for the atmosphere and ocean, JSBACH for the land and vegetation, and HAMOCC5 for marine biogeochemistry. Model components are coupled using the OASIS3 coupler (Giorgetta et al. 2013). The data are on a 1.9˚ latitude by 1.9˚ longitude grid with 47 vertical levels (Giorgetta et al. 2013).

MRI-CGCM3 is a coupled atmosphere-ocean global climate model. It consists of the atmospheric model MRI-AGCM3, the ocean-ice model MRI.COM3, and the aerosol model MASINGAR mk-2. These model components are coupled using the Scup coupler (Yukimoto et al. 2012). The model has 48 vertical layers (Yukimoto et al. 2012) with data on an approximately 1.1˚ latitude by 1.125˚ longitude grid.

Gibson et al. (2016) found these models to be good at representing synoptic patterns over Australia from 1958 to 2005 using SOMs. Similarly, Whetton et al. (2015) found the ACCESS, MPI, and MRI models to be in the top 50 % of models for simulating the southern Australian climate; the models ranked 20th, 10th, and 18th respectively out of 40 models. The authors compared the models using a skill score that incorporated temperature, rainfall, MSLP, and seasons. When examining the skill score of these models for 1.5 m temperature data and MSLP data, while these models are not the best, they are only up to 13.9 % worse than the best performing models, indicating

that they produce good representations of these variables. It must be noted that these skill scores were developed using Australia-wide data and therefore may not accurately identify the best models for the purposes of our research. For example, as noted by Whetton et al. (2015), the examination of wind, and by extension large-scale circulation, focuses on seasonal changes associated with the monsoon and subtropical ridge. Research such as ours that focuses on one season only should not prioritise models that are the best at representing seasonal changes.

Purich et al. (2014) found the above-mentioned models to be amongst the best at representing MSLP patterns associated with heatwaves over southern Australia. Gibson et al. (2017a) also showed that these models represent the spatial pattern of heatwaves over Australia well. The authors demonstrated that heatwave trends are represented well for Melbourne in all three models. However, over Adelaide the trends are too weak for all models whereas the trend is too high in MPI-ESM-LR for Perth.

Gibson et al. (2017a) noted that selectively choosing a number of CMIP5 models that represent heatwaves and their physical mechanisms well may produce better results than if models that represent heatwaves poorly are included in the analysis; this supports our decision to use a small selection of models. Our decision to use high temporal resolution daily model data, and the computing power required to do so, further suggests a need to reduce the number of models examined.

The CMIP5 models investigate the effect of differing levels of greenhouse gas emissions using a number of radiative forcing pathways, known as representative concentration pathways (RCPs). The RCPs were developed as a basis for modelling experiments to allow for consistency across different studies related to climate change. Four different pathways were developed: RCP2.6, RCP4.5, RCP6, and RCP8.5 (van Vuuren et al. 2011). Each of these represent an increase in radiative forcing by a certain

number of W/m$^2$ by 2100, for example, RCP8.5 represents an increase of 8.5 W/m$^2$ by the end of the 21$^{st}$ century (van Vuuren et al. 2011). Therefore, higher radiative forcing levels are associated with higher levels of greenhouse gas emissions.

In order to see how synoptic patterns and heatwave metrics vary with anthropogenic climate change we examine two RCPs: RCP4.5, a moderate increase in radiative forcing levels, and RCP8.5, a high increase in radiative forcing levels. To determine future change, we compare these simulations of a future with anthropogenic climate change to the historical simulations, which use observed greenhouse gas and sulphate aerosol emissions.

Here, the historical period in the models uses model data from January 1995 to March 2014, for consistency with the observational period in Chapters 4 and 5. We compare this to the future period from January 2065 to March 2084, which is the same number of years as the historical period, so that the sample sizes used for comparison are the same. Furthermore, the timing of the future period is far enough removed in time from the historical period to allow sufficient time for changes in synoptic patterns and heatwave metrics to develop due to differing levels of greenhouse gas emissions, but also not too far in the future that it is too distant in time for understanding hazards posed to cities into the future.

The CMIP5 data used consist of two sets of simulations, historical and projected runs. Since we do not examine model internal variability in this thesis, we use only one ensemble member for each model, that is r1i1p1.

To generate a historical simulation that spans the entire period of the observed data, we splice together data from the historical runs from January 1995 to December 2005 and then data from both the RCP4.5 and RCP8.5 to estimate historical forcing from January 2006 to March 2014. The historical runs use observed forcing to 2005,

while the RCP4.5 and RCP8.5 estimate forcing from 2006 to 2014. As each of the RCP4.5 and RCP8.5 show few changes in socioeconomic practice that would lead to drastically different climates in the immediate term, the RCP4.5 and RCP8.5 differ only slightly in their forcings from 2006 to 2014. The practice of 'splicing' the CMIP5 historical and projected data sets in the short term for comparison with observations beyond 2005 is common practice and has been performed extensively (e.g. King et al. 2015; Lewis and Karoly 2015).

Daily MSLP data from the three CMIP5 models are used to determine Synoptic Type distributions. We also use daily maximum and minimum temperature data from these models to identify heatwaves and examine heatwave metrics, including median and maximum heatwave temperatures, as well as number of heatwaves, number of heatwave days, and heatwave duration. We use these metrics to examine how heatwaves change over time with different climate change scenarios.

# 3. Methods

As outlined in Chapter 1, this thesis examines the magnitude of the Urban Heat Island (UHI) over three southern Australian cities. The analysis presented explores the relationship between the UHI and heatwaves (Chapter 4) and the role that the overlying synoptic conditions play in modulating the magnitude of the UHI in all three cities (Chapter 5). Using the relationships identified between synoptic conditions and the magnitude of the UHI, we then examine future changes in those UHI-related synoptic conditions with anthropogenic climate change and discuss what role these might play in influencing UHIs (Chapter 6). This includes an examination of the potential changes to the relationship between heatwaves and synoptic patterns in the future (Chapter 6). The analytical methods that will be applied throughout this thesis are now described.

## 3.1 Defining and measuring the urban heat island

The UHI is calculated as the difference between screen temperatures at urban stations and rural stations. To minimise the effects of local microclimates on station data, we use a composite of multiple stations to represent urban and rural stations where possible. Section 3.1.1 details how we select stations to represent the UHI as accurately as possible for each city, followed by a description of how we calculate the UHI in Section 3.1.2.

### 3.1.1 Station classification

In order to calculate the strength of the UHI, Automatic Weather Stations (AWSs) need to be categorised depending on their level of urbanisation. The station classification system used here is based on that applied for the ACORN-SAT dataset,

as described in Trewin (2013). Each station in Table 2.1 is assigned to one of the following classes:

- Urban – defined as stations within an urban area with a population greater than 10,000.

- Urban fringe – defined as stations within 2 km of an urban area with a population greater than 10,000. This includes stations that are located in a large green space within a population centre.

- Rural – defined as stations that are over 2 km from an urban area with a population smaller than 10,000.

Satellite images from Google Earth and population statistics from census data (available from http://www.abs.gov.au/websitedbs/censushome.nsf/home/census) are used to classify stations (see Table 2.1 and Figure 2.1).

To analyse the UHI strength, each station in and around Melbourne, Adelaide, and Perth is selected depending on the station's proximity to the greater city region, the ocean, or other large water bodies, and the station's data availability. For example, some stations are excluded as they are too close to a large water body and it is assumed that the effect of cooling of the water body will have too much influence on the strength of the UHI. For example, the Frankston AWS in southeast Melbourne, which is located on the shoreline, is consistently cooler than nearby stations. Other stations are excluded as they have large amounts of missing data between January 1995 and March 2014.

While the use of these three groups allows us to easily categorise the stations, this method ignores the variability between the stations within the same groups. For example, while Melbourne Airport and Avalon Airport are both operational airports in

outer Melbourne, their site characteristics differ. Melbourne Airport, also known as Tullamarine Airport, is the main airport for Melbourne. A greater portion of the land surface within 2 km of the station is covered by built surface, which mostly consists of the much larger airport with more runways, when compared to Avalon Airport. This likely leads to differences in the energy partitioning at the two stations. Due to the size of Melbourne Airport, more air and road traffic comes into and out of the 2 km radius surrounding the weather station, thus increasing the amount of anthropogenic heat in the area. This example shows that while we have grouped stations based on some broad similarities in the populations surrounding the stations, this does not account for all variability between stations. Further, stations in the same categories but in different cities can also show a large amount of variability in the amount of built surfaces, type and amount of vegetation cover, elevation, proximity to large water bodies, etc. surrounding the stations.

However, while there is variability between stations in the same category, due to our use of the Bureau of Meteorology's weather stations, which have standards controlling conditions in the immediate vicinity of the station (as briefly described in Section 2.1), there is a level of consistency in the land use around each of the stations in each of our three land use categories.

In order to identify and compare the strength of the UHI between Melbourne, Adelaide, and Perth, some generalisations about the stations need to be made, with the main assumption being that the variability between stations within each of the three groups is relatively small. By calculating the UHI using multiple stations from each category, as is described in detail in the following section, the effect of within group variability is reduced. This reduces the ability of each station to bias the strength of the UHI in any of the cities.

### 3.1.2 Urban heat island calculation

The UHI is calculated as the difference between urban and rural station temperatures from the AWS dataset described in Section 2.1. In Melbourne, urban and rural stations only are used to calculate the UHI. Urban fringe stations are excluded from the UHI calculation as this more clearly captures the difference between built up and non-built up environments. However, Adelaide and Perth have only one urban station each. Here, urban fringe stations are included as urban stations in the UHI calculation in order to increase the sample size and make the number of urban stations similar to the number of rural stations. However, we note that the inclusion of urban fringe stations might lead to an underestimation of the strength of the UHI in these cities.

The UHI for each time step in Melbourne is calculated as the median of urban station temperatures, minus the median of rural station temperatures for the given time step (as shown in Equation 3.1), whereas the UHIs for each time step in Adelaide and Perth are calculated as the median of the urban and urban fringe station temperatures, minus the median of the rural station temperatures for the given time step (as shown in Equation 3.2).

$$UHI_i = median(T_{u,i}) - median(T_{r,i})$$  Equation 3.1

$$UHI_i = median(T_{u,i} \cup T_{uf,i}) - median(T_{r,i})$$  Equation 3.2

Where $UHI_i$ is the strength of the UHI at time-step $i$, and $T_{u,i}$, $T_{uf,i}$, and $T_{r,i}$ are the sets of dry-bulb temperatures at time-step $i$ for the urban, urban fringe, and rural stations respectively. We calculate the UHI for each three-hourly time step to investigate the temporal progression of the UHI in each city. Hereafter, when referring

to urban stations in Adelaide and Perth, this includes both urban and urban fringe stations unless otherwise mentioned.

Throughout this thesis we refer to two forms of the UHI: the raw UHI and the anomalous UHI. Both are calculated using the quality controlled AWS data. The reasons why each is calculated are provided following the definitions.

*Raw UHI*

The raw UHI values are calculated as the median of the surface temperatures at the urban stations minus the median of the surface temperatures at the rural stations, for each three-hourly time-step for heatwave and non-heatwave periods.

*Anomalous UHI*

The anomalous UHI is calculated using temperature anomalies rather than the raw screen temperatures. The anomalies are calculated by subtracting a mean temperature for a given day and time from the raw AWS temperature data for that same day and time. The mean temperatures are calculated at each station for each three-hourly time-step of each day in the extended summer season (November to March) using a 31-day moving window centred on the day and time in question. For example, the mean for 12:00 on January 16 would use 31 days of data at 12:00 from January 1 to January 31 inclusive from 1995 to 2014. Anomalous UHI values are calculated as the median of the temperature anomalies at the urban stations, minus the median of the temperature anomalies at the rural stations.

By calculating both the raw and the anomalous UHI, we can provide more insight into the behaviour of the UHI than if we were to examine one UHI measurement only.

The raw UHI determines the size/magnitude of the UHI (or the UCI), i.e. it calculates by how many degrees Celsius the city is warmer/cooler than the surrounding

45

rural areas. A positive (negative) raw UHI (UCI) represents a city that is warmer (cooler) than the surrounding rural areas.

The calculation of the anomalous UHI determines how much warmer or cooler the UHI is when compared to average UHI conditions. Throughout this thesis, the term 'exacerbated' refers to a warmer than normal UHI, i.e. a positive anomalous UHI, whereas the term 'diminished' refers to an UHI that is cooler than normal, i.e. a negative anomalous UHI. Note that a diminished UHI does not necessarily indicate an UCI is present, it simply means that the UHI is cooler than normal. Calculating the anomalous UHI also helps to account for differences in station elevation and varying distances from each station to the coast as it assesses each station relative to itself.

## 3.2 Defining and measuring heatwaves

Heatwaves are defined here as a period of three or more consecutive days when the daily maximum temperatures exceed the 90th percentile on all days of the heatwave, and, the daily minimum temperatures exceed the 90th percentile on all days of the heatwave, except the first day. This heatwave definition is the same as that used by Pezza et al. (2012), except that the percentile thresholds for this study are computed using a 31-day moving window. Heatwaves that occur entirely during the extended summer season are identified and analysed in this research, as this is typically when the most severe heatwaves occur in southern Australia.

Note that time periods before midday on the first day of the heatwave, and after midday on the final day of the heatwave are not examined in this research. This ensures that periods prior to the start of the heatwaves, and those following cold fronts, which often herald a sudden end to heatwaves in southern Australia, are not included.

### 3.2.1 Defining heatwaves in the observational data

Heatwaves are defined using a base period from January 1910 to March 2014 because we exploit the long-term ACORN-SAT data (see Chapter 2) to compute heatwaves. However, because the AWS data from which the UHI is computed is only available from 1995, we assess heatwaves from January 1995 to March 2014 only. This definition results in 18, 25 and 22 heatwaves for Melbourne, Adelaide and Perth respectively.

Chapter 4 examines the typical nature of the UHI during heatwaves and compares this to non-heatwave conditions. To do this, we compute a climatology of the UHI during heatwaves that includes an assessment of the progression of the UHI as the heatwaves develop. To this end, the statistical analysis is stratified into three groups that are now described.

Over all three cities, heatwaves that lasted longer than three days account for only 31 % of all heatwave events (22 % in Melbourne, 32 % in Adelaide, and 36 % in Perth). The longest heatwave occurs in Adelaide and lasts for 10 days. As the majority of heatwaves last 3 days only, creating a climatology of those events that last for $n$ days, where $n$ is 4–10 days, is spurious due to the small sample size for each $n$. Instead, heatwave days are stratified into three groups defined as the 'first days,' 'middle days,' and 'final days' of the heatwaves. The first and final days of the heatwave are self-explanatory; all days that occur between the first and final days are termed 'middle days.' These groupings are selected in order to explore whether there are differences in the behaviour of the UHI as the heatwaves progress. As some heatwaves in each city persist for more than three days, the sample size for the middle days dataset is greater than that for the first or final days.

Note that the decision to stratify the heatwave days into three categories does not affect the conclusions of this study. The analysis in Chapter 4 was also applied using three-day heatwaves only to ensure the same sample size for all three groupings. While there were small differences in the magnitude of the UHI between the all heatwave and three-day only heatwave data, the general patterns of UHI evolution during heatwaves remained the same in all three cities.

**3.2.2 Defining heatwaves in the model data**

As described in Section 3.2.1, heatwaves in the observational period in Chapters 4 and 5 are identified using a base period from 1910 to 2014 (henceforth referred to as the long base period). However, since historical model simulations do not cover the entire 1910 to 2014 period, we must use a different base period when calculating heatwaves in the model data. Therefore, the heatwaves identified in Chapter 6 using model data use the same heatwave definition as that for the observational data, but with a base period from 1975 to 2005 (referred to as the short base period).

To enable us to compare heatwaves in the model simulations to those in the observational data, in Chapter 6 we recalculate heatwaves in the observational data using the short base period (1975-2005). The heatwaves identified using the short and long base periods are largely consistent, although there are a few differences (Table 3.1). Over the January 1995 to March 2014 period, the long base period identifies 59, 100, and 77 heatwave days in Melbourne, Adelaide, and Perth respectively, whereas, the short base period identifies 59, 98, and 55 heatwave days in these three cities respectively. Of these days, 56, 90, and 55 heatwave days respectively are common to both base periods. The instances in each city where heatwaves differ are shown in Table 3.1.

| Base period | Melbourne | Adelaide | Perth |
|---|---|---|---|
| Long base period 1910-2014 | 16-18 February 2013 | 12-15 February 1995<br>24-26 November 1997<br>2-4 March 2006 | 24-27 February 1999<br>11-13 November 2000<br>6 March 2001 (ext.)<br>10-12 November 2003<br>25-27 December 2004<br>24-27 February 2010<br>25-28 February 2011 |
| Short base period 1975-2005 | 12-14 January 1998 | 26-28 March 1996<br>28 November 2004 (ext.)<br>7 March 2008 (ext.)<br>21-23 November 2010 | - |

Table 3.1: Heatwaves between Jan 1995 and Mar 2014 in the observational ACORN-SAT data that only occur using one base period. Top row shows heatwaves that only occur when using the long base period (1910 to 2014) to identify heatwaves, whereas the bottom row shows heatwaves that only occur when using the short base period (1975 to 2005). Dates followed by (ext.) show heatwaves that are longer by the dates listed for a given base period.

Heatwaves in the observational dataset are identified using ACORN-SAT data as described in Chapter 2. These are point data for a number of AWSs in Australia; we choose the station closest to the CBD for each city to identify heatwaves. Since the models do not have data for the exact locations of the ACORN-SAT stations, we use data from the nearest grid point. Latitude and longitude coordinates used to represent the ACORN-SAT stations for Melbourne (Melbourne Regional Office), Adelaide (Kent Town), and Perth (Perth Airport) are shown in Tables 3.2, 3.3, and 3.4 respectively.

To identify heatwaves in the model data, we first calculate the $90^{th}$ percentile thresholds in the historical period using the 1975 to 2005 base period for each model. These thresholds are used to identify heatwaves in the past and future periods (see Section 2.4 for definition of past and future periods) using the same methodology as for the observational data. The use of the same temperature thresholds for the two periods allows for easy examination of the change in heatwave metrics with climate change. We identify heatwaves on each models' native grid to ensure heatwave identification is internally consistent in the model.

|  | ACCESS1-3 | MPI-ESM-LR | MRI-CGCM3 | Observations |
|---|---|---|---|---|
| Latitude (˚S) | 37.50 | 38.24 | 37.57 | 37.81 |
| Longitude (˚E) | 144.38 | 144.38 | 145.13 | 144.97 |
| Land fraction (%) | 90.10 | 100.00 | 95.65 | - |

Table 3.2: Latitude and longitude coordinates in the model data that are closest to Melbourne's ACORN-SAT station. Data from these coordinates are used to identify heatwaves in the model data for Melbourne. The latitude and longitude coordinates for Melbourne's observational station are listed in the far-right column. Land fraction gives the percentage of the model grid box used to represent the Melbourne ACORN-SAT station that consists of land.

|  | ACCESS1-3 | MPI-ESM-LR | MRI-CGCM3 | Observations |
|---|---|---|---|---|
| Latitude (˚S) | 35.00 | 34.51 | 35.33 | 34.92 |
| Longitude (˚E) | 138.75 | 138.75 | 138.38 | 138.62 |
| Land fraction (%) | 90.00 | 100.00 | 67.71 | - |

Table 3.3: Same as Table 3.2 but for Adelaide.

|  | ACCESS1-3 | MPI-ESM-LR | MRI-CGCM3 | Observations |
|---|---|---|---|---|
| Latitude (˚S) | 32.50 | 32.64 | 31.96 | 31.93 |
| Longitude (˚E) | 116.25 | 116.25 | 115.88 | 115.98 |
| Land fraction (%) | 63.33 | 100.00 | 38.89 | - |

Table 3.4: Same as Table 3.2 but for Perth.

## 3.3 Self-organising maps

The methods used to produce the Synoptic Typings for Chapters 5 and 6 are based on past research that analyses synoptic patterns using SOMs, with a focus on research performed in Australia (Jiang et al. 2012; Huva et al. 2015; Jiang et al. 2015; Gibson et al. 2016; Jiang et al. 2017), as well as the work of Kohonen (2014) who details the implementation of SOMs using MATLAB.

Using the methodology described below, SOMs can create similar results to k-means clustering, however one useful feature of SOMs as opposed to k-means clustering is that the patterns are ordered on the SOM plane (Kohonen 2014), that is, the typical progression of the synoptic patterns is made clear from the order of the SOM. This is useful for heatwave analysis as it allows us to see how the synoptic patterns progress from one day of the heatwave to the next.

### 3.3.1 SOM Toolbox

This research uses SOMs to determine the characteristic Synoptic Types over Melbourne, Adelaide, and Perth and identifies how often each Type occurs during both heatwave events and strong UHI events over the observational period. These Synoptic Typings are then applied to future MSLP patterns to examine changes in synoptic pattern occurrence with climate change.

In this thesis, the SOMs are created using SOM Toolbox, a MATLAB package. Various studies use SOM Toolbox to examine synoptic patterns (e.g. Verdon-Kidd and Kiem 2009; Jiang et al. 2015; Jiang et al. 2017). The SOM Toolbox package is developed by the Laboratory of Computer and Information Science (CIS) at the Helsinki University of Technology and can be downloaded freely from http://www.cis.hut.fi/projects/somtoolbox/. See Kohonen (2014) for more information about the package.

SOM Toolbox groups like data into a pre-determined number of nodes and orders them onto the SOM plane, also known as the map. When using SOMs to order MSLP data, a node corresponds to a Synoptic Type. SOM Toolbox requires the user to define a number of different input variables. The following subsections describe the settings we choose to use for this study. Section 3.3.2 details the variables we test to determine the optimal settings, whereas Section 3.3.3 details the settings we choose based solely on past research. We justify our choice for each of these settings. Settings/variables are italicised for clarity.

51

### 3.3.2 Tested SOM Toolbox settings

We test different map sizes and training lengths to determine the optimal choices for this analysis. This subsection details this process and explains the rationale behind our choices.

*Map size*

The map size determines the number of nodes (Synoptic Types) and their arrangement on the SOM plane. Map sizes vary from study to study (e.g. Gibson et al. 2017b; Jiang et al. 2017). We choose to use six nodes on a 3-by-2 map to represent six Synoptic Types over each of Melbourne, Adelaide, and Perth. These nodes are arranged on a grid with three nodes on the y-axis and two on the x-axis (e.g. see Figure 5.1). Despite the fact that a number of studies suggest using a greater number of nodes when examining MSLP data, for example Jiang et al. (2015) show that 10-20 nodes are suitable when performing cluster analysis (see Section 3.3.3 for more information about cluster analysis), we choose to limit the number of Synoptic Types to six.

The main reason for opting for a small map size is the availability of urban data. To most accurately calculate the UHI in Chapter 4 we limit our analysis to the period from January 1995 to March 2014, as described earlier. The major downside to this choice is the relatively small number of heatwave events this produces. By using a larger map size, heatwave events are scattered across many Synoptic Types that have very similar features (not shown), leaving little ability to perform robust statistical analysis of the data. We therefore opt to produce larger groupings of the heatwave days by reducing the number of Synoptic Types.

Visual inspection of the six Synoptic Types supports our choice to use a map size of 3-by-2 (Figures 5.1, 5.3, and 5.5). These six Types represent the main synoptic

patterns that affect each of the three cities, that is, the Types show a progression of frontal systems from the west to the east.

Figure 3.1 shows that the choice of a 3-by-2 SOM is valid. Ideally node-field correlations (Figure 3.1a, c, and e) should be high. This metric is calculated by matching each synoptic pattern to the most similar Synoptic Type and calculating the correlation between the two. Therefore, high node-field correlations indicate that the Synoptic Types accurately represent the synoptic patterns. On the other hand, a large spread of values in the node-node correlations (Figure 3.1b, d, and f) is preferred as this shows that the Synoptic Types represent a range of circulation patterns. This metric is calculated by finding the correlations between each Synoptic Type pair.

This method for finding suitable map sizes is explained in Gibson et al. (2016). Rather than using this methodology to determine the ideal size of the map, we use it to determine whether our chosen map size produces an adequate representation of the Synoptic Types when compared to larger map sizes.

Increasing map size generally causes increases in the mean and median of the node-field correlations and a larger spread in the node-node correlations in all cities (Figure 3.1). This shows that larger map sizes represent the synoptic patterns more accurately. However, given the increases in mean node-field correlations are relatively small (Figure 3.1a, c, and e), it is evident that using a larger map size does not greatly improve the representation of the synoptic patterns by the SOM.

There are greater improvements in the node-node correlations with increasing SOM size (Figure 3.1b, d, and f), showing that some of the circulation patterns covered by larger SOMs are not represented by a 3-by-2 SOM. However, given that the spread is fairly large for the 3-by-2 SOM, and the node-field correlations show that the circulation patterns represent the synoptic pattern data well (Figure 3.1a, c, and e), we

conclude that the node-node correlations are adequate for the purposes of this study. Therefore, in order to group heatwave days well for statistical purposes, and for ease of viewing, we maintain our earlier decision to use a 3-by-2 map size.
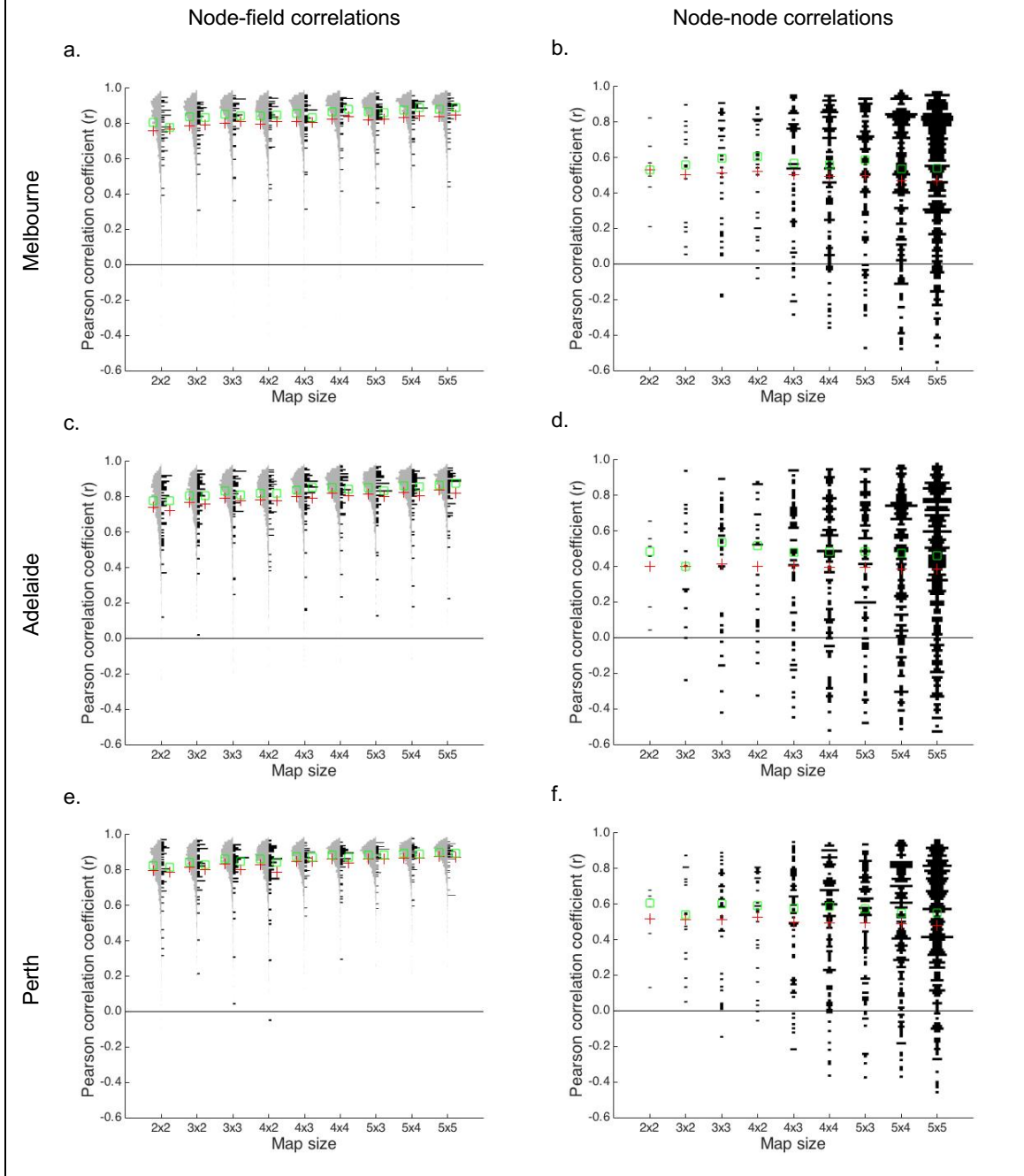


Figure 3.1: Correlation distribution plots. Subplots on the left show the distribution of correlations between each synoptic map and the Synoptic Type it is most similar to, i.e. node-field correlations, in a) Melbourne, c) Adelaide, and e) Perth, where grey bars represent all days in the sample (e.g. $n$ = 2964 days in Melbourne) and black bars represent heatwave days only (e.g. $n$ = 38 days in Melbourne). Subplots on the right show correlations between each node pair, i.e. node-node correlations, for b) Melbourne, d) Adelaide, and f) Perth. Green squares show the median of the distribution and red crosses show the mean. See Gibson et al. (2016) for more information on determining the appropriateness of different SOM map sizes.

We also use Figure 3.1a, c, and e to determine how well synoptic patterns during heatwaves are represented by the SOM. Since heatwaves are extreme events, we hypothesise that the Synoptic Types produced using MSLP patterns for all days (not just heatwave days) may not be a good representation of the synoptic patterns that occur during heatwaves.

Figure 3.1a, c, and e shows that the distributions of the node-field correlations on heatwave days are similar in shape to those for all days. This finding indicates that the 3-by-2 map size produces an adequate approximation of the synoptic patterns that occur in each of the three cities during heatwaves.

*Training lengths*

Producing a SOM using SOM Toolbox usually involves two rounds of training; coarse training, which determines the nodes (Synoptic Types), and fine training, which creates the final appearance of the node (Kohonen 2014). Training lengths, as defined by the user, are the number of iterations performed in each training phase (Kohonen 2014) and affect the quality of the SOM.

Increasing the number of iterations used to develop a SOM can improve the quality of the SOM, but after a certain number of iterations the SOMs will converge and the quality will cease to improve with increasing training lengths. To determine suitable training lengths for this analysis we create a number of 3-by-2 SOMs over Melbourne, Adelaide, and Perth with varying training lengths and compare the resulting quantisation errors (Figure 3.2).

In Melbourne and Perth, the SOMs converge after 5,000/10,000 and 1,000/2,000 iterations respectively, where the $m/n$ notation indicates that there are $m$ iterations of coarse training and $n$ iterations of fine training, see Figure 3.2a and c. This means that for both SOMs, an increase in the number of iterations above these values

does not improve the SOM. We note that small improvements in SOM quality can be seen by using a smaller number of iterations (500/1,000) in Perth (Figure 3.2c), but since this improvement is small (approximately 0.001 % improvement in quantisation error), and for consistency with Melbourne, we use training lengths of 5,000/10,000 in both cities.
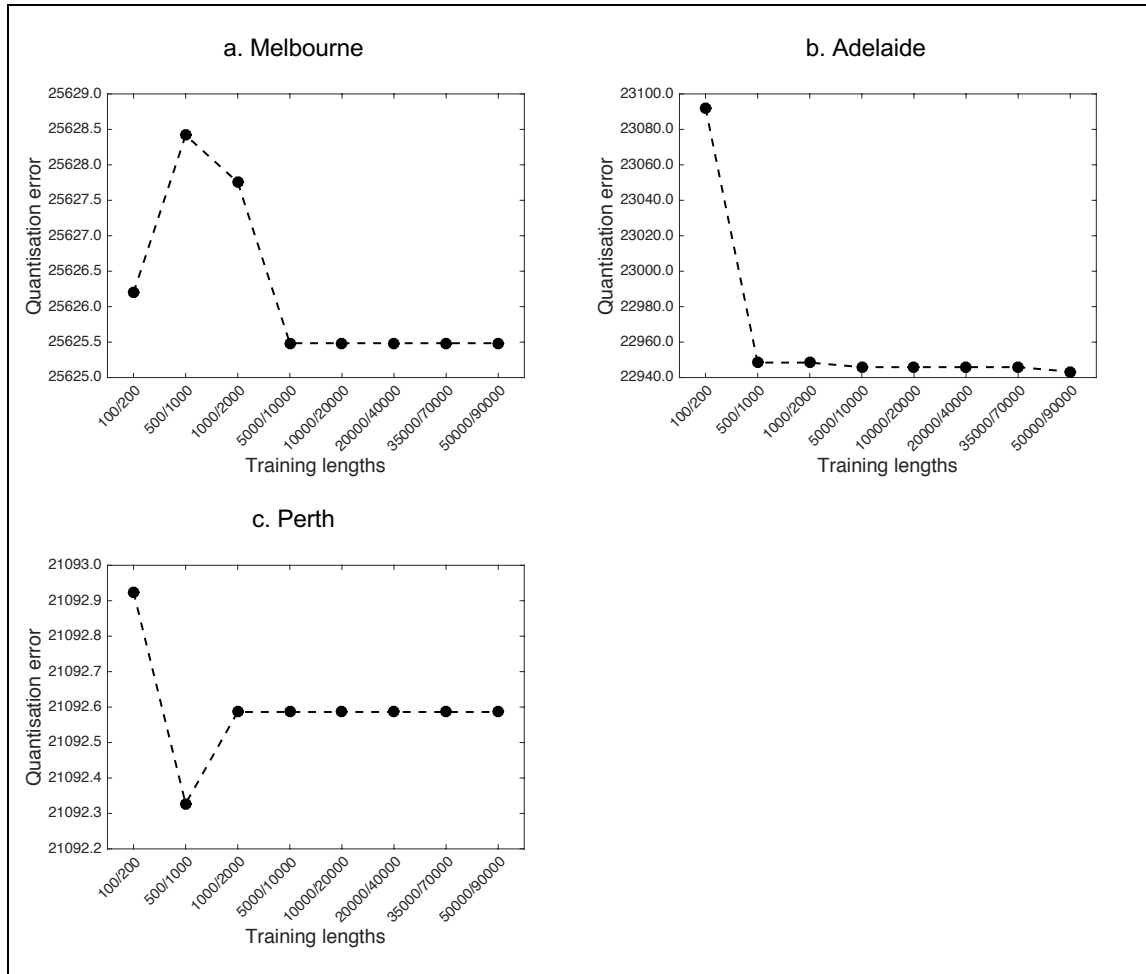


Figure 3.2: Effect of increasing training lengths on SOM quality (quantisation error) in a) Melbourne, b) Adelaide, and c) Perth using a 3-by-2 map size. Training lengths are listed on the x-axis in the format $m/n$, indicating that there are $m$ iterations of coarse training and $n$ iterations of fine training. Note: for clarity the y-axis scales differ between cities.

Adelaide on the other hand shows increasing but small improvements in the SOM quality with increasing number of iterations between 500/1,000 and 50,000/90,000 (Figure 3.2b). Since larger training lengths greatly increase the time taken to produce a SOM, and given that the corresponding increases in SOM quality

are small above training lengths of 500/1,000, we opt to use training lengths of 5,000/10,000 for Adelaide in order to be consistent with Melbourne and Perth.

Other research using SOMs to determine Synoptic Types finds that larger training lengths are necessary, but these differences might be due to differences in the city examined or data used; for example Jiang et al. (2015) use 20,000/40,000 iterations, and Jiang et al. (2012) use 50,000/90,000 iterations.

### 3.3.3 Untested SOM Toolbox settings

*Raw data*

Raw data are preferable when working primarily with weather phenomena in higher latitudes (Jiang et al. 2012; Jiang et al. 2015), i.e. when examining the passage of frontal weather systems, whereas standardised data are preferable when examining both high and low latitude data where the large variability at the high latitudes overshadows that at lower latitudes. Since this research is not concerned with tropical weather features, we use raw data for this research.

*Linear initialisation*

The training of a SOM can be started with a random set of values (random initialisation), or values determined using the principal components of the input data (linear initialisation). We choose to use linear initialisation for this work as it is quicker than random initialisation (Kohonen 2014). This choice is consistent with Jiang et al. (2012) and Jiang et al. (2015) who also use linear initialisation to create their SOMs.

*Batch training*

Different training algorithms can be used to create SOMs. Sequential training, as the name suggests, presents data to the SOM in a sequential order, with one data item presented at a time. On the other hand, batch training feeds all data items to the SOM

at once, thus the ordering of the data does not matter and the SOM converges faster (Jiang et al. 2015). Based on past research, which found batch training to be faster and more robust (Kohonen 2014) and the optimal option for research using synoptic patterns (Jiang et al. 2012; Jiang et al. 2015), we choose to use batch training in this thesis.

*Cluster analysis*

SOM analysis can be used to perform either cluster analysis or data projection. Data projection reduces topological error, that is it prioritises the order of the SOM, i.e. the placement of each of the Synoptic Types on the SOM plane in relation to one another (Jiang et al. 2015). This means that Types that frequently occur in succession will be located near one another on the SOM. On the other hand, cluster analysis prioritises reducing quantisation error, i.e. it improves the accuracy with which the Synoptic Types are grouped (Jiang et al. 2015). Since this research aims to find the synoptic patterns that are associated with either heatwaves or strong UHIs, we are most concerned with reducing quantisation error, thus increasing the accuracy of the Synoptic Types. We therefore use the cluster analysis option of SOM Toolbox. Note: while topological error is higher for cluster analysis than for data projection, nodes are still roughly ordered on the SOM plane for cluster analysis.

*Gaussian neighbourhood function*

Different neighbourhood functions can be implemented in order to optimise the SOM for the users intended purposes. The Gaussian function is the most common neighbourhood function (Kohonen 2014) and is the default in SOM Toolbox (CIS n.d.). The Gaussian neighbourhood function produces smoother patterns with less noise than using the 'ep' (Epanechikov) neighbourhood function. However, this also means the patterns using the Gaussian neighbourhood function are less accurate at fine resolution

(Liu et al. 2006). Since we are not concerned about fine detail, we choose to use the Gaussian neighbourhood function.

*Neighbourhood radii/widths*

As described in Section 3.3.2, SOM Toolbox usually requires the use of two rounds of training; coarse training and fine training (Kohonen 2014). Both rounds of training require the user to set the neighbourhood radii, which are the widths of the neighbourhood function (as described in the previous paragraph). The neighbourhood radii are a fraction of the dimensions of the SOM, thus since we use a 3-by-2 SOM, the neighbourhood radii used here must be some fraction of 3 or 2.

The neighbourhood radii used for this thesis are consistent with Jiang et al. (2015), where the radius for coarse training starts at 2 and ends at 1, and the radius for fine training starts at 2 and ends at 0. The starting radius for coarse training is the maximum of either the small dimension of the map size, or half the larger dimension (Jiang et al. 2015). Setting the final neighbourhood radius for fine training to zero makes SOM Toolbox perform cluster analysis rather than data projection (Jiang et al. 2015).

## 3.4 Verification of model data

In Chapter 5, SOMs are developed and analysis performed using ERA-Interim MSLP data from 1995 to 2014. Chapter 6 builds on these findings by fitting model data to the existing SOMs. However, since all models and observations use different resolution grids we re-grid all data to a common grid. The MSLP data are re-gridded onto the MRI-CGCM3 grid because the resolution of this model is a midpoint between that of ERA-Interim and the CMIP5 models used in this research. The MRI-CGCM3 grid has a resolution of approximately 1.1˚ by 1.125˚ for latitude and longitude

respectively. Since the ACCESS1-3 and MPI-ESM-LR grids are coarser than that of MRI-CGCM3 (see Section 2.4), data for the ACCESS and MPI models are interpolated when they are re-gridded onto the MRI grid.

To ensure the re-gridding process does not significantly alter the Synoptic Type distributions identified in Chapter 5, we verify the re-gridding process in Section 6.4.1. This validation ensures we can use the results from Chapter 5 that associate various UHI strengths and/or the presence of heatwaves with certain Synoptic Types in conjunction with the model data.

Next, we examine whether the SOMs are a good representation of the model data. These results are shown in Section 6.4.2. We fit the model MSLP data for the historical period to the SOMs created using the re-gridded ERA-Interim data. The frequency of occurrence of Synoptic Types in the model data are compared to those for the ERA-Interim data to determine if the models reproduce the observed MSLP pattern frequencies during heatwave periods and the extended summer season. Quantisation errors are also compared to ensure that the model data fit the six pre-defined Synoptic Types well.

## 3.5 Analysis methods

Analysis methods used throughout this thesis are described within the methods sections for each results chapter (Chapters 4 through 6). An overview of these methods is given below.

In this study, the typical response of the UHI during a heatwave period is examined. This behaviour is then compared to non-heatwave periods in order to determine whether UHIs are characteristically warmer, cooler, or of similar strength between heatwave and non-heatwaves periods. This methodology is detailed and results

described in Chapter 4. After determining the presence of any relationship between heatwaves and the UHI, we examine whether this potential relationship is likely due to factors other than urban-rural land surface differences, with results shown in Chapter 4, Section 4.4.

Chapter 5 describes the analysis used to identify which Synoptic Types are associated with strong UHIs and/or heatwaves and whether Synoptic Types can explain the potential relationships between heatwaves and UHI strength. These results are described in Chapter 5, Section 5.4.

Lastly, Section 6.3.4 describes the analysis used to examine future synoptic patterns. We examine how UHI strengths are likely to change in the future using changes in synoptic patterns as a proxy and identify changes in the relationship between heatwaves and synoptic patterns with anthropogenic climate change. Results from this analysis comprise Chapter 6.

# 4. Is the urban heat island exacerbated during heatwaves in southern Australian cities?

## Abstract

The extra-tropical Australian cities of Melbourne, Adelaide, and Perth are all affected by summer heatwaves and the urban heat island (UHI) effect. While research has been undertaken on both phenomena individually in Australia, they have not been studied in tandem. This research investigates the relationship between warm-season heatwaves (November to March) and the UHI in these cities from January 1995 to March 2014. Observational temperature data from six or seven Bureau of Meteorology Automatic Weather Stations in each of Melbourne, Adelaide, and Perth are used to determine the strength of the UHI during heatwave periods and these are compared to non-heatwave periods. Melbourne and Adelaide both experience an exacerbated (warmer than normal) UHI at night during heatwaves. The night-time UHI in Perth is diminished (cooler than normal) during heatwaves and often changes to an urban cool island (UCI), when compared to non-heatwave periods. Environmental factors that might affect the strength of the UHI are investigated, including wind speed and direction, and station location. Despite the proximity of all stations to the coast, coastal influences on UHI strength are minimal during heatwave conditions. Station choice is found to not affect our results, with the characteristic pattern of the UHI during heatwaves remaining consistent across all three cities in a leave-one-out sensitivity analysis.

## 4.1 Introduction

As described in Chapter 1, many cities globally experience a phenomenon known as an urban heat island (UHI), whereby urbanised areas experience higher temperatures than surrounding rural areas (Oke 1973; Oke 1982).

In urban areas, the health of the population can be adversely affected during extreme heat conditions (Nicholls et al. 2008; Loughnan et al. 2010a; Williams et al. 2012b). For example, a three-day heatwave in late January 2009 resulted in 374 additional deaths in the state of Victoria, Australia, compared to typical conditions (Department of Human Services 2009; Queensland University of Technology 2010). The negative health impacts of extreme heat are often associated with warm nights (Chestnut et al. 1998; Nicholls et al. 2008; Loughnan et al. 2010a), when any UHI effect is most prevalent (Coutts et al. 2010). If there is additional heat from an UHI during heatwave conditions, it could increase the risk of extreme heat exposure (Chestnut et al. 1998; Loughnan et al. 2010a).

The extent to which any UHI affects temperature during heatwave conditions has not yet been investigated in Australian cities. However, as described in Chapter 1, similar research conducted in other countries finds that UHI strengths are exacerbated in various cities during heatwaves, e.g. Li and Bou-Zeid (2013) in Baltimore, USA, Li et al. (2015) in Beijing, China, Heaviside et al. (2015) in Birmingham, UK, Zhou and Shepherd (2010) in Altanta, USA, and Ramamurthy and Bou-Zeid (2017) who examine multiple cities in the USA. Similarly, Fenner et al. (2014) find that the UHI at night in Berlin is exacerbated on hot days compared to the rest of the year.

If UHIs in Australian cities experience a similar pattern during heatwaves, there exists the potential to partially mitigate any associated health impacts through mitigation approaches including urban design strategies such as green roofs (Berardi et

al. 2014), or the inclusion of green spaces in the urban landscape (Fallmann et al. 2013; Zhang et al. 2014a).

This chapter will examine whether there is a relationship between heatwaves and the strength of the UHI, and if so, is the UHI exacerbated or diminished during heatwaves. This is undertaken using observational data from the Bureau of Meteorology, as described in Chapter 2 and Section 4.2, and considers different environmental factors that have the potential to affect the UHI, including wind speed and direction, geography, and station placement.

## 4.2 Data

Heatwaves and the UHI were computed using the ACORN-SAT and AWS data respectively. These data sets are described extensively in Chapter 2 so these descriptions will not be repeated here. The raw and anomalous UHIs (calculations described in Chapter 3) are computed for the three subject cities of Melbourne, Adelaide and Perth for the extended summer season (November to March) from 1995 to 2014, which is the period spanned by the AWS data at the time of the analysis.

Three-hourly wind speed and direction data are also used to examine possible causes of the relationship between heatwaves and the UHI in Section 4.4.2. These data are used to examine the likelihood that signals in the above-mentioned relationship are due to factors other than urbanisation, for example, proximity to the coast.

## 4.3 Methods

Heatwaves are identified in order to present a comparison of the UHI between heatwave and non-heatwave periods. To determine the relationships between heatwaves and the UHI in Melbourne, Adelaide, and Perth, the UHI is calculated for

each city for heatwave and non-heatwave days. The typical response of the UHI during a heatwave period is examined. This behaviour is then compared to non-heatwave periods in order to determine whether UHIs are characteristically warmer, cooler, or of similar strength between heatwave and non-heatwave periods. A complete description of the identification of heatwave periods, and of the computation of the raw and anomalous UHI were described in Chapter 3 and will not be repeated here.

**4.3.1 Urban heat island analysis**

Heatwaves are extreme and therefore rare events. Using the definition of a heatwave from Section 3.2.1, we identify 18, 25, and 22 heatwaves in Melbourne, Adelaide, and Perth respectively during the extended summer seasons between January 1995 and March 2014. Thus, to ensure an equivalent comparison during non-heatwave periods, random samples of the same sample size are selected from the observational data outside the heatwave days, hereafter referred to as bootstrapped samples.

The bootstrapped samples are generated by first selecting $n$ random UHI samples from the non-heatwave observed data, where $n$ is the number of observed heatwave days ($18 \leq n \leq 50$, where $n$ depends on city and heatwave day in question, see Section 3.2.1). This process is repeated 100 times to create 100 random UHI datasets of size $n$.

From these bootstrapped replicates of non-heatwave periods, we compute a 90 % confidence interval (5th and 95th percentile) and a median for each of the 100 random resamples. This provides an estimate of the distribution of raw and anomalous UHIs during non-heatwave periods against which we can compare the heatwave data. The median of these 100 medians, 95th percentiles, and 5th percentiles simulate the typical UHI strength, 95th percentile, and 5th percentile of the non-heatwave UHI

distribution respectively. This process is repeated for each three-hourly time-step from 00:00 to 21:00.

Using an example, Melbourne experiences 18 heatwave first/final days, and 23 middle days (see Section 3.2.1). Therefore, for each of the $i$ simulations, where $i = 100$, of UHI strength on first/final non-heatwave days in Melbourne is created using 18 random UHI observations from the non-heatwave dataset, whereas middle days are simulated using 23 random non-heatwave UHI observations. For the $i^{th}$ simulation the median, $5^{th}$ percentile, and $95^{th}$ percentile are calculated, resulting in 100 values for each statistic. The median value of each statistic is then computed.

The UHI calculation is prone to influence from missing data. To minimise these effects, the random UHI samples from non-heatwave days are discarded and then resampled if a missing data value is detected. Heatwave days with missing data are still used for UHI calculations because the sample size is already small. However, the effect of these missing data is tested by regenerating the analysis using only heatwave days with no missing temperature data. The influence on the results is negligible and, if anything, removing the days containing missing data enhances the relationships that are described in Section 4.4.1.

The Kolmogorov-Smirnov statistical test (KS-test) is employed to determine whether the distributions of the UHI during heatwave events are significantly different ($p < 0.05$) to those during non-heatwave events. Due to the difference between the sample sizes of the heatwave data ($18 \leq n \leq 50$) and the non-heatwave data from the bootstrapped samples ($1,800 \leq n \leq 5,000$), statistical significance is examined using two different methods that are defined as $KS_1$ and $KS_2$ respectively. These methods are explained in the following paragraphs. For illustrative purposes, we use the sample size for Melbourne on the first days of the heatwaves ($n = 18$) as an example.

The first method applies the KS-test at each time-step (three-hourly) by comparing the distribution of the heatwave UHI data ($n = 18$) to a distribution that consists of all randomly selected UHI data from the bootstrapped samples ($n = 1,800$, i.e. 18 random non-heatwave UHI samples multiplied by 100 repetitions of this random sampling). Time-steps with significant differences between heatwave and non-heatwave distributions computed using this method are indicated on the time series plots using grey shading (Figure 4.1). This method is referred to throughout the thesis as $KS_1$.

The second method, referred to as $KS_2$, applies the KS-test at each time-step between the distribution of heatwave UHI data ($n = 18$), and each individual bootstrapped sample ($n = 18$), thereby producing 100 different $p$-values. These results are displayed in Figure 4.1 as coloured stars, where the colour refers to the percentage of $p$-values less than alpha.

For a statistical significance level of 0.05, statistical theory dictates that around 5 % of the distributions produced from the bootstrapped sampling will yield a statistically significant result randomly and by chance, provided each sample is independent. Thus, if the proportion of $p$-values calculated using $KS_2$ is much greater than 5 %, this suggests there are real differences between the UHI distributions during heatwave and non-heatwave periods. Unless mentioned otherwise, results are discussed using $KS_1$.

### 4.3.2 Wind speed and direction analysis

The relationships between wind speed and direction and UHI anomalies are examined to determine whether geographical features that can induce local circulations (e.g. coastlines) are influencing the results. This analysis is performed for the night-

time data only, as this is when the magnitudes of the UHI anomalies are greatest (see Section 4.4.1).

The UHI anomaly strength is compared to wind speed and direction at concurrent time-steps (21:00, 00:00, and 03:00, hereafter referred to as time lag 0), and at lagged time-steps. The lagged analysis is performed in order to determine if any coastal effects, for example sea breezes, have any persistent signature on UHI anomaly strength into the evening. The lagged time-steps compare UHI anomaly strength at 21:00 with wind speed and direction 6 hours (15:00) and 3 hours (18:00) prior, referred to as lag 6 and lag 3 respectively.

The relationships between wind speed and UHI anomalies are tested using the Pearson Product moment test with a statistical significance level of 0.05.

To determine the presence of any relationship between wind direction and UHI anomaly strength, UHI data are partitioned into four groups based on wind direction. These groups are: northerly (wind direction $> 315°$ or $\leq 45°$), easterly ($45° <$ wind direction $\leq 135°$), southerly ($135° <$ wind direction $\leq 225°$), and westerly ($225° <$ wind direction $\leq 315°$). The KS-test is used to determine if there are significant differences between the distributions of UHI anomalies in each quarter compared to the distributions for all other wind directions, where the statistical significance level is again 0.05. If we identify a significant difference, we compare the median UHI anomaly for the given quarter to that for all other wind directions in order to examine the strength of the relationship.

We only examine the relationships between wind speed/direction and UHI anomaly strength where sample sizes are 20 or more for the dataset in question.

## 4.4 Results

Throughout the results section 'night-time' typically refers to times from 21:00 to 06:00. Therefore, the 'first nights' refers to 21:00 on the first days and 00:00 to 06:00 on the middle days (time-steps 8 to 11 on Figure 4.1), and 'middle nights' refers to 21:00 on the middle days and 00:00 to 06:00 on the final days (time-steps 16 to 19 on Figure 4.1).

### 4.4.1 Temporal variability of the UHI during heatwaves

The typical development of the UHI is first described using the data for non-heatwave days. Figure 4.1b, d, and f show that all cities experience an UHI. However, the magnitude can vary throughout the day and sometimes revert to a UCI during the day. In all three cities, there is typically a maximum in the UHI at night, where urban stations are warmer than rural stations, and a minimum in the UHI during the day. The minima may either remain zero or slightly positive (e.g. Figure 4.1b), or sometimes become negative, indicating that urban stations are cooler than rural stations (e.g. Figure 4.1f).

During heatwaves, a similar but stronger diurnal pattern is evident in Melbourne and Adelaide when compared to non-heatwave events (see Figure 4.1b and d respectively), whereas Perth's median raw UHI shows much less variability than during non-heatwaves (Figure 4.1f).

In all three cities, the difference between the anomalous UHI values during heatwave and non-heatwave events is greatest at night (Figure 4.1a, c, and e), demonstrating that the greatest changes in the UHI during heatwaves occur when the UHI is typically at its warmest (Figure 4.1b, d, and f; Oke et al. 1991; Coutts et al. 2010; Loughnan et al. 2013).
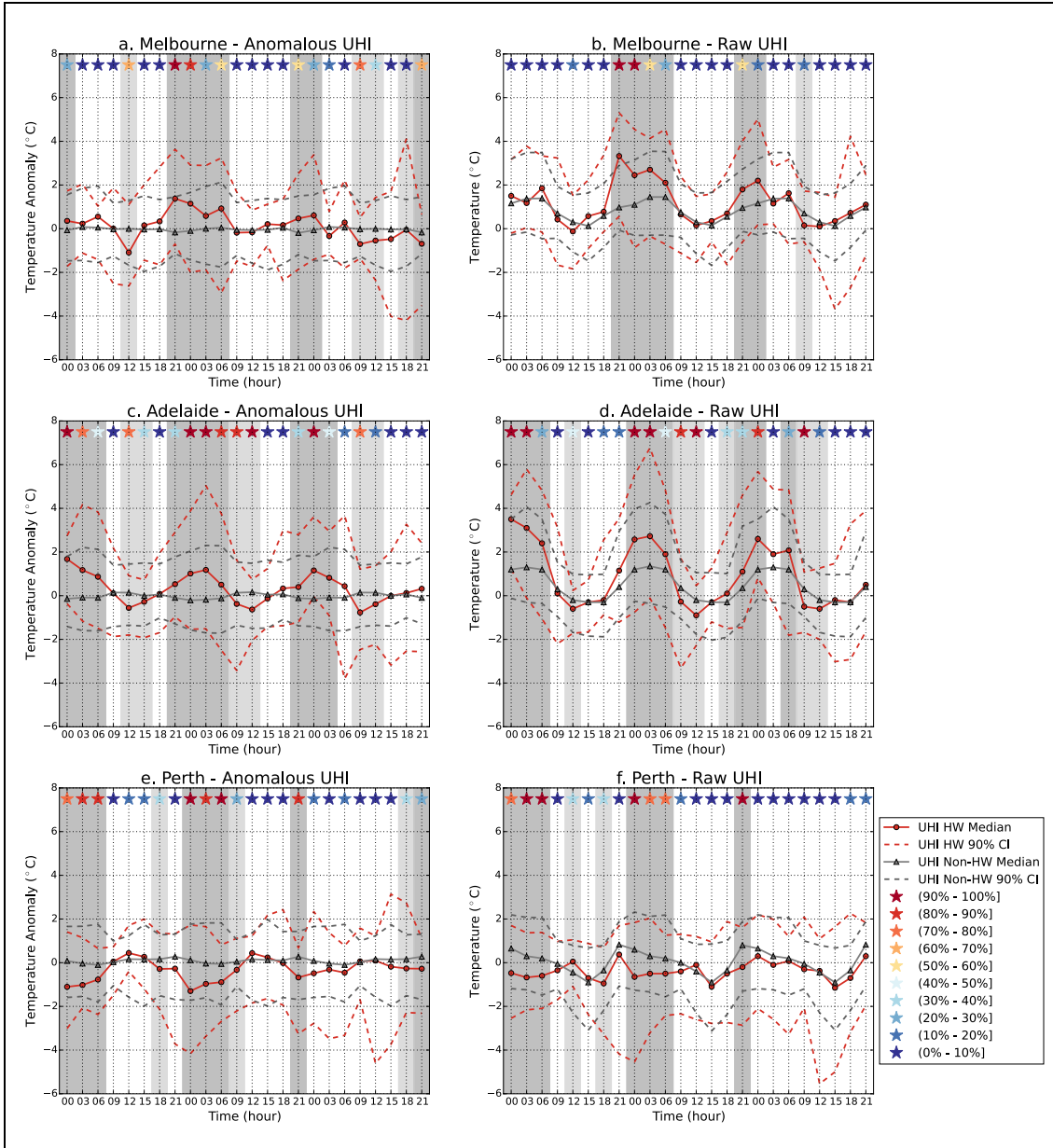
Figure 4.1: Solid red lines show the median urban heat island (UHI) over all heatwave (HW) events that occur during the extended summer season from January 1995 to March 2014. Solid grey lines show the median UHI during non-heatwave events. Solid lines in the figures in the left column show the temporal progression of the median anomalous UHI for a) Melbourne, c) Adelaide, and e) Perth. Solid lines on the figures in the right column show the temporal progression of the median raw UHI for b) Melbourne, d) Adelaide, and f) Perth. The x-axis gives the time of day over the first, middle, and final days of heatwaves in each city in three-hourly increments. Dashed lines show the 90 % confidence intervals (CI). Areas shaded dark grey (light grey) show time-steps during the night (day) where the UHI distribution during heatwaves is significantly different to that during non-heatwave events, where alpha equals 0.05 ($KS_1$). The UHI is calculated as the difference between urban stations (urban and urban fringe stations) and rural stations in Melbourne (Adelaide and Perth). Coloured stars show the percentage of randomly sampled non-heatwave UHI datasets that are significantly different to the heatwave UHI data ($KS_2$), thus higher percentages indicate more significant results, see legend for colour scale.

$KS_1$ and $KS_2$ (as described in Section 4.3.1) show strong agreement as to which time-steps are or are not significantly different between heatwave and non-heatwave conditions (Figure 4.1). The high agreement between the two methods shows that our

results are robust. As there is consistency in the two methods of measuring significance, hereafter, we describe statistical significance using $KS_1$ only.

Although all cities show statistically significant differences in the UHI anomaly at night between heatwave and non-heatwave conditions, the magnitude and sign of the UHI anomalies differs between cities. Melbourne and Adelaide show similar temporal patterns, where urban-rural temperature differences are amplified at night during heatwave conditions (Figure 4.1a and c), that is, the UHI is warmer than is typical for non-heatwave conditions.

Melbourne (Adelaide) typically experiences a raw UHI with a magnitude of up to 3.3˚C (2.7˚C) on the first nights of the heatwaves, and up to 2.2˚C (2.6˚C) on the middle nights (Table 4.1 and Figure 4.1b and d). A typical raw UHI at night during non-heatwave conditions is 1.4˚C (1.3˚C) in Melbourne (Adelaide), and so these enhanced urban temperatures correspond to an UHI anomaly that is warmer than during non-heatwave conditions by up to 1.4˚C (1.2˚C) on the first nights, and 0.6˚C (1.2˚C) on the middle nights (Table 4.1 and Figure 4.1a and c).

The UHI during the day also differs between heatwave and non-heatwave periods. A significantly negative anomalous UHI is evident in Melbourne (Adelaide) for the first and final days (all days) of the heatwave (Figure 4.1a and c). During heatwaves, the UHI anomaly reaches a minimum of -1.1˚C and -0.8˚C in Melbourne and Adelaide respectively (Table 4.1 and Figure 4.1a and c).

Cities typically experience minima in the UHI during the day due to greater heating rates in rural areas than in urban areas (Oke 1982). The above-mentioned negative anomalies suggest that the difference in the heating rates between the urban and rural areas is enhanced during heatwaves. This is evident by the steeper negative UHI gradients in Figure 4.1b and d between approximately 06:00 and midday. The

negative gradient (present during both heatwave and non-heatwave periods) shows that the rural stations heat up faster in the mornings than the urban stations, and the steeper negative gradient during heatwaves shows that this effect is enhanced during heatwaves, i.e. the heating rate at the rural stations has increased more than that at the urban stations, thus causing the negative UHI anomalies in Figure 4.1a and c.

| | | UHI size | | |
|---|---|---|---|---|
| | | Melbourne | Adelaide | Perth |
| Heatwave | First days | -0.1˚C – +0.8˚C (-1.1˚C – +0.3˚C) | -0.6˚C – -0.2˚C (-0.6˚C – +0.1˚C) | -1.0˚C – 0.0˚C (-0.3˚C – +0.4˚C) |
| | First nights | +2.1˚C – +3.3˚C (+0.6˚C – +1.4˚C) | +1.2˚C – +2.7˚C (+0.5˚C – +1.2˚C) | -0.7˚C – +0.4˚C (-1.3˚C – -0.3˚C) |
| | Middle days | +0.1˚C – +0.7˚C (-0.2˚C – +0.2˚C) | -0.9˚C – +0.1˚C (-0.6˚C – +0.3˚C) | -1.1˚C – -0.1˚C (-0.3˚C – +0.4˚C) |
| | Middle nights | +1.1˚C – +2.2˚C (-0.3˚C – +0.6˚C) | +1.1˚C – +2.6˚C (+0.4˚C – +1.2˚C) | -0.2˚C – +0.3˚C (-0.7˚C – -0.3˚C) |
| | Final days | +0.1˚C – +0.2˚C (-0.7˚C – -0.5˚C) | -0.6˚C – -0.5˚C (-0.8˚C – -0.4˚C) | -0.4˚C – -0.3˚C (+0.1˚C) |
| Non-Heatwave | Day | +0.1˚C – +0.8˚C (-0.1˚C – 0.0˚C) | -0.3˚C – +0.3˚C (0.0˚C – +0.2˚C) | -0.9˚C – 0.0˚C (0.0˚C – +0.2˚C) |
| | Night | +0.9˚C – +1.4˚C (-0.2˚C – 0.0˚C) | +0.3˚C – +1.3˚C (-0.2˚C – -0.1˚C) | +0.2˚C – +0.8˚C (-0.1˚C – +0.3˚C) |

Table 4.1: The range of the median urban heat island (UHI) for raw (no brackets) and anomalous (brackets) UHIs in Melbourne, Adelaide, and Perth for the duration of the heatwaves. For raw UHIs, a positive value represents a positive UHI, whereas a negative value represents an urban cool island. For anomalous UHIs, a positive value represents an exacerbated UHI, whereas a negative value represents a diminished UHI. UHI values during non-heatwave events are given at the bottom of the table to allow for comparison of non-heatwave and heatwave UHI strengths. For clarity, rows with night-time UHI values have been shaded.

The above-mentioned change in heating rates could be caused by rural areas potentially being drier than normal prior to heatwave events, which is typical of heatwaves in southern Australia (Gibson et al. 2017c). These dry conditions can reduce the amount of incoming short-wave radiation partitioned into latent heat, and increase that partitioned into sensible energy, thus increasing temperatures (Alexander 2011). On the other hand, urban areas are unlikely to experience an equal amount of drying since they tend to be fairly dry most of the time due to their impervious surfaces causing

rapid runoff, e.g. via storm water systems (Coutts et al. 2013). However, if the urban areas are affected by irrigation systems, this may cause urban areas to be moister during these irrigation periods. This hypothesis may explain why urban stations do not experience the same increases in heating rates as the rural stations.

Another change exhibited by the UHI during heatwaves during the day is a shift in the minima of the raw UHI. During non-heatwave events, Melbourne and Adelaide both experience minima in raw UHI magnitude in the afternoon, with Melbourne (Adelaide) experiencing minima at 15:00 (15:00 and 18:00), see Figure 4.1b and d. However, during heatwaves both cities experience minima in raw UHI magnitude at midday, three to six hours earlier than normal (Figure 4.1b and d). This tends to indicate that while rural areas are still warming faster than urban areas in the morning, the storage of heat in urban structures is at its maximum earlier than normal and thus the heating rates in urban areas become greater than those in rural areas earlier than during non-heatwaves.

Unlike Melbourne and Adelaide, the typical UHI anomaly in Perth is 1.3°C and 0.7°C cooler on the first and middle nights of the heatwave respectively, when compared to non-heatwave events (Table 4.1 and Figure 4.1e). Perth's raw UHI does not vary much during both day and night-time periods of the heatwaves, fluctuating between -1.1°C (i.e. an UCI) and 0.4°C (see Figure 4.1f). This results in a range in the raw UHI of 1.5°C, a much smaller range than for either Melbourne (3.4°C) or Adelaide (3.6°C).

Thus, during heatwave conditions, Perth's UHI does not behave like a typical UHI, which is positive and strongest at night (Coutts et al. 2010; Loughnan et al. 2013). This finding is in contrast to past research by Li and Bou-Zeid (2013), Fenner et al. (2014), Heaviside et al. (2015), and Li et al. (2015), amongst others, who examine the

UHI during heatwaves or extremely hot days in various cities around the world. None of these papers find the existence of a diminished UHI during heatwaves/hot days. The only paper to identify a diminished UHI during extreme heat events is that of Scott et al. (2018), who showed that UHIs were typically diminished during single-day heat events in various cities in the USA. The cities that showed the most strongly diminished UHIs were mainly located in the southwest of the country (see Figure 1.2).

Until now we only discuss the median raw and anomalous UHIs for each city. The 90 % confidence intervals in Figure 4.1 show there is more variability in the strength of the UHI during heatwaves than during non-heatwaves. However, the change in the spread of the confidence interval is not consistent over the duration of the heatwaves.

For all three cities, the largest changes in the confidence intervals generally occur at night-time, coinciding with the time of day when the UHI is strongest (Oke et al. 1991; Coutts et al. 2010; Loughnan et al. 2013), and when the difference between the UHI anomalies during heatwave and non-heatwave conditions is greatest (Figure 4.1a, c, and e). This demonstrates that the strength of the UHI during heatwaves is most uncertain at night. We define extreme UHIs as those greater or smaller than the 95th and 5th percentiles of all UHIs respectively. The thresholds for these extreme UHIs will now be discussed.

Night-time UHI events in Melbourne and Adelaide, which are generally exacerbated during heatwaves, show an upward shift in the 95th percentile (Figure 4.1b and d). In Melbourne (Adelaide), the 95th percentile of UHI anomaly strength during heatwaves is up to 3.6˚C (5.0˚C) larger than the median of non-heatwave events (Figure 4.1a and c). This corresponds to a raw UHI magnitude of up to 5.3˚C (6.8˚C) in Melbourne (Adelaide) during heatwaves (Figure 4.1b and d). During non-heatwaves,

the 95<sup>th</sup> percentile of the raw UHI in Melbourne (Adelaide) is much weaker, with strengths of up to 3.5˚C (4.3˚C) (Figure 4.1b and d).

While the 95<sup>th</sup> percentile of the UHIs is greater during heatwaves, Melbourne sees little change in the 5<sup>th</sup> percentile of UHI strengths (Figure 4.1b), showing that the threshold of extremely cool UHIs during heatwaves remains much the same as during non-heatwaves.

Adelaide experiences a noticeable downward shift in the 5<sup>th</sup> percentile of anomalous UHI strength from 06:00 to 12:00 on middle and final days of the heatwaves (Figure 4.1c). It is important to note that while Adelaide does experience these downward shifts in the 5<sup>th</sup> percentile in the mornings, they are smaller than the upward shifts in the 95<sup>th</sup> percentile at night.

Conversely, UHI events in Perth, which are mainly diminished, show little change in the 95<sup>th</sup> percentile of anomalous UHI strength, but a noticeable downward shift in the 5<sup>th</sup> percentile at night (Figure 4.1e).

These findings show that all three cities experience the greatest increase in the strength of extreme UHI thresholds at night, with the direction of change (i.e. an upward/downward shift in the 95<sup>th</sup>/5<sup>th</sup> percentile of the anomalous UHI) being consistent with changes in the median of the time series (Figure 4.1). For example, Melbourne experiences a positive increase in the strength of the UHI at night during heatwaves, and also experiences an increase in the threshold of extremely warm UHIs at night during heatwaves when compared to non-heatwave events (Figure 4.1a).

To summarise, Figure 4.1 shows that at night, a typical UHI during heatwaves (the median of the time series) is exacerbated in Melbourne and Adelaide but diminished in Perth, when compared to non-heatwaves. The 90 % confidence intervals show a larger spread at night during heatwaves, and hence there is more variability and

more uncertainty in the value of the UHI. However, at night there is more certainty surrounding the direction of the change in UHI strength than in the magnitude of the strength, with Melbourne and Adelaide most likely to experience a positive UHI anomaly (i.e. a warmer than normal UHI), and Perth most likely to experience a negative UHI anomaly (i.e. cooler than normal UHI).

From Figure 4.1a, c, and e, we see that all three cities experience a combination of exacerbated and diminished UHIs during heatwaves when compared to non-heatwave periods. To further investigate the characteristics of the UHI during heatwaves we examine the variability in the strength of the UHI in more detail. All UHI data outside heatwave periods are binned into quintiles, defined as strongly exacerbated ($\geq 80^{th}$ percentile), moderately exacerbated ($60^{th} – 79^{th}$ percentiles), normal ($40^{th} – 59^{th}$ percentiles), moderately diminished ($20^{th} – 39^{th}$ percentiles), and strongly diminished events ($< 20^{th}$ percentile). The heatwave data are also partitioned using the temperature thresholds from the above-mentioned categories (Figure 4.2).

The frequency of occurrence of each UHI category differs for each city (Figure 4.2). As in Figure 4.1, Figure 4.2 shows that exacerbated events are most common in Melbourne and Adelaide at night during heatwaves, whereas UHI events in Perth are frequently diminished. Figures 4.1 and 4.2 both show that the greatest changes in the UHI between heatwave and non-heatwave conditions are observed at night.

Melbourne and Adelaide both show a similar temporal distribution of UHI categories during heatwaves, this is, the UHI is more likely to be exacerbated at night and diminished during the day compared to non-heatwave conditions (Figure 4.2a and b). However, the diurnal pattern is more strongly defined in Adelaide (Figure 4.2b). Adelaide shows a minimum in the number of strongly exacerbated events on the first days at 15:00 (4 % of events are strongly exacerbated). This is followed by an increase

through the afternoon and evening to a maximum of up to 58 % at midnight, which then
decreases again through the following morning (Figure 4.2b). This pattern continues
for the duration of the heatwaves. Melbourne shows a similar pattern until midnight on
the middle nights of the heatwave. After this time, the pattern is less distinctive (Figure
4.2a).
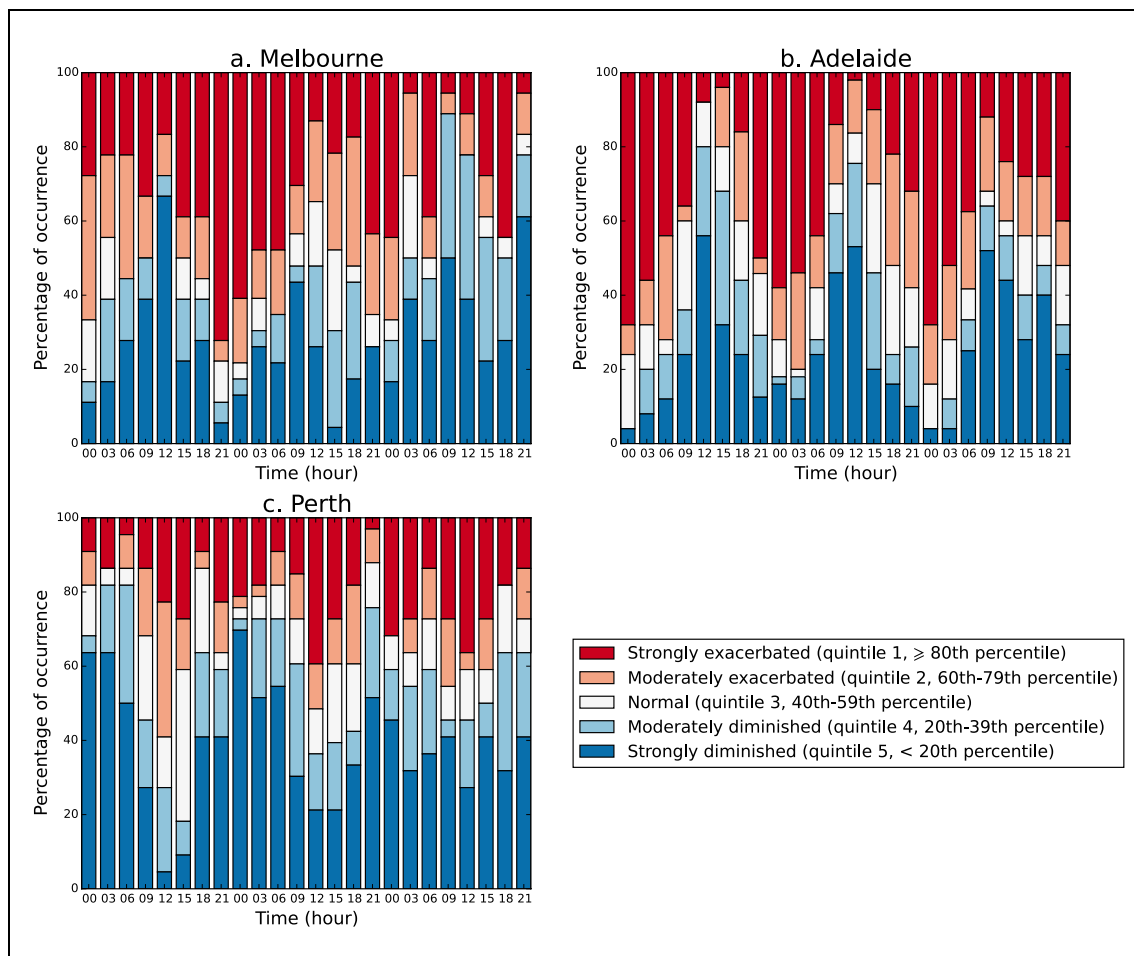


Figure 4.2: Percentage of occurrence of strongly exacerbated (dark red), moderately exacerbated (pink), normal
(white), moderately diminished (light blue), and strongly diminished (dark blue) urban heat island events during
heatwaves in a) Melbourne, b) Adelaide, and c) Perth. The x-axis gives the time of day over the first, middle, and
final days of heatwaves in each city.

In both cities, these patterns are indicative of a stronger UHI signal during
heatwaves compared to non-heatwave periods. This is further illustrated by comparing
UHIs that are broadly categorized as warmer than normal, or exacerbated, comprising
both the moderately exacerbated and strongly exacerbated categories in Figure 4.2.

These exacerbated UHIs account for up to 78 % (84 %) of heatwaves at midnight in Melbourne (Adelaide).

Perth also shows a clear diurnal pattern for the duration of the heatwaves, but one that is out of phase with Melbourne and Adelaide; that is, with mostly diminished UHIs during the night and normal or exacerbated UHIs during the day. Perth shows a minimum in the number of strongly diminished events at midday (5 % and 21 % on the first and middle days respectively), and a maximum at midnight on the first nights of the heatwaves (70 %) and at 21:00 on the middle nights (52 %), see Figure 4.2c.

If the characteristics of the UHI are the same during heatwave and non-heatwave conditions, then approximately 20 % of the heatwave data should fall into each of the pre-defined categories. However, all three cities show a tendency to produce UHIs that are disproportionately different to normal over the duration of the heatwaves (Figure 4.2). That is, the proportions of data in the strongly exacerbated/diminished and moderately exacerbated/diminished categories are inconsistent with the expected values, with each of the cities experiencing more strong events, than moderate events.

This suggests that there is more variability in the strength of the UHI during heatwaves than during non-heatwaves. For example, over all days of a heatwave, the UHI in Melbourne falls into either of the strong categories (31 % for strongly exacerbated and 28 % for strongly diminished events) more frequently than the moderate categories (18 % for moderately exacerbated and 16 % for moderately diminished). Similar patterns are experienced in Adelaide and Perth. This further demonstrates the strong relationship between heatwaves and UHI strength.

The evidence presented here shows that the magnitude of the UHI during heatwaves is stronger than during non-heatwave conditions, and that UHIs can be both exacerbated or diminished compared to non-heatwave conditions. This finding is

particularly noticeable at night during heatwaves when both the thresholds of extreme UHIs and changes in the median UHI are the greatest.

**4.4.2 Factors influencing the strength of the urban heat island**

In Section 4.4.1 we present evidence of a relationship between heatwaves and UHI strength. The assumption in this analysis so far is that the observed changes in the UHI are primarily due to differences between urban and rural land surfaces. However, other factors affect the weather stations used in the UHI calculation, such as proximity to the coast, local geography and localised microclimates might also play a role in producing the temperature differences between urban and rural stations, and the subsequent strength of the UHI we present in Section 4.4.1.

First, individual stations are examined to determine whether particular station idiosyncrasies affect the results in Section 4.4.1, for example, unique topographic or geographically induced features such as proximity to water bodies or station elevation. A leave-one-out sensitivity analysis is performed (not shown) that systematically removes each of the stations in every city and recalculates the UHI using the remaining stations only. While the removal of each station sometimes alters the magnitude of the UHI, the characteristic pattern of the UHI during heatwaves, described in detail in Section 4.4.1, remains consistent across all three cities.

As this research employs established weather stations, not all station locations are ideal for the examination of the UHI. Some stations are located relatively close to the coast and therefore are potentially affected by the advection of cool coastal air, influencing the strength of the UHI.

As described previously in Section 4.3.2, both concurrent (lag 0) and lagged winds (lag 3 and lag 6) are examined here because we hypothesise that winds during

the afternoon could have a lasting effect on night-time temperatures and hence, UHI strength. We only examine the effect of the wind on UHI strength at night because this is when the UHI effect is strongest, and when heatwave associated changes in the UHI are greatest.

The potential relationships between city-wide UHI anomaly strength, and wind speed and direction are examined by performing statistical analysis for each station in each city. We examine $p$-values, Pearson correlation coefficients ($r$), explained variances ($r^2$), and median UHI anomalies to determine any meaningful relationships. We examine lag 0 (Figure 4.3, selected stations only), lag 3, and lag 6 (not shown) in all three cities. These statistics are provided in full in Tables A1 to A6 in Appendix A. The selected statistics of interest are discussed below.

We also examine the relationship by plotting wind speed and wind direction at each station against city-wide UHI anomaly strength for lag 0 (Figure 4.3, selected stations only). A strong and significant relationship between city-wide UHI strength and wind speed and/or wind direction at a particular station indicates that that station is strongly weighting the UHI calculation. Clusters of exacerbated or diminished UHI anomalies (clusters of particular colours) in Figure 4.3 would identify this relationship. However, this is not evident in our results.

There is no clear relationship between UHI anomaly strength and wind speed and/or direction for lag 6 in any city (not shown). No stations in Melbourne show a significant relationship between wind speed and/or direction and UHI strength for lag 0 or lag 3, however significant relationships are present for both Adelaide and Perth.

Adelaide shows only one station with significant relationships between wind speed and/or wind direction and UHI anomaly for lag 0. Adelaide Airport, an urban
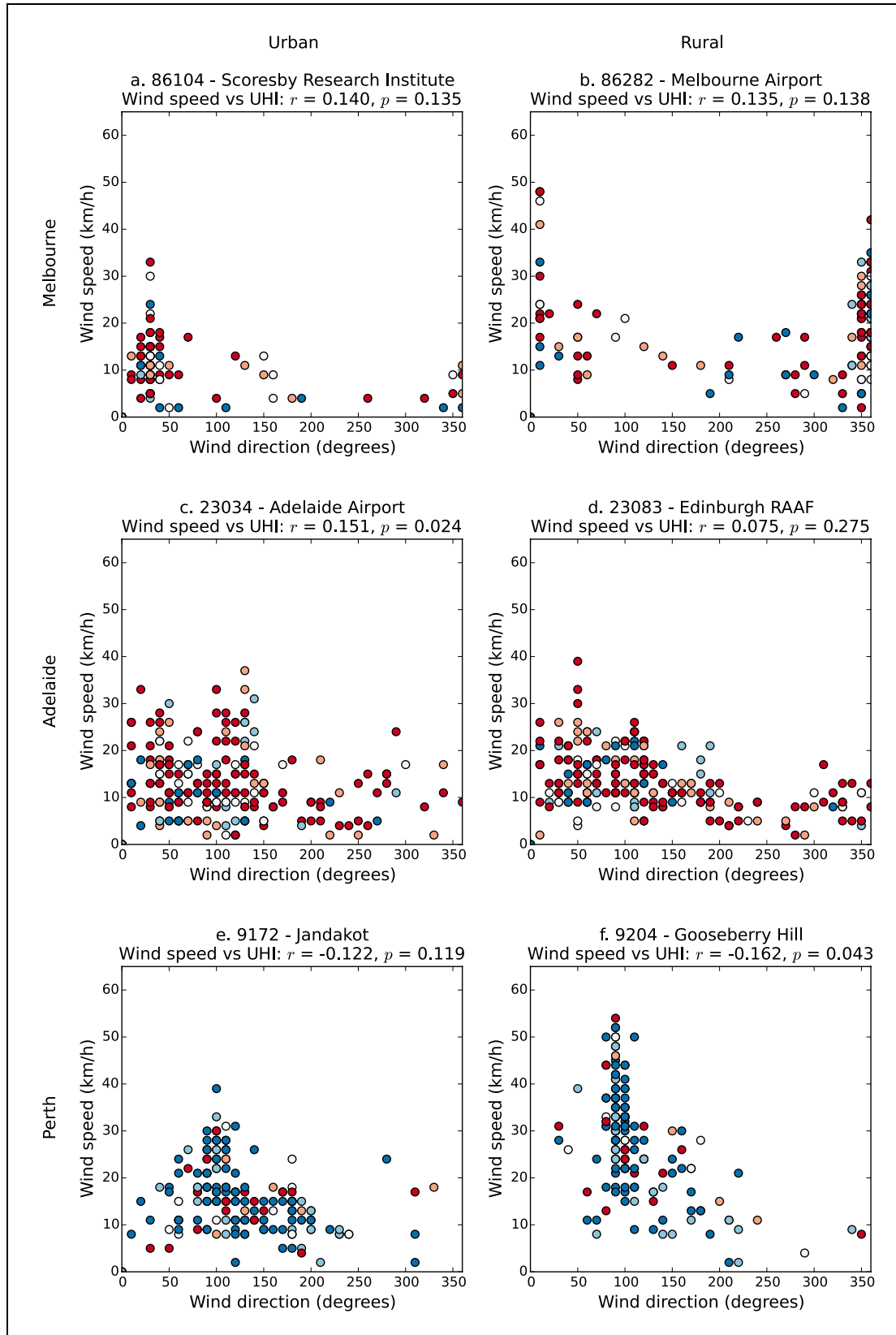
Figure 4.3: Wind speed and wind direction for the anomalous strength of the urban heat island (UHI) (colours) at time lag 0 for urban stations (left) and rural stations (right) in Melbourne (top row), Adelaide (middle row), and Perth (bottom row). One urban and one rural station are shown as representatives for each city. The correlation ($r$) between the station wind speed and city-wide UHI, and its associated $p$-value, is provided with $p < 0.05$ considered significant. As in Figure 4.2, colours represent UHIs that are strongly exacerbated (dark red), moderately exacerbated (pink), normal (white), moderately diminished (light blue), and strongly diminished (dark blue), see Figure 4.2 legend.

station, shows a significant relationship between UHI strength and both wind speed ($p = 0.02$, $r = 0.15$), and wind direction ($p = 0.03$), whereby the UHI anomalies warm with increasing wind speed, and are approximately 0.3˚C cooler when winds are easterly. However, despite the significance, this correlation is very weak to be considered near meaningless as the station explains only around 2 % of the variability in the anomalous UHI.

Similarly, for lag 3, two urban stations show a relationship between wind speed and UHI anomaly strength, these stations are Adelaide (Kent Town) ($p = 0.04$, $r = 0.23$), and Adelaide Airport ($p = 0.02$, $r = 0.26$), whereby increasing wind speed is associated with warmer UHI anomalies. One station, Adelaide (Kent Town), also shows a relationship between wind direction and UHI anomaly ($p = 0.02$), whereby Adelaide experiences a reduction in the UHI anomaly of about 0.3˚C when winds are westerly. It is important to note that the sample size at this station for westerlies is quite small ($n = 21$). As for Melbourne, although the relationships are significant, the correlations are weak, suggesting that any influence of wind speed and/or direction is relatively small.

The small explained variances for relationships with wind speed (maximum of 7 %) suggest that wind speed is not a large contributor to UHI anomaly strength. Since wind direction has a weak relationship with UHI anomaly (maximum decrease in the UHI anomaly of 0.3˚C), and since the relationship between wind direction and UHI anomaly causes a cooler UHI anomaly while Adelaide's UHI during heatwaves is typically warmer than during non-heatwaves, we can conclude that this relationship is not the main driver of the exacerbated UHI in Adelaide during heatwaves.

As for Adelaide, Perth has one station, Gooseberry Hill, with a significant relationship between wind speed and UHI anomaly for lag 0 (rural, $p = 0.04$, $r = -0.16$).

On the other hand, all stations except one (Jandakot Aero, urban) show significantly cooler UHI anomalies during easterlies, and three stations (Pearce RAAF, Perth Airport, and Perth Metro) show significantly warmer UHI anomalies during southerlies.

It is important to note that UHI anomalies are at their coolest when winds are from the east, however all wind directions experience negative median UHI anomalies (excluding wind directions with fewer than 20 samples), showing that the UHI in Perth during heatwaves is generally diminished regardless of wind direction.

Lag 3 shows no significant relationships between wind direction and UHI anomalies in Perth, but three stations show a significant relationship with wind speed, whereby stronger wind speeds are associated with cooler UHIs. These stations are Gingin Aero (rural), Jandakot Aero (urban), and Perth Metro (urban). Again, since these relationships are weak (at most 10 % of the explained variance), we can assume that this is not a large driver of UHI strength during heatwaves.

The above results imply that wind speed and wind direction are not the main drivers of UHI strength in Perth during heatwaves. This conclusion is drawn for two main reasons; first, while wind direction can affect the strength of the UHI anomaly, it does not affect the sign, and second, the wind speed relationships are weak and do not account for more than 10 % of the explained variance.

It is well documented that one of the major influences on Perth's afternoon and evening temperatures during summer is the presence of the 'Fremantle Doctor', a strong afternoon westerly sea breeze (e.g. Williams et al. 2012b). This phenomenon is expected to affect urban temperatures and the strength of the UHI during heatwaves, but due to the lack of any relationship between UHI anomaly strength and westerly

winds for lag 3 or lag 6, we can assume that the Fremantle Doctor is not having a significant effect on UHI strength at night during heatwaves.

Ramamurthy and Bou-Zeid (2017) show a change in wind direction from southerly (sea-breeze) during non-heatwaves to westerly during heatwaves is responsible for the exacerbated UHI during heatwaves in New York City. However, our results show this is not the case in Perth, highlighting the geographic differences in how UHIs operate.

Since all of Perth's urban stations are located close to the coast, relative to the rural stations, it might be assumed that the ocean has a strong moderating effect on urban station temperatures in Perth; potentially causing the diminished UHI at night during heatwaves. However, since we do not see the same effect in Adelaide, which also has all its urban stations located relatively close to the coast, this suggests that the ocean is unlikely to explain the diminished UHI in Perth.

The above-mentioned relationships show that while wind speed and direction can have a small effect on UHI anomaly strengths, they are unlikely to be a substantial modulator of the behaviour of the UHI during heatwaves in any of the three cities. Wind speed and direction are also unable to explain why Perth's UHI anomaly patterns are contradictory to those of Melbourne or Adelaide.

## 4.5 Discussion

This research quantifies the strength of the UHI during the extended summer season in Melbourne, Adelaide, and Perth, and provides robust evidence that the typical strength of the UHI changes significantly during heatwaves when compared to non-heatwave periods. We show that typical night-time UHIs in Melbourne and Adelaide are warmer during heatwaves by up to 1.4˚C and 1.2˚C respectively, when compared

to non-heatwaves. Conversely, in Perth, a typical UHI during heatwaves is 1.3˚C cooler than under non-heatwave conditions. Modelling studies would be required to determine the precise mechanisms for the exacerbated UHI in Melbourne and Adelaide, which is beyond the scope of this study.

Our results are comparable to past studies. Here, we calculate the typical raw UHI strength for Melbourne as 1.4˚C during non-heatwaves, which is comparable to that calculated by Morris and Simmonds (2000) for the entire year (0˚C to 2˚C for 75 % of days examined), despite the fact that different stations are used to calculate the UHI.

In Adelaide, Soltani and Sharifi (2017) identified a median UHI of 5.41˚C at midnight in winter using a transect study. This study calculated Adelaide's UHI as the difference between temperature measurements taken from a vehicle and the BoM's Roseworthy AWS. This study's identification of an UHI of 5.41˚C is far greater than that calculated in this thesis (1.3˚C), but it must be noted that since Soltani and Sharifi (2017) examine the UHI in winter and had greater geographic coverage of the city than is possible from the AWS data. Both aspects might explain why their calculation of the UHI is greater than determined here.

The presence of an intra-urban heat island has previously been detected in Adelaide by Erell and Williamson (2007), and Guan et al. (2013). Erell and Williamson (2007) argue that the calculation of the UHI in Adelaide using methods similar to those used for this research (i.e. by calculating the UHI as the temperature difference between urban and rural stations) is not realistic due to Adelaide's topography and the lack of an appropriate rural station.

At 3.1˚C to 4.8˚C (depending on station choice), the average night-time intra-urban heat island of Erell and Williamson (2007) is over double that calculated here for non-heatwaves (1.3˚C), but the calculation of a 1.5˚C intra-urban heat island by Guan

et al. (2013) compares well. The large differences between our UHI value and those of Erell and Williamson (2007) are likely due to differences in station selection, data sources, and seasons and time scale examined. While Erell and Williamson (2007) argue that rural stations in Adelaide are not suitable for calculating the UHI, the similarity between our calculation of the UHI and that of Guan et al. (2013), and to a lesser degree Erell and Williamson (2007), suggests that our method for determining Adelaide's UHI is sound. To our knowledge, no previous study has quantified the UHI in Perth.

The consistency between the estimates of the UHIs here compared to past studies provides further evidence that the AWSs selected highlight real temperature differences between urban and rural areas. Section 4.4.2 shows that local meteorological effects (e.g. continental winds) do not have a large effect on the regulation of the UHI during heatwaves in all three cities. This points toward an enhancement of the typical UHI process in Melbourne and Adelaide; whereby there is a significant role of urban surfaces storing and re-emitting more thermal energy compared to the surrounding rural landscapes (Oke et al. 1991). This enhancement is illustrated as an amplification of the UHI compared to non-heatwave conditions.

This finding suggests that there may be an increased ability to mitigate the UHI, and hence heatwave temperatures, through urban design features such as green roofs (Berardi et al. 2014), or the addition of more vegetation to the urban landscape (Fallmann et al. 2013; Zhang et al. 2014a).

Interestingly, the behaviour of the UHI in Perth during heatwaves, this is, that it is diminished compared to a normal UHI, has not yet been reported in the literature. Only two previous papers have shown anything other than an exacerbated UHI during heatwaves. The first is that of Zhou and Shepherd (2010) who found that the UHI in

Atlanta was not significantly different during heatwaves compared to non-heatwaves, when calculating the UHI as the difference between an urban station and a hybrid (non-rural) station. The second paper to find no significant differences in the UHI during heatwave and non-heatwave conditions was Ramamurthy and Bou-Zeid (2017), who examined UHI strength in small cities (all with populations of about 10 % of Perth's or less).

No research has identified a diminished UHI during heatwaves. However, one study does show that UHIs can be cooler during single-day heat events. Scott et al. (2018) found the UHI in multiple cities in the USA to be cooler than those prior to the heat event. Interestingly, this research found that the cities with the coolest UHIs during heat events were located in California, i.e. on the southwest coast. This is a geographically similar location to Perth, which we find often shows an UCI during heatwaves, with a median raw UHI of -0.7˚C at 00:00 on the first night of heatwaves (see Table 4.1 and Figure 4.1f). We do not suggest any mechanism to explain the similarity in the relative location of these cities, but this could suggest a further avenue for research.

Given that the UHI behaves differently in Perth compared to Melbourne, Adelaide, or any of the other studies mentioned throughout this chapter, it is important to take into account factors other than urban form that might affect the strength of the UHI. Many factors influence station temperatures, yet ideally when we calculate the UHI, the only variable that should change from urban stations to rural stations is the degree of urbanisation.

Even though we take steps to reduce the influence of other variables on temperature, for example by using anomalous data to reduce the effects of station elevation, and by undertaking a leave-one-out sensitivity analysis, we acknowledge that

some local factors cannot be easily extracted from the data and might still be affecting the UHI calculations; for example, micro and mesoscale meteorology (e.g. cool air drainage from mountains). Such factors are a major limitation to urban research seeking to characterise long-term climatological studies on the UHI. The siting of stations is also not ideal as, often, permanent meteorological stations are specifically designed to minimise any urban signal (Bureau of Meteorology 1997). Thus, many urban and urban fringe stations are purposefully sited close to large, green spaces (e.g. Moorabbin Airport and Perth Metro), reducing the influence of urban areas on the stations, potentially leading to an underestimation of the strength of the UHI.

Modelling over Melbourne has shown that the strength of the UHI is sensitive to soil moisture (Jacobs et al. 2017). While heatwaves in southern Australia tend to be dry, we cannot rule out the possibility that soil moisture has an effect on UHI strength during heatwaves. Soil moisture has also been found to have a relationship with Australian heatwave intensity and duration (Herold et al. 2016), again suggesting that soil moisture might affect our results. If there is some discrepancy in soil moisture amount between urban and rural areas during heatwaves, this may be reflected in the UHI strength. Soil moisture is likely to be naturally very low during heatwave events in the extended summer season, as little rainfall is associated with these events (not shown). There is also likely to be a period of hot, dry weather preceding the heatwaves, leading to very dry soils. On the other hand, watering and irrigation of gardens and lawns in urban areas, i.e. by councils and residents, has the potential to increase latent heat and therefore reduce sensible heat in the city (Broadbent et al. 2018a; Broadbent et al. 2018b). Research into water use and irrigation schemes in Perth may explain whether this is likely to go some way to explaining why the relationship between heatwaves and the UHI in Perth is contradictory to those in Melbourne and Adelaide.

Further, Ramamurthy and Bou-Zeid (2017) found evidence that soil moisture deficit is the most likely cause of the exacerbation of the UHI in two cities in the USA (Washington and Baltimore). These cities experienced an increased drying rate in urban areas compared to rural areas during heatwaves. On the other hand, the authors found that two cities whose urban areas were already much drier than rural areas during non-heatwave conditions (New York and Philadelphia) did not see much change in drying rates between heatwave and non-heatwave periods. These two cities therefore did not see a change in the relationship between soil moisture and UHI strength during heatwaves.

This study by Ramamurthy and Bou-Zeid (2017) shows that the influence of soil moisture on UHI exacerbation during heatwaves is dependent on urban-rural soil moisture differences during non-heatwave events. These geographical differences suggest the question must be asked for each city, does the urban-rural drying rate change during heatwaves? Since southern Australian cities tend to be fairly dry during the extended summer season, drying rates may not change much from non-heatwave to heatwave periods, thus soil moisture may not strongly influence UHI exacerbation. However, this is an important future research direction. Also, since Ramamurthy and Bou-Zeid (2017) did not show any case where the UHI was diminished during heatwaves, changes in soil moisture during heatwaves may not be able to explain why UHIs in Perth are diminished during heatwaves. More research is required to confirm or disprove this hypothesis but is outside the scope of this study.

Another limitation of this study is the number of stations used. While it is preferable to include as many AWSs as possible to accurately capture the characteristics of the cities, selected stations are excluded due to changes in urbanisation at the given station over time (e.g. Laverton AWS in suburban Melbourne), or opening/closing dates

that we deemed too late/early for our purposes (e.g. Viewbank AWS in suburban Melbourne). Other stations are excluded due to suboptimal station placement, such as if the station is too close to the coast (e.g. Frankston AWS in suburban Melbourne), or the elevation is too high.

A major limitation of this thesis is the small sample sizes of the heatwave dataset. As we use observed data, and require a number of urban and rural stations to calculate an UHI representative of our three cities, the available data are limited. A number of stations determined the length of our study due to their opening or closing dates, or because they lack reliable data outside the January 1995 and March 2014 period.

Possible solutions to the problem of small sample sizes would be to increase the time period studied by further limiting the number of stations used, or to consider using model data rather than observed data. Both of these solutions are outside the scope of this research. Further, using fewer AWSs would make the measure of UHI strength less reliable as the UHI would be more susceptible to station-specific weather conditions.

While this research characterises the differences in UHI behaviour during heatwave and non-heatwave events, the reasons for this behaviour remain unclear. Moreover, the reasons for the distinct differences between the three cities examined here have not been clearly identified. Modelling studies (e.g. Li and Bou-Zeid 2013; Heaviside et al. 2015) may be able to shed light on the effect the urban form is having on the development of the UHI during heatwaves in Perth. Again, this is outside the scope of this study.

In Melbourne, there is evidence that similar synoptic patterns are associated with both strong UHIs and heatwaves in Melbourne. Specifically, Morris and Simmonds (2000) show that the warmest UHIs in Melbourne are associated with

surface high-pressure systems in the Tasman Sea off the southeast coast of Australia. Similarly, Pezza et al. (2012) show that heatwaves in Melbourne are associated with similarly located surface high-pressure systems. Research presented later in this thesis investigates synoptic-scale patterns in Melbourne, Adelaide, and Perth, in order to determine if and how these are associated with both heatwave days and strong UHIs.

## 4.6 Conclusions

This research demonstrates that the UHI is characteristically different during heatwave conditions in three southern Australian cities with broadly similar climates. In Melbourne and Adelaide, the diurnal cycle of a typical UHI is usually exacerbated during heatwaves, resulting in UHIs at night that are warmer than normal and UHIs during the day that are cooler than normal, when compared to non-heatwave periods. Conversely, this diurnal cycle is dampened in Perth and a diminished UHI is evident at night during heatwaves. On the first night of the heatwaves, this typically results in the presence of an UCI in Perth.

Less-than-ideal station locations is a limitation of this study, yet sensitivity testing and comparisons with past studies show that urban-rural temperature differences are well represented by the stations analysed here. Further, it is unlikely that localised factors, such as sea breezes, are affecting the UHI in any of the three cities examined.

The presence of an exacerbated UHI in Melbourne and Adelaide during heatwaves, that is likely due to the urban form, highlights the possibility that urban design strategies could play a role in ameliorating extreme heat. This may have considerable benefits for vulnerable populations that are exposed to heatwaves.

# 5. The relationship between the urban heat island, heatwaves, and synoptic patterns in southern Australian cities

## Abstract

This chapter examines the synoptic weather patterns that occur with urban heat islands (UHIs) to determine whether particular synoptic conditions show a relationship with the strength of the UHI. We find that strongly exacerbated and diminished UHI events tend to occur under particular synoptic conditions that are unique to each city.

Further, we examine the coincidence of synoptic conditions during heatwaves and strong UHIs to determine whether there is evidence that the overlying synoptic conditions play a significant role in modulating the strength of the UHI during heatwaves, as identified in Chapter 4. We show that while certain synoptic patterns occur during both heatwave and strong urban heat island events, the presence of the heatwave appears to be a stronger influence on UHI strength than the overlying synoptic pattern.

Finally, we examine factors, including meridional and zonal wind components, and UHI persistence, in order to detect any relationships with the strength of the UHI. However, we show that there is no strong evidence that any of these are strong modulators of the UHI in southern Australian cities.

## 5.1 Introduction

In the previous chapter, we showed that the strength of the urban heat island (UHI) is different during heatwaves compared to non-heatwave conditions in southern Australian cities. Melbourne and Adelaide typically experience an exacerbated UHI, i.e. warmer than normal, whereas Perth typically experiences a diminished UHI, i.e. cooler than normal. However, the reasons why the UHI varies differently with heatwaves for different cities remain unknown. Throughout this chapter we mainly focus on the connection between synoptic conditions and strong UHI events, i.e. strongly exacerbated or strongly diminished UHIs, as these events have the potential to substantially alter urban temperatures.

Globally, most areas identify anticyclonic conditions as being most favourable for an UHI (Beranová and Huth 2005 and references therein). Anticyclonic conditions are relatively stable, with weak winds and often reduced cloudiness (Morris and Simmonds 2000) and precipitation (Hope et al. 2006) and a relatively stable boundary layer (Tong et al. 2005). This promotes thermal storage through radiative loading, and a lack of advection and little to no precipitation prevents removal of heat from urban areas.

Morris and Simmonds (2000) identify synoptic conditions that are associated with differing strengths of the UHI over Melbourne and show that the positioning of the centre of the anticyclone is important to the strength of the UHI. Other studies that also note a relationship between anticyclonic conditions and warmer UHIs include Unwin (1980) and Zhang et al. (2014b) in Birmingham, UK, He et al. (2013) in Changsha, China, Beranová and Huth (2003) in Prague, Czech Republic, Yagüe et al. (1991) in Madrid, Spain, and Unger (1996) in Szeged, Hungary.

Observational studies show that synoptic patterns have a well-established relationship with heatwaves in Melbourne (Pezza et al. 2012; Boschat et al. 2015; Gibson et al. 2017b), Adelaide, and Perth (Pezza et al. 2012; Gibson et al. 2017b). In all three cities, heatwaves are typically associated with high-pressure systems to the southeast of the city; that is, high-pressure systems are located over the Tasman Sea for heatwaves in Melbourne and Adelaide, and over the Great Australian Bight for heatwaves in Perth.

The relationship between the UHI and synoptic patterns has been little studied in Australia. However, one study by Morris and Simmonds (2000) showed that warm UHIs were associated with particular synoptic patterns in Melbourne. Interestingly, the synoptic patterns for which Morris and Simmonds (2000) reported the warmest UHIs in Melbourne strongly resemble those patterns that are most closely associated with heatwaves in Melbourne.

The similarity between the locations of the high-pressure systems associated with both heatwaves and warm UHIs in Melbourne could suggest that the relationship between UHI strength and heatwaves identified in Chapter 4 is, in part, due to pre-conditioning from the overlying synoptic conditions. If this similarity in synoptic patterns can explain the relationship between heatwaves and the strength of the UHI, it may also be able to explain the difference in the heatwave-UHI relationship in Perth as compared to Melbourne and Adelaide.

This work extends that of Morris and Simmonds (2000) and determines the relationships between synoptic patterns and the strength of the UHI over the three Australian cities – Melbourne, Adelaide, and Perth. The synoptic conditions and related UHI during heatwaves are then examined more closely in order to determine any contribution to the exacerbated (diminished) UHIs observed in Melbourne and

Adelaide (Perth) during heatwaves in Chapter 4. Further we examine whether the relationship between synoptic patterns and UHIs in Perth can help to explain why we see mainly strongly diminished UHIs in Perth during heatwaves. Perth is an anomaly in the heatwave-UHI connection, with heatwaves in Melbourne, Adelaide, and most cities where similar research has been undertaken are associated with warm UHIs (e.g. Li and Bou-Zeid 2013; Heaviside et al. 2015; Li et al. 2015).

Here, Synoptic Types over Melbourne, Adelaide, and Perth are generated for the extended summer season in order to examine which Synoptic Types are associated with exacerbated or diminished UHIs (Section 5.4.1). Section 5.4.2 determines which of these Synoptic Types are associated with heatwaves for each of the three cities, and Section 5.4.3 examines whether there are any relationships between all of heatwaves, the UHI, and synoptic patterns.

## 5.2 Data

This chapter builds on the research of Chapter 4 and therefore makes use of the high-quality Bureau of Meteorology's Australian Climate Observations Reference Network – Surface Air Temperature (ACORN-SAT) observational data for heatwave identification as well as the Bureau of Meteorology's Automatic Weather Station (AWS) three-hourly observational data for calculation of UHI strength. The ERA-Interim mean sea level pressure (MSLP) data are used to determine synoptic typings of each city during the extended summer season. A detailed description of all datasets is provided in Chapter 2 of this thesis, and data used in this chapter are briefly described below.

### 5.2.1 ACORN-SAT data

As described in Chapter 2, daily maximum and minimum temperatures from the Bureau of Meteorology's high-quality ACORN-SAT dataset are used to identify heatwaves from the observations for the extended summer season from January 1995 to March 2014. We use the stations closest to the centre of each city which are: Melbourne Regional Office (MRO, #86071), Adelaide (Kent Town, #23090), and Perth Airport (#9021). This is consistent with Chapter 4.

### 5.2.2 Automatic weather station data

As described in Chapter 2, three-hourly dry-bulb temperature data from the Bureau of Meteorology's AWSs in urban and rural locations are used to calculate the strength of the UHI during heatwave periods and the extended summer season in Melbourne, Adelaide, and Perth.

### 5.2.3 ERA-Interim data

Six-hourly ERA-Interim MSLP data are used to determine MSLP patterns for the observational period. We use these data to produce the Synoptic Types used throughout this chapter. ERA-Interim 10 m u and v-wind components are also examined to determine whether the wind may have a differing influence on the strength of the UHI depending on the Synoptic Type.

While the ERA-Interim data are reanalysis data we will refer to these as observational data throughout this work. We perform our analysis on the UHI in this chapter at midnight only. However, since ERA-Interim data are six-hourly in UTC we are unable to get data at midnight for all three cities, we therefore select the data closest

in time to midnight. We make the assumption that there are no significant changes in MSLP patterns and wind components between the times used and midnight.

## 5.3 Methods

This work examines UHIs in Melbourne, Adelaide, and Perth during heatwave periods and during the extended summer season, and relates these to synoptic patterns both individually and together. To examine the synoptic conditions associated with both UHIs and/or heatwaves we employ self-organising maps (SOMs). As described extensively in Chapter 3, SOMs are a clustering algorithm that determines the main nodes of a dataset by grouping the data based on similarities (Kohonen 2014). When working with MSLP data, the nodes correspond to Synoptic Types. Here we apply the SOM algorithms to the ERA-Interim MSLP data (see Chapter 2).

The methods employed in this Chapter are now described where they have not already been provided in Chapter 3.

### 5.3.1 Defining heatwave days

As explained in Chapter 3, heatwave days are defined using a percentile threshold method over an extended summer season (November to March) from January 1995 to March 2014. Subsequently, 18, 25, and 22 heatwaves are detected in Melbourne, Adelaide, and Perth, respectively.

Since this chapter examines the UHI at night, and the heatwave definition states that all nights of the heatwave, except the first night, must be greater than the $90^{th}$ percentile, we examine all nights of the heatwave, except the first night. This results in a sample size of heatwave days of 41, 75, and 55 for Melbourne, Adelaide, and Perth (Table 5.1). The main reason for excluding the first night of the heatwaves is that this

occurs before the heatwave has set in and potentially before the extreme temperatures have begun, thus the inclusion of these days could result in the inclusion of pre-heatwave synoptic patterns.

| City | Number of stations | | Sample size (days) | | Number of days with undefined UHI | |
|---|---|---|---|---|---|---|
| | Urban | Rural | All | Heatwaves | All | Heatwaves |
| Melbourne | 3 | 4 | 2964 | 41 | 0 (0.00%) | 0 (0.00%) |
| Adelaide | 3 | 3 | 2964 | 75 | 17 (0.57%) | 0 (0.00%) |
| Perth | 3 | 3 | 2964 | 55 | 3 (0.10%) | 0 (0.00%) |

Table 5.1: Station and data statistics for Melbourne, Adelaide, and Perth. Columns two and three show the number of urban and rural stations in each city. Columns four and five show the total number of days used in this study (i.e. the extended summer season) and the number of heatwave days (excluding heatwave start days). Columns six and seven show the number of extended summer days and heatwave days respectively where the UHI was undefined, as a number (no brackets) and as a percentage (brackets). Days with an undefined UHI are days where the calculation of the UHI is not possible because either temperature data for all urban stations are missing, or temperature data for all rural stations are missing, i.e. we are unable to calculate median($T_{urban}$) or median($T_{rural}$). If only some data are missing from urban and/or rural stations, an UHI is still calculated.

### 5.3.2 Calculating the urban heat island

In each of the three cities, the UHI is calculated as the difference between the median of urban and rural AWS dry-bulb temperature data as shown in Equations 3.1 and 3.2. See Chapter 3 for more detail on the calculation of the UHI. Since the relationship between heatwaves and the UHI is greatest at night (as shown in Chapter 4), this study examines the UHI at midnight only.

### 5.3.3 SOM Toolbox

To compute the SOMs, we use the SOM Toolbox MATLAB package described in Chapter 3. We choose to analyse a 3-by-2 SOM, producing six Synoptic Types for each city. This configuration produces robust synoptic patterns that represent the passage of high and low-pressure systems over each of the cities.

The methods applied in this chapter are based on past research analysing synoptic patterns, with a focus on research performed in Australia (Jiang et al. 2012;

Huva et al. 2015; Jiang et al. 2015; Gibson et al. 2016; Jiang et al. 2017), as well as the work of Kohonen (2014) who details the implementation of SOMs using MATLAB.

### 5.3.4 SOM analysis

The SOM analysis is performed in order to help answer three questions:

1. Which Synoptic Types are associated with strong UHI events?
2. Which Synoptic Types are associated with heatwaves?
3. Are Synoptic Types that are associated with heatwaves the same as those associated with strong UHIs?

We also examine whether two factors, persistence of the UHI, and the meridional and zonal wind components, affect the strength of the UHI for certain Synoptic Types. Given that one of the main drivers of the UHI is heat stored in the urban fabric, if stored heat takes more than one day to dissipate, the strength of the UHI on any given day might affect the strength of the UHI on the following day. To determine whether there is persistence of the UHI, we compare UHI anomaly sign on day $i$ to that on day $j$, where day $j$ follows day $i$. For example, is an exacerbated UHI more likely to be followed by an exacerbated UHI, or is there no relationship? And do the strengths of the northerly and easterly wind components affect the strength of the UHI within each Synoptic Type. These methods are explained in the results section of this chapter as they depend on results that are yet to be explained.

## 5.4 Results

Section 5.4.1 details the relationships between UHIs and synoptic patterns in the three cities previously examined in Chapter 4: Melbourne, Adelaide, and Perth. The relationships between heatwaves and these synoptic patterns are examined in Section 5.4.2. Lastly, Section 5.4.3 examines the relationships between distributions of anomalous UHI strengths and synoptic patterns during heatwave days and the extended summer season in all three cities.

### 5.4.1 Urban heat island strength and synoptic patterns

This subsection introduces the Synoptic Types developed using SOMs. Due to the limited number of heatwave events within our chosen study period, six Synoptic Types only are selected to allow for robust statistical analysis of UHI strength during heatwaves (see Chapter 3 for further details). The six Synoptic Types identify the six most prominent synoptic patterns for each of Melbourne, Adelaide, and Perth. These results are displayed in Figures 5.1, 5.3, and 5.5 respectively. It is important to note that Synoptic Types differ between cities, i.e. Type 6 for Melbourne (Figure 5.1) is not the same as Type 6 for Adelaide or Perth (Figures 5.3 and 5.5 respectively).

To examine the relationship between UHI strength and Synoptic Type, we first bin the UHI anomalies into quintile categories. For each category, the anomalous UHI is defined as strongly exacerbated ($\geq 80^{th}$ percentile), moderately exacerbated ($60^{th} - 79^{th}$ percentiles), normal ($40^{th} - 59^{th}$ percentiles), moderately diminished ($20^{th} - 39^{th}$ percentiles), and strongly diminished ($< 20^{th}$ percentile). Using these five UHI categories, the distributions of the strengths of UHI anomalies during each of the Synoptic Types are examined.

Figures 5.2, 5.4, and 5.6 show the frequency of occurrence of each UHI anomaly category (coloured bars) for each Synoptic Type for Melbourne, Adelaide, and Perth respectively. The error bars represent the expected frequency of occurrence of each UHI anomaly category assuming that each category is equally likely to occur for a given Synoptic Type. Thus, the error bars show a 90 % confidence interval produced from $n$ random samples from a uniform distribution, where $n$ is the number of events in the Synoptic Type in question. If the strength of the UHI has no relationship with Synoptic Type, we expect the frequencies of anomalous UHI strengths to lie within these error bars. Therefore, if the observed frequencies lie outside the expected range we can conclude that there is a relationship between UHI strength and Synoptic Type. Throughout this section we only discuss results that are statistically significant, that is the observed frequencies lie outside the 90 % confidence interval, unless stated otherwise.

*MELBOURNE*

Melbourne's SOM (Figure 5.1) describes the passage of high and low-pressure systems over the city with a typical anticlockwise progression of the Synoptic Types. Type 1, which occurs for 13.83 % of the days in the study period, represents a postfrontal setup with a low-pressure system to the southeast of Melbourne. Both Type 2 and Type 3, with relative frequencies of 17.81 % and 15.22 % respectively, have a high-pressure system to the west/southwest of Melbourne, with southerly flow over the city. All three of these Types result in advection of cool oceanic air towards Melbourne from the south or southwest.
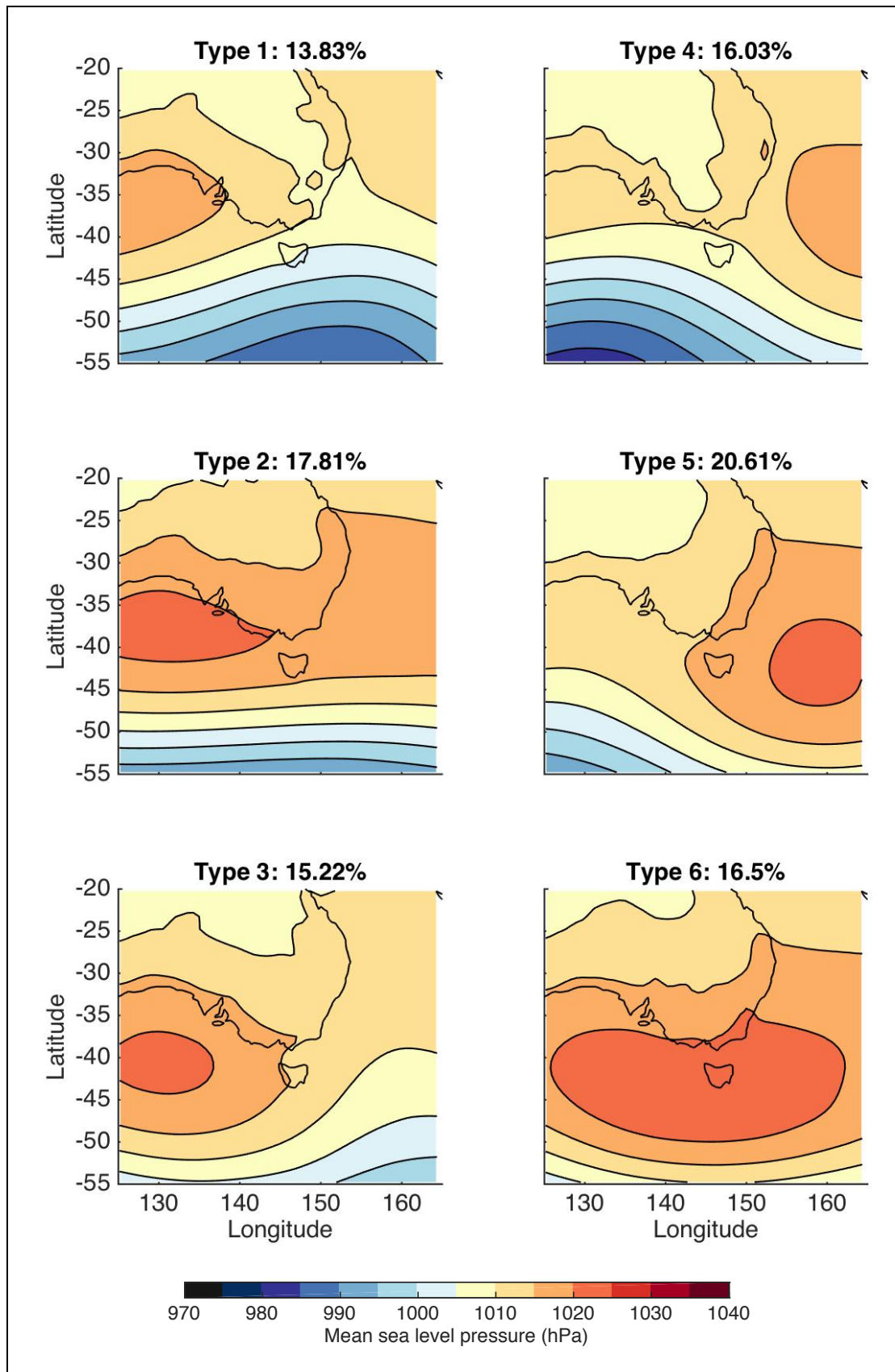
Figure 5.1: Figure showing SOMs for Melbourne using data from January 1995 to March 2014 for the extended summer season. Coloured contours show MSLP (hPa). Percentages at the top of each Type show how frequently each Type occurs during the extended summer season (November to March) from January 1995 to March 2014.

Type 6, with a relative frequency of 16.5 %, shows a broad high-pressure system centred to the south of Melbourne with ridging along the east coast of Australia and light easterly to northeasterly flow. Type 5, with a relative frequency of 20.61 %, has a high-pressure system over the Tasman Sea (to the west of Melbourne) and ridging along the east coast resulting in northerly to northeasterly flow over Melbourne. Type 4, with a relative frequency of 16.03 %, has a cold front approaching Melbourne and shows a similar high-pressure system to that in Type 5, but one that is weaker and located further northeast.

All six Types occur with a similar frequency (between 13.83 % and 20.61 %). The most frequently occurring Type, Type 5, is similar to the synoptic patterns associated with both heatwaves (Pezza et al. 2012; Boschat et al. 2015; Gibson et al. 2017b) and the warmest UHIs in Melbourne (Morris and Simmonds 2000).

Figure 5.2 shows how frequently each UHI category occurs in each Synoptic Type. As in Chapter 4, Figure 5.2 shows that the largest departures from the expected range of UHI occurrence are for the strong UHI events (i.e. both strongly exacerbated and strongly diminished events). We therefore examine strong UHIs in more detail throughout this chapter than moderate or normal events.

Strongly exacerbated UHI events occur significantly more frequently than expected during Synoptic Types 1, 4, and 5 (Figure 5.2). These Types show frequencies 0.7 %, 2.5 %, and 1.6 % above the maximum expected value given the random uniform distribution (Figure 5.2). As well as an increase in strongly exacerbated events, Types 1 and 4 are significantly less likely to coincide with strongly diminished UHI events, with frequencies 7.3 % and 2.5 % below the lowest expected value. There is no change in the frequency of strongly diminished events for Type 5 (Figure 5.2). Types 4 and 5 are also consistent with the synoptic patterns that Morris and Simmonds (2000)

identified as being associated with warm UHIs over Melbourne, i.e. anticyclonic systems to the east of Melbourne and ridges along the Great Dividing Range.
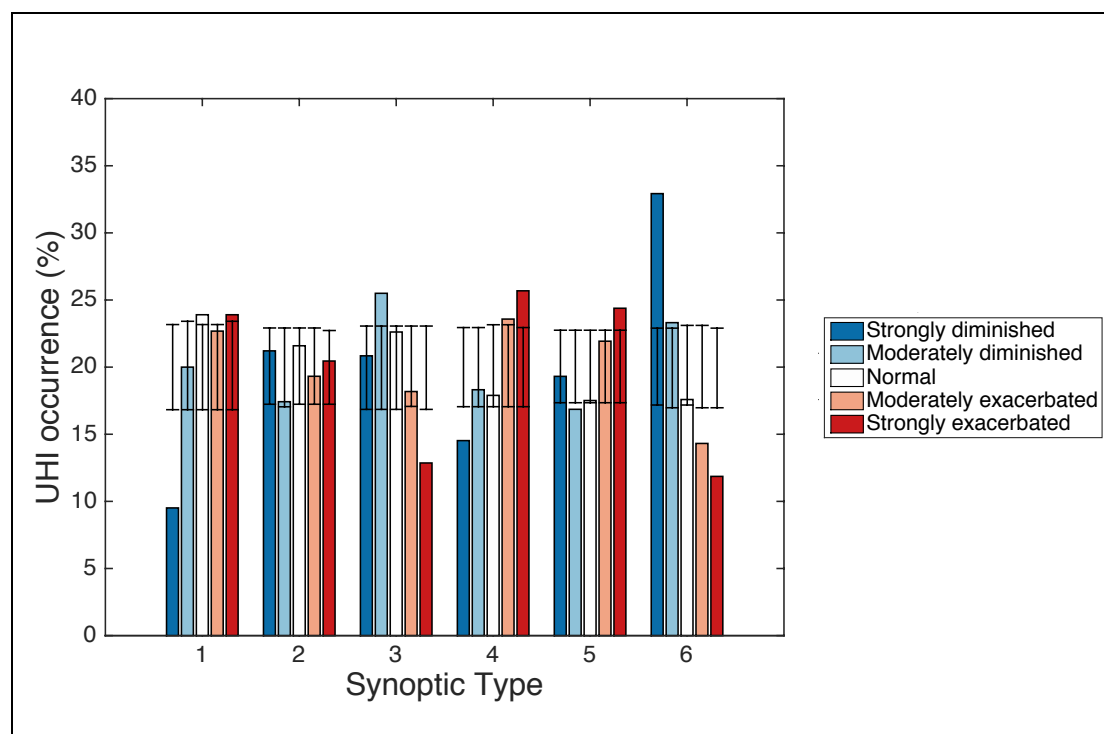


Figure 5.2: Bar graph showing the relationship between Synoptic Type (x-axis) and frequency of occurrence of each UHI category (y-axis) in Melbourne. Refer to Figure 5.1 for Synoptic Types. The UHI events are stratified into the following categories: strongly diminished (dark blue), moderately diminished (light blue), normal (white), moderately exacerbated (pink), and strongly exacerbated (red). Error bars show the 90 % confidence interval of frequencies, if UHI categories are randomly and uniformly distributed.

On the other hand, strongly exacerbated events occur significantly less frequently than expected during Types 3 and 6, by 4.2 % and 5.3 % respectively (Figure 5.2). Type 6 also shows statistically significantly more strongly diminished events than expected randomly and by chance, with a frequency 10.0 % above what is expected with the random uniform distribution (Figure 5.2). Despite Types 3 and 6 both being associated with fewer strongly exacerbated UHIs, they are associated with different weather conditions over Melbourne. While Type 3 has southerly flow over the city, Type 6 shows more stable conditions with easterly to northeasterly flow (Figure 5.1). Morris and Simmonds (2000) do not identify synoptic patterns that match Types 3 and

6, however the most similar synoptic patterns in their research are associated with UHIs between 0°C and 2°C, i.e. not their coolest UHI category.

Given that UHIs of similar strengths in Melbourne are neighbours on the SOM plane (Figures 5.1 and 5.2), this implies that the anomalous strength of the UHI may persist for a number of days. If heat stored in buildings takes more than one day to dissipate, this could provide a mechanism for a persistent UHI anomaly.

To test whether the strength of the UHI anomaly persists from one day to the next we pair all Synoptic Types and determine the frequency with which UHI anomalies of the same sign co-occur when the pair of Synoptic Types occur in succession, i.e. how often an exacerbated (diminished) UHI for Type $j$ follows an exacerbated (diminished) UHI for Type $i$.

The frequency of consistency between successive Synoptic Types is then compared to a frequency calculated for the same pairs of Synoptic Types that do not necessarily occur consecutively, i.e. the two days that comprise the pair of non-consecutive Synoptic Types are independently chosen at random from the given Types. These random pairs are determined for each pair of Synoptic Types $i$ and $j$ by randomly selecting $n$ UHI samples from each of Synoptic Types $i$ and $j$, where $n$ equals 10,000. The randomised pairs of Synoptic Types are used to generate a confidence interval for comparison to the consecutively occurring pairs. Therefore, the comparison shows whether the strength of the UHI anomaly is dependent on prior Synoptic Types, not on the Types themselves.

Table 5.2 shows the frequency with which UHI anomaly signs are consistent for a given Synoptic Type progression. For example, in Melbourne, when Synoptic Types progress from Type 4 to Type 1, the sign of the UHI anomaly is consistent from day 0 to day 1 (i.e. positive on both days or negative on both days), 52 % of the time

(Table 5.2). This value lies within the 90 % confidence interval computed from randomised days. So, there is no evidence that the strength of the UHI anomaly for Synoptic Type 4 influences the UHI anomaly for Synoptic Type 1 in any appreciable way (Table 5.2). We repeat this analysis for Adelaide and Perth later in this section (Figures 5.3 and 5.4).

| | | Synoptic Type (day 1) | | | | | |
|---|---|---|---|---|---|---|---|
| | | 1 | 2 | 3 | 4 | 5 | 6 |
| Synoptic Type (day 0) | 1 | 0.55 (196) | 0.60 (75) | 0.55 (77) | 0.58 (48) | 0.55 (11) | 0.00 (3) |
| | 2 | 0.60 (30) | 0.51 (225) | 0.61 (62) | 0.53 (51) | 0.49 (89) | 0.51 (71) |
| | 3 | 0.41 (22) | 0.38 (45) | 0.56 (187) | 0.56 (25) | *0.41 (78)* | *0.64 (94)* |
| | 4 | 0.52 (141) | 0.54 (79) | 0.46 (28) | 0.50 (198) | 0.54 (28) | 0.00 (1) |
| | 5 | 0.55 (20) | 0.49 (77) | 0.48 (67) | 0.53 (148) | 0.51 (255) | 0.56 (43) |
| | 6 | 1.00 (1) | 0.58 (26) | *0.70 (30)* | 0.80 (5) | 0.57 (150) | *0.63 (277)* |

Table 5.2: Frequency of instances of consistency in the sign of the UHI anomaly between days with successive Synoptic Types for Melbourne. Values show the frequency with which $UHI_{anom}$(day 1)/$UHI_{anom}$(day 0) is greater than 0, i.e. the magnitude/sign of the UHI is consistent over two consecutive days. Values in brackets show total sample size for given Synoptic Type progressions. Italicised values lie outside the 90 % confidence interval. Shaded cells correspond to pairs of Synoptic Types where both Types typically show significantly more (dark shading) or fewer (light shading) strongly exacerbated events respectively. Type progressions with a sample size smaller than 20 are shown in grey font to indicate a less robust sample size.

Since Chapter 4 identified an exacerbation (diminishment) of the strength of the UHI during heatwaves in Melbourne and Adelaide (Perth), we focus the persistence analysis on pairs of Synoptic Type where both Types are associated with significantly more or fewer strongly exacerbated (diminished) UHI magnitudes. These pairs of Types are easily identifiable as the shaded cells in Tables 5.2 to 5.4. Note that we also limit our analysis to Synoptic Type pairs with sample sizes of 20 or more to ensure sufficient sample size for analyses.

While Figure 5.1 indicates that the Synoptic Types generally progress in an anticlockwise progression, this is further clarified in Table 5.2. However, it is important to note that for all cities, a day with Synoptic Type *S* is most likely to be followed by Type *S* on the following day (Table 5.2). This is likely because of two reasons. The first

is the slow-moving nature of transitory systems over Melbourne, which is distinctly sub-tropical in the warmer months. The second reason is because we have chosen a relatively small number of Synoptic Types, the reasons for which are discussed in Chapter 3.

Strong UHI events, whether exacerbated or diminished, tend to occur in those Synoptic Types for which there is a typical temporal progression in Melbourne. The Types associated with an increased number of strongly exacerbated UHIs generally progress from Type 5, to Type 4, to Type 1 (Table 5.2 and Figure 5.2). Similarly, the Types associated with significantly fewer strongly exacerbated events, Types 3 and 6 (Figure 5.2), also tend to occur in succession with Type 3 typically preceding Type 6 (Table 5.2). This suggests that a strong UHI state might be the result of maintenance or enhancement by one or more Synoptic Types, rather than directly caused by a particular Synoptic Type. Thus, the order of successive Synoptic Types over Melbourne might be as important as the Types themselves for the generation of a strong UHI anomaly, whether it be an enhanced or diminished UHI.

Table 5.2 shows some evidence of a relationship between UHI anomaly strengths on consecutive days in Melbourne, but the relationship is weak. The progressions between Types with a higher chance of strongly exacerbated events (Types 1, 4, and 5) show no instances where persistence is more likely than chance. However, when those Synoptic Types that are associated with fewer exacerbated events occur successively, there is a greater chance that the UHI strength in both Synoptic Types is consistent (Table 5.2). This is evident as progressions from Types 3 to 3, 6 to 3, and 6 to 6 have frequencies of consistent UHI anomalies of at least 63 %, which are unlikely to occur due to chance. Therefore, the sign of the UHI anomaly is only weakly related to the order of progression of the Synoptic Types.

*ADELAIDE*

Adelaide's Synoptic Types are shown in Figure 5.3. Types 1 and 4, with relative frequencies of 16.73 % and 8.84 % respectively, show a high-pressure centre to the west of Adelaide, both of which are postfrontal but with the systems located further east in Type 1. These patterns result in light winds over Adelaide from the south or southwest. Types 2 and 3, with relative frequencies of 19.33 % and 16.36 % respectively, have high-pressure systems centred to the south of Adelaide or to the west, with a ridge along the Great Dividing Range (Figure 5.3). This results in the advection of air towards Adelaide from the east or southeast. Types 5 and 6, with relative frequencies of 17.68 % and 21.05 % respectively, feature a high-pressure system over the Tasman Sea and ridging along Australia's Great Dividing Range causing advection of air to Adelaide from Australia's warm interior (Figure 5.3).

In Adelaide, Synoptic Types 5 and 6 show 8.8 % and 10.9 % more strongly exacerbated events respectively than would expected due to chance (Figure 5.4), with both Types showing that strongly exacerbated UHIs in Adelaide are associated with high-pressure system over the Tasman Sea and light winds from the east or northeast (Figure 5.3). The slow moving warm air is conducive to a warm UHI as light winds are often associated with warm UHIs (e.g. Oke 1982; Unger 1996; Morris et al. 2001). All other Synoptic Types in Adelaide (Types 1 to 4) show significantly fewer strongly exacerbated events than expected by between 0.8 % and 8.7 % (Figure 5.4), thus showing a clear relationship between the strength of the UHI anomaly and Synoptic Type in Adelaide.

While the SOMs for Melbourne and Adelaide are not directly comparable as they are computed independently, there is a consistency in the location of the anticyclone over the Tasman Sea and a strongly exacerbated UHI in Melbourne and
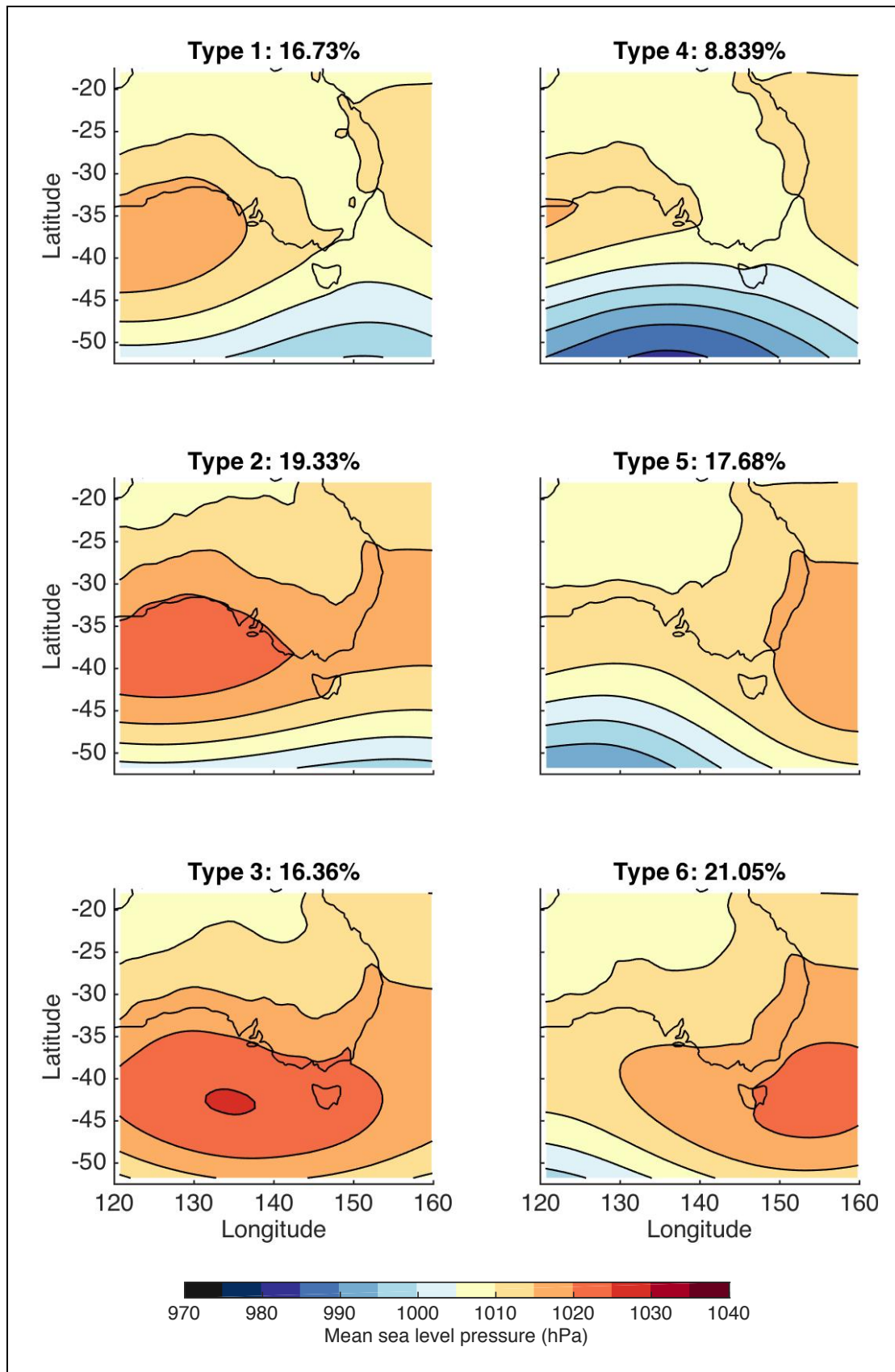
Figure 5.3: Same as Figure 5.1 but for Adelaide.

Adelaide. Specifically, the locations of the high-pressure systems of Types 5 and 6 in Adelaide are similar to Types 4 and 5 in Melbourne and both cities have light winds from the north or northeast under these synoptic setups (Figure 5.3 and 5.1 respectively). This suggests that similar large-scale mechanisms are associated with UHI formation in the two cities.
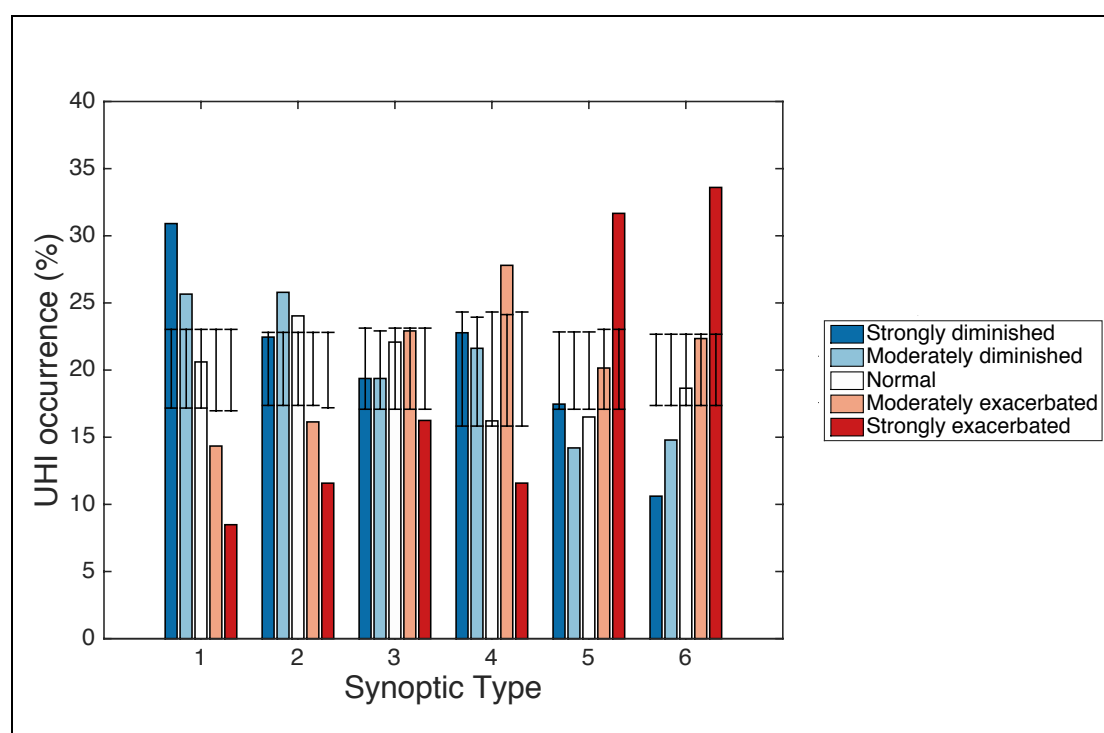


Figure 5.4: Same as Figure 5.2 but for Adelaide. Refer to Figure 5.3 for Synoptic Types.

Types 1 and 6 are the only Types in Adelaide that show significant changes in the frequency of strongly diminished events compared to what would be expected if the UHI had no connection to Synoptic Type (Figure 5.4). Type 1 shows a high-pressure system to the east of Adelaide with southerly flow from the ocean to the city (Figure 5.3). There is a significant increase in the likelihood of strongly diminished UHIs for Type 1 of 7.9 % (Figure 5.4), that is, the strength of the UHI is more likely to lie in the bottom quintile. Type 6 shows a high-pressure system to the southwest of Adelaide

with easterly flow from the warm continental interior to the city (Figure 5.3). There is a decrease of 6.8 % in the chance of strongly diminished UHIs for Type 6 (Figure 5.4).

In Adelaide, strongly diminished UHIs have a weaker relationship with Synoptic Type than that for strongly exacerbated UHI events, that is, frequencies of strongly diminished events for four of six Synoptic Types lie within the 90 % confidence interval (Figure 5.4).

As discussed earlier, there is an increase in the occurrence of strongly exacerbated UHIs in Melbourne and Adelaide when there is a high-pressure system over the Tasman Sea (Figures 5.1 to 5.4). However, not all comparable Types in the two cities show a similar consistency in UHI strength. Type 1 in Melbourne and Type 1 in Adelaide have quite similar MSLP patterns (Figure 5.1 and 5.3), that is, for both cities, Type 1 is associated with a high-pressure system over the Great Australian Bight and light southerly or southwesterly flow from over the ocean (Figure 5.1 and 5.3). Given that light winds tend to be associated with the formation of a warm UHI (e.g. Oke 1982; Unger 1996; Morris et al. 2001) we might expect Type 1 to be associated with strongly exacerbated UHIs in both cities. However, despite their similarity, these respective patterns are associated with opposing UHI strengths for each city. Melbourne has a higher change of strongly exacerbated events for Type 1 (Figure 5.2), whereas Adelaide has fewer strongly exacerbated events and a higher frequency of strongly diminished events (Figure 5.4).

On the other hand, the passage of relatively cool oceanic air over each of these cities when Synoptic Type 1 is present may lead to cool temperatures in the cities and therefore a decrease in the number of strongly exacerbated events and an increase in strongly diminished events as this cool air can disrupt the formation of the boundary layer, and hence the formation of a warm UHI. This result is observed in Adelaide but

not in Melbourne (Figure 5.2 and 5.4). These contrasting results suggest different mechanisms may drive the formation of the UHIs in Melbourne and Adelaide.

The above discussion shows that the typical strength of the UHI is not always clear from visual examination of the Synoptic Types. One possible explanation for the inconsistent results between the two cities is our hypothesis that the strength of the UHI on day $j$ is somewhat dependent on the UHI on day $i$. While we find persistence of the sign of the UHI to be weak in Melbourne, if UHI persistence is stronger in Adelaide this might explain why the distributions of UHI categories are different for Type 1 for the two cities. That is, in Adelaide, are strongly exacerbated UHIs less likely for Type 1 than due to chance, because Type 4 also has fewer strongly exacerbated UHIs?

In Table 5.3 we investigate whether the strength of the UHI persists for more than one day. As for Table 5.2 for Melbourne, Table 5.3 shows the frequency of consistency in the sign of the UHI anomaly in successively occurring pairs of Synoptic Types for Adelaide. The table also shows how often each pair of Types occurs in the observational data.

| | | Synoptic Type (day 1) | | | | | |
|---|---|---|---|---|---|---|---|
| | | 1 | 2 | 3 | 4 | 5 | 6 |
| Synoptic Type (day 0) | 1 | *0.69 (205)* | *0.68 (119)* | 0.66 (29) | 0.58 (26) | 0.54 (76) | 0.61 (41) |
| | 2 | 0.50 (42) | *0.61 (251)* | 0.61 (124) | 0.60 (5) | 0.53 (40) | 0.54 (111) |
| | 3 | 0.80 (5) | 0.56 (34) | *0.60 (269)* | - (0) | 0.29 (7) | 0.54 (170) |
| | 4 | *0.62 (79)* | *0.72 (25)* | - (0) | 0.52 (129) | 0.56 (27) | 0.50 (2) |
| | 5 | 0.53 (123) | 0.49 (75) | 0.71 (7) | 0.46 (97) | *0.57 (187)* | 0.46 (35) |
| | 6 | 0.57 (42) | 0.50 (68) | *0.59 (56)* | 0.6 (5) | *0.58 (187)* | *0.57 (265)* |

Table 5.3: As for Table 5.2 but for Adelaide.

While Melbourne shows little evidence of persistence of the UHI from one day to the next, there is more evidence of a relationship in Adelaide. Over half of the pairs of Synoptic Types shaded in Table 5.3 show a significant relationship between UHI

strengths on consecutive days. That is, neighbouring pairs of Synoptic Types with typically strong UHIs of the same sign are more likely than not to have UHIs of the same signs on consecutive days than if UHI samples for the given pair are randomised.

Conversely, for progressions from Types associated with more (fewer) strongly exacerbated UHIs than can be expected due to chance, to those with fewer (more) strongly exacerbated UHIs, i.e. the cells in Table 5.3 that are not shaded, few significant relationships exist between successive Synoptic Types and the strength of the UHI anomaly. Only one of these twelve pairs of Types (Type 6 to Type 3) shows a statistically significantly higher chance of consistency in the sign of the UHI anomaly from one day to the next (Table 5.3).

These findings are evidence that the prior state of the UHI may influence the strength of the UHI anomaly in pairs of Types that are predisposed to strong UHIs of the same sign. This persistence may explain why the relationship between heatwaves and the strength of the UHI anomaly in Adelaide remains strong for the entire duration of the heatwaves, whereas UHI anomalies in Melbourne on the middle nights of the heatwaves are weaker than on first nights (see Figure 4.2a and b). This hypothesis is further investigated in Section 5.4.2.


*PERTH*

Perth's Synoptic Types are shown in Figure 5.5 and are now described. As previously, the Synoptic Types show an anticlockwise progression on the SOM, revealing the eastward passage of frontal weather systems. Three of the Synoptic Types for Perth have troughs along Australia's west coast that result in advection of air from Australia's warm interior, towards Perth. These Synoptic Types are Types 3, 5, and 6, and account for 16.36 %, 21.86 %, and 16.09 % of extended summer season days

respectively. Each Type is differentiated by the location of the high-pressure system. In Type 3 this system is located to the southwest of Perth, in Type 5 the high is located to the west, and in Type 6 the system is located to the southeast (Figure 5.5).

High-pressure systems to the west of Perth typify Types 1 and 2, with relative frequencies of 14.68 % and 19.3 % respectively. These systems cause the advection of air towards Perth from the southeast or east (Figure 5.5). Type 4, with a relative frequency of 11.71 %, shows a similar, but weaker, high-pressure system to the west of Perth and a prefrontal system located to the south of Perth causing stable conditions (Figure 5.5).

In Perth, Type 4 shows a higher likelihood of strongly exacerbated UHI events by 4.9 % and a decrease in the number of strongly diminished events by 7.8 % (Figure 5.6). The stable atmospheric conditions induced by the low pressure gradients over the city are generally conducive to the formation of a warm UHI. Types 1 and 2 are also associated with fewer strongly diminished events by 7.8 % and 1.2 % respectively (Figure 5.6). As for Type 4, these Types are also associated with weak southerly or southeasterly flow (Figure 5.5).

Conversely, Synoptic Types 3 and 6 show an increased occurrence of strongly diminished (cooler than normal) UHI events by 6.8 % and 9.0 % respectively and corresponding decreases in the number of strongly exacerbated events by 1.4 % and 2.7 % (Figure 5.6). These Types are neighbours on the SOM plane and, as mentioned earlier, have similar synoptic features that induce northeasterly flow over Perth. We also noted earlier that Type 5 has similar synoptic features to both Types 3 and 6, but with weaker winds, however Type 5 does not have a similar distribution of UHI anomaly categories as shown in Figure 5.6. That is, northeasterly flow in Types 3 and
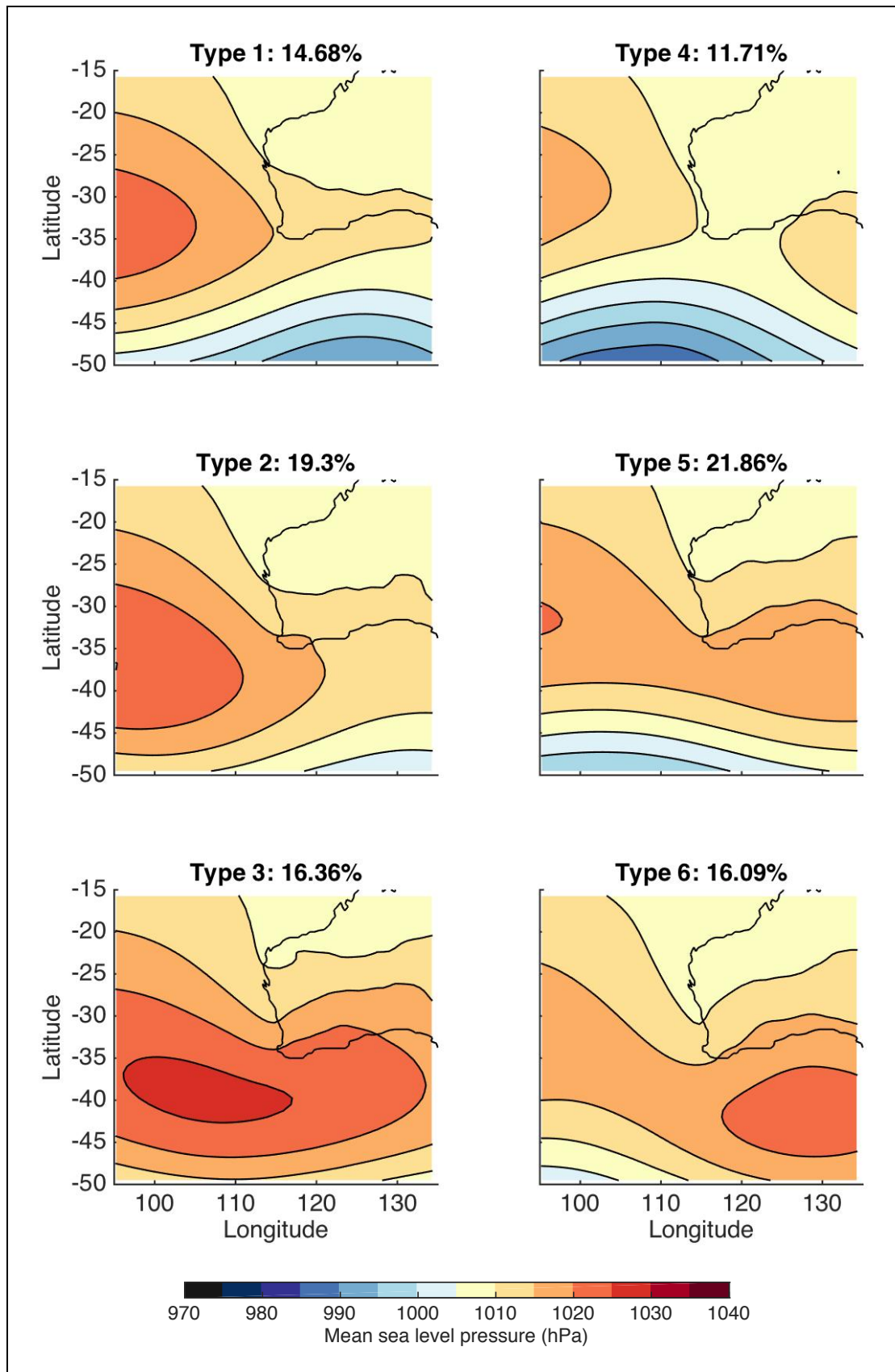
Figure 5.5: Same as Figure 5.1 but for Perth.

6 predispose Perth to a higher frequency of strongly diminished UHIs, but the same cannot be said for Type 5. Rather, all UHI categories for Type 5 occur as frequently as can be expected due to random chance as they lie within the 90 % confidence interval. As with Melbourne and Adelaide, we now examine UHI anomaly signs and their persistence from one day to the next for Perth in Table 5.4.
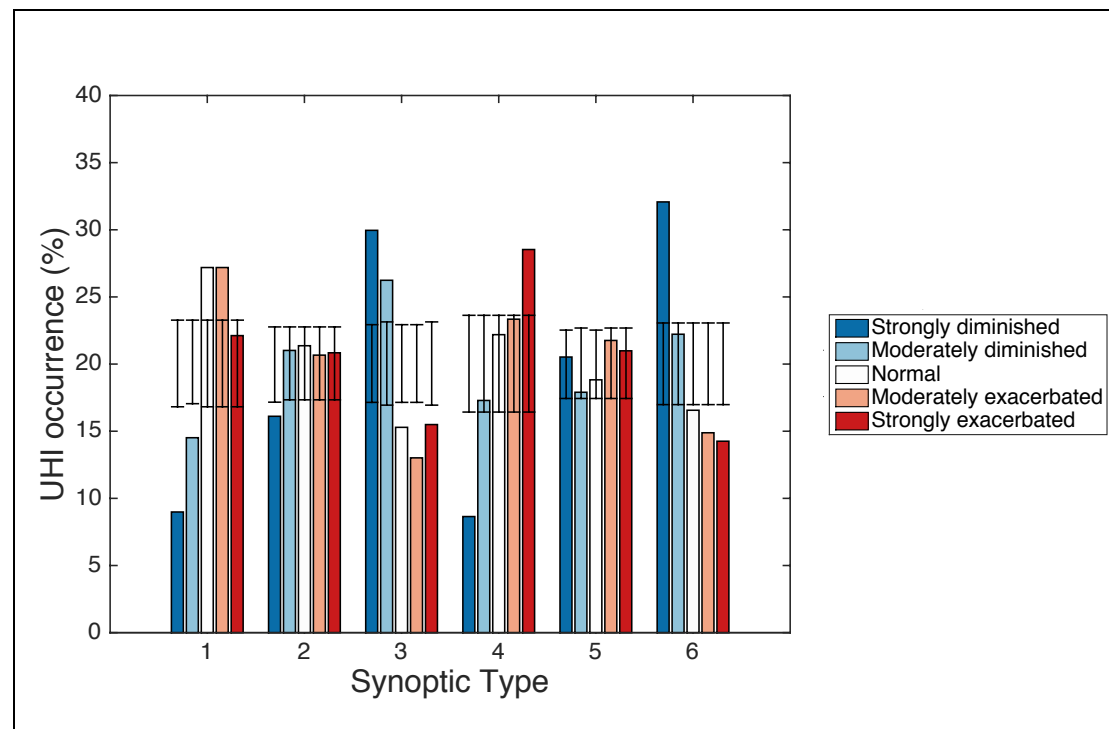


Figure 5.6: Same as Figure 5.2 but for Perth. Refer to Figure 5.5 for Synoptic Types.

| | | Synoptic Type (day 1) | | | | | |
|---|---|---|---|---|---|---|---|
| | | 1 | 2 | 3 | 4 | 5 | 6 |
| Synoptic Type (day 0) | 1 | *0.67 (177)* | 0.61 (92) | 0.50 (16) | *0.79 (42)* | 0.47 (100) | 0.43 (7) |
| | 2 | *0.66 (41)* | 0.55 (252) | 0.55 (122) | 0.50 (2) | 0.52 (90) | 0.54 (65) |
| | 3 | 0.50 (2) | 0.51 (37) | *0.65 (289)* | 0.00 (1) | 0.59 (41) | *0.68 (115)* |
| | 4 | 0.55 (111) | 0.50 (8) | - (0) | 0.61 (185) | 0.45 (42) | 1.00 (1) |
| | 5 | 0.57 (90) | 0.56 (117) | 0.62 (21) | 0.58 (80) | *0.58 (286)* | *0.63 (54)* |
| | 6 | 0.50 (14) | 0.52 (66) | 0.50 (36) | 0.46 (37) | 0.48 (89) | *0.59 (235)* |

Table 5.4: As for Table 5.2 but for Perth and light and dark shaded values correspond to Synoptic Types that show significantly more or fewer strongly diminished events respectively.

Consecutive days that both occur in Types associated with more strongly diminished UHIs, Types 3 and 6 (Figure 5.6), show more consistency in UHI sign than

can be expected due to chance (Table 5.4). However, those Synoptic Types that show fewer strongly diminished events, Types 1, 2, and 4, show no such relationship (Table 5.4 and Figure 5.6). As for Adelaide, this is evidence that the Synoptic Type progression can reinforce the anomalous UHI over Perth, but unlike Adelaide, this occurs only for Synoptic Types that are predisposed to strongly diminished UHIs. Thus, we suggest that strongly diminished UHIs are more likely to persist in Perth compared to strongly exacerbated events and might help to explain why UHIs are typically diminished during heatwaves in Perth (as shown in Chapter 4) assuming that Types 3 and/or 6 occur during heatwaves in Perth. This will be examined in Section 5.4.2.

In summary, these findings suggest that persistence may contribute to the relationship between heatwaves and the strength of the UHI anomaly in Adelaide and Perth, as seen in Chapter 4, but is unlikely to affect the UHI during heatwaves in Melbourne.

*WIND ANALYSIS*

As each Synoptic Type is essentially a composite of the synoptic patterns associated with that Type, variability in atmospheric conditions within each Type has the potential to explain why we see intra-Type variation in the strength of the UHI anomaly. So, to further elucidate the intra-Type variation in the UHI, we examine the relationship between the UHI anomaly and the meridional and zonal components of the 10 m winds.

This analysis is similar to that done in Chapter 4 to determine whether wind direction and/or strength has a strong influence on the UHI. However, in this chapter we consider the 10 m meridional and zonal wind components instead of 2 m direction and strength. Also, rather than using BoM AWS wind data, in this chapter we use

ERA-Interim wind data. Thus, results for the two analyses might show different findings. This is because the 10 m analysis examines how large scale winds affect the UHI, without taking smaller scale influences into account, such as sea breezes and station specific conditions. On the other hand, these smaller influences were considered in the 2 m wind analysis in Chapter 4. By examining different aspects of the wind, we gain a better understanding of how both large and small-scale influences can affect the strength of the UHI.

The examination of the meridional and zonal wind components allows us to determine whether advection of air from a particular region is likely to affect the strength of the UHI, and in particular, whether the advection of warm continental air towards each of the cities is associated with a warmer UHI. If this hypothesis is correct, this would mean that exacerbated UHIs in Melbourne, Adelaide, and Perth would be associated with northerly, northeasterly, and eastly winds respectively.

Our examination of wind direction in the previous chapter was performed predominately to determine whether winds from the direction of the coast caused a cooling of the UHI during heatwaves by cooling the urban stations, which generally tend to be closer to the coast than the rural stations. We also examined wind strength in Chapter 4.

Since weak winds tend to be associated with warmer UHIs (e.g. Oke 1982; Unger 1996; Morris et al. 2001), if we found winds during heatwaves to be stronger over Perth than over Melbourne and Adelaide, this may have been able to explain the opposing relationships between heatwaves and the strength of the UHI in Melbourne and Adelaide, when compared to Perth.

By examining wind components, as opposed to wind strength, we investigate whether there is a relationship between the strength of the wind and UHI, stratified by

direction (e.g. when the wind is from the north, south, etc.). Further, by stratifying the results depending on Synoptic Type, we are able to determine whether some synoptic setups and their resulting winds have a stronger effect on the strength of the UHI than others. While there are likely to be some similarities in the results for the wind analyses in both Chapters 4 and 5, the use of two different approaches allows us to gain a deeper understanding of the relationship between the wind, advection of air, and the strength of the anomalous UHI. Throughout this section we use a significance level of 5 %.

Figure 5.7 shows the strength of the UHI anomaly plotted against the 10 m ERA-Interim v-wind data, for the grid box closest to Melbourne Regional Office (Melbourne's ACORN-SAT station), and Figure 5.8 shows the same but for u-wind data. The data are stratified into Synoptic Types to determine whether there is a relationship between meridional and zonal wind component and UHI anomaly for one or more Types.

Types 2, 3, 4, and 6 have significant negative relationships between meridional wind component and the strength of the anomalous UHI in Melbourne at the 5 % significance level (Figure 5.7). While these relationships are weak and account for less than 4.2 % of explained variance, Figure 5.7b shows that moderately strong northerly wind components for Synoptic Type 4, a prefrontal setup, are associated with the warmest UHIs. This can be seen from the five UHI events in Type 4, with UHI anomalies greater than 4 °C, as all of these events are associated with moderately strong northerly wind components (approximately -5 m/s). Melbourne's proximity to the coast may affect the influence of wind on the strength of the UHI. For example, stronger winds from inland areas may reduce the effectiveness of any sea breeze in cooling urban
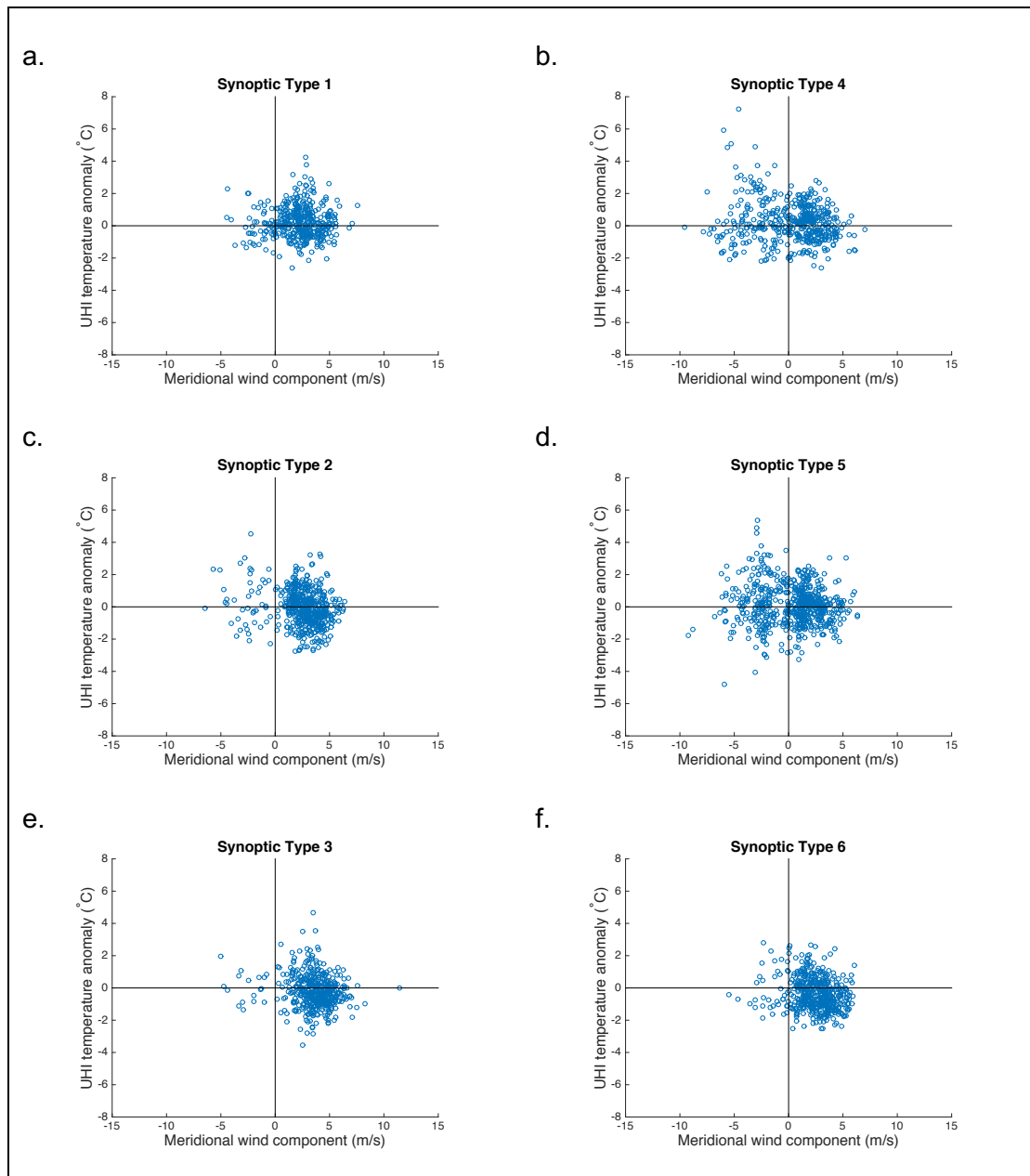
Figure 5.7: Scatterplot showing the relationship between meridional wind component (x-axis) and UHI temperature anomaly (y-axis) in Melbourne for six Synoptic Types.

areas, thus promoting a warmer UHI. This finding suggests that our earlier hypothesis that warm northerly winds can be conducive to a warmer UHI in Melbourne is accurate as the warmest UHIs occur when the winds are northerly.

However, these events comprise a small number of the total sample size in this Synoptic Type, with the majority of UHI events showing little relationship between
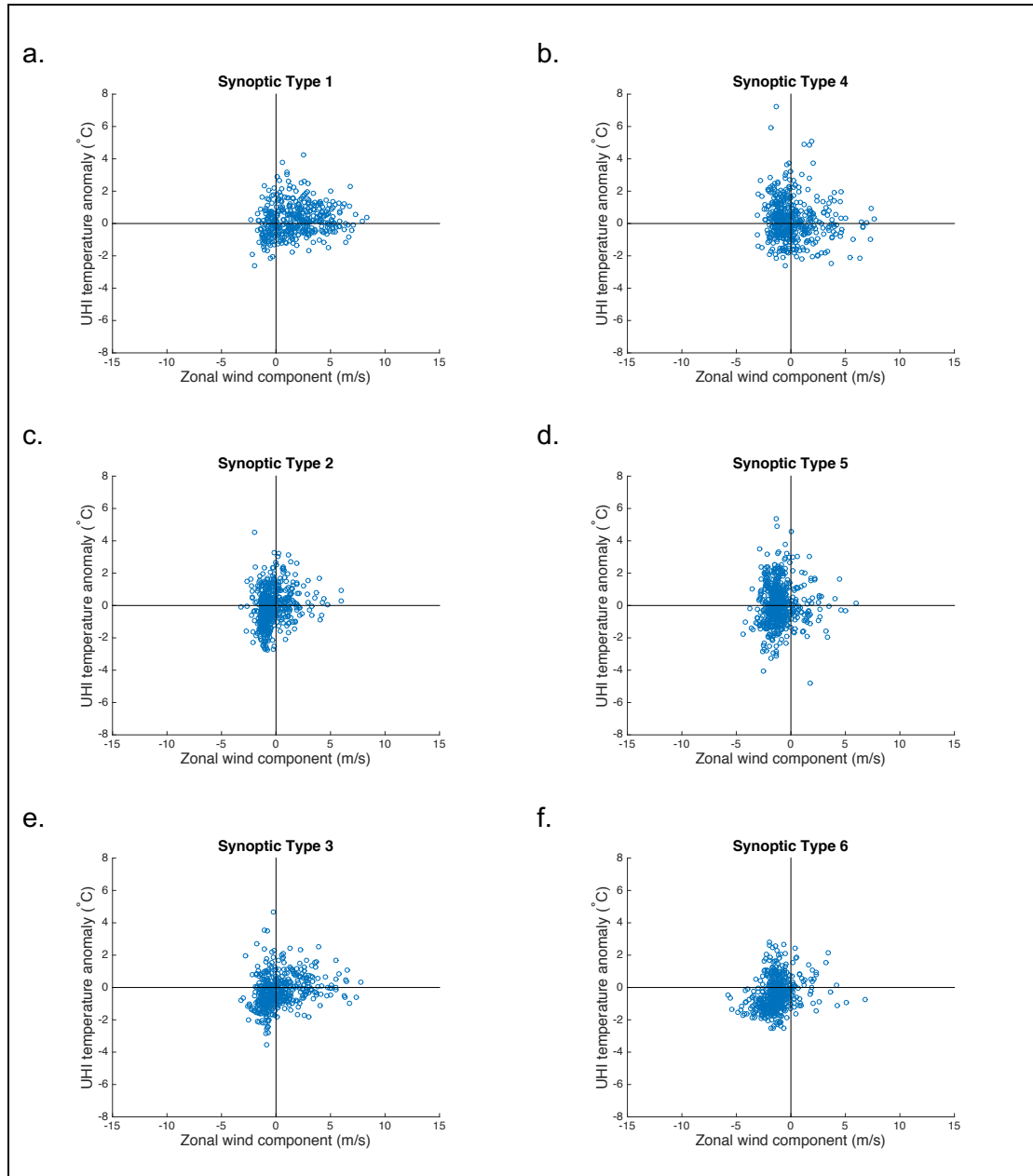
Figure 5.8: Scatterplot showing the relationship between zonal wind component (x-axis) and UHI temperature anomaly (y-axis) in Melbourne for six Synoptic Types.

meridional component and UHI anomaly. Further, we note that all Synoptic Types show a spread of exacerbated and diminished UHIs regardless of the sign or magnitude of the meridional wind component. While we identified weak linear relationships between meridional wind component and UHI anomaly for certain Synoptic Types, it is clear that the meridional wind is not a strong predictor of the strength of the UHI.

All Types except Type 5 show a linear relationship between zonal wind component and the strength of UHI anomalies that is statistically significant at the 5 % level (Figure 5.8). This means that westerly winds are more favourable for UHI development than easterlies in Synoptic Types 1, 2, 3, and 6, and easterlies are associated with warmer UHIs for Type 4. However, as previously, all relationships are weak. The strongest relationships are for Types 3 and 6 with 5.9 % and 5.8 % explained variance respectively, both of which are associated with cooler UHIs and easterly winds. This relationship shows that the stronger the easterly component of the wind in Types 3 and 6, the cooler the UHI, however the zonal wind components in these Types are generally weak (i.e. less than 5 m/s).

These results contrast to those from Chapter 4, which found no significant relationships between wind speed and/or direction and the strength of the UHI during heatwaves in Melbourne. Further, since the wind analysis here examines 10 m wind components, whereas Chapter 4 examined 2 m wind strength and direction, these results suggest that large scale wind flow is potentially more influential to UHI development in Melbourne than small scale, station specific wind conditions. However, as noted earlier, the contribution of large scale flow to the strength of the UHI is very small.

The differing results between Chapters 4 and 5 could also suggest that the wind has a stronger effect on the strength of the UHI during the extended summer season, as opposed to during heatwave periods, as Chapter 4 examined this relationship only during heatwave events. It must be noted that this means there is a large difference in the sample sizes used for the wind analyses in the two chapters, which may also affect our results. Despite the differences between the results in this chapter and those of Chapter 4, both draw the same conclusion. That is, wind direction and strength are not key driving mechanisms modulating the strength of the anomalous UHI in Melbourne.

Similar to Melbourne, Figure 5.9 (5.10) shows the relationship between meridional (zonal) wind component and the strength of the UHI anomaly in Adelaide. The wind components over Adelaide show a stronger relationship with UHI anomalies than for Melbourne. Four of six Types show a negative relationship between meridional wind component and UHIs, they are Type 1, 2, 3, and 6 (Figure 5.9). Types 2 and 3 show the strongest relationship with 7.8 % and 13.5 % explained variance respectively (Figure 5.9c and e). These Types also happen to be associated with cool UHIs, showing that stronger southerly wind components in Types 2 and 3 are associated with cool UHIs.

The zonal wind component shows a significant negative relationship with UHI anomalies for all Types (Figure 5.10). Type 5 shows the strongest relationship with 14.1 % explained variance (Figure 5.10d), where warm UHIs are associated with winds with a stronger easterly component. Type 6 has a similar but weaker relationship to that of Type 5 (5.7 % explained variance) and shows that the warmest UHIs are associated with moderate easterly winds. Since Types 5 and 6 are both associated with a higher frequency of strongly exacerbated UHIs, this suggests that for these Synoptic Types, winds with an easterly component over Adelaide cause the advection of warm continental air from the east, thus increasing heat storage in the city during the day and heat release at night, consequently a warm nocturnal UHI is formed. All other Types have much weaker relationships between zonal wind component and the strength of the UHI anomaly (maximum of 3.6 % explained variance, Figure 5.10). These results, and the presence of linear trends in Figures 5.9 and 5.10, show that the warmest UHIs are generally not associated with calm conditions.
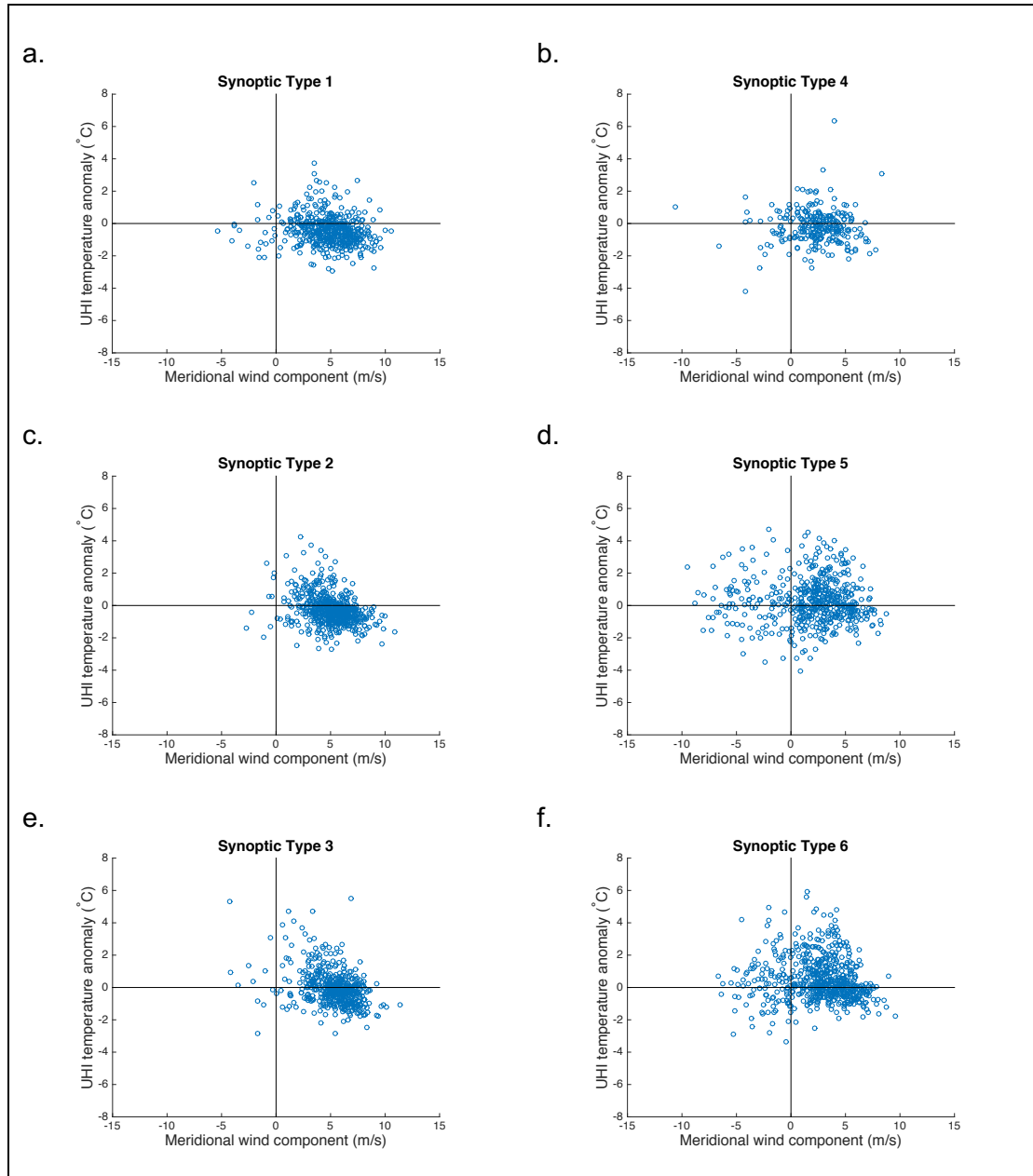
Figure 5.9: Same as Figure 5.7 but for Adelaide.

These results differ to those from Chapter 4, which found that AWSs in Adelaide did not show relationships between UHI anomalies during heatwaves and wind speed and/or direction at numerous stations across the city. As for Melbourne, this may suggest that large scale winds are more influential to the strength of the UHI than local wind speed and direction. However, the large differences in samples sizes may be skewing our results.
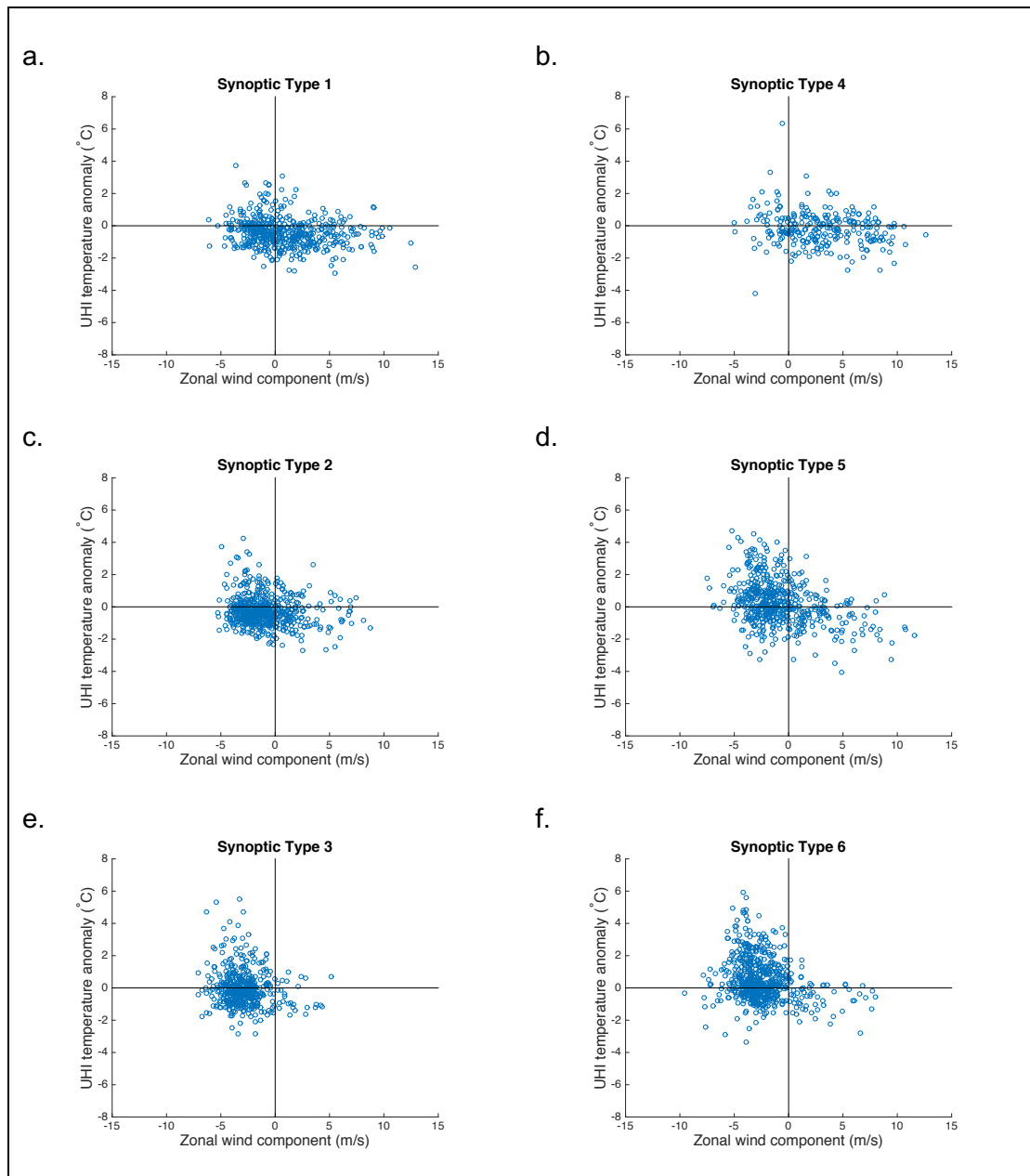
Figure 5.10: Same as Figure 5.8 but for Adelaide.

Since Chapter 4 only examined heatwave periods, the inconsistency in the relationships between winds and UHI strength may also imply that the influence of the wind on the strength of the UHI is weaker during heatwave periods. However, since these chapters examined different wind metrics, i.e. Chapter 4 examined observational 2 m local winds whereas Chapter 5 examines ERA-Interim 10 m winds, this hypothesis requires more analysis before it can be confirmed.

The relationships between anomalous UHIs and meridional and zonal wind components in Perth are now described in Figures 5.11 and 5.12.

In Perth, Synoptic Types 2 through 6 show significant positive relationships between meridional wind component and the anomalous strength of the UHI (Figure 5.11b to f). That is, stronger northerly (southerly) components lead to cooler (warmer) UHIs.

Type 5 shows the strongest relationship with 13.2 % explained variance (Figure 5.11d). The coolest UHIs for this Type occur with weak to moderate northerly winds. Types 3 and 6 show 8.3 % and 6.6 % explained variance respectively but the coolest UHIs in these Types are associated with weak meridional wind components (less than 5 m/s, Figure 5.11e and f). Meridional wind components for all other Types explain less than 5 % of the variance in the strength of the UHI in Perth (Figure 5.11).

All Types except Type 3 show statistically significant relationships between zonal components and UHI, but all relationships are weak, with less than 2.7 % explained variance (Figure 5.12). However, we can see from Types 3, 5, and 6 that the coolest UHIs are all associated with moderately strong easterly winds (approximately 5 m/s, Figure 5.12e, d, and f).

By considering Figures 5.11 and 5.12 consecutively, we can see that the coolest UHIs are associated with moderately strong northeasterly to easterly winds. These results might appear counterintuitive as northeasterly to easterly winds suggest advection of warm air towards Perth from Australia's continental interior, which might be assumed to lead to high heat absorption by the urban fabric and thus a warmer UHI at night.
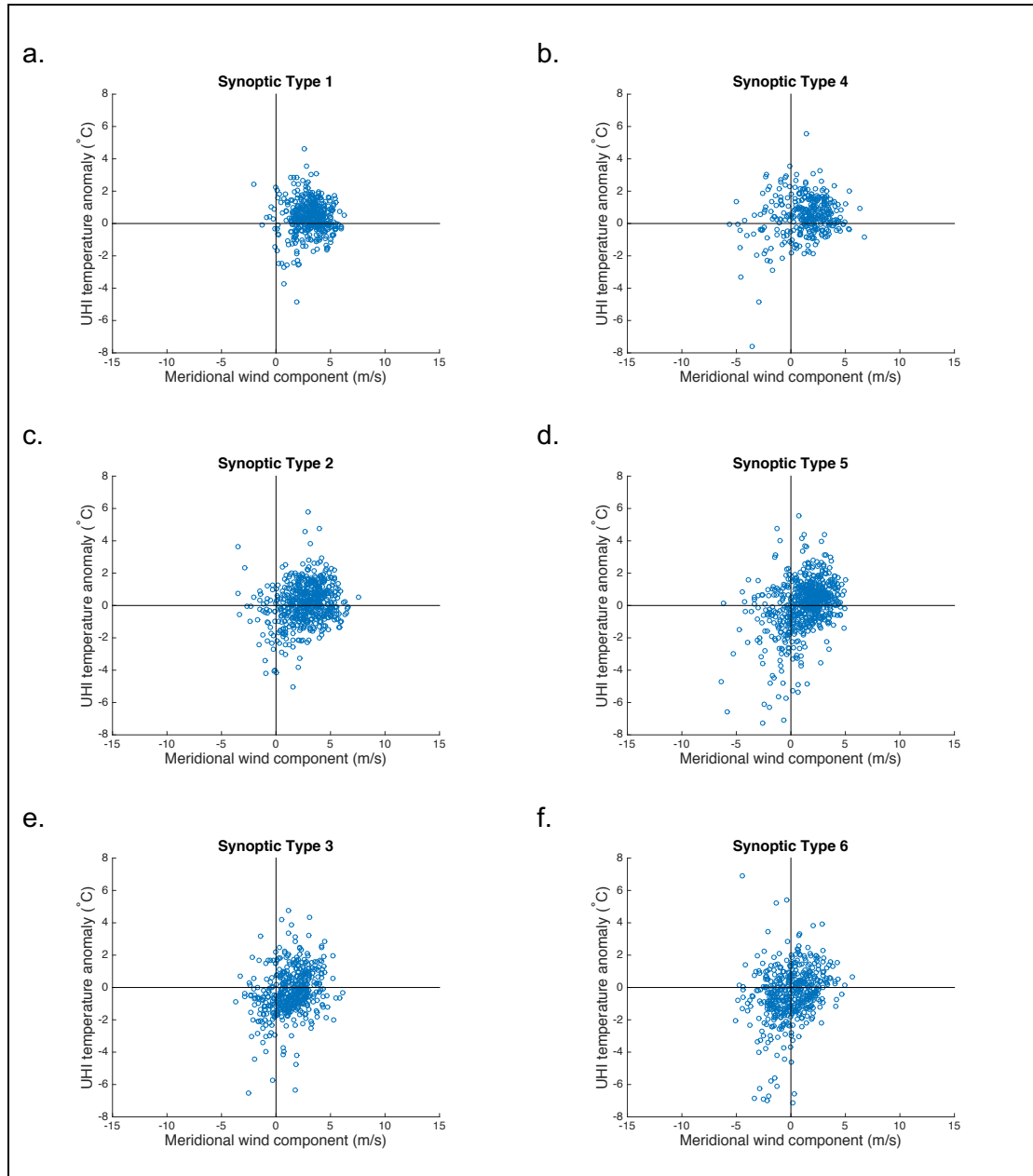
Figure 5.11: Same as Figure 5.7 but for Perth.

Using a case study in Melbourne, Morris and Simmonds (2000) found that a northwesterly wind was responsible for a strong UCI (< -1˚C). They found that the city prevented warm air northwest of the city from being advected to their urban station while the air was able to warm the rural stations. The finding that urban areas can inhibit the advection of warm air might explain our results for Perth. That is, given that Perth's rural stations are located further east than the urban stations, it is possible that when
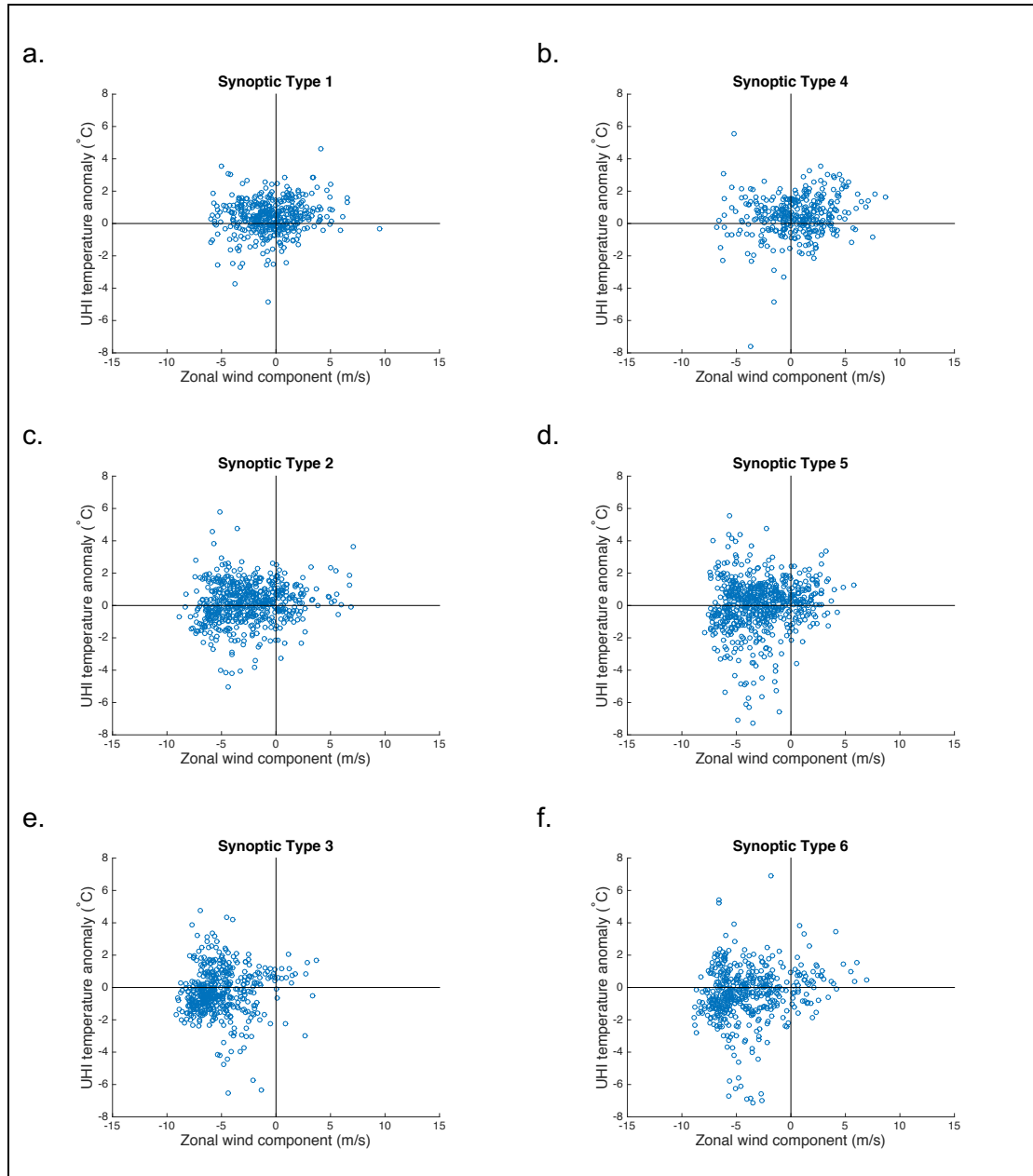
Figure 5.12: Same as Figure 5.8 but for Perth.

winds are northeasterly to easterly, the warm continental air is advected to the rural stations, but not the urban stations, due to the city blocking the advection of the warm air. Further, this hypothesis might explain why Types 3 and 6, which are associated with the advection of air from the warm continental interior (Figure 5.5), have a higher frequency of strongly diminished UHIs than are expected due to chance (Figure 5.6).

This analysis for Perth shows that while the strength of the UHI has a weak relationship with the wind component, this relationship is not always significant and is

dependent on the Synoptic Type. These findings are consistent with those from Chapter 4 that found that all stations, except one urban station, had significantly cooler UHIs when winds were from the east. Relationships between winds and UHI anomalies in Chapter 4 were also found to be weak.

As for our results for Melbourne and Adelaide, Figures 5.11 and 5.12 suggest that the common assumption that weaker winds favour a warm UHI (e.g. Oke 1982; Unger 1996; Morris et al. 2001) is not always the case. That is, the coolest UHIs in Perth, as seen in Types 3, 5, and 6 (Figures 5.11e, d, and f and 5.12e, d, and f), are associated with weak to moderate meridional and zonal wind components, whereas some of the warmest UHIs are associated with moderate easterly winds (Figure 5.12b to f). This analysis also shows that easterly winds in Perth are associated with both the warmest and coolest UHIs, further implying that wind direction is not a major driver of the strength of the UHI.

While the wind components can explain some of the variance in the strength of the UHI anomaly in each of the cities, we again confirm that the wind is not a primary modulator of the UHI. We find that warm continental flow for certain Synoptic Types in Melbourne (Type 4) and Adelaide (Types 5 and 6) is associated with warmer UHIs, whereas in Perth, easterlies are associated with both the warmest and coolest UHIs. As in Chapter 4, this chapter finds consistent results between Melbourne and Adelaide, and contrasting results for Perth, thus further suggesting that aspects of wind speed and/or wind direction are unable to explain why the relationship between heatwaves and the strength of the UHI in Perth is inconsistent with those for Melbourne and Adelaide.

Further, while our analysis of the relationship between wind component and the strength of the UHI shows that a small fraction of the variance in the strength of the UHI can be explained by the wind, the weakness of these relationships is evidence that

the wind does not explain the relationship between Synoptic Type and the strength of the UHI in any city. Rather, we suggest that other factors that are dependent on Synoptic Type, such as radiation loading and the stability of the boundary layer, have a greater effect on the strength of the UHI.

**5.4.2 Heatwaves and synoptic patterns**

Chapter 4 of this thesis showed that heatwaves in Melbourne and Adelaide are typically associated with strongly exacerbated (warmer than normal) UHI events, and heatwaves in Perth with strongly diminished (cooler than normal) UHI events. However, the chapter did not identify a mechanism behind these relationships. The remainder of Chapter 5 examines whether synoptic typing may aid in explaining those results. This is, whether the Synoptic Types associated with heatwaves are typically also coincident with strongly exacerbated or diminished UHIs, even during the entire extended summer season (as described in Section 5.4.1).

Here, we stratify those Synoptic Types described in Section 5.4.1 into extended summer season days (i.e. the pooled group of heatwave and non-heatwave days) and heatwave days only. Note that "heatwave days" refers to nights between the first and final days of the heatwaves to be consistent with Chapter 4. As we describe in Section 5.2.3, we only perform our analysis on MSLP data at midnight (or the closest available time) as relationships between heatwaves and the UHI are strongest at night in all three cities (see Chapter 4).

The Synoptic Types that we identify as being associated with heatwaves are largely consistent with previous studies examining heatwaves and synoptic patterns in Melbourne (Pezza et al. 2012; Boschat et al. 2015; Gibson et al. 2017b), Adelaide, and

Perth (Pezza et al. 2012; Gibson et al. 2017b), despite differences in the methodologies used between the studies.

Synoptic Type distributions during heatwaves are described in Figure 5.13 and compared to those during the extended summer season. For a fair comparison, we generate distributions of extended summer season days that are the same sample size as heatwave days by randomly sampling *n* samples from the extended summer season dataset, where *n* is the number of heatwave days. This process is repeated 10,000 times, with the $5^{th}$ percentile and $95^{th}$ percentile used to produce a 90 % confidence interval. We compute the median as the typical value. Figure 5.13a, c, and e shows that each city has one or two Synoptic Type(s) that occur much more frequently than any others during heatwave days. These are Type 5 in Melbourne, Types 5 and 6 in Adelaide, and Type 6 in Perth. Throughout this Chapter we will refer to these four Synoptic Types as "Dominant Heatwave Types" or "Dominant Types". It is important to note that Dominant Types are not consistent across cities. This is, i.e. even though Type 5 in Melbourne and Adelaide are both associated with heatwaves, they do not represent the same synoptic pattern, however similarities sometimes occur.

As heatwaves consist of three or more consecutive hot days (and two or more consecutive hot nights) it is important to consider the progression of Synoptic Types throughout the heatwaves in each city. Further, we showed in Section 5.4.1 that the progression of Synoptic Types plays a role in maintaining UHI strength in Adelaide and Perth, and to a lesser extent in Melbourne, which might also be important during heatwaves. Figure 5.13 shows the difference in Synoptic Type distributions on all heatwave days (left subplots) compared to those for stratified heatwave days, that is with middle and final days plotted separately (right subplots).
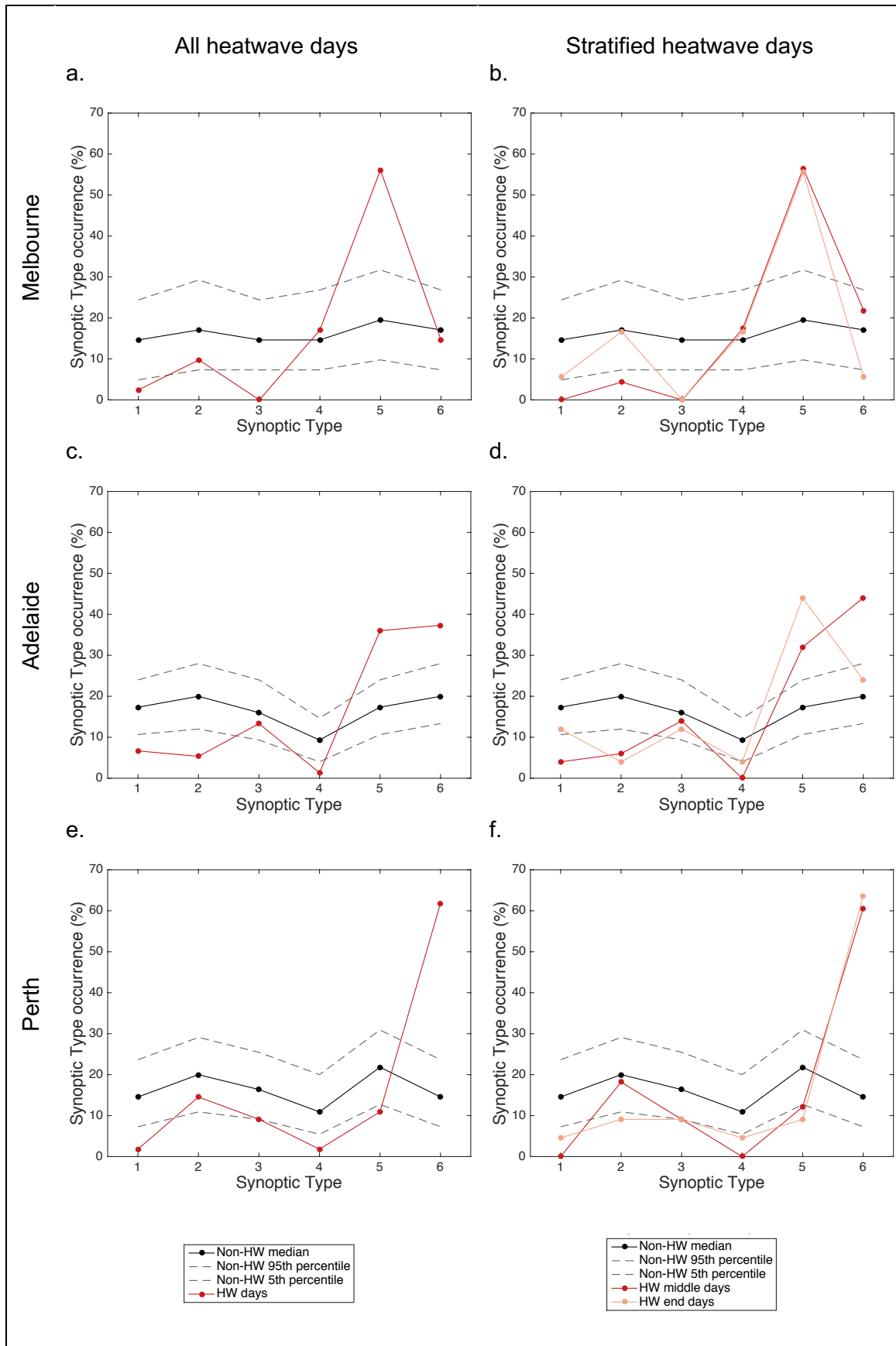
Figure 5.13: The frequency of occurrence of Synoptic Types in Figures 5.1, 5.3, and 5.5 during all heatwave days at midnight (red) in a) Melbourne, c) Adelaide, and e) Perth. Frequency of occurrence of Synoptic Types in Figures 5.1, 5.3, and 5.5 during middle (red) and final (pink) heatwave days in b) Melbourne, d) Adelaide, and f) Perth. Frequency of Synoptic Types during the extended summer season (denoted as non-HW on figures) are determined using random sampling with the median shown by the black solid line, and the 90 % confidence interval shown by the dashed lines.

In Melbourne and Perth, there are negligible differences in the frequency of the Dominant Type for stratified heatwave days when compared to grouped heatwave days (all heatwave days). That is, Type 5 in Melbourne and Type 6 in Perth show very similar frequencies for middle, final, and all heatwave days of approximately 56 % and 62 % respectively (Figure 5.13a, b, e, and f). This suggests that for the duration of a heatwave the Synoptic Types over a city remain fairly consistent because they are slow moving systems (Parker et al. 2013; Nairn and Fawcett 2014). This supports our decision to group the 'middle days' of a heatwave together where the number of days in the heatwave is greater than three (see Chapter 3).

There are some differences between the frequencies of Synoptic Types that occur on the middle and end days of the heatwaves in Melbourne and Perth for the Non-Dominant Types (e.g. Synoptic Types 1 and 2 in Figure 5.13b). However, these differences are small and equate to a handful of days only. Thus, the distributions of the Synoptic Types on the middle and end days of the heatwaves are largely the same and so can be grouped for analysis in Melbourne and Perth.

The greatest differences between middle and final day Synoptic Type frequencies are observed in Adelaide, where the most frequently occurring Type differs for middle and final days (Figure 5.13d). On middle days, Type 6 occurs most frequently (44.0 % of heatwave days) with Type 5 the second most frequently occurring Type (32.0 %). This ranking is reversed on final days where Type 5 occurs most frequently (44.0 %) and Type 6 is the second most frequently occurring Type (24.0 %). Thus, when the middle and final heatwave days are combined, the resulting distribution of Synoptic Types reflects the finding that both Types 5 and 6 occur most frequently during heatwave days (Figure 5.13c). For all heatwave days, Types 5 and 6 occur significantly more frequently than during the entire extended summer season and

account for 36.0 % and 37.3 % of heatwave days respectively. Due to the similarities in the frequencies of each Synoptic Type for middle and final heatwave days, we are justified in examining only the un-stratified heatwave data (all days data). We now describe the Synoptic Types that occur frequently during heatwaves (i.e. the Types that occur as frequently or more frequently than during the entire extended summer season).

Heatwaves in Melbourne are dominated by Synoptic Type 5 (Figure 5.13a), a pre-frontal trough with a high-pressure system to the east, over the Tasman Sea (Figure 5.1) (Pezza et al. 2012; Boschat et al. 2015; Gibson et al. 2017b). This Synoptic Type occurs for the majority of heatwave days (56.1 %), which is significantly more than for extended summer season days (Figure 5.13a). This Synoptic Type is typical of a slow-moving high-pressure system that delays or diverts the passage of a cold front over Melbourne. Thus, temperatures remain high for an extended period of time. This is the only Type that occurs significantly more frequently during heatwaves than during the extended summer season in Melbourne (Figure 5.13a).

Synoptic Types 4 and 6 both occur as frequently during heatwaves as during the extended summer season (Figure 5.13a). These two Synoptic Types represent those conditions that would often occur before (Type 6) or after (Type 4) Synoptic Type 5 (Table 5.2). Type 6 shows a broad high-pressure system centred further east than that in Type 5, whereas Type 4 features a high-pressure system further to the west with a cold-front approaching Melbourne (Figure 5.1). These two events account for a combined 31.7 % of heatwave days (Figure 5.13a).

Types 1, 2, and 3 all have sample sizes of four or less and a frequency of occurrence that is either below the 90 % confidence interval or close to the lower bound. Therefore, these Types are not discussed further as they occur too rarely to produce robust findings.

As described earlier, Adelaide has two Synoptic Types that occur more frequently during heatwaves than the extended summer season; they are Type 5, a high-pressure system over the Tasman Sea with a cold front approaching Adelaide, and Type 6, also a high-pressure system over the Tasman Sea, but with higher surface pressure over the Tasman Sea and the high extending further to the west, thus frontal systems are also located further to the west, i.e. further away from Adelaide (Figures 5.3 and 5.13c).

Synoptic Types 5 and 6 account for 36.0 % and 37.3 % of all heatwave days respectively, a total of 73.3 % of all heatwave days, with both occurring more frequently than during the extended summer season (Figure 5.13c). As heatwaves are defined as consecutive hot days, it is not surprising that the most frequently occurring Synoptic Types are neighbours on the SOM plane (Figure 5.3), with Type 5 often following Type 6 (Table 5.3). The typical progression of these Synoptic Types and the large proportion of heatwave days associated with just two Types suggests that heatwaves in Adelaide are slow moving transitory systems that result in persistent heatwave conditions over a number of days. This is consistent with Chapter 4, which showed that of the three cities examined in this thesis, the longest heatwaves occur in Adelaide, ranging from a minimum of 3 days to a maximum of 10 days in the observations (see Chapter 4).

A smaller proportion of heatwave days occur for Type 3 conditions, which shows a high-pressure system to the south of Adelaide (13.3 %, $n$=10). This Type occurs as frequently during heatwaves and the extended summer season (Figure 5.13c) and often occurs before Type 6 (Table 5.3).

Type 6 for Perth, a high-pressure system to the south of the Great Australian Bight with high-pressure extending to the west (Figure 5.5), is the Synoptic Type that

is most typically observed on heatwave days (61.8 %, Figure 5.13e). Types 2 and 3 also coincide with some heatwaves, but they occur about as frequently as during the extended summer season (14.6 % and 9.1 % respectively, Figure 5.13e). Types 2 and 3 consist of high-pressure systems off the southwest coast of Australia.

The above findings are largely consistent with Pezza et al. (2012), whose MSLP patterns for heatwaves largely resembles the Dominant Heatwave Types in all three cities (Figures 5.1, 5.3, and 5.5). Our findings are also consistent with Gibson et al. (2017b) and Gibson et al. (2017c) who show that heatwaves in Perth are generally associated with a high-pressure system over the Great Australian Bight or to the west/southwest of Perth, and heatwaves in Adelaide and Melbourne tend to be associated with high-pressure systems over the Tasman Sea.

The relationships between heatwaves and the strength of the UHI are now compared to those Synoptic Types identified above to determine the contribution of the synoptic state during heatwaves to the UHI in all three cities.

### 5.4.3 The relationship between heatwaves, strong urban heat islands, and synoptic patterns

By comparing Figures 5.2, 5.4, and 5.6 with Figure 5.13, it is evident that the Dominant Synoptic Types during heatwaves are the same as those Types that provide a favourable environment for the development of a strongly exacerbated (diminished) UHI during the extended summer season in Melbourne and Adelaide (Perth) (see Section 5.4.1). Chapter 4 determined that heatwaves are associated with exacerbated (diminished) UHIs at night in Melbourne and Adelaide (Perth). Thus, it is possible that the Synoptic Type plays a role in modulating the strength of the UHI during heatwaves. Establishing a connection between the strength of the UHI and synoptic patterns during

heatwaves can provide useful information for urban temperature forecasts during heatwave events.

The UHI-heatwave-Synoptic Type relationship is examined in two parts; first we examine the Dominant Synoptic Type(s) that occur during heatwaves in each city and determine whether the distributions of UHI categories are what we expect given the distributions in Figures 5.2, 5.4, and 5.6. This is, for a given Synoptic Type are there more or fewer strongly exacerbated or diminished UHIs during heatwaves compared to the extended summer season. Second, we explore whether the distributions of the strength of the anomalous UHI during heatwaves for the Dominant Heatwave Type(s) differ to those for the Non-Dominant Heatwave Types. For example, during heatwaves in Melbourne, if we see an increase in the frequency of strongly exacerbated UHI events for the Dominant Heatwave Type (Type 5) compared to the extended summer season, is this pattern also visible for the Non-Dominant Synoptic Types (Types 1, 2, 3, 4, and 6)? Through the above analysis we examine whether the increased chance of exacerbated UHIs is most closely associated with the overlying synoptic conditions, or with the increased urban heat storage during heatwave conditions.

We examine UHIs for the Dominant Heatwave Type(s) by stratifying UHIs into quintiles (see Section 5.4.1 for a description of UHI categories). To determine whether there is a higher occurrence of any UHI categories for the Dominant Heatwave Type(s), we compare the frequency of anomalous UHI categories during heatwaves to those during the extended summer season, as shown in Figure 5.14.
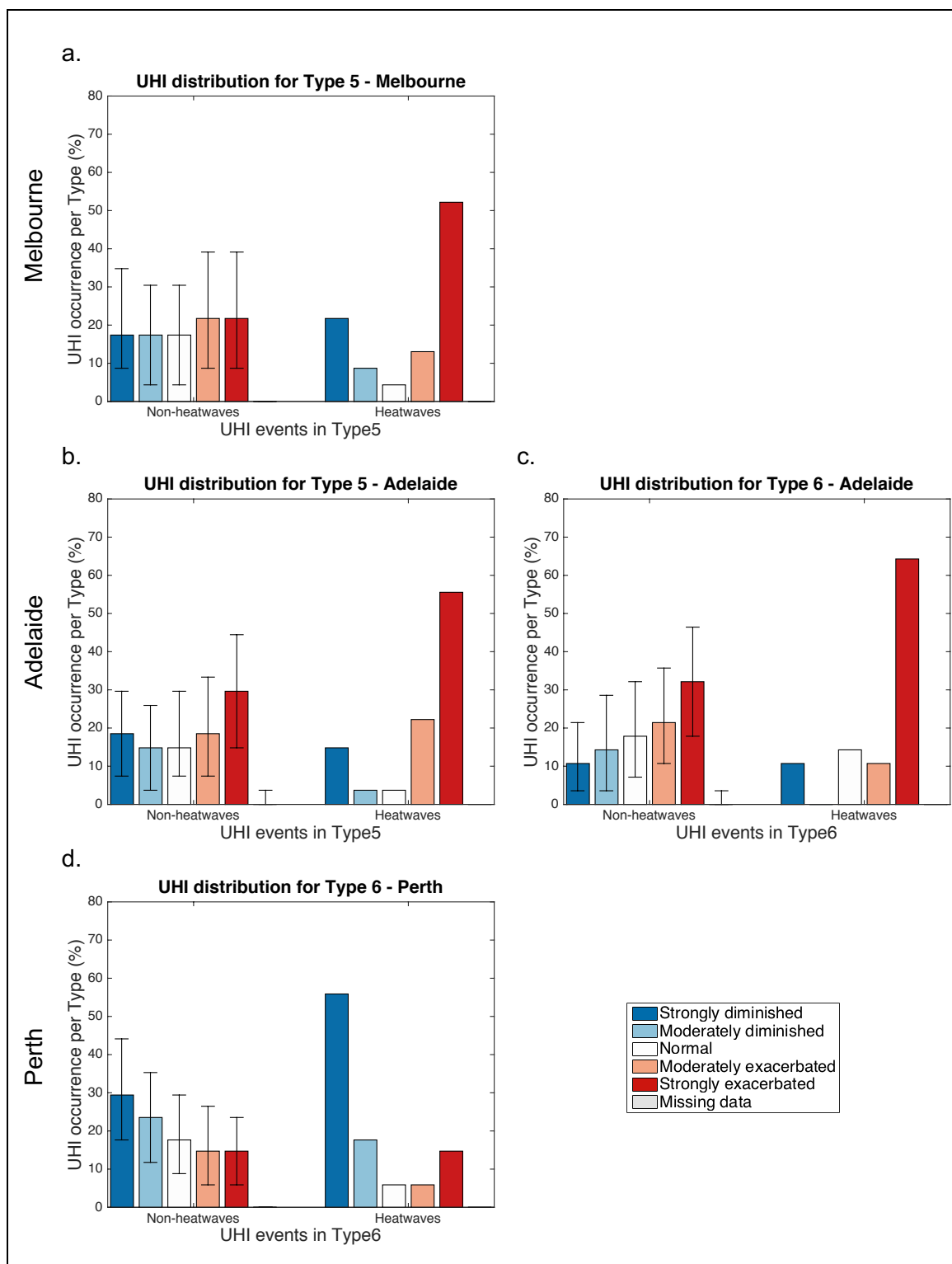
Figure 5.14: Distributions of the anomalous strength of the UHI during heatwaves for a) Type 5 in Melbourne, b) Type 5 in Adelaide, c) Type 6 in Adelaide, and d) Type 6 in Perth. Bars on the left of each subplot show distributions of anomalous UHI strength categories during the extended summer season (labelled non-heatwaves on the subplots). Bars on the right of each subplot show distributions of anomalous UHI strength categories during heatwave days. Extended summer season samples are created using random sampling with replacement of the extended summer season dataset. Error bars show the 90 % confidence interval of the random sampling and the bar height shows the median.

Distributions of the anomalous UHI during the extended summer season for a given Synoptic Type are simulated using bootstrapped random sampling of the extended summer season data to produce replicates with the same sample size as for the heatwave days. Each random sample consists of $n$ samples, where $n$ is the number of heatwave days for the Synoptic Type in question. We produce 10,000 bootstrapped replicates for a robust calculation of a 90 % confidence interval of the frequency of occurrence for each UHI category. This random sampling estimates the expected distribution of the extended summer season data for the same sample size as the heatwave dataset. Thus, we can determine whether the distributions of the anomalous UHI that occur for the Dominant Heatwave Types during heatwaves is likely due to chance, or whether there is a statistically significant difference in the distribution compared to those days in the extended summer season.

As described in Section 5.4.2, Synoptic Type 5 occurs most frequently during heatwaves in Melbourne ($n$ = 23, Figure 5.13a). Strongly exacerbated UHI events account for 52.2 % of Type 5 heatwave days (Figure 5.14a). This is significantly more than during the extended summer season as the frequency lies above the upper bound of the 90 % confidence interval for extended summer season days (39.1 %, Figure 5.14a). Thus, UHIs in Type 5 are more likely to be strongly exacerbated during heatwaves than during the extended summer season.

Other UHI categories lie within the 90 % confidence interval. This means that during heatwaves there are no significant changes in the frequency of occurrence of any UHI categories other than the strongly exacerbated group.

Synoptic Types 5 and 6 in Adelaide, the Dominant Heatwave Types, show similar distributions of anomalous UHI strengths to one another on heatwave days (Figures 5.14b and c). Both Synoptic Types have a significantly higher than expected

proportion of strongly exacerbated events (55.6 % and 64.3 % respectively) during heatwaves compared to the extended summer season. Each Synoptic Type also shows a significant decrease in one UHI category. Type 5 shows a decrease in normal UHIs and Type 6 shows a decrease in moderately diminished UHIs compared to the extended summer season. Therefore, heatwaves that occur in either of these Types are more likely to have strongly exacerbated UHIs than extended summer season days in the same Types.

Heatwaves that occur in Synoptic Type 6 in Perth have an UHI that is strongly diminished 55.9 % of the time (Figure 5.14d). This means that heatwaves occurring with this Type are significantly more likely to have a strongly diminished UHI when compared to the extended summer season (Figure 5.14d).

Concurrently, normal UHIs during heatwaves in Perth significantly decrease in frequency during heatwaves (Figure 5.14d). However, the significance of this result is sensitive to the bootstrap sampling and therefore is not robust.

Figure 5.14 shows that the distribution of anomalous UHI for the Dominant Heatwave Types in Figures 5.2, 5.4, and 5.6 are amplified during heatwaves for all three cities. That is, if a particular Synoptic Type typically has a high proportion of strongly exacerbated (diminished) events, this proportion increases when heatwave days only are considered. We do not undertake the above analysis for those Synoptic Types where there are fewer than 20 samples during heatwaves as the results would not be robust, thus we are not able to examine the Non-Dominant Synoptic Types in detail.

The distributions of the anomalous UHI categories during heatwaves for each Synoptic Type are shown in Figure 5.15. From a brief examination of this figure it is not clear whether these distributions differ significantly between Synoptic Types. Although there is a pre-disposition toward strongly exacerbated or diminished UHIs in

all three cities due to the Synoptic Type(s), our results suggest that the Synoptic Type becomes less important relative to the capacity for thermal energy storage during heatwave conditions. This is, during heatwaves in Melbourne and Adelaide, it is the heatwave itself that provides the first order effect on the strength of the UHI because very hot conditions and high radiative loading increase thermal storage in urban surfaces. The mechanism behind the strongly diminished UHIs in Perth during heatwaves remains unclear. This hypothesis is difficult to test as the sample sizes in the Non-Dominant Synoptic Types are small (10 or fewer samples in each Non-Dominant Type during heatwaves). Thus, it is unclear whether they show statistically similar distributions of anomalous UHI to the Dominant Synoptic Type(s) or whether the distributions are different.

To understand the relationship between UHIs and Synoptic Types during heatwaves further, we group the distributions of anomalous UHIs for all Non-Dominant Types and compare them to those for Dominant Heatwave Type(s) in each city. For example, for Melbourne, we compare the UHIs for heatwaves that occur during Type 5 (the Dominant Type) to those that occur in a pooled dataset of Types 1–4 and 6 (Non-Dominant Types). This provides an indication as to whether distributions of anomalous UHI strengths robustly differ between Synoptic Types during heatwaves and the extended summer season. Sample sizes for the combined sets of Non-Dominant Heatwave Types are 18 in Melbourne, 20 in Adelaide, and 21 in Perth. These sample sizes are comparable to those for the Dominant Types, which are 23, 55, and 34 respectively. The results of this analysis are shown in Figure 5.16.
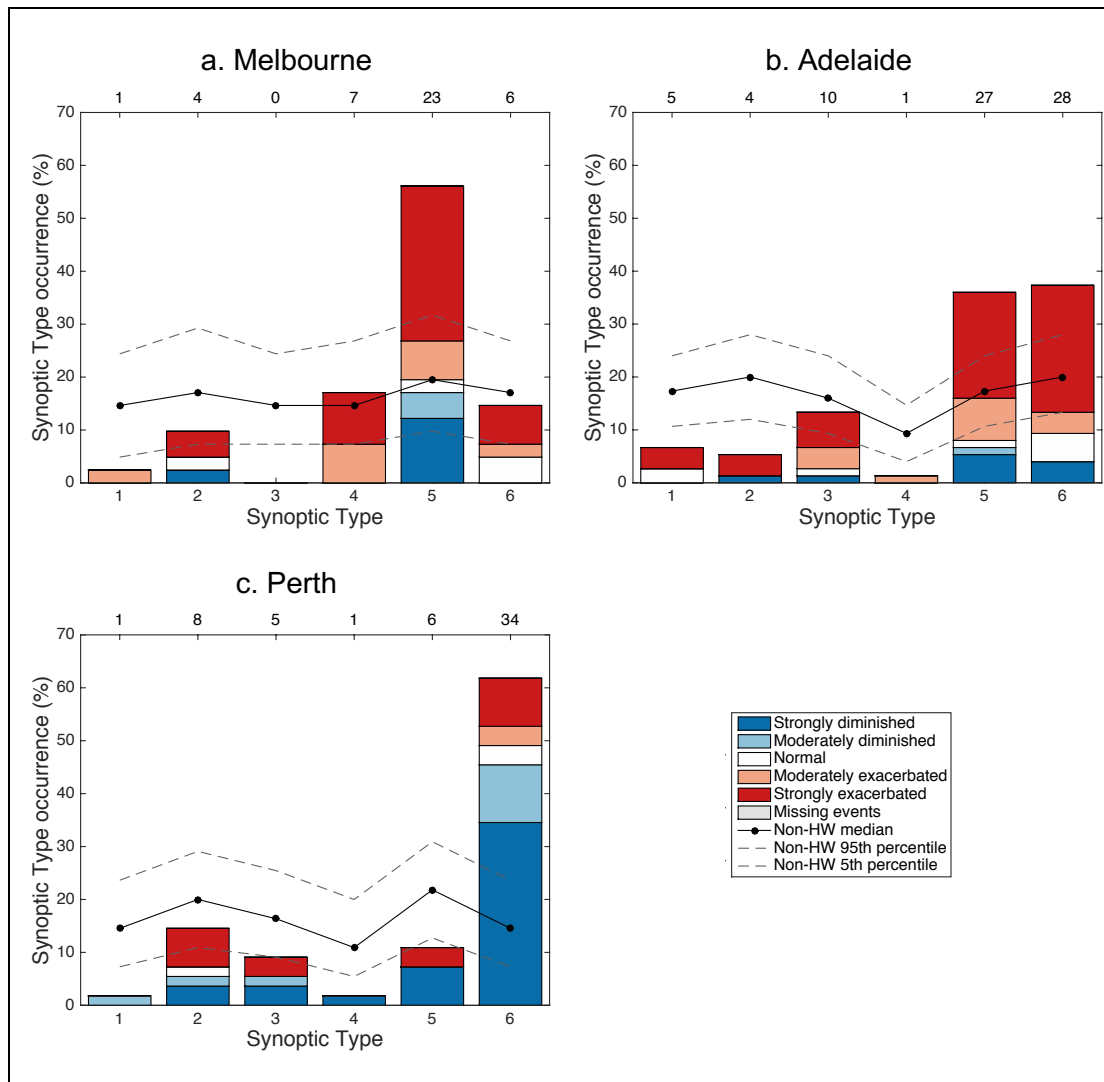
Figure 5.15: Stacked bar plots showing the distribution of UHI events in each Synoptic Type (x-axis) stratified into five categories: strongly exacerbated (red), moderately exacerbated (pink), normal (white), moderately diminished (light blue), and strongly diminished (dark blue). Grey bars indicate missing data at all urban stations and/or all rural stations. See Chapter 3 for more information on missing data. Black, circle markers with solid lines indicate the median percentages of occurrence of each Synoptic Type for extended summer season days (y-axis). The 90 % confidence intervals of Synoptic Type frequency on extended summer season days for each Type are shown with grey, dashed lines. The extended summer season is referred to as non-HW in the figure. Median percentages of occurrence and confidence intervals of extended summer season days are created using random sampling of the entire extended summer season (i.e. heatwave and non-heatwave data) with bootstrapping. Values on the upper x-axis show the number of heatwave events in each Synoptic Type.

Figure 5.16 shows similar distributions of UHIs between the Dominant and Non-Dominant Types for Melbourne and Adelaide. This is particularly noticeable in Adelaide where there are similar frequencies between Non-Dominant and Dominant Synoptic Types for all five UHI categories, most notably, the high rate of occurrence of strongly exacerbated events (55.0 % and 60.0 % respectively, see Figure 5.16b). Melbourne also shows similar frequencies for strongly exacerbated UHI events for the

pooled Non-Dominant Types (50.0 %) and the Dominant Type (52.2 %) that occurs during heatwaves (Figure 5.16a).
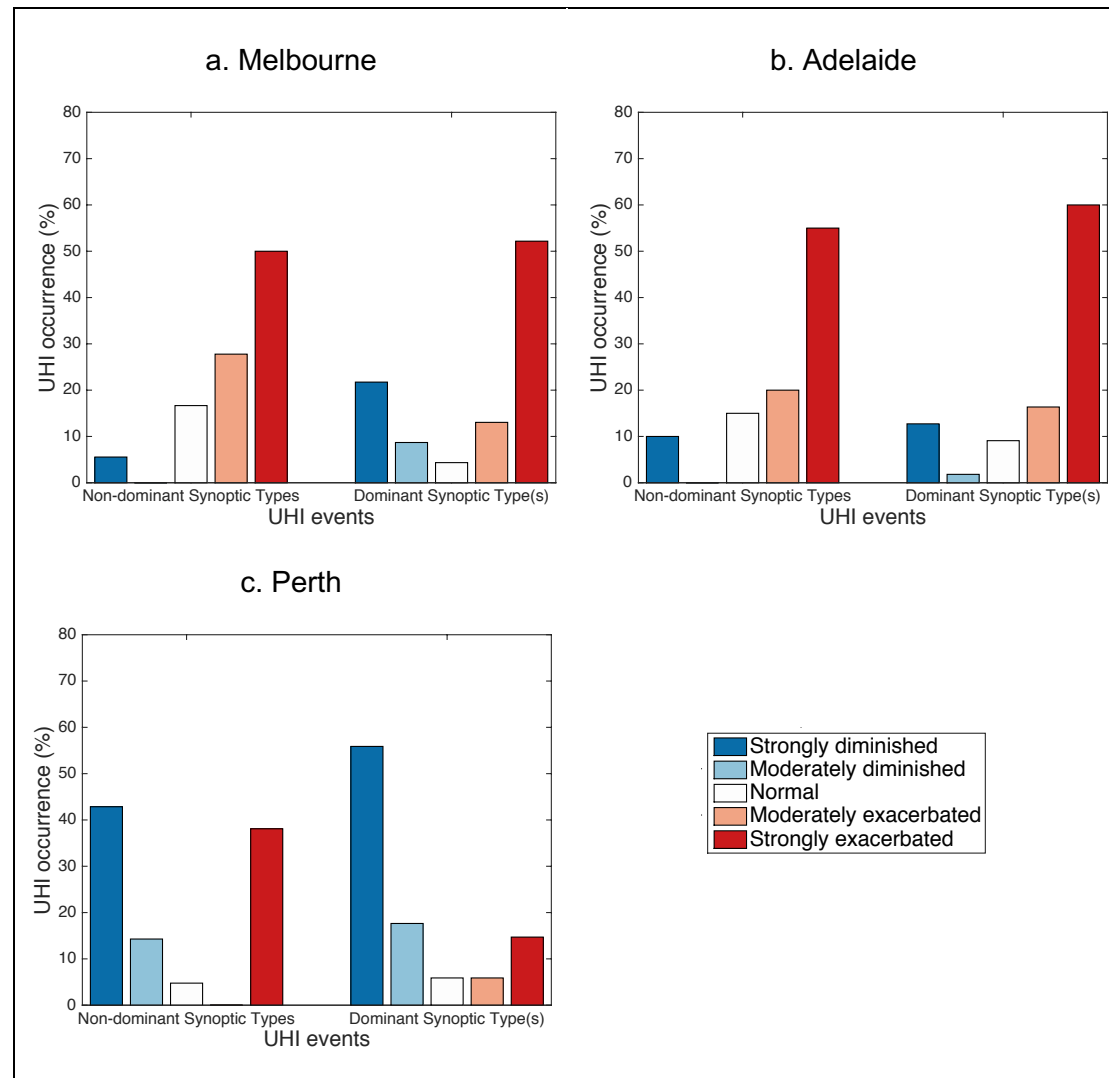


Figure 5.16: Bar plots showing distributions of the anomalous UHI during heatwaves for the pooled Non-Dominant Heatwave Types (left) and Dominant Heatwave Types (right). UHI events in each Synoptic Type are stratified into five categories: strongly exacerbated (red), moderately exacerbated (pink), normal (white), moderately diminished (light blue), and strongly diminished (dark blue). Subplots show distributions for a) Melbourne, b) Adelaide, and c) Perth. Dominant Heatwave Types comprise Type 5 in Melbourne, Types 5 and 6 in Adelaide, and Type 6 in Perth. Pooled Non-Dominant Types consist of all remaining Types.

Perth shows some differences in the distributions of the UHIs between the Dominant and Non-Dominant Synoptic Types. While strongly diminished UHI events remain the most frequently occurring UHI category (42.9 % and 55.9 % for Non-Dominant and Dominant Types respectively), there are notably more strongly

exacerbated UHIs for the Non-Dominant Types (38.1 %) when compared to the Dominant Types (14.7 %, Figure 5.16c). Thus, there is some evidence that the strength of the anomalous UHI during heatwaves in Perth is at least partially dependent on the overlying synoptic conditions. However, the dependence of the strength of the UHI in Perth on the synoptic environment only provides a partial explanation as to why there is typically a strongly diminished UHI in Perth during heatwave conditions, as shown in Chapter 4. This is because there is still a high proportion of strongly diminished events in Perth during heatwaves for all Synoptic Types, not just those Types typically associated with diminished UHI events.

Our results demonstrate that while all three cities show an amplification of the distributions of the UHI categories for those Synoptic Types that are pre-dominant during heatwaves, these patterns are not necessarily unique to those Dominant Synoptic Types. That is, a similar pattern also occurs in those Synoptic Types that are less common during heatwaves, i.e. the Non-Dominant Types. This is particularly prevalent in Melbourne and Adelaide, but less so in Perth. Our finding that UHI patterns during heatwaves for Non-Dominant Types are very similar to those identified for Dominant Types in Melbourne and Adelaide implies that the presence of a heatwave is a better predictor of an exacerbated UHI in these cities than is Synoptic Type. Our results for Perth on the other hand suggest that the city may experience a stronger relationship between synoptic pattern and the strength of the UHI, but without a larger sample of heatwave data, this hypothesis is difficult to confirm.

To determine whether the distribution patterns for UHI strength in Figure 5.16 for Non-Dominant Types are unique to heatwave events, i.e. they aren't an enhanced form of the pattern present during the extended summer season, we replicate this analysis in Figure 5.17 using data for the entire extended summer season.
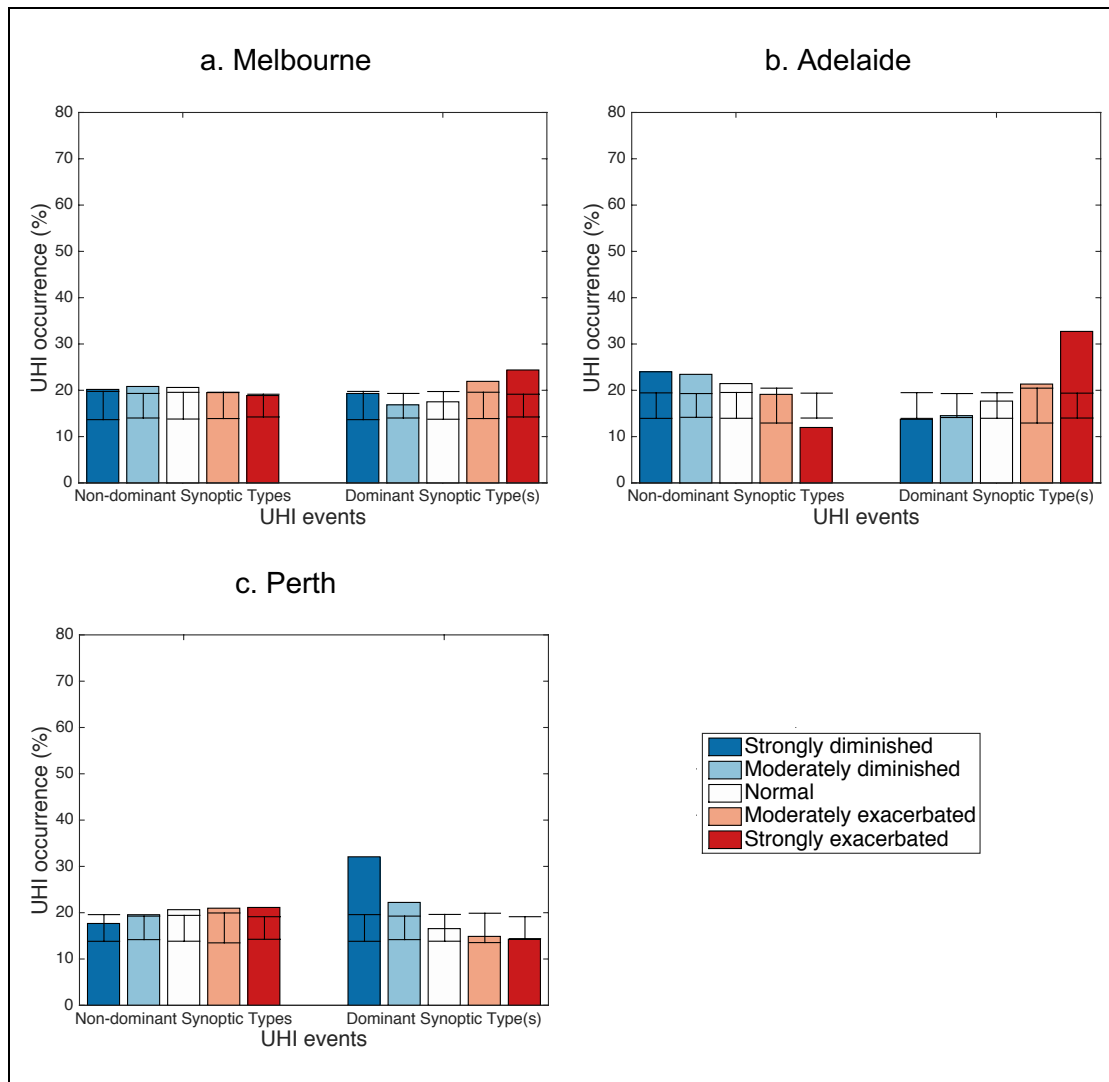
Figure 5.17: Bar plots showing distributions of anomalous UHI categories for the extended summer season for Non-Dominant Heatwave Types (left) and Dominant Heatwave Types (right). UHI events in each Synoptic Type are stratified into five categories: strongly exacerbated (red), moderately exacerbated (pink), normal (white), moderately diminished (light blue), and strongly diminished (dark blue). Subplots show distributions for a) Melbourne, b) Adelaide, and c) Perth. Error bars show the 90 % confidence interval.

Comparing Figures 5.16 and 5.17 clearly demonstrates that the distributions of the UHI categories differ for heatwave periods when compared to the entire extended summer season. Figure 5.16 shows similar distributions of the anomalous UHI between Dominant and Non-Dominant Heatwave Types, whereas the same analysis for the extended summer season show distinctly different patterns (Figure 5.17).

The main discrepancy between the distributions of anomalous UHI categories for heatwave and extended summer data for each city is the difference in the range of frequencies of the UHI categories. Where UHI category frequencies vary between

about 5 % and 60 % for heatwave days, they range from approximately 12 % to 30 % for the extended summer season. This shows that the UHI is more predictable on heatwave days than the extended summer season days, most likely due to a greater capacity of the urban form to retain heat.

The second most notable difference between Figures 5.16 and 5.17 is the fact that the distributions of the UHI categories for Dominant Type(s) and Non-Dominant Types look broadly similar in Figure 5.16, but not in Figure 5.17. That is, during heatwaves in Melbourne and Adelaide, there are high frequencies of strongly exacerbated UHI events for both the Dominant and Non-Dominant heatwave groupings, whereas Perth sees mainly strongly diminished events (Figure 5.16). Conversely, Figure 5.17 shows that there are more notable differences between the Dominant and Non-Dominant groups for the extended summer season, i.e. all days, heatwaves and non-heatwaves alike. That is, the Dominant Type(s) in Melbourne and Adelaide experience mainly exacerbated UHIs whereas the Non-Dominant groupings experience more diminished UHIs. Similarly, in Perth, the Dominant Type experiences mainly diminished UHIs but the Non-Dominant Types experience more exacerbated UHIs. From this analysis we conclude that the UHI on heatwave days is less dependent on Synoptic Type than it is on extended summer season days and that any influence of Synoptic Types on the strength of the UHI during heatwaves is overwhelmed by the presence of the heatwave. Conversely, the Synoptic Type has a stronger role to play in modulation of the UHI on extended summer season days.

## 5.5 Discussion

In Section 5.4 we determine the relationships between Synoptic Type, the strength of the UHI, and the presence of heatwaves in Melbourne, Adelaide, and Perth. We also investigate whether Synoptic Type is likely to be an important driver of the relationship between heatwaves and UHIs as identified in Chapter 4. Ultimately, our results provide evidence that for heatwaves, it is the presence of the heatwave and the associated high radiative loading and very warm temperatures that contribute to the anomalous UHI in Melbourne and Adelaide. The results for Perth show that synoptic conditions might play some role in modulating a diminished UHI, but they are not the dominant factor. The reason why Perth shows strongly diminished UHIs during heatwaves remains unclear. For those Synoptic Types that are most frequently associated with heatwaves, the distribution of UHI categories is enhanced during heatwaves conditions (Figure 5.14). Notably these are Types that are associated with strongly exacerbated (strongly diminished) UHIs in Melbourne and Adelaide (Perth) over the entire extended summer season.

While the above findings suggest that Synoptic Type contributes to the strength of the UHI during heatwaves, we also show that UHI categories for Non-Dominant Heatwave Types during heatwaves (grouped, see Figure 5.16) tend to produce similar patterns to those of the Dominant Heatwave Type(s). These findings are largely consistent across all three cities, but similarities are weaker in Perth. We therefore hypothesise that the presence of the heatwave is more influential to the strength of the UHI than Synoptic Type. While we identify a relationship between UHIs and synoptic patterns during the warmer months (November to March), this Synoptic Type-UHI strength relationship weakens in the presence of a heatwave. While Figure 5.16c shows some evidence that synoptic patterns have an effect on the strength of the UHI during

147

heatwaves in Perth, this hypothesis is difficult to test robustly given the limited availability of AWS data.

Further, the similar distributions of anomalous UHI categories for all Synoptic Types (Dominant and Non-Dominant Types) during heatwaves suggest that heat storage is the main driver of the strength of the UHI on heatwave days. Sun et al. (2017) show that urban landscapes are able to store more heat on extremely hot days, i.e. heatwaves, than on cooler days, thus releasing more stored heat at night into urban areas. This may lead to a warmer UHI, and increases the likelihood of a strongly exacerbated UHI event occurring.

The above hypothesis can explain why strongly exacerbated UHIs are more frequent in Melbourne and Adelaide during heatwaves, and can also explain why the distribution of UHI categories is similar across all Synoptic Types when there is a heatwave. This idea suggests that a large enough increase in heat loading in urban areas has the ability to overpower the influence that Synoptic Type has on the UHI. More research would be required to determine whether this relationship holds for all hot days or only for heatwaves as is studied here.

However, this hypothesis does not appear to explain why the UHI is occasionally strongly diminished during heatwaves in Melbourne and Adelaide (Figure 5.15a and b) or why Perth predominantly experiences strongly diminished UHIs during heatwaves (Figures 4.1 and 5.15c). In Chapter 4 we hypothesised that a potential relationship between heatwaves, UHIs, and Synoptic Types might explain why we get vastly different results in Chapter 4 for Perth than for Melbourne and Adelaide. However, we were unable to find evidence of this relationship with the available data.

As described in Chapter 4, our lack of inclusion of soil moisture in this study is a potential limitation. Soil moisture is influential to the strength of the UHI (Jacobs et

al. 2017) and heatwave intensity (Herold et al. 2016) in Australia, therefore soil moisture variability is likely to affect UHIs during heatwaves in Melbourne, Adelaide, and Perth. That is, if a heatwave was to occur during a period when soil moisture was low, then the resulting UHI might be different to an UHI that occurred when a heatwave was present during a period of higher soil moisture. However, this analysis is beyond the scope of this PhD.

The effect of soil moisture on the strength of the UHI may be able to explain our results for Perth, whereby strongly diminished UHIs occur more frequently than expected during heatwaves. From satellite images (Google Earth, not shown), the rural stations surrounding Perth are sparsely vegetated with grasses or native vegetation, thus if water is limited during extremely hot conditions, the evapotranspiration rate is likely to drop significantly (Reichstein et al. 2013) and the dry earth may act in a similar way to urban building materials, that is, most of the incoming solar energy would be partitioned into sensible energy and stored in the rural landscape during the day then released at night. This would erode any UHI effect felt by the city at night. This hypothesis is supported by the findings of Scott et al. (2018), who showed that UHIs decrease with increasing temperatures due to larger temperature increases in rural areas than in urban areas. They found that the coolest UHIs during heat events occured in cities located in the southwest of the USA, i.e. in a geographically similar location to Perth. Further, if urban areas are irrigated to prevent vegetation loss during hot weather, this might further diminish the UHI. This hypothesis may also explain why UHIs are occasionally diminished during heatwaves in Melbourne and Adelaide.

Given that Chapters 4 and 5 both note small significant relationships between easterly winds and the strength of the UHI in Perth, and since Perth's rural stations are all located further east than the urban stations, it is possible that hot continental

easterlies warm the rural stations during heatwaves but are unable to penetrate the urban areas. Morris and Simmonds (2000) note a similar phenomenon in Melbourne, whereby the urban area prevents the advection of warm air from rural areas, thus the city remains relatively cool compared to the rural stations.

Further research is required to determine whether the above hypotheses are correct. Specifically, an examination of diurnal changes in temperatures and soil moisture at individual stations on heatwave days and during the extended summer season may help to determine whether hot continental air is able to advect into Perth's urban areas on heatwave days with strongly diminished UHIs.

As mentioned in Chapter 4, one of the major limitations of this research is the limited sample sizes; including number of heatwaves and availability of AWS data for stations with suitable temporal extent. This lack of data affects the number of heatwaves we have to work with and means that sample sizes are often too small to allow detailed statistical analysis to be carried out. We are unable to perform statistical analysis on individual Non-Dominant Types during heatwaves due to small numbers of events, thus we cannot determine whether UHI distributions for each of these Types differ significantly between heatwave periods and the extended summer season. This could help us determine whether the presence of a heatwave generally overpowers the influence of Synoptic Type on UHI patterns during heatwaves. See Chapter 4 for a more discussion of the limitations of sample size on this study.

Pezza et al. (2012) and Gibson et al. (2017b) both identify the synoptic patterns that occur during heatwaves over Melbourne, Adelaide, and Perth. Our methodology for identifying Synoptic Types is similar to that of Gibson et al. (2017b), that is we both identify a number of Synoptic Types then determine in which Types the heatwaves occur. Pezza et al. (2012) on the other hand determines the composite of MSLP for all

heatwave days. Despite differences in methodologies, the synoptic patterns from both of these studies are similar to those identified in our research, suggesting that the results are robust.

To date, a study by Morris and Simmonds (2000) on the UHI in Melbourne remains the only research to investigate the connection between synoptic conditions and UHIs in Australia. However, their methodology differs to ours in a number of ways. Morris and Simmonds (2000) find composites of MSLP for pre-defined UHI categories, while we use the opposite approach and examine the strength of the UHI for each of our pre-defined Synoptic Types. Furthermore, the stations used to calculate the UHI and the time periods over which Morris and Simmonds (2000) examined the UHI are not consistent with this thesis.

Despite the differences in the studies, there is consistency between the results of Morris and Simmonds (2000) and what we show here. For example, Morris and Simmonds (2000) noted a relationship between high-pressure systems centred along the southeast coast of Australia (a hybrid of Types 4, 5, and 6 in Figure 5.1) and warm UHIs. We find that as well as Types 4 and 5, Type 1, a post-frontal system, is associated with strongly exacerbated UHIs. This Type is most similar to a synoptic pattern in Morris and Simmonds (2000) that is associated with a 0˚C to 1˚C UHI, showing that this Synoptic Type is associated with positive UHIs for both studies.

Another important difference between our study and Morris and Simmonds (2000) is that they examined UHIs over the entire year, whereas we limit our analysis to the extended summer season (November to March). The authors note that stronger UHIs occur more frequently in the summer, therefore the synoptic patterns identified in their study may differ if developed using summer data only.

In a recent study, Scott et al. (2018) identify a relationship between synoptic weather conditions and UHIs in many cities in the USA. Rather than examining MSLP patterns as we have, the authors compare UHIs on moist days to those on dry days, finding that the strength of the UHI is reduced for moist weather conditions. However, given that heatwaves in southern Australia tend to be predominantly associated with dry conditions (Boschat et al. 2015), if there exists a similar relationship between Australian synoptics and UHIs, it is not likely to be relevant for the majority of heatwaves in Melbourne, Adelaide, and Perth.

## 5.6 Conclusions

The results in this chapter show that in all three cities, particular synoptic weather patterns are associated with a greater frequency of heatwaves. In Melbourne and Adelaide (Perth), these Types are also associated with anomalously warm (cool) UHIs, during both heatwave periods and the extended summer season. Thus, our results show that the synoptic conditions pre-dispose the overlying atmosphere toward a state that is favourable for the formation of a stronger or weaker than normal UHI. We demonstrate that outside heatwave conditions, overlying synoptic conditions are an important factor in determining whether there will be an UHI and the strength of that UHI. Our results show that the mechanisms for the relationships between synoptic conditions and UHIs are different for Melbourne and Adelaide than they are for Perth.

However, we also show that the dominant mechanism affecting the strength of the UHI changes during heatwaves. That is, during heatwaves the UHI is more strongly affected by the presence of the heatwave rather than a pre-disposition toward greater/lesser heat loading by synoptic patterns. However, how this manifests in each city is different. Melbourne and Adelaide show mostly exacerbated UHIs during

heatwaves that are unrelated to Synoptic Type. Conversely, Perth shows mostly diminished UHIs during heatwaves while also showing some evidence that Synoptic Types may influence UHIs during heatwaves, but we are unable to determine this conclusively. As described in the Section 5.5, the reasons for the differences between the cities are unclear, but we speculate that this could be related to the behaviour of the rural stations, rather than the urban stations in Perth.

# 6. Future synoptic patterns, relationships with heatwaves, and implications for the urban heat island

## Abstract

This chapter examines changes to synoptic patterns under high (RCP8.5) and moderate (RCP4.5) future radiative forcing pathways, and uses these changes to examine possible future changes to those synoptic environments that are related to UHIs of certain strengths in the present day. Further, we examine the relationship between synoptic patterns and heatwaves and how this may change in the future and provide a discussion of the implications for the UHI.

Our analysis uses projections from three climate models and shows that those synoptic patterns that are associated with strongly diminished (exacerbated) UHIs in Melbourne in the present day become more (less) likely in the future. Results for Adelaide suggest future synoptic patterns that presently favour weaker UHIs are likely to occur more frequently, whereas results for Perth show more variability across the models and therefore the likely direction of change in synoptic patterns is less clear.

The model experiments show a weakening of the relationship between heatwaves and synoptic patterns in the future in Melbourne and Perth, with a larger range of synoptic patterns being associated with future heatwaves. In Adelaide, this relationship is projected to stay relatively unchanged in the future. However, these changes are model dependent.

## 6.1 Introduction

While the UHI is a well-known phenomenon and has been quantified in many cities around the world, future changes in the strength of the UHI are not well understood. As described in Chapter 1, increasing rates of urbanisation due to population growth (e.g. Coutts et al. 2008; Argüeso et al. 2014) and increases in heat loading due to climate change (e.g. Sachindra et al. 2016; Roberge and Sushama 2018; Scott et al. 2018; Zhang and Ayyub 2018) are two of the most well understood influences on the future strength of the UHI.

In Chapter 5 we showed the strength of the UHI in southern Australian cities to be closely related to the overlying synoptic patterns. The strong association between synoptic patterns and the strength of the UHI provides another potential source of modulation of the UHI into the future. Furthermore, synoptic patterns are expected to change in the future with climate change (e.g. Demuzere et al. 2009; Gibson et al. 2017c). While various studies have examined how the UHI will change in the future due to changes in urbanisation and/or climate change (Sachindra et al. 2016; Roberge and Sushama 2018; Zhang and Ayyub 2018) and other studies have examined the influence of synoptic patterns on past UHIs (Morris and Simmonds 2000; Beranová and Huth 2005; He et al. 2013), no studies have examined how those synoptic patterns related to particular strengths of the UHI might change with anthropogenic climate change. This chapter will bridge this gap by examining whether Synoptic Types that are associated with warmer or cooler UHIs are expected to increase or decrease in frequency with anthropogenic climate change.

We note that potential changes in the strength of the UHI associated with future synoptic pattern changes are independent of any modifications to urban environments and therefore may act to enhance or weaken changes to the UHI due to increased

urbanisation or changes to the urban fabric. We do not assess these factors in this chapter and focus on synoptic patterns only.

Here, we make the assumption that the relationships between the synoptic environment and the UHI will remain somewhat stationary into the future. Beranová and Huth (2005) showed trends in the strength of the UHI in Prague, Czech Republic, associated with various synoptic patterns from 1961 to 1990. They found that increases in the strength of the UHI under anticyclonic patterns were larger than those under cyclonic patterns. However, these results do not elucidate whether or not the relationships between synoptic patterns and the strength of the UHI are non-stationary i.e. change in any significant way. Their results suggest only differences in the UHI trends between synoptic patterns, which is likely to be dominated by changes to land surface factors. Given the strong relationships identified in Chapter 5, we argue that examining changes in the synoptic patterns associated with UHIs of certain strengths is a worthwhile exercise for elucidating any influence of synoptic patterns as a modulating mechanism on the UHI.

While we know that heatwaves in Australia will get hotter, longer, and more intense due to climate change (Perkins et al. 2012; Perkins and Alexander 2013; Cowan et al. 2014a; Cowan et al. 2014b), the effect of heatwaves on urban populations is not as clear due to the relationships between heatwaves and the UHI identified in Chapter 4. This influence of future heatwave on the UHI is especially unclear given the inconsistent relationships between these two factors in Melbourne and Adelaide compared to Perth. Since Chapter 5 showed that synoptic patterns have a relationship with both heatwaves and the strength of the UHI, we now examine changes in future synoptic patterns and draw conclusions about how these changes might affect future heatwaves and the strength of the UHI. This chapter shows how the changes in Synoptic

Types that are most strongly associated with either heatwaves or strong anomalous UHIs (i.e. strongly exacerbated or strongly diminished UHIs) in the present day will change over the southern Australian cities of Melbourne, Adelaide, and Perth. The differences between high and moderate radiative forcing pathways are described.

## 6.2 Data

This study uses observational and model data for analysis. The projections of future changes to the synoptic conditions associated with the UHI are performed using climate model simulations. However, we first validate the ability of the models to simulate MSLP patterns over the extended summer season and during heatwave conditions by comparing the model output to the observational data. Here, we briefly describe the datasets used throughout Chapter 6, but a more comprehensive description is provided in Chapter 2.

### 6.2.1 ACORN-SAT data

As described in Chapter 2, daily maximum and minimum dry-bulb temperature data from the Bureau of Meteorology's high quality Australian Climate Observations Reference Network – Surface Air Temperature (ACORN-SAT) dataset are used to identify heatwaves from the observational period for the extended summer season from January 1995 to March 2014. We use the stations closest to the centre of each city, these are: Melbourne Regional Office (MRO, #86071), Adelaide (Kent Town, #23090), and Perth Airport (#9021). This is consistent with Chapters 4 and 5.

### 6.2.2 ERA-Interim data

Six-hourly ERA-Interim MSLP data are used to determine MSLP patterns for the observational period. We use these data to produce the SOMs used throughout this chapter and to examine the distribution of synoptic weather patterns for comparison with the climate model simulations. While the ERA-Interim data are reanalysis data we refer to it as observational data throughout this work. To be consistent with Chapter 5 we perform our analysis in this chapter at midnight only. Since ERA-Interim data are six-hourly in UTC we are unable to get data at midnight for all three cities, we therefore select the data closest in time to midnight. We make the assumption that there are no significant changes in MSLP patterns between the times used and midnight.

### 6.2.3 CMIP5 data

The climate model simulations are taken from the CMIP5 archive. Daily MSLP data are procured from three CMIP5 models, ACCESS1-3, MPI-ESM-LR, and MRI-CGCM3 (henceforth referred to as the ACCESS, MPI and MRI models). The models are described in detail in Chapter 2. These models are chosen as they represent MSLP patterns over southern Australia well during heatwaves (Purich et al. 2014; Gibson et al. 2017a) and over the entire calendar year (Gibson et al. 2016).

We use the ACCESS, MPI and MRI models to determine the frequencies of certain Synoptic Types over the extended summer season and during heatwave periods for the historical period that overlaps with the observational data 1995 to 2014, and for future projections for the period, 2065 to 2084. We use moderate and high radiative forcing pathways, RCP4.5 and RCP8.5 respectively (van Vuuren et al. 2011), to provide a range of projected future changes. Note that the historical simulations in the CMIP5 models finish in 2005. In order to span the equivalent period of the observations

in Chapters 4 and 5, we splice the historical data from 1995 to 2005 with data from 2006 to 2014 from the RCP4.5 and RCP8.5. This creates two "historical" periods for comparison with the observations and is common practice in other studies where observational data are available for comparison to models beyond 2005 (e.g. King et al. 2015; Lewis and Karoly 2015).

## 6.3 Methods

### 6.3.1 Defining and measuring the urban heat island

The anomalous magnitudes of the UHI that are described in this chapter are the same as those computed in Chapter 4. This analysis uses dry-bulb temperature data from the Bureau of Meteorology's Automatic Weather Stations (AWSs) in and around Melbourne, Adelaide, and Perth to calculate the UHI. See Chapter 2 for more detail on these stations. We only consider anomalous UHI strengths at midnight in this chapter to be consistent with Chapter 5. See Chapter 3 for more detail on how the UHI is calculated.

### 6.3.2 Defining and measuring heatwaves

As is comprehensively described in Chapter 3, heatwaves are defined as periods of three or more days where maximum temperature is greater than the $90^{th}$ percentile and minimum temperature is greater than the $90^{th}$ percentile for all days except the first. The heatwaves in the observational data are identified using ACORN-SAT data as described in Chapter 2.

Heatwaves in the historical and future periods are identified using CMIP5 model data (Chapter 2). Heatwave temperature thresholds are calculated for the historical period and applied to both the historical and future data to identify heatwaves

for these two periods. The use of the same temperature thresholds allows for comparison of heatwave metrics between the two periods, such as number of heatwaves and average temperature.

Note that the definition of heatwaves in this chapter uses a different base period, 1975 to 2005 (short base period), to that used in previous chapters, which used 1910 to 2014 (long base period). This is because a portion of the long base period, 2006 to 2014, lies outside the CMIP5 historical period, which ends in 2005. The new short base period allows us to be consistent across the observational and model data and allows for comparison of heatwave metrics between the two datasets over the historical period (January 1995 to March 2014). See Chapter 3, Section 3.2 for more detail on identifying heatwaves.

### 6.3.3 Validation of the use of model data with observed Synoptic Types

This research builds on the work done in Chapter 5 where SOMs were produced for the extended summer season in each of Melbourne, Adelaide, and Perth, using ERA-Interim MSLP data from 1995 to 2014. Here, we fit the model data to the above-mentioned SOMs for the historical and future periods to ensure a like-with-like comparison. We then determine how frequently each of the predefined Synoptic Types occur over the extended summer season and during heatwave periods using the model data and compare these to the frequencies computed from the observed data.

In order to constrain MSLP data from the ERA-Interim dataset and the CMIP5 models to the same SOMs, we re-grid the data to a common grid. To ensure the re-gridding process does not significantly alter the Synoptic Type distributions we identified from the observations (Chapter 5) we compare the re-gridded Type distributions to those from Chapter 5. The main features of the SOMs' Synoptic Types,

the mean quantisation error, and the topographic error are compared to determine the validity of the re-gridding process.

The ERA-Interim and CMIP5 model data are re-gridded onto the MRI model grid spacing because the resolution of this model is a midpoint between the ERA-Interim grid and the grids used for the other CMIP5 models used in this research. The MRI grid has a resolution of approximately 1.1˚ by 1.125˚ for latitude and longitude respectively.

Next, we examine how well the models simulate the observed SOMs. The CMIP5 data are fitted to the SOMs created using ERA-Interim data. That is, for each MSLP pattern in the CMIP5 data, we find which Synoptic Type is the best fit to the data. We then compare the frequency distributions of the six Synoptic Types generated from the six CMIP5 runs to those generated from ERA-Interim (all on the MRI grid) to determine if the observational and model data create similar frequency distributions of the incidence of the observed Synoptic Types during the extended summer season and heatwave periods. We also compare quantisation error to make sure the model data fit the six pre-defined Synoptic Types relatively well.

**6.3.4 Urban heat islands and heatwaves in the future**

Since our findings in Chapter 5 show no conclusive relationship between all three of heatwaves, UHI strength, and synoptic patterns, we do not examine all three factors together in Chapter 6. The analysis for this chapter is therefore split into two parts: 1) an examination of synoptic patterns in the future and possible implications for UHI strength, and 2) an examination of the relationships between heatwaves and synoptic patterns in the future. We again constrain our analysis to the extended summer season.

We begin this portion of the analysis by fitting the future model data to the pre-defined Synoptic Types developed using re-gridded ERA-Interim MSLP data from January 1995 to March 2014. This method is the same as that used when verifying the use of the model data, see Section 3.4. We then determine the distribution of Synoptic Types during the future period using the model data. To determine how synoptic patterns are likely to change in the future, we compare the Synoptic Type distributions created using the future periods to those for the historical periods. From changes in the frequency of Synoptic Types over time we can examine how those Synoptic Types related to particular magnitudes of the UHI might change in the future.

To investigate how the relationship between heatwaves and synoptic patterns is likely to change with anthropogenic climate change, we examine how Synoptic Type distributions during heatwaves periods differ between the historical and future periods.

## 6.4 Results

Certain MSLP patterns are associated with observed heatwaves (Pezza et al. 2012; Gibson et al. 2017b; Chapter 5) and the strength of the UHI (Morris and Simmonds 2000; Chapter 5) in Australia. This section of the thesis compares future and historical synoptic patterns using CMIP5 model data applied to the Synoptic Types identified in Chapter 5 to investigate how heatwaves and those Synoptic Types related to exacerbated or diminished UHIs may change under future anthropogenic climate change. Our re-gridding methodology is verified in Section 6.4.1 and the use of CMIP5 MSLP data in conjunction with an ERA-Interim trained SOM is examined in Section 6.4.2.

Section 6.4.3 investigates how those synoptic patterns related to the UHI in the present day might change into the future with anthropogenic warming. To do this, we

examine the frequencies of Synoptic Types associated with UHIs of certain strengths in the historical period and compare them to Synoptic Type frequencies in the future. Similarly, in Section 6.4.4 we examine frequencies of future synoptic patterns during heatwaves to determine how the synoptic patterns associated with future heatwaves differ to those for the historical period.

### 6.4.1 Validation of re-gridding methodology

As described in Section 6.3.3, the ERA-Interim MSLP data are re-gridded onto the MRI grid for direct comparison between model and observational data. To make sure our re-gridding methods are suitable for use with the observational dataset, and the model data can accurately simulate the synoptic situations that occur during heatwaves, we verify our re-gridding methodology prior to undertaking any analysis. If the Synoptic Types produced using the re-gridded data are similar to those created using the native grid, the results from Chapter 6 can be easily compared to the results from Chapter 5.

The original SOMs from Chapter 5 are compared to the SOMs created using the re-gridded ERA-Interim data in subplots a and b respectively of Figures 6.1 to 6.3. These figures show that the original and re-gridded SOMs have visually similar synoptic patterns in each of the six Synoptic Types.

For all three cities, there is a reduction in the quantisation error but an increase in the topographic error for the re-gridded SOMs (subplots a and b for Figures 6.1 to 6.3). This means that the observational data fit the re-gridded SOM better, but the ordering on the SOM is slightly less accurate. This can be attributed to the reduction in resolution after re-gridding.
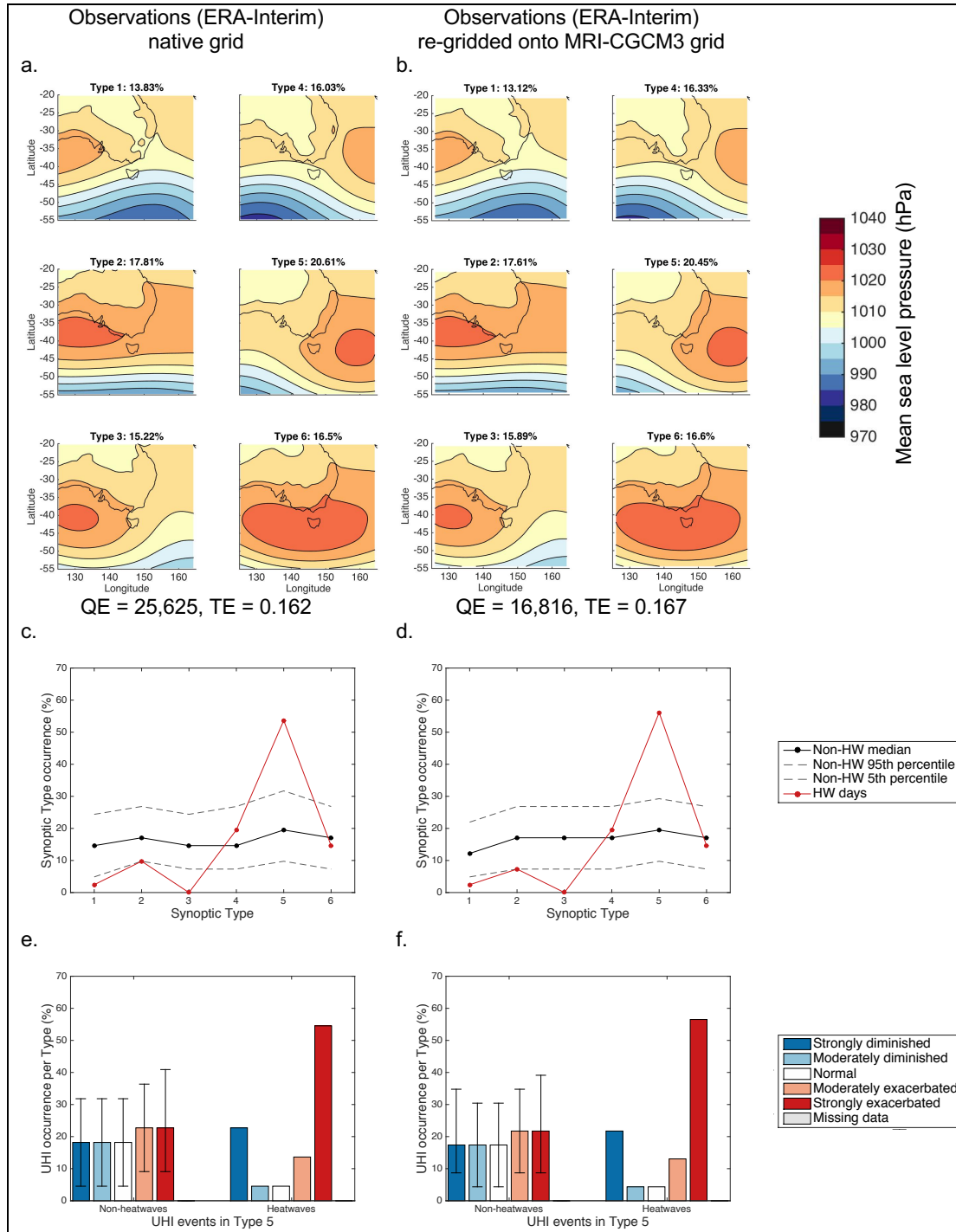
Figure 6.1: Comparison plots for observational data (ERA-Interim) for native grid (left) and re-gridded onto the MRI-CGCM3 grid (right) in Melbourne. a) and b) show the SOMs for the observational data using different grids. Contour lines show mean sea level pressure (hPa). Mean quantisation error (QE) and topographic error (TE) are shown under subplots a) and b). Subplots c) and d) show the distributions of Synoptic Types for heatwave days. e) and f) show the distributions of UHI strength categories during the extended summer season (denoted as non-heatwave days on the plot) and on heatwave days for the Dominant Heatwave Type.
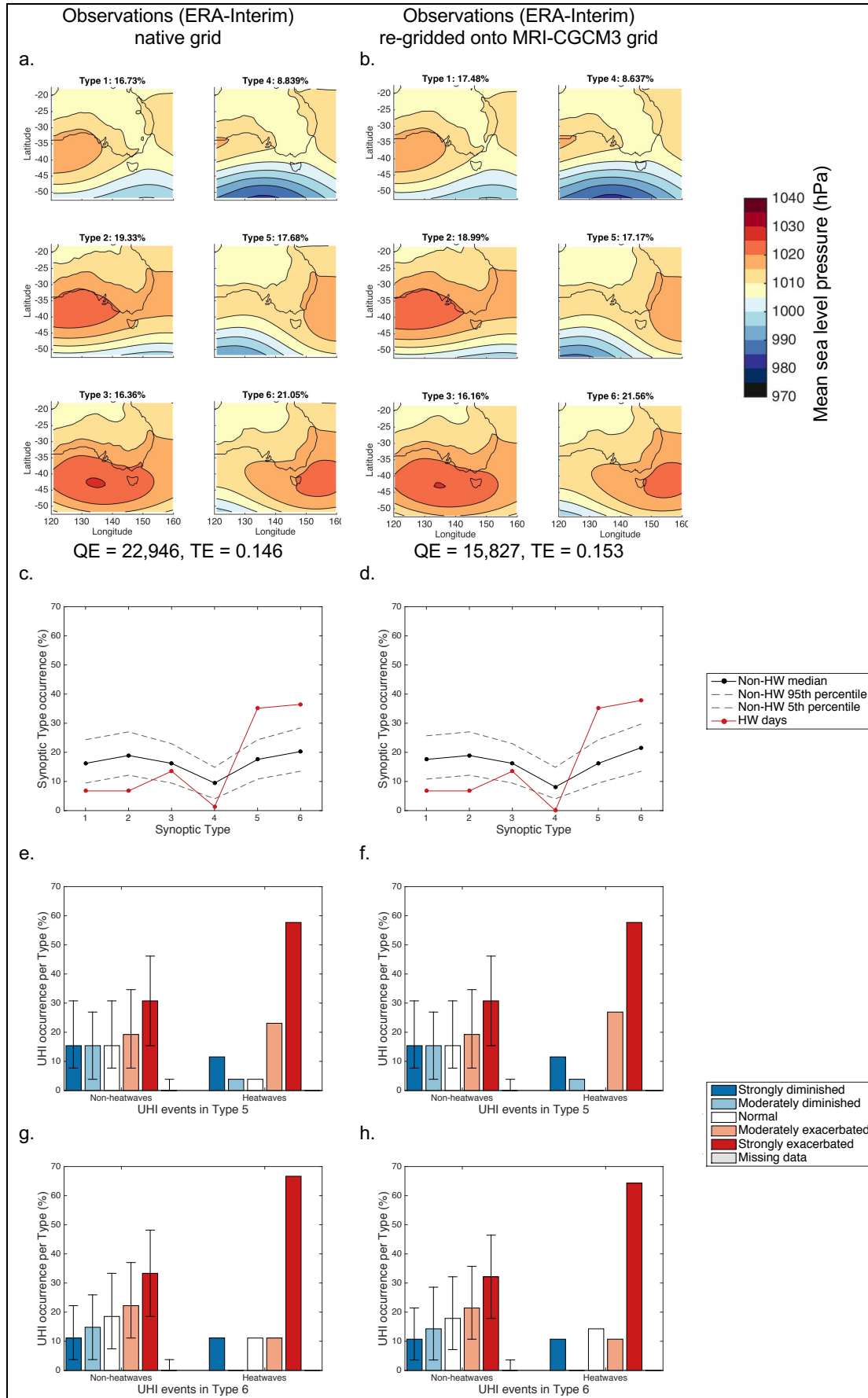
Figure 6.2: Same as Figure 6.1 but for Adelaide. Subplots e), f), g), and h) show the distributions of UHI strength categories during the extended summer season (denoted as non-heatwave days on the plot) and on heatwave days for the two Dominant Heatwave Types.

165
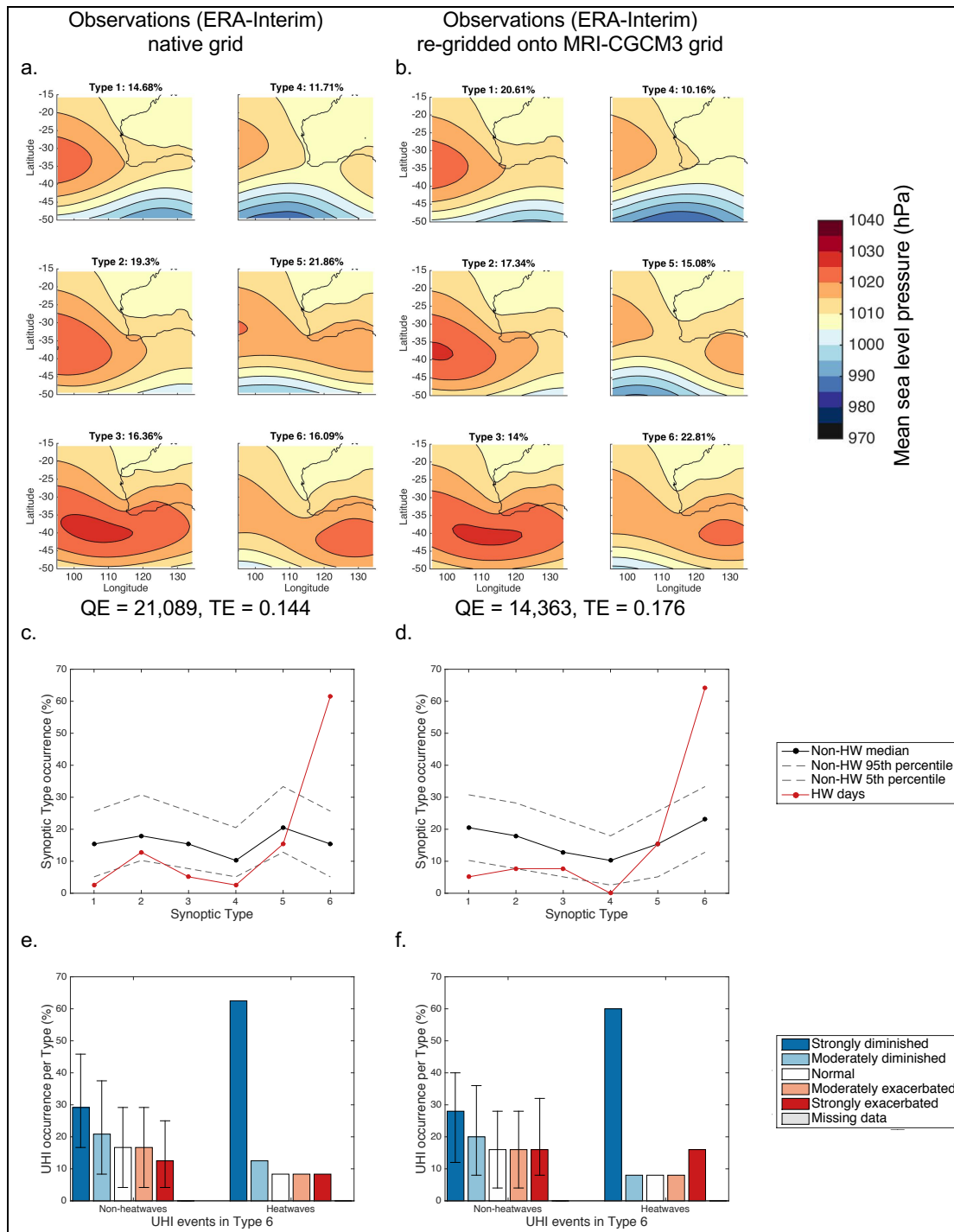
Figure 6.3: Same as Figure 6.1 but for Perth.

We further compare the native and re-gridded SOMs for each city by comparing Synoptic Type occurrence during heatwaves in subplots c and d of Figures 6.1 to 6.3. These subplots show very similar patterns for both the native and re-gridded data for all three cities. The number of heatwave days in each Synoptic Type are given in Table 6.1. While there are some differences between the distributions, all differences are small (maximum of 5.1 % difference, or two heatwave days). Overall, the SOMs show no significant differences. The main features of the Synoptic patterns are well captured and the Dominant Heatwave Types, this is, Types that are above the 90 % confidence interval, remain the same (subplots c and d of Figures 6.1 to 6.3). That is, Type 5 is the Dominant Heatwave Type in Melbourne (Figure 6.1c and d), Types 5 and 6 are dominant in Adelaide (Figure 6.2c and d), and Type 6 is dominant in Perth (Figure 6.3c and d) for both native and re-gridded SOMs.

| Type | Melbourne | | Adelaide | | Perth | |
|---|---|---|---|---|---|---|
| | Native grid | MRI grid | Native grid | MRI grid | Native grid | MRI grid |
| 1 | 1 | 1 | 5 | 5 | 1 | 2 |
| 2 | 4 | 3 | 5 | 5 | 5 | 3 |
| 3 | 0 | 0 | 10 | 10 | 2 | 3 |
| 4 | 8 | 8 | 1 | 0 | 1 | 0 |
| 5 | 22 | 23 | 26 | 26 | 6 | 6 |
| 6 | 6 | 6 | 27 | 28 | 24 | 25 |

Table 6.1: Number of heatwave days (middle and end) associated with each Synoptic Type in Melbourne, Adelaide, and Perth for ERA-Interim data on the native grid and when re-gridded onto the MRI grid.

The distribution of UHI strength categories during the extended summer season remain the same between the SOMs created using native and re-gridded data (Figure 6.1e and f for Melbourne, Figure 6.2e to h for Adelaide, and Figure 6.3e and f for Perth). Similarly, UHI category distributions during heatwaves do not differ much between the two SOMs (Figure 6.1e and f for Melbourne, Figure 6.2e to h for Adelaide, and Figure 6.3e and f for Perth). The main features from each of the Dominant Heatwave Types

does not change, that is, Type 5 in Melbourne and Types 5 and 6 in Adelaide are associated with significantly more strongly exacerbated events than are expected during the extended summer season, and Type 6 in Perth is associated with significantly more strongly diminished events. Thus, the distribution of Synoptic Types on heatwave days is an enhanced form of the distributions on days during the extended summer season. The native grid shows a similar enhanced distribution on heatwave days (Figure 6.1e and f for Melbourne, Figure 6.2e to h for Adelaide, and Figure 6.3e and f for Perth). Recall that exacerbated and diminished UHIs refer to UHIs that are warmer or cooler than normal respectively, and that a diminished UHI is not necessarily an UCI.

Our comprehensive analysis, above, shows that the re-gridding methodology does not significantly alter the representation of Synoptic Types either during heatwaves or during the extended summer season. As the re-gridded SOMs are very similar to the SOMs for the native grid, we can seamlessly use the findings from Chapter 5 in conjunction with our findings from this chapter. Therefore, we use the SOMs computed from the re-gridded data for the remainder of this chapter, as shown below in Figures 6.4 to 6.6.
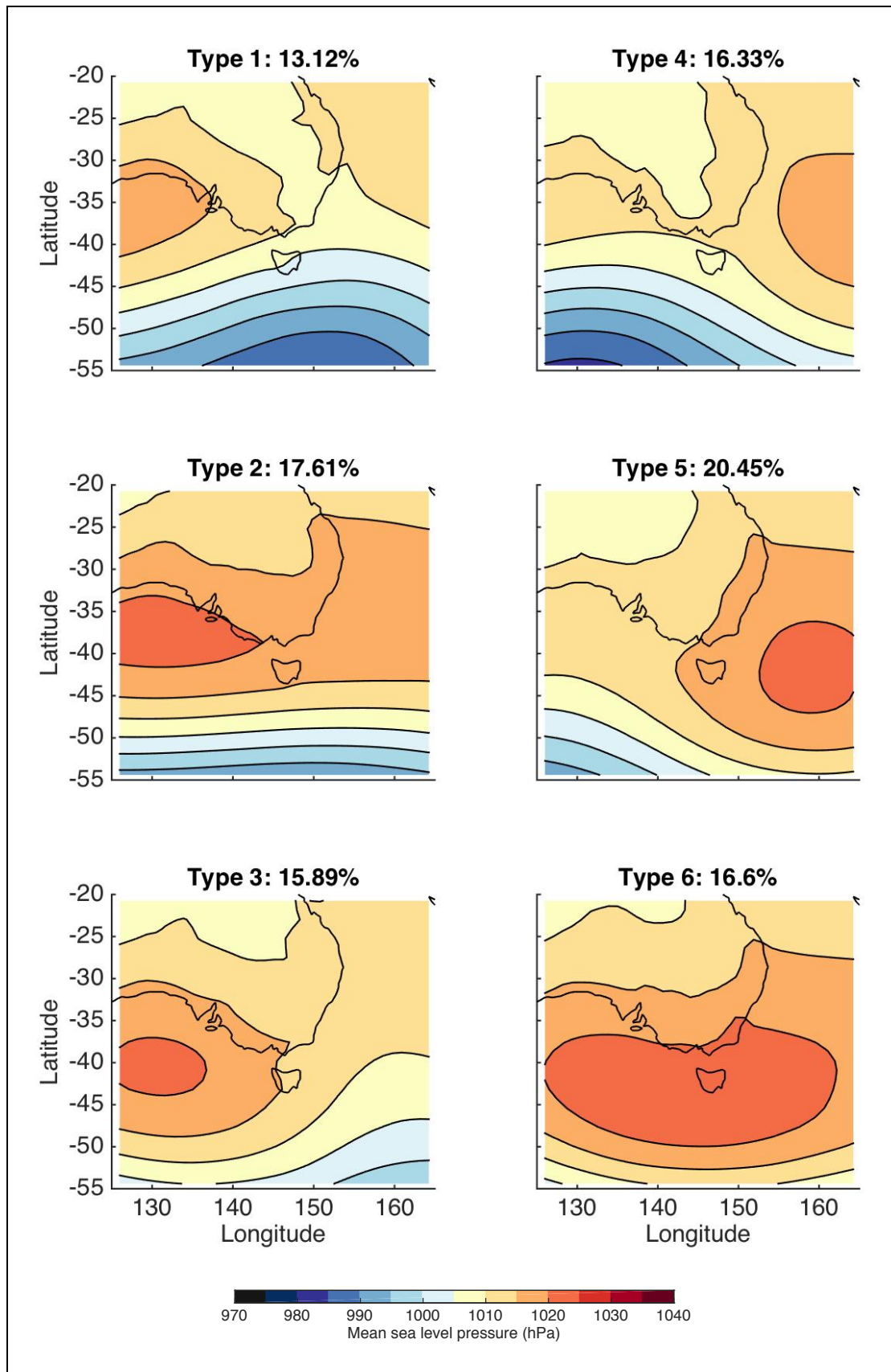
Figure 6.4: SOM created using ERA-Interim MSLP data re-gridded onto the MRI-CGCM3 CMIP5 model grid for Melbourne, using data from the historical period (Jan 1995 to Mar 2014) for the extended summer season (Nov to Mar). Coloured contours show MSLP (hPa) at the six-hourly time step closest to midnight. Percentages at the top of each Synoptic Type show how frequently each Type occurs. Note: this figure is the same as Figure 6.1b but has been enlarged for clarity.
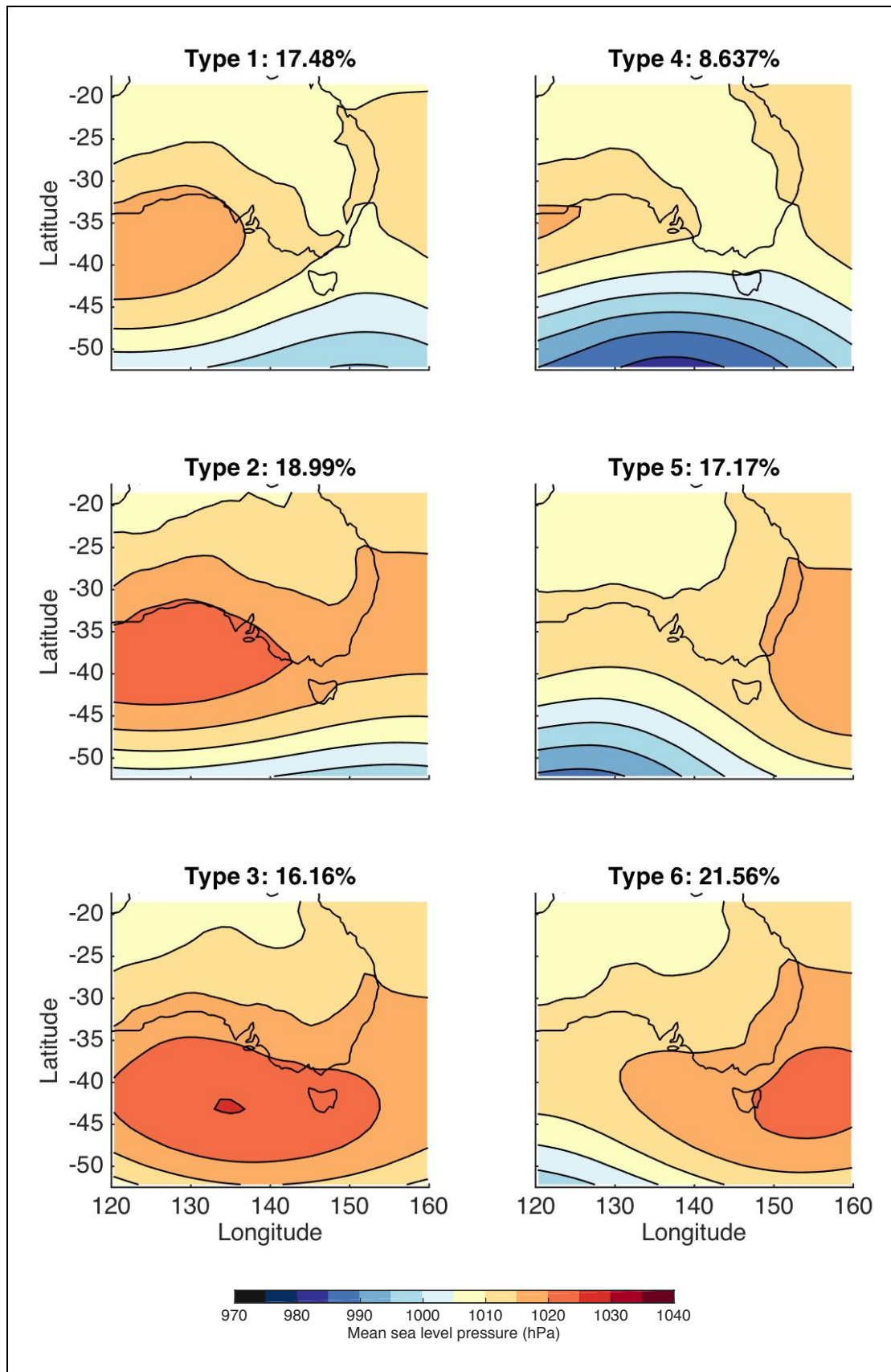
Figure 6.5: Same as Figure 6.4 but for Adelaide. Note: this figure is the same as Figure 6.2b but has been enlarged for clarity.
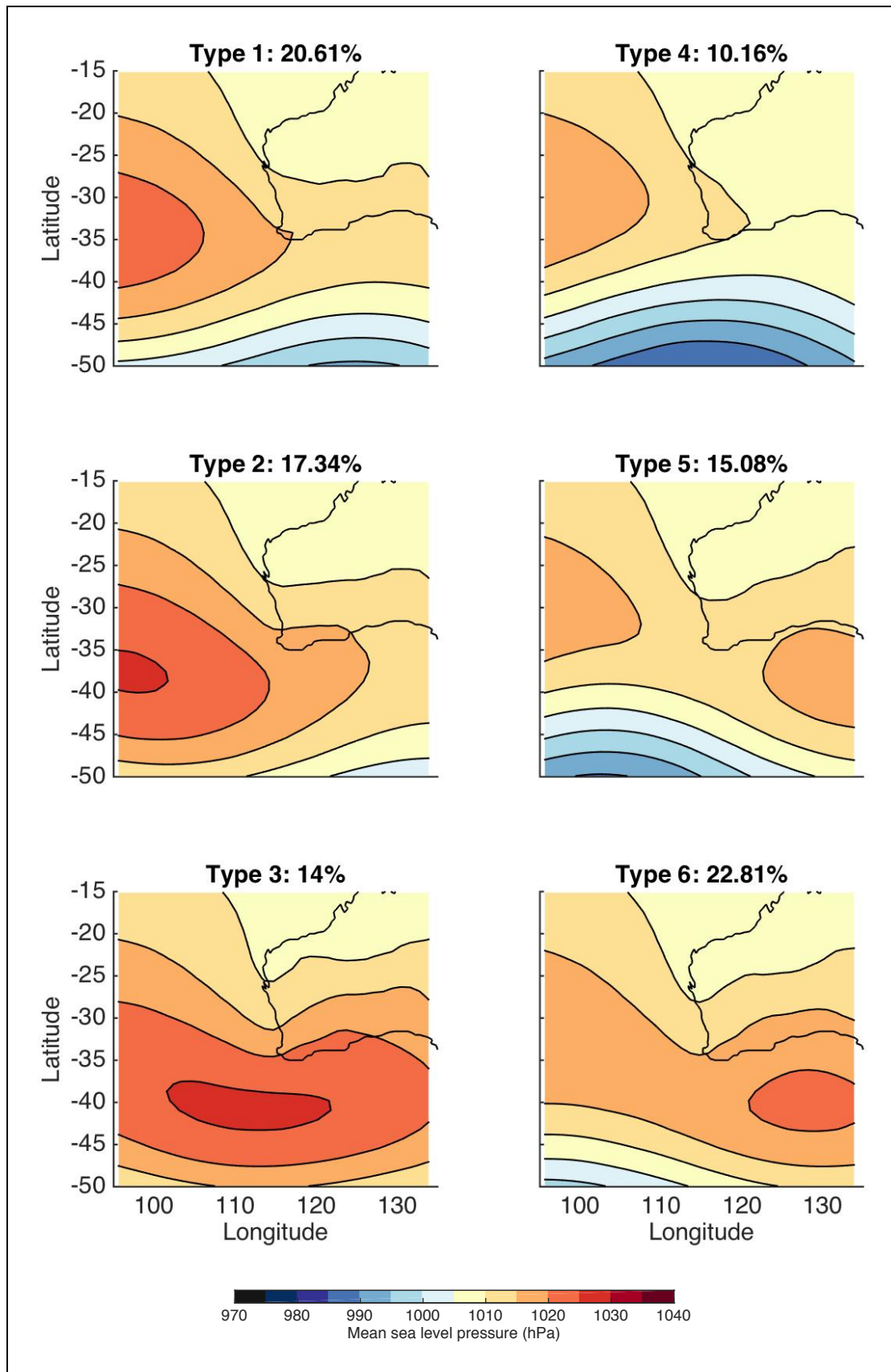
Figure 6.6: Same as Figure 6.4 but for Perth. Note: this figure is the same as Figure 6.3b but has been enlarged for clarity.

### 6.4.2 Verification of model simulations of synoptic patterns

Here we determine whether data from the ACCESS, MPI, and MRI models are suitable for our proposed analyses by comparing the frequency of the Synoptic Types produced in the model simulations to those in the observations. If any of the models cannot reasonably reproduce the distribution of synoptic patterns associated with heatwaves then they are not suitable for these analyses. We use the SOM trained with the re-gridded ERA-Interim data and determine the best matching units (BMUs) in the model data; that is, we determine which of the six Synoptic Types is the best fit for each daily synoptic pattern in the dataset. In this section of the thesis we examine the distribution of Synoptic Types during all days and during heatwave days and examine quantisation error (goodness of fit of each synoptic pattern to the ERA-Interim Synoptic Types).

*DISTRIBUTION OF SYNOPTIC TYPES DURING THE EXTENDED SUMMER SEASON*

Figures 6.7, 6.8, and 6.9 show the range of likely frequencies of Synoptic Types in Melbourne, Adelaide, and Perth respectively for the extended summer season. These figures show how frequently each Synoptic Type is likely to occur for observational and model data over the historical and future periods by employing random sampling with replacement for both datasets, i.e. bootstrapping. By comparing the 10,000 bootstrapped samples for the historical model data to those for the observational data, we can determine whether the two samples are significantly different. These figures show that the differences between the observed and modelled distributions of Synoptic Types for the historical period are generally statistically insignificant. That is, the medians of the bootstrapped samples of the frequencies of modelled historical Synoptic

Types (solid blue lines) generally lie within the 90 % confidence interval of the bootstrapped samples of the frequencies of observational Synoptic Types (dashed black lines).

The only model to show significant differences between observed and modelled Synoptic Types is the MRI model. In Melbourne, this model shows a high model bias for the frequency of Types 1 and 2 for RCP4.5 and Type 1 for RCP8.5 (Figure 6.7e and f), that is, these Types occur too frequently in the model. In Adelaide, the MRI shows a high bias in the frequency of Type 4 and a low bias for Types 3 and 6 for RCP8.5 (Figure 6.8f). Model biases for both cities are between -8.4 % and +10.7 % of the observed values (Tables 6.2 and 6.3). There are no significant differences for Perth (Table 6.4 and Figure 6.9).

This analysis shows that ACCESS and MPI produce better representations of the distributions of the Synoptic Types in Melbourne and Adelaide over the historical period than the MRI model. Further, the MPI tends to produce better representations than ACCESS as there are fewer large deviations between observed and modelled Synoptic Type frequencies (Figures 6.7 and 6.8). All three models produce a good representation of the distribution of Synoptic Types in Perth. The bootstrapped samples of the frequencies of Synoptic Types for the modelled and observed data show a maximum difference between the medians of 5.6 % (Table 6.4).

To further verify the use of our chosen models we compare the quantisation error for the historical period using the model data to that for the observational data (Table 6.5). This comparison shows how well the model data fit the SOMs in Figures 6.4 to 6.6.
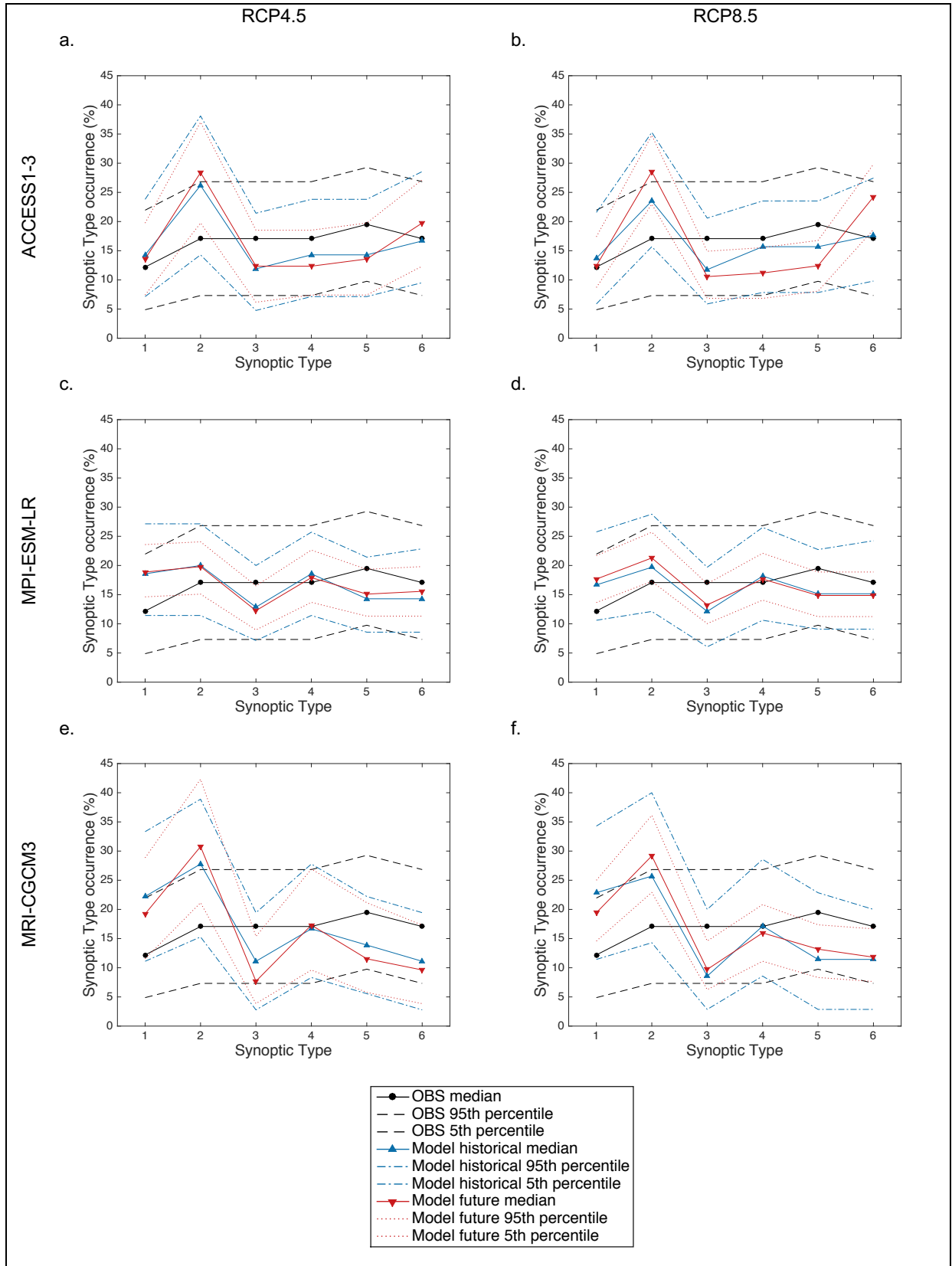
Figure 6.7: Frequency of occurrence of each Synoptic Type over Melbourne during the extended summer season. Black lines (circle markers) show the median of the bootstrapped samples of the frequencies of Synoptic Types for observational data (OBS), and blue lines (upward-pointing triangle markers) show the median of the bootstrapped samples of the frequencies of Synoptic Types for model data over the historical period (Jan 1995 to Mar 2014). Red lines (downward-pointing triangle markers) show the median of the bootstrapped samples of the frequencies of Synoptic Types for model data for the future period (Jan 2065 to Mar 2084). Dashed and/or dotted lines show the 90 % confidence intervals for each of the bootstrapped samples.
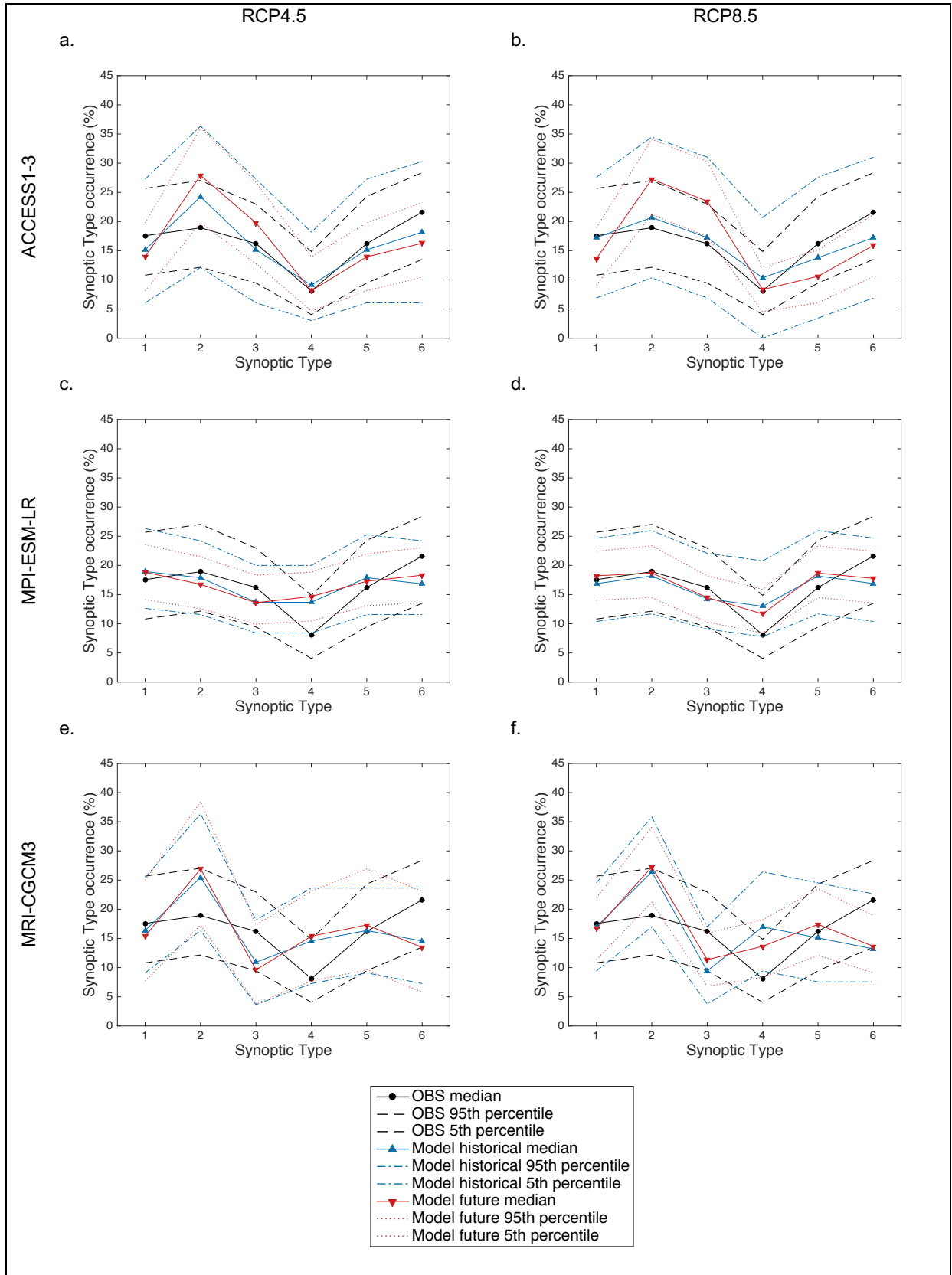
Figure 6.8: Same as Figure 6.7 but for Adelaide.
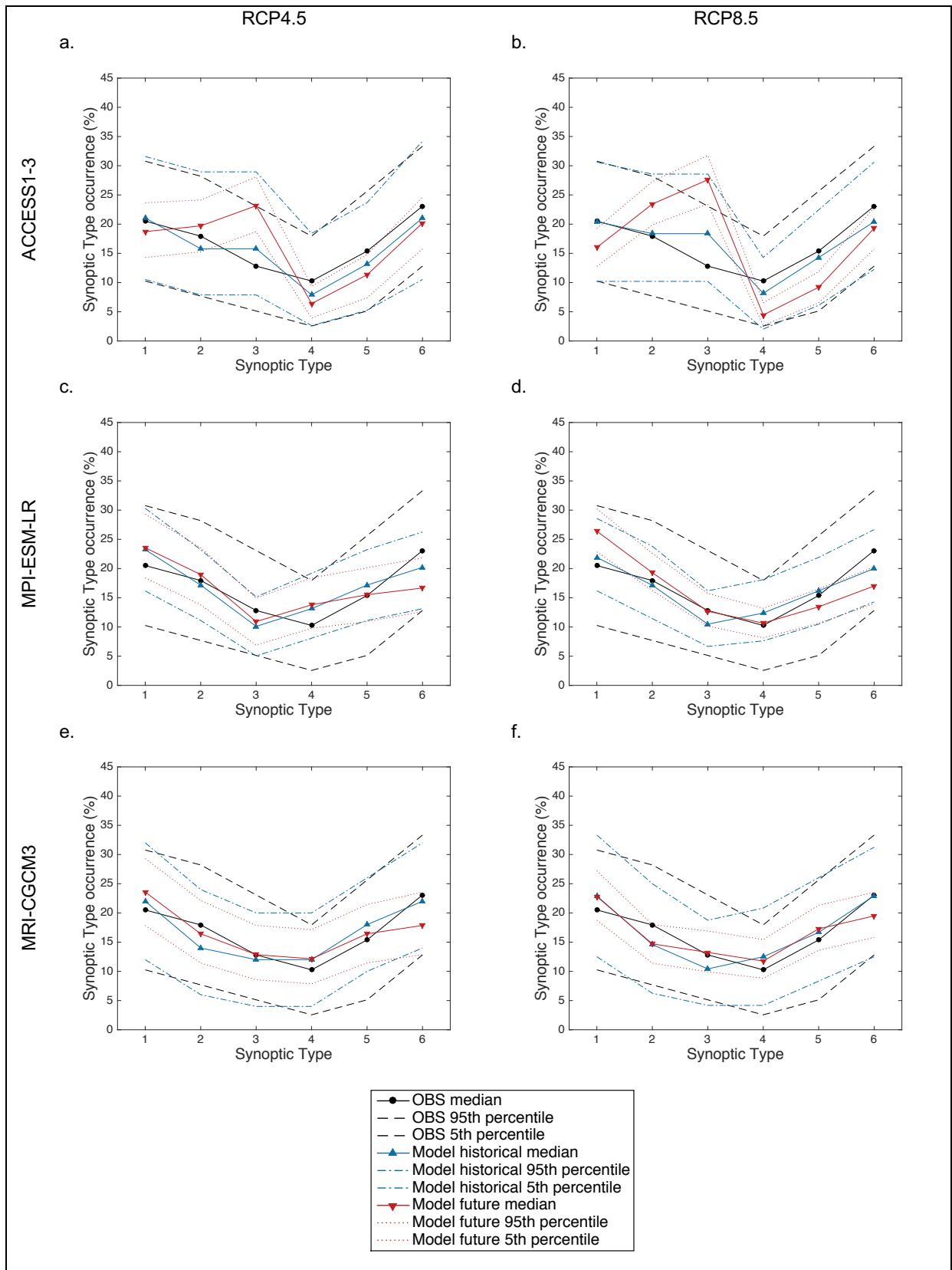
Figure 6.9: Same as Figure 6.7 but for Perth.

| Type | OBS | ACCESS1-3 | | MPI-ESM-LR | | MRI-CGCM3 | |
|---|---|---|---|---|---|---|---|
| | | RCP4.5 | RCP8.5 | RCP4.5 | RCP8.5 | RCP4.5 | RCP8.5 |
| 1 | 12.2 | 14.3% (2.1) | 13.7% (1.5) | 18.6% (6.4) | 16.7% (4.5) | *22.2% (10.0)* | *22.9% (10.7)* |
| 2 | 17.1 | 26.2% (9.1) | 23.5% (6.5) | 20.0% (2.9) | 19.7% (2.6) | *27.8% (10.7)* | 25.7% (8.6) |
| 3 | 17.1 | 11.9% (-5.2) | 11.8% (-5.3) | 12.9% (-4.2) | 12.1% (-5.0) | 11.1% (-6.0) | 8.6% (-8.5) |
| 4 | 17.1 | 14.3% (-2.8) | 15.7% (-1.4) | 18.6% (1.5) | 18.2% (1.1) | 16.7% (-0.4) | 17.1% (0.1) |
| 5 | 19.5 | 14.3% (-5.2) | 15.7% (-3.8) | 14.3% (-5.2) | 15.2% (-4.4) | 13.9% (-5.6) | 11.4% (-8.1) |
| 6 | 17.1 | 16.7% (-0.4) | 17.7% (0.6) | 14.3% (-2.8) | 15.2% (-1.9) | 11.1% (-6.0) | 11.4% (-5.6) |

Table 6.2: Median of the percentages of occurrence for the bootstrapped samples of each Synoptic Type for observational and model data in Melbourne over the historical period. Values in brackets show the difference between modelled and observed values. Italicised values show where models are significantly different to observations.

| Type | OBS | ACCESS1-3 | | MPI-ESM-LR | | MRI-CGCM3 | |
|---|---|---|---|---|---|---|---|
| | | RCP4.5 | RCP8.5 | RCP4.5 | RCP8.5 | RCP4.5 | RCP8.5 |
| 1 | 17.6 | 15.2% (-2.4) | 17.2% (-0.3) | 19.0% (1.4) | 16.9% (-0.7) | 16.4% (-1.2) | 17.0% (-0.6) |
| 2 | 18.9 | 24.2% (5.3) | 20.7% (1.8) | 17.9% (-1.0) | 18.2% (-0.7) | 25.5% (6.5) | 26.4% (7.5) |
| 3 | 16.2 | 15.2% (-1.1) | 17.2% (1.0) | 13.7% (-2.5) | 14.3% (-1.9) | 10.9% (-5.3) | *9.4% (-6.8)* |
| 4 | 8.1 | 9.1% (1.0) | 10.3% (2.2) | 13.7% (5.6) | 13.0% (4.9) | 14.6% (6.4) | *17.0% (8.9)* |
| 5 | 16.2 | 15.2% (-1.1) | 13.8% (-2.4) | 17.9% (1.7) | 18.2% (2.0) | 16.4% (0.1) | 15.1% (-1.1) |
| 6 | 21.6 | 18.2% (-3.4) | 17.2% (-4.4) | 16.8% (-4.8) | 16.9% (-4.7) | 14.6% (-7.1) | *13.2% (-8.4)* |

Table 6.3: Same as Table 6.2 but for Adelaide.

| Type | OBS | ACCESS1-3 | | MPI-ESM-LR | | MRI-CGCM3 | |
|---|---|---|---|---|---|---|---|
| | | RCP4.5 | RCP8.5 | RCP4.5 | RCP8.5 | RCP4.5 | RCP8.5 |
| 1 | 20.5 | 21.1% (0.5) | 20.4% (-0.1) | 23.2% (2.7) | 21.9% (1.4) | 22.0% (1.5) | 22.9% (2.4) |
| 2 | 18 | 15.8% (-2.2) | 18.4% (0.4) | 17.2% (-0.8) | 17.1% (-0.8) | 14.0% (-4.0) | 14.6% (-3.4) |
| 3 | 12.8 | 15.8% (3.0) | 18.4% (5.6) | 10.1% (-2.7) | 10.5% (-2.3) | 12.0% (-0.8) | 10.4% (-2.4) |
| 4 | 10.3 | 7.9% (-2.4) | 8.2% (-2.1) | 13.1% (2.9) | 12.4% (2.1) | 12.0% (1.7) | 12.5% (2.2) |
| 5 | 15.4 | 13.2% (-2.2) | 14.3% (-1.1) | 17.2% (1.8) | 16.2% (0.8) | 18.0% (2.6) | 16.7% (1.3) |
| 6 | 23.1 | 21.1% (-2.0) | 20.4% (-2.7) | 20.2% (-2.9) | 20.0% (-3.1) | 22.0% (-1.1) | 22.9% (-0.2) |

Table 6.4: Same as Table 6.2 but for Perth.

| City | OBS | ACCESS1-3 | | MPI-ESM-LR | | MRI-CGCM3 | |
|---|---|---|---|---|---|---|---|
| | | RCP4.5 | RCP8.5 | RCP4.5 | RCP8.5 | RCP4.5 | RCP8.5 |
| Melbourne | 16816 | 17527 (4.2%) | 17381 (3.4%) | 18409 (9.5%) | 18391 (9.4%) | 18056 (7.4%) | 17954 (6.8%) |
| Adelaide | 15827 | 16632 (5.1%) | 16504 (4.3%) | 17367 (9.7%) | 17371 (9.8%) | 16963 (7.2%) | 16910 (6.8%) |
| Perth | 14363 | 14618 (1.8%) | 14416 (0.4%) | 16290 (13.4%) | 16241 (13.1%) | 15181 (5.7%) | 15297 (6.5%) |

Table 6.5: Mean quantisation error (QE) for ERA-Interim observational (OBS) and model data after fitting to SOM created using ERA-Interim (OBS) data from Jan 1995 to Mar 2014 (extended summer months only). Values in brackets show the difference between the model and observational QEs as a percentage of the observed QE, i.e. a positive value shows that the error for the model data is greater than that for the observations. Model and observational data are re-gridded onto MRI-CGCM3 grid.

Given that the SOMs are trained using the observational data (ERA-Interim), it is expected that quantisation errors will be greater for the model runs than for the observations. Table 6.5 shows that the quantisation errors for all model runs is greater than those for the observational data. However, the increases in the errors are small in percentage terms. ACCESS shows the smallest quantisation errors (maximum of 5.1 % increase on observational error), showing that of the three models, synoptic patterns simulated by ACCESS are the best fit for the SOMs, whereas MPI shows the greatest errors (maximum of 13.4 % increase on observational error). Next, we examine how well the models simulate the frequency of Synoptic Types during heatwaves.

*DISTRIBUTION OF SYNOPTIC TYPES DURING HEATWAVES*

Figures 6.10 to 6.12 show the bootstrapped samples of the distribution of Synoptic Types for historical and future model simulations for heatwaves and the extended summer season. Bootstrapped distributions for the observational data are also shown for comparison. These figures demonstrate that while the frequency distributions of Synoptic Types during heatwave periods are simulated reasonably well by the models, there are some departures from the observed distributions.

In Melbourne, model biases that occur during heatwaves tend to mirror those that occur for the entire extended summer season. For example, while there is a high bias for Type 2 in MRI RCP4.5 during heatwaves (Figure 6.10e compared to Figure 6.10g), a similar bias exists for the extended summer season (Figure 6.7e). Thus, the Dominant Heatwave Types in the observations are the same for all model runs (Figure 6.10). All model runs have a slightly weaker relationship between heatwaves and
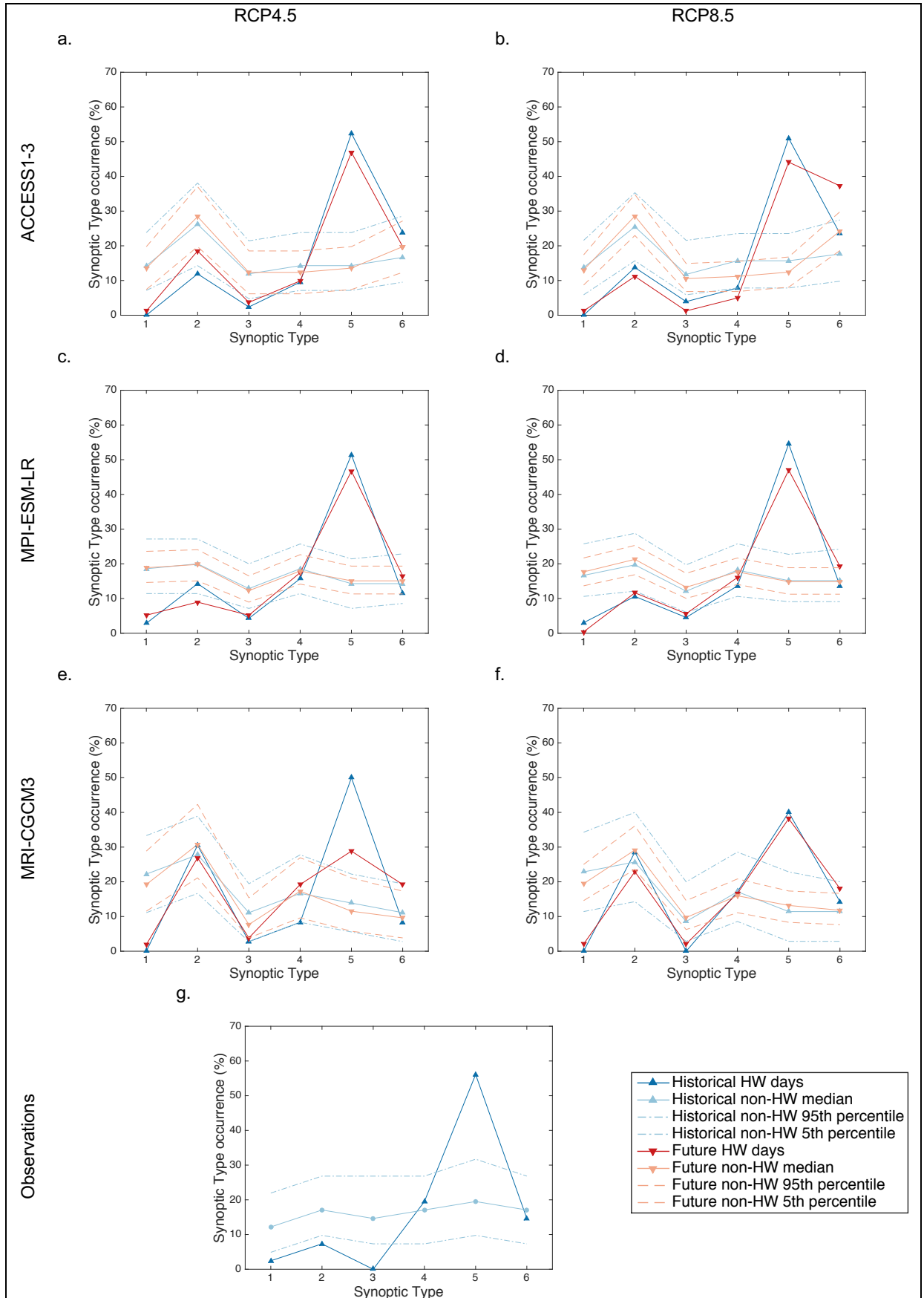
Figure 6.10: Frequency of Synoptic Types during heatwaves (HW) for the future (Jan 2065 to Mar 2084, solid red lines) and historical (Jan 1995 to Mar 2014, solid dark blue lines) periods in Melbourne. Solid pink and light blue lines show the median of the bootstrapped extended summer season days (denoted as non-HW days on the plot). Dashed lines show the 90 % confidence intervals. Subplots on the first, second, and third rows are simulations created using ACCESS1-3, MPI-ESM-LR, and MRI-CGCM3 respectively. The subplots on the left show simulations using the RCP4.5 radiative forcing pathway and those on the right use RCP8.5. Subplot g shows frequency distributions of Synoptic Types using observational data (Jan 1995 to Mar 2014). Data used are for midnight, or the closest available time period.

synoptic patterns as shown by the consistent low biases in the frequency of Type 5 during heatwaves. The models show low Type 5 biases of between -1.6 % and -16.1 % (Table 6.6).

| Type | OBS | ACCESS1-3 | | MPI-ESM-LR | | MRI-CGCM3 | |
|---|---|---|---|---|---|---|---|
| | | RCP4.5 | RCP8.5 | RCP4.5 | RCP8.5 | RCP4.5 | RCP8.5 |
| 1 | 2.4 | 0.0% (-2.4) | 0.0% (-2.4) | 2.9% (0.4) | 3.0% (0.6) | 0.0% (-2.4) | 0.0% (-2.4) |
| 2 | 7.3 | 11.9% (4.6) | 13.7% (6.4) | 14.3% (7.0) | 10.6% (3.3) | 30.6% (23.2) | 28.6% (21.3) |
| 3 | 0.0 | 2.4% (2.4) | 3.9% (3.9) | 4.3% (4.3) | 4.6% (4.6) | 2.8% (2.8) | 0.0% (0.0) |
| 4 | 19.5 | 9.5% (-10.0) | 7.8% (-11.7) | 15.7% (-3.8) | 13.6% (-5.9) | 8.3% (-11.2) | 17.1% (-2.4) |
| 5 | 56.1 | 52.4% (-3.7) | 51.0% (-5.1) | 51.4% (-4.7) | 54.6% (-1.6) | 50.0% (-6.1) | 40.0% (-16.1) |
| 6 | 14.6 | 23.8% (9.2) | 23.5% (8.9) | 11.4% (-3.2) | 13.6% (-1.0) | 8.3% (-6.3) | 14.3% (-0.3) |

Table 6.6: Validating the use of the SOM developed over Melbourne using ERA-Interim reanalysis data (referred to as OBS in table) with CMIP5 model data. The SOM was created using data for the extended summer season (Nov to Mar) using data from Jan 1995 to Mar 2014. Values show the frequency of occurrence of each Synoptic Type for the ERA-Interim data (OBS) and each model run during heatwaves. Values in brackets show the differences between the percentage of occurrence for the ERA-Interim data and each model run.

Figure 6.11 shows the frequencies of each Synoptic Type during heatwave periods over the historical and future periods in Adelaide. This Figure shows that biases in Types 1 to 4 during heatwaves are mirrored by those during the extended summer season. However, Types 5 and 6, both of which represent a high-pressure system over the Tasman Sea, tell a different story. While Types 5 and 6 are Dominant Heatwave Types in the observations (Figure 6.11g), only Type 6 is consistently classified as a Dominant Heatwave Type in the model runs (Figure 6.11a to f). We see evidence for this as Type 6 occurs as frequently or more frequently in the models than in the observations, whereas Type 5 does not occur frequently enough for all but one model run (MRI RCP4.5).

Despite the low biases in Type 5 during heatwaves, in ACCESS RCP4.5 and MRI RCP4.5 there is a stronger relationship between heatwaves and high-pressure systems over the Tasman than in the observations. We see evidence for this as both
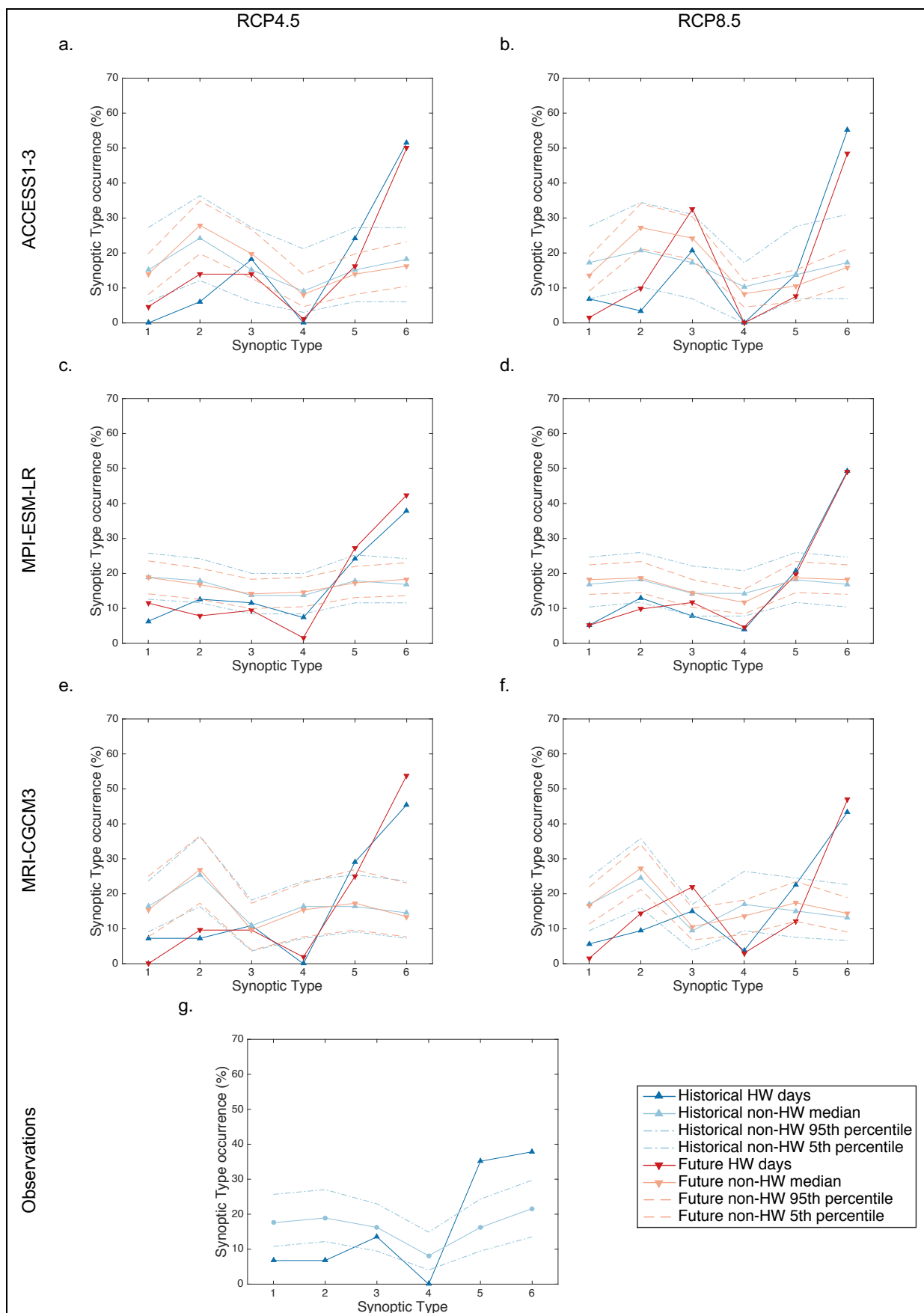
Figure 6.11: Same as Figure 6.10 but for Adelaide.

model runs show a higher frequency of Types 5 and 6 combined than the observations (Table 6.7). Further, since the low biases in Type 5 are compensated for with high biases in Type 6, the high-pressure systems over the Tasman Sea during heatwaves are shifted westward in these model runs (Figure 6.5). On the other hand, all historical RCP8.5 runs and MPI RCP4.5 have a weaker relationship between synoptic patterns and heatwaves than the observational data, as the model runs show greater low biases in Type 5 compared to high biases in Type 6 (Table 6.7).

| Type | OBS | ACCESS1-3 | | MPI-ESM-LR | | MRI-CGCM3 | |
|------|-----|-----------|-----------|------------|------------|-----------|-----------|
| | | RCP4.5 | RCP8.5 | RCP4.5 | RCP8.5 | RCP4.5 | RCP8.5 |
| 1 | 6.8 | 0.0% (-6.8) | 6.9% (0.1) | 6.3% (-0.4) | 5.2% (-1.6) | 7.3% (0.5) | 5.7% (-1.1) |
| 2 | 6.8 | 6.1% (-0.7) | 3.5% (-3.3) | 12.6% (5.9) | 13.0% (6.2) | 7.3% (0.5) | 9.4% (2.7) |
| 3 | 13.5 | 18.2% (4.7) | 20.7% (7.2) | 11.6% (-1.9) | 7.8% (-5.7) | 10.9% (-2.6) | 15.1% (1.6) |
| 4 | 0.0 | 0.0% (0.0) | 0.0% (0.0) | 7.4% (7.4) | 3.9% (3.9) | 0.0% (0.0) | 3.8% (3.8) |
| 5 | 35.1 | 24.2% (-10.9) | 13.8% (-21.4) | 24.2% (-10.9) | 20.8% (-14.4) | 29.1% (-6.1) | 22.6% (-12.5) |
| 6 | 37.8 | 51.5% (13.7) | 55.2% (17.3) | 37.9% (0.0) | 49.4% (11.5) | 45.5% (7.6) | 43.4% (5.6) |

Table 6.7: As in Table 6.6 but for Adelaide.

Figure 6.12 shows the frequencies of each Synoptic Type during heatwave periods over the historical and future periods in Perth. All model runs, except ACCESS RCP4.5, accurately show that Type 6 occurs significantly more frequently during heatwaves in Perth than during the extended summer season. Since the frequency of Type 6 in ACCESS RCP4.5 during heatwaves lies on the upper bound of the 90 % confidence interval of the bootstrapped simulations for the extended summer season, we still consider this a Dominant Heatwave Type. The low biases for Type 6 are between 16.2 % and 29.9 % for all model runs (Table 6.8).

The low biases toward fewer Synoptic Type 6 patterns during heatwaves in Perth are partially compensated for by high biases in Type 3 of between 12.5 % and
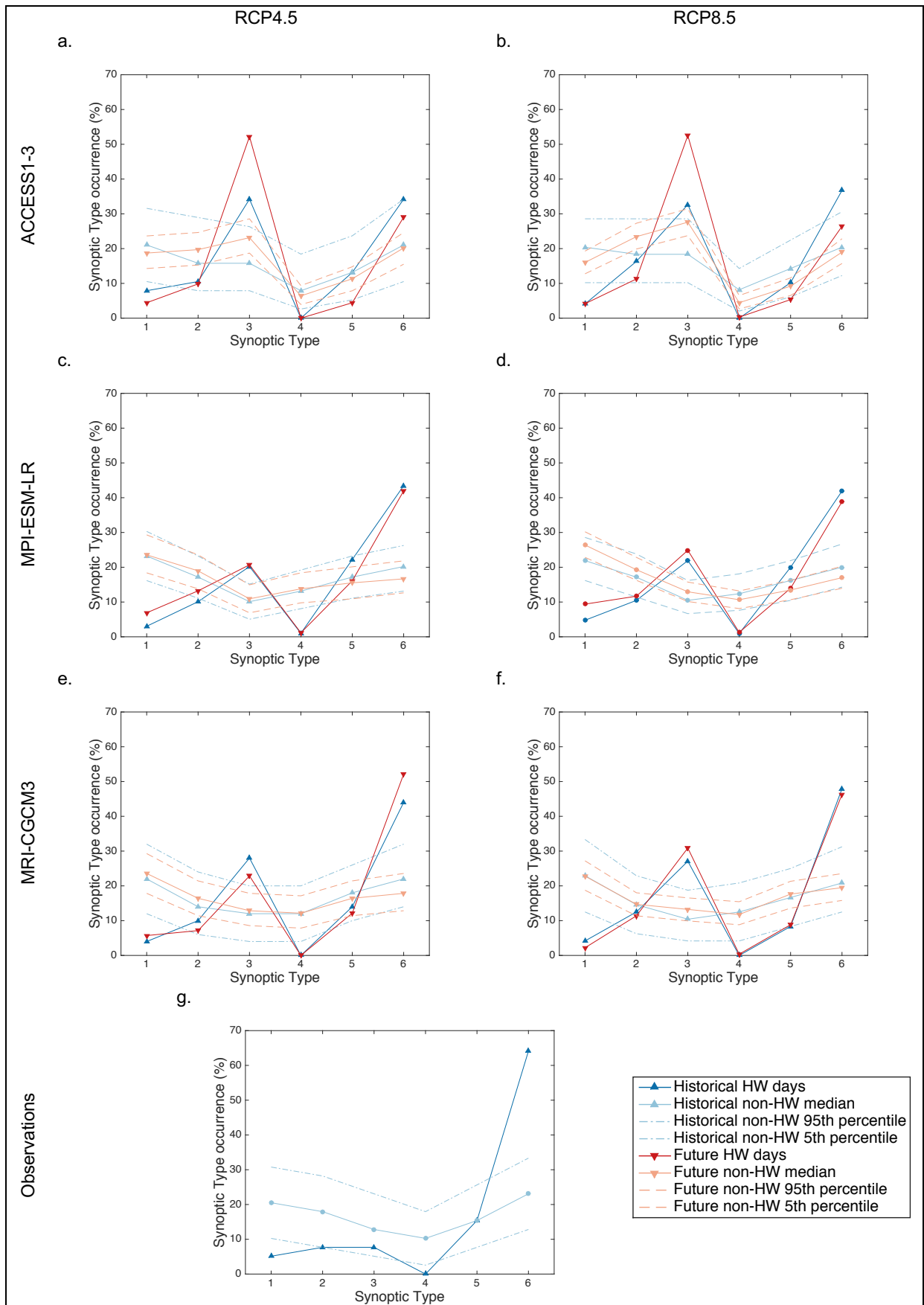
Figure 6.12: Same as Figure 6.10 but for Perth.

26.5 % (Table 6.8 and Figure 6.12). This finding indicates that Types 3 and 6 are both Dominant Heatwave Types in all model runs (Figure 6.12a to f). These biases in the frequency of Types 3 and 6 during heatwaves do not coincide with biases of similar magnitude and/or direction during the extended summer in all model runs (Table 6.4 and Figure 6.9). Thus, the three models are not simply fitting more patterns to Type 3 instead of Type 6, but that heatwaves are associated with different synoptic patterns in the models.

| Type | OBS | ACCESS1-3 | | MPI-ESM-LR | | MRI-CGCM3 | |
|------|-----|-----------|-----------|------------|------------|-----------|-----------|
| | | RCP4.5 | RCP8.5 | RCP4.5 | RCP8.5 | RCP4.5 | RCP8.5 |
| 1 | 5.1 | 7.9% (2.8) | 4.1% (-1.1) | 3.0% (-2.1) | 4.8% (-0.4) | 4.0% (-1.1) | 4.2% (-1.0) |
| 2 | 7.7 | 10.5% (2.8) | 16.3% (8.6) | 10.1% (2.4) | 10.5% (2.8) | 10.0% (2.3) | 12.5% (4.8) |
| 3 | 7.7 | 34.2% (26.5) | 32.7% (25.0) | 20.2% (12.5) | 21.9% (14.2) | 28.0% (20.3) | 27.1% (19.4) |
| 4 | 0.0 | 0.0% (0.0) | 0.0% (0.0) | 1.0% (1.0) | 1.0% (1.0) | 0.0% (0.0) | 0.0% (0.0) |
| 5 | 15.4 | 13.2% (-2.2) | 10.2% (-5.2) | 22.2% (6.8) | 20.0% (4.6) | 14.0% (-1.4) | 8.3% (-7.1) |
| 6 | 64.1 | 34.2% (-29.9) | 36.7% (-27.4) | 43.4% (-20.7) | 41.9% (-22.2) | 44.0% (-20.1) | 47.9% (-16.2) |

Table 6.8: As in Table 6.6 but for Perth.

The locations of the high-pressure systems in Types 3 and 6 are different. The system is centred to the southwest of Perth in Type 3 and to the southeast of the city in Type 6 (Figure 6.6). However, despite these differences, both Types show a ridge along the southwest coast of Australia that brings warm continental air towards Perth, thus the mechanism driving the heatwave does not change significantly.

While the discrepancies between the frequencies of occurrence of Types 3 and 6 during heatwaves in the observations and those in the models are significant, if we examine a combined Type 3 and 6, the differences become small. That is, the differences in the frequencies of occurrence are between -0.3 % and +10.9 % for all model runs (not shown). The fact that this difference occurs in all three models suggests a possible systematic bias of the simulation of heatwaves over Perth, with the anticyclonic systems associated with heatwaves occurring further to the west. However,

as we use three models only we could not examine if this is a systematic bias in all climate models.

*SIMULATION OF HEATWAVE FREQUENCY AND MAGNITUDE IN THE MODEL DATA*

Table 6.9 shows a comparison of the number of heatwaves identified using each of the model simulations compared to the observations. The MRI model under-predicts the number of heatwaves in Melbourne and Adelaide but provides a similar estimation in Perth (MRI simulates 17 heatwaves to the observed 16, Table 6.9). The MPI model generally over-predicts the number of heatwaves in all three cities. The ACCESS model under-predicts the number of heatwaves for the RCP4.5 historical simulations. Whereas for the RCP8.5 historical simulations, the number of heatwaves is under-predicted in Adelaide and overestimated in Melbourne and Perth (Table 6.9).

| City | Period | OBS | ACCESS1-3 | | MPI-ESM-LR | | MRI-CGCM3 | |
|------|--------|-----|-----------|-----------|------------|------------|-----------|-----------|
| | | | RCP4.5 | RCP8.5 | RCP4.5 | RCP8.5 | RCP4.5 | RCP8.5 |
| Melbourne | Historical | 18 (41) | 17 (42) | 21 (51) | 23 (70) | 24 (66) | 15 (36) | 13 (35) |
| | Future | - (-) | 27 (81) | 61 (161) | 64 (212) | 81 (249) | 20 (52) | 50 (144) |
| Adelaide | Historical | 24 (74) | 13 (33) | 12 (29) | 28 (95) | 24 (77) | 21 (55) | 20 (53) |
| | Future | - (-) | 25 (86) | 42 (132) | 55 (191) | 63 (214) | 21 (52) | 42 (132) |
| Perth | Historical | 16 (39) | 15 (38) | 19 (49) | 34 (99) | 33 (105) | 17 (50) | 17 (48) |
| | Future | - (-) | 62 (203) | 100 (337) | 60 (174) | 120 (394) | 44 (140) | 78 (272) |

Table 6.9: Number of heatwaves (heatwave days) during the historical (Jan 1995 to Mar 2014) and future (Jan 2065 to Mar 2084) periods during the extended summer season in Melbourne, Adelaide, and Perth.

On average, the number of heatwaves simulated by the models differs to the number of observed heatwaves by 26.4 %, with a maximum difference of 54.5 % and a minimum difference of 4.0 % (Table 6.9). Overall this suggests that the models do a relatively good job of simulating the number of heatwaves over each of the three cities.

The description of the models' abilities to simulate number of heatwaves uses thresholds for heatwaves that are internally consistent for each model i.e. the heatwave thresholds are calculated for each model individually. Next, we assess the maximum temperature biases associated with heatwaves in each model for the historical period (Figure 6.13). Biases differ for each model. That is, Figure 6.13a shows that the median of the observed heatwave temperatures in Melbourne are typically cooler than those in the ACCESS and MRI models, but warmer than those for MPI. In Adelaide and Perth, both ACCESS and MRI produce median heatwave temperatures that are too cool, but those produced using the MPI model are close to the observed values (Figure 6.13b and c).

Historical coolest maximum temperatures, i.e. the minimum of the maximum temperatures, during heatwaves are generally simulated well, except in Melbourne for the MPI model runs, and to a lesser extent Perth for the MRI model, whereby the coolest maximum temperatures are too cool (Figure 6.13).

Hottest maximum temperatures, i.e. the maximum of the maximum temperatures, during heatwaves are generally well simulated during the historical period. The most notable exceptions include an underestimation of the hottest maximum temperatures in MPI for Melbourne and in ACCESS and MRI for Adelaide and Perth.

There is generally more underestimation of heatwave temperatures than overestimation (Figure 6.13). This does not appear to be related to whether number of heatwaves is over or underestimated for the given city (Table 6.9). The above findings are considered when discussing projected changes to future heatwaves in Section 6.4.4.
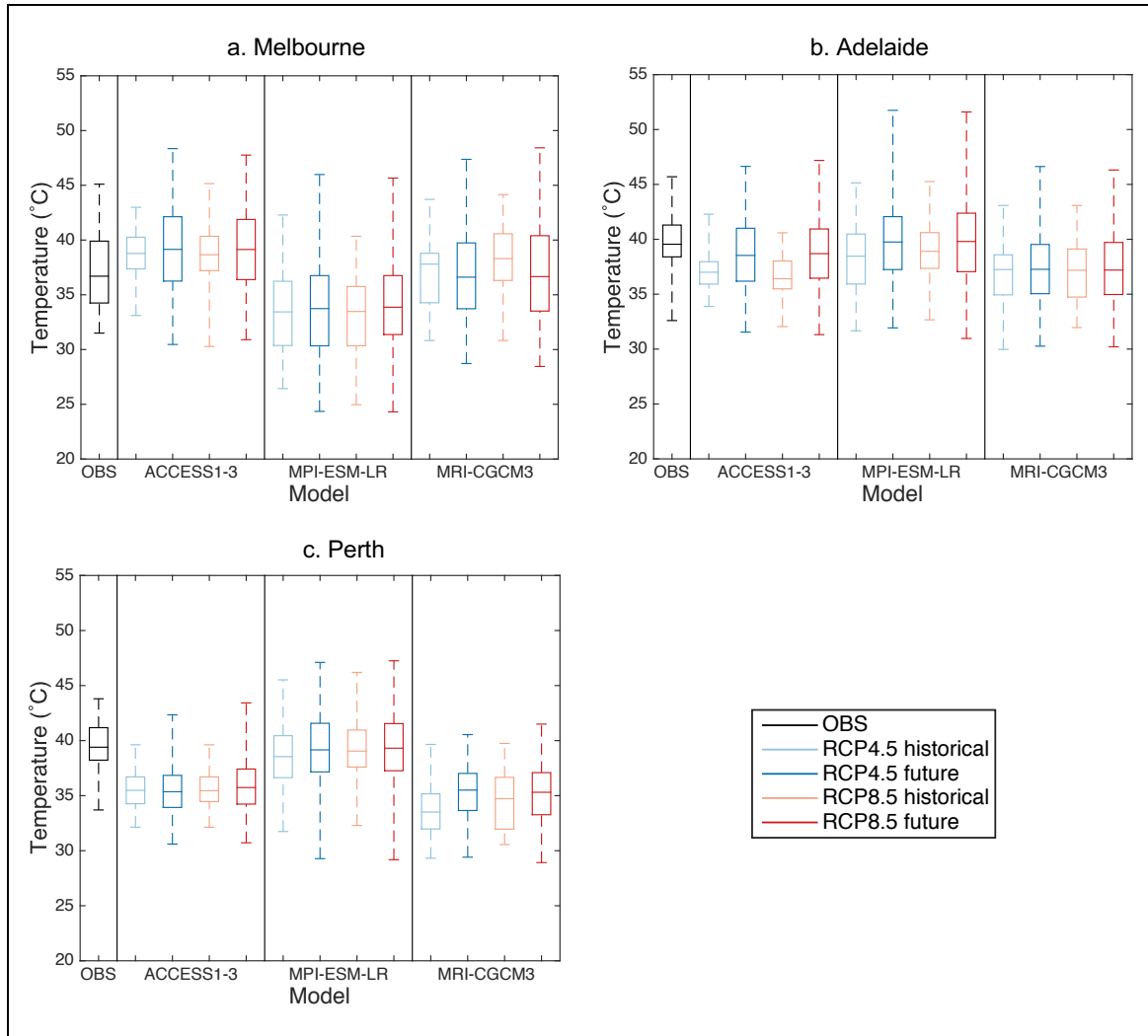
Figure 6.13: Boxplots showing variability of maximum temperatures during heatwaves for observational and model data. Black boxes show observational data. Light (dark) coloured boxes show historical (future) model data. Light blue and dark blue (pink and red) boxes show RCP4.5 (RCP8.5) model data. The central line in each box shows the median, the upper and lower edges show the 75$^{th}$ and 25$^{th}$ percentiles respectively. Upper and lower whiskers show the maximum and minimum of the maximum temperatures during heatwave respectively.

## 6.4.3 Future changes to synoptic patterns related to UHI strength

This section of the thesis examines how synoptic patterns are likely to change during the extended summer season in the future and relates these changes to the relationships between synoptic patterns and the strength of the UHI. As was described in the previous chapter, there are strong relationships between overlying synoptic patterns and the strength of the UHI. Thus, changes to the likelihood of synoptic patterns with anthropogenic climate change could be an important modulator of future

UHIs. The synoptic patterns in simulations from the ACCESS, MPI, and MRI models are assessed using two radiative forcing pathways, the RCP4.5 and RCP8.5.

To analyse how synoptic patterns might change in the future, we fit the future CMIP5 MSLP data to our pre-defined Synoptic Types in the ERA-Interim trained SOMs (Figures 6.4 to 6.6). To assess whether the future data are well represented by these Synoptic Types we compare quantisation errors for the CMIP5 historical and future periods in Table 6.10. This demonstrates that future data fit the SOMs as well as the historical data, with a range in difference of quantisation errors between the periods from -4.0 % to +2.6 % (Table 6.10). This result shows that there does not appear to be any systematic change to the synoptic patterns themselves in the future over the extended summer season. This is, the same patterns occur, just at differing frequencies.

| City | Scenario | ACCESS1-3 | MPI-ESM-LR | MRI-CGCM3 |
|---|---|---|---|---|
| Melbourne | RCP4.5 | 17853 (1.9%) | 18492 (0.5%) | 17977 (-0.4%) |
| | RCP8.5 | 17702 (1.8%) | 18371 (-0.1%) | 17787 (-0.9%) |
| Adelaide | RCP4.5 | 16920 (1.7%) | 17610 (1.4%) | 17013 (0.3%) |
| | RCP8.5 | 16771 (1.6%) | 17315 (-0.3%) | 16677 (-1.4%) |
| Perth | RCP4.5 | 14797 (1.2%) | 16226 (-0.4%) | 15029 (-1.0%) |
| | RCP8.5 | 14797 (2.6%) | 15590 (-4.0%) | 14728 (-3.7%) |

Table 6.10: Mean quantisation error (QE) of future CMIP5 data (Jan 2064 to Mar 2084), extended summer season only, where data are fit to the SOM created using ERA-Interim data over the historical period (Jan 1995 to Mar 2014). Values in brackets show the differences between QE for CMIP5 historical and future periods as a percentage of QE for the historical period, i.e. a positive value shows the error for the future period is greater than that for the past period. Model and ERA-Interim data are re-gridded onto the MRI-CGCM3 grid.

Changes in the frequency of Synoptic Types from the historical to the future periods are now investigated and changes to those Types that are most closely associated with strongly exacerbated or diminished UHIs are highlighted. We examine the direction of change in the frequency of each Synoptic Type for each city and establish whether these changes are consistent between models. We define that a change in the frequency of Synoptic Types is robust if at least five of the six simulations

show a change that is consistent in sign, for example at least five of six model runs show an increase in the frequency of a given Synoptic Type.

This approach requires the RCP4.5 and RCP8.5 model runs to be pooled to give us six runs for the three models. If the frequencies of Synoptic Types change linearly with increases in forcing, the direction of change should be the same between the RCP4.5 and RCP8.5 scenarios. Any inconsistencies in the changes in synoptic patterns between the different forcing pathways from the same model are most likely to be due to internal model variability.

Those Synoptic Types that are associated with UHIs of a particular nature (e.g. strongly exacerbated or diminished), as determined in Chapter 5, are pooled and examined together. For example, for Melbourne, we combine Types 1, 4, and 5 as these Types are all associated with a higher likelihood of strongly exacerbated UHIs (see Chapter 5). This allows us to determine the net effect of changing frequencies of Synoptic Types associated with particular UHI anomalies.

In Melbourne, Adelaide, and Perth we create four pooled groups of Synoptic Types. The first pooled group includes Synoptic Types that are associated with a higher likelihood of strongly exacerbated events ($HL_{exacerbated}$). The second pooled group includes those Synoptic Types that are associated with a lower likelihood of strongly diminished events ($LL_{diminished}$). These two pools represent Types that are associated with warmer than normal UHIs. Conversely, the third and fourth pooled groups include Synoptic Types associated with a higher likelihood of strongly diminished UHIs ($HL_{diminished}$) and a lower likelihood of strongly exacerbated UHIs ($LL_{exacerbated}$), thus these groups represent cooler than normal UHIs. The pooled Synoptic Types are listed in the captions for Tables 6.11 to 6.13. Note that $HL_{exacerbated}$ ($HL_{diminished}$) and $LL_{diminished}$ ($LL_{exacerbated}$) are likely to show consistent changes as they comprise some

of the same Synoptic Types. Synoptic Types that do not show a significantly higher or lower likelihood of strong UHI events when compared to random sampling are not considered in these pooled data.

*MELBOURNE*

There are consistent changes in the frequency of two Synoptic Types in the model simulations for Melbourne. Type 2 shows an increase of up to 21.4 % (149 days over the 20-year period) and Type 4 shows a decrease of a maximum of 28.7 % (134 days, Table 6.11 and Figure 6.7). Type 2 does not favour exacerbated or diminished UHIs. However, Type 4 is associated with a higher likelihood of strongly exacerbated UHIs and a lower likelihood of strongly diminished UHIs in the present day (see Chapter 5, Figure 5.2). Thus, should the relationships between the strength of the UHI and synoptic patterns remain relatively stationary into the future, a decrease in Type 4 represents a decrease in the likelihood of synoptic conditions that promote warm UHIs over Melbourne. The magnitudes of these changes are largest in the ACCESS and MRI models (Table 6.11 and Figure 6.7).

Type 2 changes linearly from RCP4.5 to RCP8.5 in all models (Table 6.11). That is, the frequencies of Type 2 in the future are larger under RCP8.5 than RCP4.5. The direction of change is consistent across all model runs, except MPI for RCP4.5, which shows a small reduction in occurrence by approximately 6 days over the 20-year period. Type 4 for ACCESS shows a stronger change for RCP8.5 than RCP4.5, with a decrease of 134 and 58 days for RCP8.5 and RCP4.5 respectively over the 20-year period. However, MPI shows changes of similar strength between the RCPs, and MRI shows changes with inconsistent signs for Type 4 (Table 6.11). The ACCESS model shows that higher greenhouse gas emissions, and therefore warmer temperatures, may

cause a decrease in the frequency of synoptic patterns associated with warmer UHIs, i.e. Type 4. However, this result is dependent on model choice.

| Type | ACCESS1-3 | | MPI-ESM-LR | | MRI-CGCM3 | |
|---|---|---|---|---|---|---|
| | RCP4.5 | RCP8.5 | RCP4.5 | RCP8.5 | RCP4.5 | RCP8.5 |
| 1 | 13.6% (-21) | 12.4% (-39) | 18.9% (9) | 17.7% (30) | 19.2% (-89) | 19.4% (-101) |
| 2 | 28.4% (66) | 28.6% (149) | 19.8% (-6) | 21.3% (47) | 30.8% (89) | 29.2% (103) |
| 3 | 12.4% (13) | 10.6% (-36) | 12.3% (-18) | 13.3% (33) | 7.7% (-101) | 9.7% (34) |
| 4 | 12.4% (-58) | 11.2% (-134) | 17.9% (-19) | 17.7% (-15) | 17.3% (19) | 16.0% (-35) |
| 5 | 13.6% (-21) | 12.4% (-97) | 15.1% (24) | 14.9% (-9) | 11.5% (-70) | 13.2% (52) |
| 6 | 19.8% (91) | 24.2% (195) | 15.6% (38) | 14.9% (-9) | 9.6% (-44) | 11.8% (11) |
| ◆HL$_{exacerbated}$ | 39.5% (-100) | 36.0% (-269) | 51.9% (13) | 50.2% (6) | 48.1% (-139) | 48.6% (-84) |
| ◆LL$_{diminished}$ | 25.9% (-79) | 23.6% (-173) | 36.8% (-10) | 35.3% (15) | 36.5% (-70) | 35.4% (-136) |
| ■ HL$_{diminished}$ | 19.8% (91) | 24.2% (195) | 15.6% (38) | 14.9% (-9) | 9.6% (-44) | 11.8% (11) |
| ■ LL$_{exacerbated}$ | 32.1% (105) | 34.8% (159) | 27.8% (20) | 28.1% (25) | 17.3% (-146) | 21.5% (45) |

Table 6.11: Percentage of occurrence of each Synoptic Type over the future period (Jan 2065 to Mar 2084) during the extended summer season in Melbourne. Values in brackets give the change in the number of days from the historical (Jan 1995 to Mar 2014) to the future period. Each 20-year period consists of 2964 days. Dark grey (light grey) shaded cells indicate Synoptic Types that show consistent increases (decreases) in frequency across at least 5 model runs in the future. The pool with a higher likelihood of strongly exacerbated UHIs (HL$_{exacerbated}$) comprises Types 1, 4, and 5. The pool with a lower likelihood of strongly diminished UHIs (LL$_{diminished}$) comprises Types 1 and 4. The pool with a higher likelihood of strongly diminished UHIs (HL$_{diminished}$) comprises Type 6. The pool with a lower likelihood of strongly exacerbated UHIs (LL$_{exacerbated}$) comprises Types 3 and 6. The pools denoted with a red diamond show the pools that are associated with warmer than normal UHIs (HL$_{exacerbated}$ and LL$_{diminished}$) and the pools denoted with a blue square show the pools that are associated with cooler than normal UHIs (HL$_{diminished}$ and LL$_{exacerbated}$).

Further, all Synoptic Types in ACCESS, except Type 3, show consistent changes in sign under both radiative forcing pathways, with stronger changes under RCP8.5 (Table 6.11). The results from the ACCESS model suggest that the higher the greenhouse gas emissions, the greater the changes in synoptic pattern frequency over Melbourne are likely to be when compared to the historical period. That is, the greater the magnitude of emissions increases, the greater the magnitude of changes in synoptic pattern frequencies. MPI and MRI do not show changes that are consistent in sign across most Types, highlighting that internal variability is larger than any forced response in these models.

By comparing the pooled Synoptic Types in Table 6.11 we see a clear indication that ACCESS projects a higher likelihood of those Synoptic Types associated with cooler UHIs ($HL_{diminished}$ and $LL_{exacerbated}$) and a lower likelihood in those associated with warmer UHIs ($HL_{exacerbated}$ and $LL_{diminished}$) in Melbourne, regardless of emission scenario. The MRI model shows a similar reduction in Types associated with warmer UHIs but changes in Types associated with cooler UHIs are inconsistent in sign. This pattern is much weaker in the MPI model, which shows small increases in $LL_{exacerbated}$ for both radiative forcing pathways (up to 25 days over the 20-year period), but only shows a small decrease in $LL_{diminished}$ for RCP4.5 (10 days over the 20-year period, Table 6.11).

In summary, ACCESS shows that changes to the frequencies of the pooled groups are stronger with increased emissions, i.e. higher (lower) likelihood of Types associated with cooler (warmer) UHIs under RCP8.5 compared to RCP4.5 (Table 6.11). This pattern is not replicated by MPI or MRI. No model shows a preference for a higher likelihood of Synoptic Types associated with more strongly exacerbated UHIs in the future, that is, all models show that it is unlikely that there will be an increase in synoptic patterns associated with warmer UHIs in the future in Melbourne.

*ADELAIDE*

In Adelaide, Types 1 and 2 show consistent changes in frequency across five of six model runs from the 1995-2014 to 2065-2084 period (Table 6.12 and Figure 6.8). Type 1 shows a decrease in frequency of up to 107 days over the 20-year period, whereas Type 2 shows an increase of up to 195 days. Both Types 1 and 2 are associated with a decreased likelihood of strongly exacerbated UHIs in the present day when compared to chance, and Type 1 is also associated with an increased chance of strongly

diminished UHIs (Chapter 5, Figure 5.4). So, an increase in Type 2 and decrease in Type 1 counterbalance to some extent and so the resulting change to all Types associated with strongly exacerbated UHIs in the present day is unclear.

| Type | ACCESS1-3 | | MPI-ESM-LR | | MRI-CGCM3 | |
|---|---|---|---|---|---|---|
| | RCP4.5 | RCP8.5 | RCP4.5 | RCP8.5 | RCP4.5 | RCP8.5 |
| 1 | 14.0% (-36) | 13.6% (-107) | 18.9% (-3) | 18.2% (40) | 15.4% (-29) | 16.7% (-9) |
| 2 | 27.9% (109) | 27.3% (195) | 16.8% (-34) | 18.7% (15) | 26.9% (44) | 27.3% (25) |
| 3 | 19.8% (137) | 23.5% (185) | 13.6% (-2) | 14.5% (6) | 9.6% (-38) | 11.4% (57) |
| 4 | 8.1% (-28) | 8.3% (-60) | 14.7% (29) | 11.7% (-39) | 15.4% (25) | 13.6% (-99) |
| 5 | 14.0% (-36) | 10.6% (-94) | 17.3% (-18) | 18.7% (15) | 17.3% (28) | 17.4% (69) |
| 6 | 16.3% (-56) | 15.9% (-39) | 18.3% (44) | 17.8% (26) | 13.5% (-32) | 13.6% (13) |
| ◆HL$_{exacerbated}$ | 30.2% (-92) | 26.5% (-134) | 35.6% (26) | 36.5% (41) | 30.8% (-4) | 31.1% (82) |
| ◆LL$_{diminished}$ | 16.3% (-56) | 15.9% (-39) | 18.3% (44) | 17.8% (26) | 13.5% (-32) | 13.6% (13) |
| ■ HL$_{diminished}$ | 14.0% (-36) | 13.6% (-107) | 18.9% (-3) | 18.2% (40) | 15.4% (-29) | 16.7% (-9) |
| ■ LL$_{exacerbated}$ | 69.8% (182) | 72.7% (214) | 63.9% (-10) | 63.1% (22) | 67.3% (1) | 68.9% (-26) |

Table 6.12: Same as Table 6.11 but for Adelaide. The pool with a higher likelihood of strongly exacerbated UHIs (HL$_{exacerbated}$) comprises Types 5 and 6. The pool with a lower likelihood of strongly diminished UHIs (LL$_{diminished}$) comprises Type 6. The pool with a higher likelihood of strongly diminished UHIs (HL$_{diminished}$) comprises Type 1. The pool with a lower likelihood of strongly exacerbated UHIs (LL$_{exacerbated}$) comprises Types 1, 2, 3, and 4.

Changes in frequencies for the other Synoptic Types are often inconsistent across the different radiative forcing pathways for MPI and MRI. ACCESS on the other hand shows stronger changes under RCP8.5 than RCP4.5 for all Types (except Type 6), with consistent signs over both RCPs (Table 6.12). Similarly to Types 1 and 2, Types 3 and 4 are also associated with fewer strongly exacerbated UHIs (Figure 5.4). These Types show a respective increase (up to 185 days in the 20-year period) and decrease (up to 60 days) in frequency in ACCESS. Types 5 and 6, which are associated with an increased chance of strongly exacerbated UHIs (Figure 5.4), show decreases of up to 94 days for the 20-year period in ACCESS. This means that Types 2 and 3 are the only Types to increase in frequency with anthropogenic forcing. Both of these Types are associated with fewer strongly exacerbated UHIs than can be expected due to chance (Figure 5.4).

These results tend to suggest that fewer synoptic patterns associated with strong UHIs, both exacerbated and diminished, are likely to occur in the two decades centred on the year 2075.

Pooled Types that are associated with a higher likelihood of strongly diminished UHIs ($HL_{diminished}$) are the only group to show a change in frequency that is consistent across most model runs in Adelaide (all runs except RCP8.5 for the MPI model) (Table 6.12). Thus, Types associated with strongly diminished UHIs are likely to occur less frequently in the future according to these model results. When considering the ACCESS model only, Types that are associated with a lower chance of strongly exacerbated UHIs ($LL_{exacerbated}$) are likely to be more frequent in the future when compared to the historical period. The Synoptic Types associated with warmer UHIs ($HL_{exacerbated}$ and $LL_{diminished}$) both show a decrease in occurrence for RCP4.5 and RCP8.5 in the ACCESS model (up to 134 day decrease in the 20-year period). The increase of $LL_{exacerbated}$ and decreases in $HL_{exacerbated}$ and $HL_{diminished}$ in the ACCESS model suggest that Types associated with strong UHIs, both exacerbated and diminished, will be less likely in the future. These changes in frequencies are not replicated by the MPI or MRI models, which often show inconsistent results across the different radiative forcing pathways, again highlighting their strong internal variability compared to the ACCESS model.

All individual Synoptic Types and pooled groups in the ACCESS model show consistent changes across the two radiative forcing pathways (Table 6.12). Further, all changes in frequencies are stronger under the higher radiative forcing pathway except for Type 6 and the $LL_{diminished}$ group. These results show that the ACCESS model has a stronger response to anthropogenic forcing compared to the MRI and MPI models.

Interestingly, the models have a tendency to show an overall reduction in the frequency of Types that are associated with strong UHIs. That is, decreases in $HL_{diminished}$ (except RCP8.5 for the MPI model) and $HL_{exacerbated}$ (ACCESS RCP4.5 and RCP8.5, and MRI RCP4.5 only). This implies that future synoptic conditions over Adelaide may favour weaker UHIs than those in the historical period, provided those relationships between UHI strength and synoptic conditions are relatively stationary.

*PERTH*

Four of six Synoptic Types in Perth show consistent changes across the models and radiative forcings. Future projections in Perth show increases in the frequencies of Types 2 and 3 of up to approximately 150 days and 274 days respectively over the 20-year period. Types 5 and 6 show decreases in the frequencies of up to 151 days and 123 days respectively (Table 6.13 and Figure 6.9). In general, the ACCESS model shows changes with greater magnitudes than those for the MPI and MRI models (Table 6.13 and Figure 6.9). This is consistent with Melbourne and Adelaide which both show that the ACCESS model has a stronger response in synoptic conditions to radiative forcing than the MPI and MRI.

Types 3 and 6, both of which are associated with cooler than normal UHIs, show opposing changes in frequencies. That is, there is an increase in the frequency of Type 3 and a decrease in Type 6 (Table 6.13 and Figure 5.6). This coincides with an increase in the frequency of Type 2 and a decrease in Types 5 (Table 6.13). Types 2 and 5 are associated with a reduced or normal chance of cool UHIs in the present day (Figure 5.6). As there are competing changes, it is unclear whether the net effect is toward future increases or decreases in those types of Synoptic Types that favour more or fewer strongly diminished UHIs in the present day.

| Type | ACCESS1-3 | | MPI-ESM-LR | | MRI-CGCM3 | |
|---|---|---|---|---|---|---|
| | RCP4.5 | RCP8.5 | RCP4.5 | RCP8.5 | RCP4.5 | RCP8.5 |
| 1 | 18.7% (-69) | 16.0% (-130) | 23.6% (10) | 26.4% (133) | 23.6% (47) | 22.8% (-4) |
| 2 | 19.7% (116) | 23.4% (150) | 19.0% (53) | 19.3% (64) | 16.4% (72) | 14.7% (4) |
| 3 | 23.2% (218) | 27.6% (274) | 10.9% (24) | 12.7% (66) | 12.9% (25) | 13.2% (84) |
| 4 | 6.4% (-44) | 4.5% (-110) | 13.8% (20) | 10.7% (-51) | 12.1% (4) | 11.8% (-22) |
| 5 | 11.3% (-54) | 9.2% (-151) | 15.5% (-49) | 13.5% (-81) | 16.4% (-47) | 17.3% (18) |
| 6 | 20.2% (-25) | 19.3% (-33) | 16.7% (-105) | 17.0% (-89) | 17.9% (-123) | 19.5% (-102) |
| ◆ $HL_{exacerbated}$ | 6.4% (-44) | 4.5% (-110) | 13.8% (20) | 10.7% (-51) | 12.1% (4) | 11.8% (-22) |
| ◆ $LL_{diminished}$ | 44.8% (3) | 43.9% (-90) | 56.3% (83) | 56.4% (146) | 52.1% (123) | 49.3% (-22) |
| ■ $HL_{diminished}$ | 43.4% (193) | 46.9% (240) | 27.6% (-80) | 29.7% (-23) | 30.7% (-97) | 32.7% (-18) |
| ■ $LL_{exacerbated}$ | 43.4% (193) | 46.9% (240) | 27.6% (-80) | 29.7% (-23) | 30.7% (-97) | 32.7% (-18) |

Table 6.13: Same as Table 6.11 but for Perth. The pool with a higher likelihood of strongly exacerbated UHIs ($HL_{exacerbated}$) comprises Type 4. The pool with a lower likelihood of strongly diminished UHIs ($LL_{diminished}$) comprises Type 1, 2, and 4. The pool with a higher likelihood of strongly diminished UHIs ($HL_{diminished}$) comprises Types 3 and 6. The pool with a lower likelihood of strongly exacerbated UHIs ($LL_{exacerbated}$) comprises Types 3 and 6.

In Perth, the strength of the projected changes in the frequencies of the pooled Synoptic Types depends on the choice of model, i.e. no pooled groups show consistent changes across all models (Table 6.13).

Both ACCESS RCPs show an increase in the percentage of those Synoptic Types associated with strongly diminished UHI events ($HL_{diminished}$) and a decrease in Types associated with strongly exacerbated UHIs ($HL_{exacerbated}$), thus ACCESS favours Types that are associated with cooler UHIs in the present day. On the other hand, both MPI scenarios and the MRI RCP4.5 show future increases in the $LL_{diminished}$ group and all scenarios for the MPI and MRI simulations show decreases in $HL_{diminished}$, thus suggesting that these models favour changes toward more of those Synoptic Types that are associated with warmer and/or weaker UHIs in the present day. These differences mean that changes in the frequencies of the pooled groups are inconsistent across the models and radiative forcing pathways.

When stratified by RCP, the simulations from the ACCESS and MPI models show stronger changes in Synoptic Type frequencies for RCP8.5 than for RCP4.5 for all individual Types, except Types 4 and 6 for the MPI model only (Table 6.13). This

suggests a linear forced response in many synoptic patterns in these two models. However, this result is not replicated by the MRI model, which shows inconsistent changes between RCPs. This shows that the changes in synoptic patterns in ACCESS and MPI are likely driven by the radiative forcings in the models, whereas for the MRI model, internal variability appears to have a larger influence on changes in the synoptic conditions than the forcings.

The above results show that there is little consistency across the models on the direction of the projected change in Synoptic Types over Perth. ACCESS tends to favour those Types that are associated with cooler UHIs in the present day, whereas MPI and MRI favour Types that are associated with weaker (i.e. more moderate and fewer strong UHIs) and/or warmer UHIs in the present day. Due to the differences between the directions of change across the models, as reflected in the differing results for the pooled Types (Table 6.13), changes in those patterns associated with UHI strength in Perth are uncertain.

The above analysis shows that future changes to synoptic patterns that are associated with anomalous UHIs of certain strengths in the present day are unclear. The results are frequently inconsistent across all models. If the earth system responds linearly to increases in emissions one would expect the results should be consistent in sign across radiative forcing pathways as when compared to the historical period. This is, changes in frequencies of the Synoptic Types would be in the same direction for the two RCPs and greater in magnitude for RCP8.5. Differences in signs between RCPs suggest one of two things. The first is that internal model variability still dominates any anthropogenic climate change signal of changes to synoptic conditions in the mid-late $21^{st}$ century. The second is that there are non-linearities in changes to synoptic

conditions. Further investigation of each of these is beyond the scope of this thesis, however, given the strength of the RCP forcing it's more likely that internal variability is dominating.

However, one consistency across all cities is that no city shows any robust future increase in those types of synoptic patterns that are associated with strongly exacerbated UHIs in the present day. Instead, some cities show either no consistent significant change over the majority of model runs (Perth) or some evidence of a change toward those synoptic systems that are presently associated with UHIs that are cooler and/or weaker in magnitude when compared to those in the historical period (Melbourne and Adelaide). Given that past research shows that UHIs are likely to become warmer with increasing urbanisation (Coutts et al. 2008; Argüeso et al. 2014) and fundamental surface warming associated with anthropogenic climate change (Sachindra et al. 2016; Roberge and Sushama 2018; Zhang and Ayyub 2018) in the future, we may expect the UHIs of Melbourne, Adelaide, and Perth to become warmer. However, our results from three climate models show that if the relationship between synoptic systems and UHI strength remains largely stationary, the changes in synoptic patterns are more likely to ameliorate this warming than intensify it.

**6.4.4 Future changes to synoptic patterns and implications for heatwaves**

In Chapter 5, we showed that the dominant mechanism affecting the strength of the UHI changes during heatwaves compared to the entire extended summer season. Specifically, during heatwaves the UHI is more strongly affected by the presence of the heatwave itself and the association between the strength of the UHI and synoptic pattern decreases compared to the extended summer season. In this sense, the synoptic pattern becomes less important to the likelihood of an anomalous UHI during heatwaves. These

results suggest that the incidence of heatwaves will affect future UHIs, regardless of Synoptic Type, i.e. if more heatwaves occur for a wider variety of Synoptic Types, this could affect the strength of the UHIs associated with each Type.

Given the previously identified relationship between heatwaves and the UHI, projected changes to the synoptic patterns associated with heatwaves imply a further change to the relationship between synoptic patterns and the strength of the UHI. This cannot be examined directly unless we perform downscaled, high-resolution simulations of the UHI over Australian cities, which is outside the scope of this project. However, examining changes in the frequency of synoptic patterns during heatwaves at least identifies whether non-stationarity in the relationships between synoptic patterns and the UHI could be introduced.

*FUTURE HEATWAVES*

Before examining changes in Synoptic Types associated with future heatwaves, we investigate how heatwave metrics are likely to change in the future. As discussed in Chapter 1, heatwaves are expected to get hotter, longer, and more frequent in the future (Meehl and Tebaldi 2004; Alexander and Perkins 2013; Cowan et al. 2014a; Cowan et al. 2014b; Fallmann et al. 2017). We examine changes in heatwave temperatures between the historical and future periods in Figure 6.13, and changes in the number of heatwaves, number of heatwave days, and heatwave duration in Table 6.14.

Consistent with past research, Table 6.14 shows that the number of heatwaves is expected to increase in the future, with 101.8 %, 62.9 %, 151.5 % more heatwaves in Melbourne, Adelaide, and Perth respectively in the future for the moderate RCP (Table 6.14). The high RCP further enhances these increases with 231.0 %, 162.5 %, and 331.9 % more heatwaves in Melbourne, Adelaide, and Perth respectively compared to the

historical period (Table 6.14). Greater increases are seen for the future number of heatwave days, with up to 255.2 %, 190.7 %, and 380.1 % more heatwave days in Melbourne, Adelaide, and Perth respectively (Table 6.14). Thus, there is also an increase in the duration of heatwaves of up to an average of 11.8 %, 10.5 %, and 11.0 % (Table 6.14).

| City | Period | Number of heatwaves | | Number of heatwave days | | Heatwave duration | |
|---|---|---|---|---|---|---|---|
| | | RCP4.5 | RCP8.5 | RCP4.5 | RCP8.5 | RCP4.5 | RCP8.5 |
| Melbourne | Historical | 9.2 | 9.7 | 33.8 | 35.0 | 3.7 | 3.6 |
| | Future | 18.5 | 32.0 | 76.0 | 124.3 | 4.1 | 3.9 |
| | Change | 101.8% | 231.0% | 124.6% | 255.2% | 11.8% | 7.7% |
| Adelaide | Historical | 10.3 | 9.3 | 40.8 | 35.8 | 4.0 | 3.8 |
| | Future | 16.8 | 24.5 | 71.7 | 104.2 | 4.3 | 4.3 |
| | Change | 62.9% | 162.5% | 75.5% | 190.7% | 7.7% | 10.5% |
| Perth | Historical | 11.0 | 11.5 | 42.2 | 45.2 | 3.8 | 3.9 |
| | Future | 27.7 | 49.7 | 113.8 | 216.8 | 4.1 | 4.4 |
| | Change | 151.5% | 331.9% | 170.0% | 380.1% | 7.1% | 11.0% |

Table 6.14: Number of heatwaves, number of heatwaves days, and mean heatwave duration for Melbourne, Adelaide, and Perth, averaged over the ACCESS1-3, MPI-ESM-LR, and MRI-CGCM3 models over the historical (Jan 1995 to Mar 2014) and future (Jan 2065 to Mar 2084) periods. Here we include heatwave start, middle, and end days in our calculation of these values. Values are given for moderate (RCP4.5) and high (RCP8.5) radiative forcing pathways. The rows labelled "change" show the percentage difference between the historical and future periods.

All cities show increases in the number of heatwaves, number of heatwave days, and duration in the future. This means that the future period consists of more heatwave days than the historical period. Heatwaves in the historical period account for an average of 2.3 %, 2.6 %, and 2.9 % of days in the extended summer season for Melbourne, Adelaide, and Perth respectively, whereas future heatwaves account for 6.8 %, 5.9 %, and 11.2 % of the season. These values are averaged over the three models and two RCPs. Changes in number of heatwaves, number of heatwave days, and duration are greater for the higher forcing scenario, except for heatwave duration in Melbourne where the increase in duration is slightly smaller for RCP8.5 (7.7 %) than RCP4.5 (11.8 %), when compared to the historical period.

Figure 6.13 shows us that maximum heatwave temperatures in the future are expected to get hotter, as shown by increases in the median of the boxplots. While the hottest maximum temperatures during heatwaves are often underestimated by the models in the historical period, for example MPI for Melbourne (Figure 6.13a), all models simulations show consistent increases in the hottest heatwave temperatures in the future for all cities.

Maximum heatwave temperatures are also expected to become more variable in the future. This is evident because while all model runs show an increase in the hottest maximum heatwave temperatures, most also show a decrease in the coolest maximum temperatures when compared to the historical period (Figure 6.13).

*MELBOURNE*

During future heatwaves in Melbourne, four of six Synoptic Types show consistent changes in frequencies when compared to the historical period (Table 6.15 and Figure 6.10). Future projections show that Types 1, 3, and 6 occur more frequently during heatwaves when compared to the historical period. Moreover, Type 5, which is the Dominant Heatwave Type for the historical model data, shows a consistent decrease in the frequency of occurrence during future heatwave days (Table 6.15 and Figure 6.10). This is, the types of synoptic conditions under which a heatwave occurs diversifies when compared to the historical period. Note that although there is a reduction in Type 5, it remains a Dominant Heatwave Type for all models and scenarios as its frequency remains above the 90 % confidence interval for the future period (Figure 6.10a to f).

Also, due to increases in the number of heatwaves in the future, while the relative frequency of Type 5 decreases, the total number of heatwave days in Type 5

increases from an average of 25 to 66 heatwave days (not shown). Throughout this section, rather than discussing changes in the number of heatwave days for a given Synoptic Type, we discuss the change in the frequency of that Type during heatwaves.

| Type | ACCESS1-3 | | MPI-ESM-LR | | MRI-CGCM3 | |
|---|---|---|---|---|---|---|
| | RCP4.5 | RCP8.5 | RCP4.5 | RCP8.5 | RCP4.5 | RCP8.5 |
| 1 | 1.2% (1.2) | 1.2% (1.2) | 5.2% (2.3) | 0.4% (-2.6) | 1.9% (1.9) | 2.1% (2.1) |
| 2 | 18.5% (6.6) | 11.2% (-2.6) | 9.0% (-5.3) | 11.7% (1.0) | 26.9% (-3.6) | 22.9% (-5.7) |
| 3 | 3.7% (1.3) | 1.2% (-2.7) | 5.2% (0.9) | 5.6% (1.1) | 3.9% (1.1) | 2.1% (2.1) |
| 4 | 9.9% (0.4) | 5.0% (-2.9) | 17.5% (1.7) | 16.1% (2.4) | 19.2% (10.9) | 16.7% (-0.5) |
| 5 | 46.9% (-5.5) | 44.1% (-6.9) | 46.7% (-4.7) | 47.0% (-7.6) | 28.9% (-21.2) | 38.2% (-1.8) |
| 6 | 19.8% (-4.1) | 37.3% (13.7) | 16.5% (5.1) | 19.3% (5.6) | 19.2% (10.9) | 18.1% (3.8) |

Table 6.15: Mean percentage of occurrence of Synoptic Types during heatwaves in Melbourne for the ACCESS1-3, MPI-ESM-LR, and MPI-CGCM3 models. Values in brackets show the difference between the percentage of occurrence of future and historical periods. Dark grey (light grey) shaded cells indicate Synoptic Types that show consistent increases (decreases) in frequency across at least 5 model runs.

Over Melbourne, there is an increase in Type 6 for future simulations for all models runs except ACCESS1-3 RCP4.5 (Table 6.15 and Figure 6.10a to f). This results in both Types 5 and 6 being classified as Dominant Heatwave Types in the future simulations for all models under RCP8.5, and for the MRI model for RCP4.5. This is compared to the historical period where only Type 5 is a Dominant Type for all model runs (Figure 6.10a to f). That is, frequencies of both Types 5 and 6 on future heatwave days are greater than the 90 % confidence interval for the extended summer season (Figure 6.10a to f). The increase in Type 6 and decrease in Type 5 suggests that hotter background temperatures are causing a change in the synoptic patterns that are associated with heatwaves.

It is not clear what causes the above-mentioned change in the relationship between synoptics and heatwaves, i.e. what causes Type 6 to become a Dominant Heatwave Type. Our first hypothesis is that there is a westward shift in the synoptic patterns associated with heatwaves. Synoptic Types 5 and 6 both have high-pressure

systems influencing the weather in Melbourne, with the high-pressure system in Type 6 located further west than that in Type 5 (Figure 6.4). Thus, an increase of Synoptic Type 6 during heatwaves at the expense of Type 5 suggests a westward shift of this system. This hypothesis is consistent with the findings of Purich et al. (2014) who noted a westward shift of synoptic patterns during future heatwaves over Melbourne.

Our second hypothesis for this shift in Synoptic Types during heatwaves is that since increased greenhouse gas emissions are associated with warmer background temperatures, yet heatwave thresholds are still identified using the 1975 to 2005 base period, it is easier for heatwave thresholds to be exceeded in the future. Thus, future heatwaves are less dependent on synoptic patterns. This is evident by the increases in the frequencies of Types 1, 3, and 6 during heatwaves. The increase in the frequency of Type 6 during heatwaves, which is often followed by Type 5 (Table 5.2), implies that heatwaves are starting earlier. Further, the small but consistent increases in the frequencies of Types 1 and 3 during future heatwaves (Table 6.15), shows that a wider range of synoptic patterns are conducive to future heatwave formation when compared to the historical period.

Lastly, we compare changes in the frequencies of Synoptic Types for the different radiative forcing pathways. It might be assumed that the changes described above would be stronger for higher RCPs, as higher emissions are related to higher background temperatures thus heatwaves are more likely to be less constrained by Synoptic Type, but this is not observed in Table 6.15 or Figure 6.10a to f. This suggests that there may be more variability in the relationship between heatwaves and synoptic patterns in the future, or that there is a non-linearity in the effect of rising temperatures on this relationship. Alternatively, model biases and internal variability, as identified in Section 6.4.2, may be obscuring the signal.

*ADELAIDE*

Only Type 5 in Adelaide shows a consistent change in the frequency of occurrence for future heatwaves (Table 6.16 and Figure 6.11). In Chapter 5, Types 5 and 6 were both identified as Dominant Heatwave Types using observational data. However, as we show in Section 6.4.2, this pattern is not replicated well by the models. Type 5 tends to occur too infrequently in the models, resulting in it not being classified as a Dominant Heatwave Type (Figure 6.11). The reduction in Type 5 in the future is therefore potentially not representative of the real world given the models show low biases in their simulations of this Synoptic Type in the historical period.

| Type | ACCESS1-3 | | MPI-ESM-LR | | MRI-CGCM3 | |
|------|-----------|-----------|-----------|-----------|-----------|-----------|
| | RCP4.5 | RCP8.5 | RCP4.5 | RCP8.5 | RCP4.5 | RCP8.5 |
| 1 | 4.7% (4.7) | 1.5% (-5.4) | 11.5% (5.2) | 5.1% (-0.1) | 0.0% (-7.3) | 1.5% (-4.1) |
| 2 | 14.0% (7.9) | 9.9% (6.4) | 7.9% (-4.8) | 9.8% (-3.2) | 9.6% (2.4) | 14.4% (5.0) |
| 3 | 14.0% (-4.2) | 32.6% (11.9) | 9.4% (-2.2) | 11.7% (3.9) | 9.6% (-1.3) | 22.0% (6.9) |
| 4 | 1.2% (1.2) | 0.0% (0.0) | 1.6% (-5.8) | 4.7% (0.8) | 1.9% (1.9) | 3.0% (-0.7) |
| 5 | 16.3% (-8.0) | 7.6% (-6.2) | 27.2% (3.0) | 19.6% (-1.2) | 25.0% (-4.1) | 12.1% (-10.5) |
| 6 | 50.0% (-1.5) | 48.5% (-6.7) | 42.4% (4.5) | 49.1% (-0.3) | 53.9% (8.4) | 47.0% (3.6) |

Table 6.16: Same as Table 6.15 but for Adelaide.

Further examining these changes, in four of six runs (ACCESS RCP4.5 and all models for RCP8.5) the Types classified as Dominant Heatwave Types remain unchanged, that is Type 6 is the only Dominant Type for the historical and future periods (Figure 6.11). The future simulations for the MPI and MRI for RCP4.5 both show a change in Dominant Types associated with heatwaves, but these changes are not consistent between the two models. The Dominant Types in MPI RCP4.5 change from only Type 6 to both Types 5 and 6, and MRI sees the opposite, changing from 5 and 6 to only 6. The inconsistency between MPI and MRI for the RCP4.5 scenario suggests that the changes in the Dominant Synoptic Types are not robust.

Changes in frequencies for certain Synoptic Types are often inconsistent across the different radiative forcing pathways. These results, along with our earlier findings that most Types do not show consistent changes during future heatwaves, show that future changes to synoptic patterns over Adelaide during heatwaves have no robust forced signal.

*PERTH*

In Perth, three of six Types show consistent increases or decreases in frequency during heatwave events over the 2065 to 2084 period compared to 1995 to 2014. Type 3 shows an increase in frequency whereas Types 5 and 6 show decreases (Table 6.17).

| Type | ACCESS1-3 | | MPI-ESM-LR | | MRI-CGCM3 | |
|------|-----------|-----------|-----------|-----------|-----------|-----------|
|  | RCP4.5 | RCP8.5 | RCP4.5 | RCP8.5 | RCP4.5 | RCP8.5 |
| 1 | 4.4% (-3.5) | 4.2% (0.1) | 6.9% (3.9) | 9.4% (4.6) | 5.7% (1.7) | 2.2% (-2.0) |
| 2 | 9.9% (-0.7) | 11.3% (-5.1) | 13.2% (3.1) | 11.7% (1.2) | 7.1% (-2.9) | 11.4% (-1.1) |
| 3 | 52.2% (18.0) | 52.5% (19.9) | 20.7% (0.5) | 24.9% (3.0) | 22.9% (-5.1) | 30.9% (3.8) |
| 4 | 0.0% (0.0) | 0.3% (0.3) | 1.2% (0.1) | 1.3% (0.3) | 0.0% (0.0) | 0.4% (0.4) |
| 5 | 4.4% (-8.7) | 5.3% (-4.9) | 16.1% (-6.1) | 14.0% (-6.0) | 12.1% (-1.9) | 8.8% (0.5) |
| 6 | 29.1% (-5.2) | 26.4% (-10.3) | 42.0% (-1.5) | 38.8% (-3.1) | 52.1% (8.1) | 46.3% (-1.6) |

Table 6.17: Same as Table 6.15 but for Perth.

While only Type 6 is identified as a Dominant Heatwave Type using observational data (Chapter 5 and Figure 6.12g), Section 6.4.2 identifies both Types 3 and 6 as Dominant Heatwave Types using historical model data (Figure 6.12a to f). That is, there is a high bias in the frequency of Type 3 in the models resulting in this Type occurring more frequently during heatwaves than can be expected due to chance. The future model data also shows Types 3 and 6 to be Dominant Heatwave Types (Figure 6.12a to f), thus heatwaves in the future and historical periods are predominantly associated with similar synoptic conditions.

Type 3 features a high-pressure system to the southwest of Perth, whereas Type 6 has a high-pressure system to the southeast of the city (Figure 6.6). While the locations of the pressure centres are vastly different in the two Types, both Types are associated with northeasterly flow due to the presence of a ridge along the western coast of Australia (Figure 6.6). This ridge brings warm continental air to Perth and therefore explains why both Types 3 and 6 are often associated with heatwaves.

Future heatwaves are projected to be associated with an increase in the frequency of Type 3 (high pressure to the southwest of Perth) and a decrease in Type 6 (high pressure to the southeast of Perth), see Table 6.17 and Figure 6.6. As for Melbourne, this result suggests a westward shift in the synoptics associated with future heatwaves or an earlier onset of future heatwaves. However, since our previous discussion shows that the frequency of Type 3 is overestimated during historical heatwaves in the models, it is unclear whether this further increase in Type 3 during future heatwaves is a true reflection of how MSLP patterns will change, or another overestimation of Type 3.

Table 6.17 also shows a decrease in the frequency of Type 5 during future heatwaves. Type 5 often occurs after Type 6 (Table 5.4) and shows a cold front approaching Perth. This supports our hypothesis above that heatwaves in the future are either starting earlier or the anticyclonic system has shifted westwards.

For the ACCESS and MPI models, Types 3, and 6 also show changes in frequencies that depend on the RCP. The changes in the frequencies of Types 3 and 6 are stronger in magnitude for RCP8.5 than for RCP4.5. This results in Type 3 being more frequent and Type 6 less frequent with higher radiative forcing. Thus, stronger forcing enhances the possible westward shift of the anticyclone associated with heatwaves in Perth.

Interestingly, all cities show a decrease in one Dominant Heatwave Type during heatwaves; that is Type 5 in Melbourne, Type 5 in Adelaide, and Type 6 in Perth, which generally coincides with an increase in the number of heatwaves and heatwave days in the future (Table 6.9). The consistency between these models suggests a change in the synoptic setup associated with heatwaves and/or a weakening of the relationship between heatwaves and synoptic patterns. The choice of RCP is generally unrelated to the strength of the changes in Synoptic Type frequencies in Melbourne and Adelaide, however Perth shows stronger changes in frequencies for two of six Types with increasing radiative forcing.

Given that the above-mentioned decreases in frequencies of Dominant Synoptic Types in Melbourne and Perth occur concurrently with increases in similar anticyclonic systems that are located further west, both of these cities will potentially see a westward shift of the synoptic patterns associated with heatwaves in the future. Alternatively, since pressure systems travel west to east over southern Australia, this suggests an earlier onset for heatwaves in a warmer world simply because the thresholds, computed from present day data, are more easily exceeded. This hypothesis is strengthened by the fact that future heatwaves last longer for all model runs than past heatwaves (except MPI RCP4.5 in Adelaide and MRI RCP4.5 in Perth). Although, rather than this earlier start to heatwaves being due to some change in the physical mechanism responsible for the relationship between heatwaves and synoptic patterns, this could be due to our earlier suggestion that hotter background temperatures under anthropogenic climate change make heatwave thresholds easier to exceed.

As we note earlier in this section, both Type 5 in Adelaide and Type 6 in Perth show low biases in the model simulations during heatwaves in the historical period (Tables 6.7 and 6.8), so how realistic the projected future changes are remains unclear.

Examining changes to the frequencies of synoptic patterns with heatwaves at least identifies that non-stationarity in the relationships between synoptic patterns and the UHI could be introduced.

## 6.5 Discussion

Most of the literature on the future strength of the UHI focuses on increases in urbanisation (Coutts et al. 2008; Argüeso et al. 2014) and background temperature increases due to anthropogenic climate change (Sachindra et al. 2016; Roberge and Sushama 2018; Zhang and Ayyub 2018). In contrast, this thesis approaches the problem in a novel way by examining future synoptic patterns over urban areas that are associated with anomalous UHI strengths in the present day (Chapter 5).

The most commonly applied method for examining future changes in the UHI is to downscale climate model simulations. For Australian cities, all studies show increases in the strength of the UHI regardless of the future scenario (Argüeso et al. 2014; Sachindra et al. 2016). For example, Sachindra et al. (2016) calculate future UHIs using downscaled general-circulation model data over Melbourne and show an increase in the UHI.

This thesis provides further insight into some of the causes of the processes causing changes to the UHI, specifically those concerned with the overlying atmospheric conditions. While the synoptic environment may not provide a first order effect, like changing urban surfaces, Chapter 5 demonstrated their importance as a contributor to modulating the strength of the UHI. Specifically, this could have effects that either act to dampen or amplify what is expected with urban expansion and warming.

While this chapter finds that heatwaves in the future remain associated with the same Dominant Heatwave Types from the historical period, there is also a change in the frequency of the synoptic patterns associated with heatwaves in Melbourne and Perth. This change is potentially due to either a weakening of the relationship between synoptics and heatwaves, or a westward shift in the position of the high-pressure systems associated with heatwaves. These findings are consistent with Purich et al. (2014) who find that future heatwaves in southeast and southwest Australia are associated with a weakening of MSLP patterns and a southwest shift of these systems, thus heatwaves in a warmer world can occur with a wider range of synoptic setups.

The consistency between our findings and those of Purich et al. (2014) demonstrate the robustness of the two studies given that they use different methodologies. While we determine our Synoptic Types then find how many heatwave days occur in each Type, Purich et al. (2014) found MSLP composites of all heatwave days. The fact that the different methods produce very similar results suggests that the results are not purely a product of the methodology.

While the lack of a relationship between all three of heatwaves, the UHI, and synoptic patterns means we cannot make any direct conclusions about how the strength of the UHI during heatwaves might change in the future using changes in synoptic patterns as a proxy, we can still develop a hypothesis on the potential changes based on other findings in this thesis.

Similarly, the increase in the number of future heatwave days over the extended summer season in most model runs (Table 6.9) is a mechanism for changing the strength of the UHI. Since heatwaves in Melbourne and Adelaide are associated with warmer than normal UHIs (Chapter 4), an increase in the number of heatwave days implies that, on average, the strength of the UHI in the future will be warmer in these

cities. Conversely, since heatwaves in Perth are associated with cooler UHIs (Chapter 4) and this could be, at least in part, due to the overlying synoptic conditions (Chapter 5), we might assume that future UHIs will have at least one mechanism that promotes a predisposition toward cooling. It is likely that this cooling will be counteracted and even superseded by increases in urbanisation (Coutts et al. 2007; Coutts et al. 2008; Argüeso et al. 2014; Sachindra et al. 2016). However, by understanding the mechanisms, we gain more insight into what is causing the changes that will be observed into the future. For example, if Perth UHIs during heatwaves warm at a rate that is less than expected, our findings help to elucidate the reasons why. However, this cannot be determined directly without downscaled, high-resolution projections for Perth that also incorporate expected changes in the urban form.

In Chapter 4 we found that the UHI in Melbourne and Adelaide at night is exacerbated during heatwaves whereas it is diminished in Perth. In Chapter 5 we came to the conclusion that the presence of a heatwave was likely to be a stronger influence on the strength of the UHI than synoptic pattern. In Melbourne and Adelaide, we assume that warmer temperatures during heatwaves results in more heat storage in the urban structure, thus more heat is emitted at night and the UHI is exacerbated. Given that most model runs show that heatwaves are expected to get hotter in the future, we might expect that the strength of the UHI in Melbourne and Adelaide during heatwaves will become warmer too. This hypothesis is supported by Zhao et al. (2018) who used the Community Earth System Model (CESM) to examine the UHI during heatwaves in 50 cities in the USA. The authors found that due to increased heat release at night, the relationships between the strength of the UHIs and heatwaves at night become stronger in the future.

Using this logic, describing how the UHI in Perth might behave during future heatwaves is difficult. While the logical conclusion, based on our analysis earlier in this thesis, would be that UHIs in Perth during future heatwaves would be cooler than in the historical period, there is no obvious mechanism to explain this. From the analysis in this thesis, we are unable to determine why the UHI is cooler than normal in Perth during observed heatwaves. However, we provide a hypothesis in Chapter 5 that on extremely hot, dry days, the rural stations may store a similar amount of heat, or more, than urban stations, causing a diminished UHI. Thus, from our investigation of future synoptic patterns, it is not clear how Perth's UHI may change in the future given the mechanism for these cooler than normal UHIs during heatwaves remains unclear.

Melbourne and Perth show weaker relationships between heatwaves and Synoptic Type in the future, which is likely due to the mean background warming associated with anthropogenic climate change. Thus, there is a greater range of synoptic conditions that can occur during future heatwaves. Given that the presence of a heatwave has a stronger influence on the strength of the UHI than the synoptic conditions, the presence of more future heatwaves occurring in more Synoptic Types suggests there may be a weakening of the relationship between Synoptic Types and the strength of the UHI. While a similar but weaker reduction in the relationship between heatwaves and Synoptic Type is noted in Adelaide, this is potentially due to model bias.

While changes in the synoptic patterns associated with heatwaves suggests the typical strength of the UHI in certain Synoptic Types may change in the future, thus affecting the average UHI for each city, the number of heatwave days remains significantly smaller than the number of non-heatwave days, with heatwave days accounting for up to 11.2 % of the extended summer season in the future. Therefore, any changes in the strength of the UHI associated with changes in heatwaves and their

associated Synoptic Types may be obscured by a greater warming of the UHI that is expected due to increased urbanisation and/or background temperatures (Coutts et al. 2007; Coutts et al. 2008; Argüeso et al. 2014; Sachindra et al. 2016).

The changes in the frequencies of certain Synoptic Types during future heatwaves could also affect the strength of the relationship between heatwaves and the strength of the UHI. In Chapter 4, the relationship between the strength of the UHI and heatwaves was strong over the entire duration of the heatwaves in Adelaide (Figure 4.1c), whereas in Melbourne the relationship was stronger on the first night of the heatwaves and weaker on the middle nights (Figure 4.1a). We suggested that this difference in the strength of the relationship might be due to persistence of the sign of the UHI from one day to the next, as persistence of the UHI was more prevalent for Adelaide than for Melbourne (see Chapter 5).

In Chapter 6, we show that Types 1, 3, and 6 are likely to occur more frequently during future heatwaves in Melbourne (Table 6.15). This coincides with a decrease in the frequency of Type 5 during heatwaves. Pairs of Synoptic Types that occur on consecutive days and progress from Type 3 to 5, 3 to 6, 6 to 3, and 6 to 6 show a greater likelihood of consistency in the sign of the UHI over the two days (Table 5.2). Thus, since Type 5 remains a Dominant Heatwave Type in the future (Figure 6.10a to f), and we show that Types 3 and 6 are likely to occur more frequently during future heatwaves than during the historical period (Table 6.15), this suggests a strengthening of the relationship between heatwaves and the strength of the UHI on middle nights of heatwaves in Melbourne.

These changes are not mirrored in Adelaide and Perth. In contrast to Melbourne, the Dominant Heatwave Types in Adelaide (Types 5 and 6) and Perth (Type 6) were associated with a high level of consistency in the sign of the UHI in the historical period

(Tables 5.3 and 5.4 for Adelaide and Perth respectively). As the Types that are expected to occur more frequently during future heatwaves (Type 5 in Adelaide, and Type 3 in Perth) were also associated with persistence of the sign of the UHI, we do not expect any significant change in the strength of the relationship between heatwaves and the strength of the UHI due to persistence of the sign of the UHI.

This study employed two future simulations (RCPs) from three different climate models. There was evidence that internal model variability was large given the inconsistency in the sign of trends in most cities for most RCPs. Thus, a clearer signal in changes to the synoptic environment over these three Australian cities might be better revealed by including more models in the analysis. However, this was not possible due to the time constraints of this thesis. Instead, we sought to ensure we produced the most reliable results possible by selecting models that reproduce MSLP patterns during heatwaves well. We did this by using some of the models that Purich et al. (2014) found to be most accurate compared to present-day observations. Our decision to limit the number of models in this study is supported by the findings of Gibson et al. (2017a), who noted that selectively choosing a number of CMIP5 models that represent heatwaves and their physical mechanisms well may produce better results than simply using more models.

Throughout this chapter we considered the contribution of synoptic patterns to changes in the strength of the UHI in the future – a highly novel approach. Other influences on the UHI, including urbanisation and urban design (e.g. Coutts et al. 2007; Coutts et al. 2008; Argüeso et al. 2014), increases in urban heat storage and release due to climate change (Zhao et al. 2018), and population behaviour (Earl et al. 2016), have not been considered but are likely to affect the future strength of the UHI. However, even if changes to the synoptic environment contribute a lower order effect to changes

in the strength of the UHI, our work demonstrates that determining exactly if and how the relationships between synoptic patterns and UHIs change in the future during the extended summer season is an important avenue for research. This is because Chapter 5 showed the relative importance of the overlying synoptic conditions to the modulation of the strength of the UHI outside heatwave conditions.

## 6.6 Conclusions

This chapter investigated potential future changes in those synoptic patterns that are most closely related to strong anomalous UHI conditions in the present day. Understanding how these synoptic patterns might change in the future provides an estimate of change for an important modulator of the UHI that has not been studied to date. Further, we examined the relationship between heatwaves and synoptic patterns in the future with anthropogenic climate change to provide insight into how the synoptic pattern and UHI relationship might change as the threshold for a heatwave is more easily exceeded.

Section 6.4.3 found that results were inconsistent between the three cities. Melbourne showed some decreases in the frequency of those Synoptic Types that are associated with a strongly exacerbated UHI in the observations, suggesting that synoptic patterns may favour cooler UHIs in the future, but the results were model dependant. Also, it is unclear how warmer background temperatures affect the synoptic pattern-UHI relationship. So, this cooling may be negligible compared to the expected warming, including that associated with more frequent heatwaves. Adelaide showed decreases in Synoptic Types associated with strong UHI events, both exacerbated and diminished, which tends to suggest that future synoptic patterns may favour weaker UHIs in Adelaide. Again, the results were dependent on model choice. Perth's results

were also model dependent with less consistency across the models than in Melbourne and Adelaide. Changes in Synoptic Type frequencies across all cities were sometimes stronger under the higher radiative forcing pathway, suggesting that these changes are a forced response.

Melbourne and Perth show a westward shift and/or a weakening of the relationship between heatwaves and synoptic patterns in the future. This coincides with a general increase in the number of heatwaves in the future, showing that heatwaves become less dependent on synoptic setup. Adelaide did not show a similar shift in synoptic patterns or weakening of the Synoptic Type-heatwave relationship in the future, leading us to conclude that synoptic setup for future heatwaves in Adelaide is unlikely to differ significantly to that in the historical period.

The increase in the range of Synoptic Types associated with heatwaves in the future, and the fact that heatwaves have a stronger relationship with the strength of the UHI than synoptic setup, suggests that the relationship between the strength of the UHI and Synoptic Type may also weaken in the future in Melbourne and Perth. Due to model bias, changes in the future relationship between Synoptic Type and the strength of the UHI in Adelaide are less clear. However, heatwaves, as we define them today, still only account for 11 % or less of the extended summer season in the future. We showed in Chapter 5 that the overlying synoptic conditions were an important regulator of the strength of an UHI. Thus, future changes in synoptic patterns provide an indication in just one part of this highly complex land-atmosphere interaction – and one that has not been examined to date.

# 7. Summary and synthesis

This thesis set out to address gaps in the scientific literature surrounding urban heat islands (UHIs) and their modulation by atmospheric mechanisms, namely synoptic patterns. The thesis also sought to examine the relationship between the UHI and heatwaves in southern Australian cities. This research represents the first body of work to thoroughly examine these aspects of the UHI for southern Australia. Due to a relative lack of research on UHIs in cities in the Southern Hemisphere, and an absence of research examining the contribution of synoptic patterns to UHIs under anthropogenic climate change, we provide an important contribution to the general understanding of the mechanisms regulating UHIs beyond land surface influences.

Understanding the processes that regulate the UHI is crucial for developing accurate forecasts of urban temperatures, particularly minimum temperatures during heatwaves. This is important because of the association between high minimum temperatures and negative health implications (Chestnut et al. 1998; Nicholls et al. 2008; Loughnan et al. 2010a). By gaining a better understanding of how heatwaves and synoptic patterns can interact to affect minimum temperatures in urban areas, as we do in this thesis, we have built on this body of knowledge on the UHI's regulating mechanisms. This information could potentially be exploited by a variety of applications, for example, for the improvement of forecasting urban temperatures.

This thesis addressed the following aims:

1. Quantify the relationship between heatwaves and the strength of the UHI in southern Australian cities.

2. Determine the relationship between synoptic patterns and the strength of the UHI during heatwaves and the extended summer season.

3. Examine future changes related to those atmospheric mechanisms identified in 1 and 2 that are important for the UHI.

    a. Future changes in synoptic patterns from 2 to determine the potential change to those synoptic environments most closely associated with strong anomalous UHIs.

    b. Future changes in heatwaves.

In this chapter, we reiterate the main findings of the thesis and address the three aims, above. We also discuss how these findings fit with the current understanding of non-land surface influences on UHIs and consider some of the questions that have arisen from this work.

*SUMMARY*

The first aim of this thesis was to determine whether there is a relationship between UHIs and heatwaves in southern Australian cities. A number of studies from around the world have already shown that UHIs are exacerbated during heatwaves (e.g. Zhou and Shepherd 2010; Li and Bou-Zeid 2013; Heaviside et al. 2015; Li et al. 2015; Ramamurthy and Bou-Zeid 2017), but no studies have focused on the southern hemisphere. Our findings that UHIs in Melbourne and Adelaide are exacerbated during

heatwaves are consistent with previous studies, all of which examine cities in the northern hemisphere.

We investigated whether the UHI-heatwave relationships in Melbourne and Adelaide were likely to be due to the urban form or local and regional atmospheric influences. We asked the question, is the relationship between the UHI and heatwaves due to increases in heat storage and release during heatwaves, or can this relationship be at least partially explained by changes in local circulations, illustrated through relationships with characteristics of the winds or MSLP? We concluded that the lack of any significant relationships between the strength of the UHI and any of wind speed, wind direction, and wind components, showed that the relationships between the strength of the UHI and heatwaves in Melbourne and Adelaide were not due to surface wind characteristics.

Further, we found that synoptic patterns do not have a strong influence on the strength of the UHI on heatwave days in Melbourne or Adelaide. We concluded that the exacerbation of UHIs in Melbourne and Adelaide during heatwaves was more likely due to the presence of the heatwave, and that any predisposition by the synoptic environment became negligible during heatwave conditions. Thus, the exacerbated UHIs in Melbourne and Adelaide during heatwaves were most likely due to increased energy absorption and release during heatwaves. This hypothesis is consistent with past research (e.g. Li and Bou-Zeid 2013; Heaviside et al. 2015).

While our identification of exacerbated UHIs during heatwaves in Melbourne and Adelaide is fairly consistent with existing research, this thesis is the first study to show that cities can have a diminished UHI during heatwaves. We found that UHIs in Perth are diminished during heatwaves, often resulting in an urban cool island at night. However, ultimately, the reasons for this diminished UHI remain unclear.

The contrasting results in Perth were initially thought to be due to the presence of a strong afternoon sea breeze, but subsequent analysis showed that this was not the case. Rather, at most stations there was evidence of a weak association between easterly winds and cooler UHIs. When combined with the significant relationship between Synoptic Types and heatwaves in Perth in Chapter 5, this evidence shows that at least part of the reason that Perth experiences diminished UHIs during heatwaves is because the synoptic environment induces easterly flow over the city. However, the reason why easterly flow aids in inducing a diminished UHI remains unclear and should be the subject of future research. Moreover, the influence is relatively weak and so other factors must also be involved.

If the city structure were to block the advection of warm air from inland Australia to the urban stations, this could explain why easterly winds were associated with anomalously warm rural stations, when compared to the urban areas, during heatwaves in Perth. A similar effect has been noted by Morris and Simmonds (2000) when examining a case study in Melbourne. The authors found that one of the coolest UHIs occurred under a northwesterly, where the city prevented the advection of the warm air to the urban stations, but not the rural stations. If a similar mechanism for the blocking of warm air exists in Perth, this might be able to explain the cooler than normal UHIs that occur during heatwaves.

While we did not identify a relationship between the strength of the UHI and synoptic patterns in Melbourne and Adelaide during heatwaves, a relationship was detected in Perth. Here, the Dominant Synoptic Type for heatwaves was overwhelmingly associated with diminished (i.e. anomalously cool) UHIs during heatwaves. Conversely, when a heatwave occurred with other Synoptic Types, although many UHIs were still significantly diminished in strength, a significant proportion

became strongly exacerbated. These results point to some predisposition toward diminished UHIs during heatwaves in Perth that are associated with the overlying synoptic environment. However, the mechanisms causing this relationship remain unclear.

Interestingly, for a number of cities in the USA Scott et al. (2018) found that UHIs are often diminished during heat events (defined as single days of extreme heat) when compared to the days prior to the event. A number of coastal Californian cities, which are located in the southwest of the USA, showed the coolest UHIs during heat events (Figure 1.2). That is, the UHIs of these cities were more than 3˚C cooler during the heat events than four days prior to the events. These results show stark similarities to those of Chapter 4 for Perth. Further, Perth and the Californian cities are all located on the western coast of their respective continents at similar distances from the equator; Perth is located at approximately 32˚S (Figure 1.3), whereas the Californian cities are located between approximately 33˚N and 38˚N (Figure 1.2). Perth and the Californian cities also have large deserts to the east. The coincidences between the findings in both studies suggest a possible geographical influence on UHIs during heatwaves, which should be investigated.

Our findings reveal an important avenue for future research. We cannot unequivocally determine that the differences in the relationships (or lack thereof) between Perth, and Melbourne and Adelaide are due to geographical differences between the cities. However, our results, in conjunction with those of Chapter 4 and Scott et al. (2018), strengthen the hypothesis that the location of the cities might affect the response of the UHI to heatwaves, in the case of Perth, partially via the synoptic setup. Therefore, more research is required to determine whether the UHI during

heatwaves is influenced by the city's location and surroundings, and the mechanism behind this influence.

In Chapter 5 we examined whether the u and v-wind components could explain the strength of the UHI for each Synoptic Type in each city. Since past research has shown that UHIs are strongest during calm conditions, we expected to see a relationship between weak winds and warm UHIs in Melbourne, Adelaide, and Perth. However, we found that the warmest UHIs were occasionally associated with moderate wind speeds (approximately 5 m/s). This further suggests a geographical influence on the strength of the UHI and implies that the advection of air from certain regions can affect the strength of the UHI.

Chapter 5 identified a relationship between synoptic patterns and the strength of the UHI for the extended summer season (i.e. during both heatwave and non-heatwave periods), and past research has shown that synoptic patterns are expected to change with anthropogenic climate change (Demuzere et al. 2009; Gibson et al. 2017c). This past research prompted us to examine projected future changes in those synoptic patterns most closely related to strong anomalous UHIs in each city in Chapter 6.

The results showed that those synoptic patterns associated with cooler UHIs in the present day are expected to become more frequent in the future in Melbourne. In Adelaide, those synoptic patterns associated with weaker UHIs (i.e. Synoptic Types with fewer strong UHIs and a higher frequency of normal and/or moderate UHIs) are expected to occur more frequently in the future. The changes in synoptic patterns in Perth were inconclusive due to inconsistencies across the different models and/or emissions pathways.

One of the important findings here is that no city showed any notable, robust future change toward synoptic patterns that are typically associated with warm UHIs in

the present day. Other research shows that UHIs are expected to become warmer in the future due to climate change (Sachindra et al. 2016; Roberge and Sushama 2018; Zhang and Ayyub 2018) and increases in urbanisation (Coutts et al. 2007; Coutts et al. 2008; Argüeso et al. 2014). Our results show that, provided the relationships between synoptic patterns and anomalous UHI remain relatively stationary, future synoptic patterns could act to dampen expected future increases in the strength of the UHI, providing some amelioration to the warming over cities.

*LIMITATIONS AND REMAINING QUESTIONS*

While we investigated the causes of the diminished UHI in Perth during heatwaves, the reasons why remain unclear and more research is required to understand the Perth UHI behaviour during heatwaves. One hypothesis was around the dryness of rural stations, causing them to behave like urban stations. If the rural stations are extremely dry during heatwaves, causing a reduction in evapotranspiration rates and therefore removing the potential for latent cooling, more incoming radiative energy would be stored in the rural surface during the day and released at night. This would increase rural temperatures and reduce the UHI effect. An examination of energy fluxes and evapotranspiration rates at the AWSs in and around Perth during heatwave and non-heatwave conditions could help determine whether this hypothesis is correct. Specifically, if there is a notable decrease in evapotranspiration rates at the rural stations during heatwaves, this could explain the diminished UHIs. Further, if urban stations show an increase in evapotranspiration rates during heatwaves, potentially due to urban irrigation, this may produce an additional cooling of the UHI during heatwaves. Alternatively, soil moisture measurements may be able to be used as a proxy for plant productivity without the need to set up new equipment in the field.

While Chapter 6 assumed that the relationship between UHIs and synoptic patterns will remain stationary into the future, this assumption is likely to be too simplistic. We showed that heatwaves, as we define them in the present day, occur more frequently and last longer in future climate change scenarios across all cities. In Melbourne and Adelaide, we showed that the Synoptic Type-UHI relationship broke down during heatwave conditions. Thus, with more heatwaves, it's likely that at least some aspects of the Synoptic Type-UHI relationship will change into the future.

Further, Beranová and Huth (2005) identified changes in the relationship between synoptic patterns and the strength of the UHI in Prague, Czech Republic. They identified trends in the strength of the UHI over time, with the strongest trends occurring under anticyclonic weather patterns. The reason for the differences between trends in the UHI for anticyclonic and cyclonic patterns are unclear, but the authors suggest that meteorological factors might be the cause. It is also unclear whether the trends in the UHI are to do with changes to the weather patterns themselves, changes to simple background warming, changes to urbanisation, or a combination of all three factors.

The presence of any trend in UHI magnitude in southern Australia is important to identify as this could strengthen or weaken the conclusions drawn in Chapter 6. However, identifying any potential trend in UHI magnitudes in the three cities will not be a simple task. Due to limited data availability at a number of stations, we concluded at the start of this thesis that this research had to be limited to a 20-year time period, thus the data available may not be long enough to identify any trends that exist.

However, if it is possible to accurately calculate the UHI in each of these cities using fewer stations, a more accurate trend analysis could be undertaken. UHIs calculated using fewer urban and rural stations could be compared to the UHIs

calculated in this thesis with the full set of stations. If similar UHI magnitudes are produced using each set of stations, a trend analysis could be performed over a longer time frame using the smaller set of stations.

Alternatively, if we were able to set up the ideal urban station network for this study, the results would be more accurate and would likely show stronger UHIs in all three cities as the green space surrounding the Bureau of Meteorology's weather stations has the potential to dampen the impact of urbanisation on the stations' measurements. Since we wanted to determine how much the UHI could change during heatwave events, we wanted to identify the strongest UHI possible. Thus, a number of stations would ideally be placed in the most built up parts of each of the cities, that is, in the CBD of each city. Rural station placement would be done in order to make sure that the stations were far enough away from the cities so as not to be affected by the city, but close enough that the weather systems affecting the city in question would also affect the rural stations nearby. All weather stations would be placed a similar distance from the coast to ensure that if there was advection of cool air from the coast, it would not affect the urban or rural stations disproportionately.

Further, if a number of additional stations were to be placed in less built up areas, i.e. suburban areas. This would allow us to calculate both an UHI and a suburban heat island, thus we could determine how urban density affects the relationship between heatwaves and the UHI in each of the cities. This could have implications for how cities are designed or redeveloped in the future.

In Chapter 5 we were unable to determine whether the strength of the UHI during heatwaves differed between Synoptic Types due to limited sample sizes. To increase sample sizes, we may be able to use fewer stations with longer data availability, as discussed above. Similarly, this research could be expanded to examine

extremely hot days, rather than only heatwaves, however this may result in weaker relationships between UHIs and synoptic patterns.

Our results in Chapter 6 for each city showed some consistency across the three models, but occasionally showed some large differences. By examining more model simulations we may be able to develop a clearer idea of how future synoptic patterns and UHIs are likely to change.

Since undertaking the research for this thesis, new model simulations have been developed for CMIP6. Assuming that CMIP6 model simulations are able to produce more accurate projections of future synoptic patterns than those in CMIP5, CMIP6 may be able to provide a clearer idea of how future UHIs may change due to changes in synoptic patterns.

Similarly, since commencing this PhD some of the new ERA5 data have become available, with the remainder of the data due to be available by the end of 2019. This improved dataset may be able to produce a more accurate climatology of historical synoptic patterns over the three cities, thus improving the robustness of our results and conclusions from Chapter 5.

This thesis has improved the understanding of external influences on UHIs and has addressed the lack of research on UHIs in southern Australia. As opposed to all existing literature, we have shown that UHIs can be diminished during heatwaves in some cases, thus prompting the need for a more thorough investigation of the mechanisms causing UHIs, and those that affect the relationship between UHIs and heatwaves. We identified the synoptic patterns that are related to warm and cool UHIs in Melbourne, Adelaide, and Perth, and used model simulations to gain some insight into how changing synoptic patterns may change future UHIs and heatwaves.

# References

Alcoforado MJ, Andrade H (2008) Global warming and the urban heat island. In: Urban Ecology: An International Perspective on the Interaction Between Humans and Nature. Springer US, pp 249-262. doi:10.1007/978-0-387-73412-5_14

Alexander L (2011) Climate science: Extreme heat rooted in dry soils. *Nature Geoscience* **4**:12-13 doi:10.1038/ngeo1045

Alexander LV, Arblaster JM (2009) Assessing trends in observed and modelled climate extremes over Australia in relation to future projections. *Int J Climatol* **29**:417-435 doi:10.1002/joc.1730

Alexander LV, Perkins SE (2013) Debate heating up over changes in climate variability. *EnvironResLett* **8**:041001 doi:10.1088/1748-9326/8/4/041001

Argüeso D, Evans JP, Fita L, Bormann KJ (2014) Temperature response to future urbanization and climate change. *Climate Dynamics* **42**:2183-2199 doi:10.1175/JCLI-D-11-00073.1

Arnds D, Böhner J, Bechtel B (2017) Spatio-temporal variance and meteorological drivers of the urban heat island in a European city. *Theor Appl Climatol* **128**:43-61 doi:10.1007/s00704-015-1687-4

Australian Bureau of Statistics (2013a) 3222.0 - Population Projections, Australia, 2012 (base) to 2101: Projection Results — Australia. http://abs.gov.au/ausstats/abs@.nsf/Lookup/3222.0main+features52012 (base) to 2101. Accessed August 29 2017

Australian Bureau of Statistics (2013b) 3222.0 - Population Projections, Australia, 2012 (base) to 2101: Projection Results — States and Territories. http://www.abs.gov.au/ausstats/abs@.nsf/Lookup/3222.0main+features62012 (base) to 2101. Accessed November 14 2018

Australian Bureau of Statistics (2014) 3218.0 - Regional Population Growth, Australia, 2012-13: Feature Article: Capital Cities: Past, Present and Future. http://www.abs.gov.au/ausstats/abs@.nsf/Previousproducts/3218.0Feature Article22012-13?opendocument&tabname=Summary&prodno=3218.0&issue=2012-13&num=&view=. Accessed April 16 2018

Australian Bureau of Statistics (2017) 3218.0 - Regional Population Growth, Australia, 2016: Main Features. http://www.abs.gov.au/ausstats/abs@.nsf/mf/3218.0. Accessed April 16 2018

Australian Bureau of Statistics (2018) 3218.0 - Regional Population Growth, Australia, 2016-17: Main Features. http://abs.gov.au/ausstats/abs@.nsf/0/B7616AB91C66CDCFCA25827800183B7B?Opendocument. Accessed November 14 2018

Bejarán RA, Camilloni IA (2003) Objective method for classifying air masses: An application to the analysis of Buenos Aires' (Argentina) urban heat island intensity. *Theor Appl Climatol* **74**:93-103 doi:10.1007/s00704-002-0714-4

Beranová R, Huth R (2003) The heat island of Prague under different synoptic conditions. *Meteorol Zpr* **56**:137-142 [in Czech with English summary]

Beranová R, Huth R (2005) Long-term changes in the heat island of Prague under different synoptic conditions. *Theor Appl Climatol* **82**:113-118 doi:10.1007/s00704-004-0115-y

Berardi U, GhaffarianHoseini A, GhaffarianHoseini A (2014) State-of-the-art analysis of the environmental benefits of green roofs. *Applied Energy* **115**:411-428 doi:10.1016/j.apenergy.2013.10.047

Bi D et al. (2013) The ACCESS coupled model: description, control climate and evaluation. *Aust Meteorol Oceanogra J* **63**:41-64 doi:10.22499/2.6301.004

Boschat G, Pezza A, Simmonds I, Perkins S, Cowan T, Purich A (2015) Large scale and sub-regional connections in the lead up to summer heat wave and extreme rainfall events in eastern Australia. *Climate Dynamics* **44**:1823-1840 doi:10.1007/s00382-014-2214-5

Broadbent AM, Coutts AM, Tapper NJ, Demuzere M (2018a) The cooling effect of irrigation on urban microclimate during heatwave conditions. *Urban Climate* **23**:309-329 doi:10.1016/j.uclim.2017.05.002

Broadbent AM, Coutts AM, Tapper NJ, Demuzere M, Beringer J (2018b) The microscale cooling effects of water sensitive urban design and irrigation in a suburban environment. *Theor Appl Climatol* **134** doi:10.1007/s00704-017-2241-3

Bureau of Meteorology (1997) Guidelines for the siting and exposure of meteorological instruments and observing facilities. Bureau of Meteorology, Australia

Bureau of Meteorology (2014) Meteorological Observations and Reports Instrument Siting Requirements. Commonwealth of Australia. http://www.bom.gov.au/met-authority/docs/MA8a_Meteorological_Observations_and_Reports_Instrument_Siting_Requirements_V1.0.pdf. Accessed February 4 2019

Bureau of Meteorology (2015) Long-term temperature record - Methods. Commonwealth of Australia. http://www.bom.gov.au/climate/change/acorn-sat/ - tabs=Methods. Accessed October 19 2015

Bureau of Meteorology (2018) Observation of air temperature. Commonwealth of Australia. http://www.bom.gov.au/climate/cdo/about/airtemp-measure.shtml - link1. Accessed February 4 2019

Chestnut LG, S. Breffle W, Smith JB, Kalkstein LS (1998) Analysis of differences in hot-weather-related mortality across 44 U.S. metropolitan areas. *Environ Sci Policy* **1**:59-70

CIS (n.d.) som_batchtrain documentation. Helsinki University of Technology,. http://www.cis.hut.fi/projects/somtoolbox/package/docs2/som_batchtrain.html . Accessed June 13 2016

Collier M, Uhe P (2012) CMIP5 datasets from the ACCESS1. 0 and ACCESS1. 3 coupled climate models. Centre for Australian Weather and Climate Research,

Coumou D, Rahmstorf S (2012) A decade of weather extremes. *Nat Clim Change* **2**:491-496 doi:10.1038/nclimate1452

Coutts A, Beringer J, Tapper N (2010) Changing Urban Climate and CO2 Emissions: Implications for the Development of Policies for Sustainable Cities. *Urban Policy and Research* **28**:27-47 doi:10.1080/08111140903437716

Coutts AM, Beringer J, Tapper NJ (2007) Impact of increasing urban density on local climate: Spatial and temporal variations in the surface energy balance in Melbourne, Australia. *J Appl Meteorol Climatol* **46**:477-493 doi:10.1175/jam2462.1

Coutts AM, Beringer J, Tapper NJ (2008) Investigating the climatic impact of urban planning strategies through the use of regional climate modelling: A case

study for Melbourne, Australia. *Int J Climatol* **28**:1943-1957 doi:10.1002/joc.1680

Coutts AM, Tapper NJ, Beringer J, Loughnan M, Demuzere M (2013) Watering our cities: The capacity for Water Sensitive Urban Design to support urban cooling and improve human thermal comfort in the Australian context. *Prog Phys Geogr* **37**:2-28 doi:10.1177/0309133312461032

Cowan T, Purich A, Boschat G, Perkins S (2014a) Future projections of Australian heat wave number and intensity based on CMIP5 models. *Bulletin of the Australian Meteorological and Oceanographic Society* **27**:134-138

Cowan T, Purich A, Perkins S, Pezza A, Boschat G, Sadler K (2014b) More frequent, longer, and hotter heat waves for Australia in the Twenty-First Century. *J Clim* **27**:5851-5871 doi:10.1175/JCLI-D-14-00092.1

Da Silva VJ, Da Silva CR, Almeida LS, Da Silva CR, Carvalho HP, De Camargo R (2018) Mobile transect for identification of intra-urban heat islands in Uberlandia, Brazil. *Rev Ambiente Agua* **13** doi:10.4136/ambi-agua.2187

De Bono A, Giuliani G, Kluser S, Peduzzi P (2004) Impacts of Summer 2003 Heat Wave in Europe vol 2. UNEP/DEWA/GRID-Europe,

Dee DP et al. (2011) The ERA‑Interim reanalysis: Configuration and performance of the data assimilation system. *Q J R Meteorol Soc* **137**:553-597 doi:10.1002/qj.828

Demographia (2017) Demographia World Urban Areas 13th Annual Edition: 2017:04.

Demuzere M, Werner M, van Lipzig NPM, Roeckner E (2009) An analysis of present and future ECHAM5 pressure fields using a classification of circulation patterns. *Int J Climatol* **29**:1796-1810 doi:10.1002/joc.1821

Department of Human Services (2009) January 2009 Heatwave in Victoria: an Assessment of Health Impacts. Victorian Government, Melbourne, Victoria

Earl N, Simmonds I, Tapper N (2016) Weekly cycles in peak time temperatures and urban heat island intensity. *EnvironResLett* **11** doi:10.1088/1748-9326/11/7/074003

ECMWF (2018) ERA-Interim. European Centre for Medium-Range Weather Forecasts. https://www.ecmwf.int/en/forecasts/datasets/archive-datasets/reanalysis-datasets/era-interim. Accessed December 11 2018

Erell E, Williamson T (2007) Intra-urban differences in canopy layer air temperature at a mid-latitude city. *Int J Climatol* **27**:1243-1255 doi:10.1002/joc.1469

Fallmann J, Emeis S, Suppan P (2013) Mitigation of urban heat stress -a modelling case study for the area of Stuttgart. *Erde* **144**:202-216 doi:10.12854/erde-144-15

Fallmann J, Wagner S, Emeis S (2017) High resolution climate projections to assess the future vulnerability of European urban areas to climatological extreme events. *Theor Appl Climatol* **127**:667-683 doi:10.1007/s00704-015-1658-9

Fenner D, Meier F, Scherer D, Polze A (2014) Spatial and temporal air temperature variability in Berlin, Germany, during the years 2001–2010. *Urban Climate* **10, Part 2**:308-331 doi:10.1016/j.uclim.2014.02.004

Gibson PB, Perkins-Kirkpatrick SE, Alexander LV, Fischer EM (2017a) Comparing Australian heat waves in the CMIP5 models through cluster analysis. *Journal of Geophysical Research* **122**:3266-3281 doi:10.1002/2016JD025878

Gibson PB, Perkins-Kirkpatrick SE, Uotila P, Pepler AS, Alexander LV (2017b) On the use of self-organizing maps for studying climate extremes. *Journal of Geophysical Research* **122**:3891-3903 doi:10.1002/2016JD026256

Gibson PB, Pitman AJ, Lorenz R, Perkins-Kirkpatrick SE (2017c) The Role of Circulation and Land Surface Conditions in Current and Future Australian Heat Waves. *J Clim* **30**:9933-9948 doi:10.1175/JCLI-D-17-0265.1

Gibson PB, Uotila P, Perkins-Kirkpatrick SE, Alexander LV, Pitman AJ (2016) Evaluating synoptic systems in the CMIP5 climate models over the Australian region. *Climate Dynamics* **47**:2235-2251 doi:10.1007/s00382-015-2961-y

Giorgetta MA et al. (2013) Climate and carbon cycle changes from 1850 to 2100 in MPI‐ESM simulations for the Coupled Model Intercomparison Project phase 5. *Journal of Advances in Modeling Earth Systems* **5**:572-597 doi:https://doi.org/10.1002/jame.20038

Guan H et al. (2013) Characterisation, Interpretation and Implications of the Adelaide Urban Heat Island. Flinders University, Adelaide, South Australia

Haashemi S, Weng Q, Darvishi A, Alavipanah SK (2016) Seasonal variations of the surface urban heat Island in a semi-arid city. *Remote Sens* **8** doi:10.3390/rs8040352

He GX, Yu CWF, Lu C, Deng QH (2013) The influence of synoptic pattern and atmospheric boundary layer on PM10 and urban heat island. *Indoor and Built Environment* **22**:796-807 doi:10.1177/1420326x13503576

Heaviside C, Cai XM, Vardoulakis S (2015) The effects of horizontal advection on the urban heat island in Birmingham and the West Midlands, United Kingdom during a heatwave. *Q J R Meteorol Soc* **141**:1429-1441 doi:10.1002/qj.2452

Herbel I, Croitoru AE, Rus AV, Roşca CF, Harpa GV, Ciupertea AF, Rus I (2018) The impact of heat waves on surface urban heat island and local economy in Cluj-Napoca city, Romania. *Theor Appl Climatol* **133**:681-695 doi:10.1007/s00704-017-2196-4

Herold N, Kala J, Alexander LV (2016) The influence of soil moisture deficits on Australian heatwaves. *EnvironResLett* **11** doi:10.1088/1748-9326/11/6/064003

Hinkel KM, Nelson FE, Klene AE, Bell JH (2003) The urban heat island in winter at Barrow, Alaska. *Int J Climatol* **23**:1889-1905 doi:10.1002/joc.971

Hope PK, Drosdowsky W, Nicholls N (2006) Shifts in the synoptic systems influencing southwest Western Australia. *Climate Dynamics* **26**:751-764 doi:10.1007/s00382-006-0115-y

Horton DE, Johnson NC, Singh D, Swain DL, Rajaratnam B, Diffenbaugh NS (2015) Contribution of changes in atmospheric circulation patterns to extreme temperature trends. *Nature* **522**:465-469 doi:10.1038/nature14550

Huth R, Kyselý J, Pokorná L (2000) A GCM simulation of heat waves, dry spells, and their relationships to circulation. *Clim Change* **46**:29-60

Huva R, Dargaville R, Rayner P (2015) The impact of filtering self-organizing maps: A case study with Australian pressure and rainfall. *Int J Climatol* **35**:624-633 doi:10.1002/joc.4008

Jacobs SJ, Gallant AJE, Tapper NJ (2017) The sensitivity of urban meteorology to soil moisture boundary conditions: A case study in Melbourne, Australia. *J Appl Meteorol Climatol* **56**:2155-2172 doi:10.1175/JAMC-D-17-0007.1

Jiang N, Cheung K, Luo K, Beggs PJ, Zhou W (2012) On two different objective procedures for classifying synoptic weather types over east Australia. *Int J Climatol* **32**:1475-1494 doi:10.1002/joc.2373

Jiang N, Luo K, Beggs PJ, Cheung K, Scorgie Y (2015) Insights into the implementation of synoptic weather-type classification using self-organizing maps: An Australian case study. *Int J Climatol* **35**:3471-3485 doi:10.1002/joc.4221

Jiang N et al. (2017) Visualising the relationships between synoptic circulation type and air quality in Sydney, a subtropical coastal-basin environment. *Int J Climatol* **37**:1211-1228 doi:10.1002/joc.4770

Kim S, Sinclair VA, Räisänena J, Ruuhelac R (2018) Heat waves in Finland: Present and projected summertime extreme temperatures and their associated circulation patterns. *Int J Climatol* **38**:1393-1408 doi:10.1002/joc.5253

King AD, Van Oldenborgh GJ, Karoly DJ, Lewis SC, Cullen H (2015) Attribution of the record high Central England temperature of 2014 to anthropogenic influences. *EnvironResLett* **10** doi:10.1088/1748-9326/10/5/054002

Kohonen T (2014) MATLAB Implementations and Applications of the Self-Organizing Map

Lai J et al. (2018) Identification of typical diurnal patterns for clear-sky climatology of surface urban heat islands. *Remote Sens Environ* **217**:203-220 doi:10.1016/j.rse.2018.08.021

Lee SH, Baik JJ (2010) Statistical and dynamical characteristics of the urban heat island intensity in Seoul. *Theor Appl Climatol* **100**:227-237 doi:10.1007/s00704-009-0247-1

Lewis SC, Karoly DJ (2015) Are estimates of anthropogenic and natural influences on Australia's extreme 2010–2012 rainfall model-dependent? *Climate Dynamics* **45**:679-695 doi:10.1007/s00382-014-2283-5

Li D, Bou-Zeid E (2013) Synergistic interactions between urban heat islands and heat waves: The impact in cities is larger than the sum of its parts. *J Appl Meteorol Climatol* **52**:2051-2064 doi:10.1175/JAMC-D-13-02.1

Li D, Sun T, Liu M, Yang L, Wang L, Gao Z (2015) Contrasting responses of urban and rural surface energy budgets to heat waves explain synergies between urban heat islands and heat waves. *EnvironResLett* **10** doi:10.1088/1748-9326/10/5/054009

Liu Y, Weisberg RH, Mooers CNK (2006) Performance evaluation of the self-organizing map for feature extraction. *Journal of Geophysical Research: Oceans* **111** doi:10.1029/2005JC003117

Loughnan M, Nicholls N, Tapper N (2010a) Mortality-temperature thresholds for ten major population centres in rural Victoria, Australia. *Health and Place* **16**:1287-1290 doi:10.1016/j.healthplace.2010.08.008

Loughnan ME, Nicholls N, Tapper NJ (2010b) The effects of summer temperature, age and socioeconomic circumstance on Acute Myocardial Infarction admissions in Melbourne, Australia. *Int J Health Geogr* **9** doi:10.1186/1476-072X-9-41

Loughnan ME, Tapper NJ, Thu P, Lynch K, McInnes JA (2013) A spatial vulnerability analysis of urban populations during extreme heat events in Australian capital cities. National Climate Change Adaptation Research Facility, Gold Coast, Australia

Ma S, Pitman A, Hart M, Evans JP, Haghdadi N, MacGill I (2017) The impact of an urban canopy and anthropogenic heat fluxes on Sydney's climate. *Int J Climatol* **37**:255-270 doi:10.1002/joc.5001

Meehl GA, Tebaldi C (2004) More intense, more frequent, and longer lasting heat waves in the 21st century. *Science* **305**:994-997 doi:10.1126/science.1098704

Met Office (2016) The Russian heatwave of summer 2010. https://www.metoffice.gov.uk/learning/learn-about-the-weather/weather-phenomena/case-studies/russian-heatwave. Accessed February 6 2019

Mishra V, Ganguly AR, Nijssen B, Lettenmaier DP (2015) Changes in observed climate extremes in global urban areas. *EnvironResLett* **10** doi:10.1088/1748-9326/10/2/024005

Morris CJG, Simmonds I (2000) Associations between varying magnitudes of the urban heat island and the synoptic climatology in Melbourne, Australia. *Int J Climatol* **20**:1931-1954 doi:10.1002/1097-0088(200012)20:15<1931::aid-joc578>3.0.co;2-d

Morris CJG, Simmonds I, Plummer N (2001) Quantification of the influence of wind and cloud on the nocturnal urban heat island of a large city. *J Appl Meteorol* **40**:169-182 doi:10.1175/1520-0450(2001)040<0169:QOTIOW>2.0.CO;2

Moss JL, Doick KJ, Smith S, Shahrestani M (2019) Influence of evaporative cooling by urban forests on cooling demand in cities. *Urban For Urban Greening* **37**:65-73 doi:10.1016/j.ufug.2018.07.023

Nairn JR, Fawcett RJB (2014) The excess heat factor: A metric for heatwave intensity and its use in classifying heatwave severity. *Int J Environ Res Public Health* **12**:227-253 doi:10.3390/ijerph120100227

Nicholls N, Skinner C, Loughnan M, Tapper N (2008) A simple heat alert system for Melbourne, Australia. *International Journal of Biometeorology* **52**:375-384 doi:10.1007/s00484-007-0132-5

Oke TR (1973) City size and the urban heat island. *Atmos Environ Part A Gen Top* **7**:769-779 doi:10.1016/0004-6981(73)90140-6

Oke TR (1982) The energetic basis of the urban heat island. *Q J R Meteorol Soc* **108**:1-24 doi:10.1002/qj.49710845502

Oke TR, Johnson GT, Steyn DG, Watson ID (1991) Simulation of surface urban heat islands under 'ideal' conditions at night part 2: Diagnosis of causation. *Boundary-Layer Meteorology* **56**:339-358 doi:10.1007/bf00119211

Oleson KW, Bonan GB, Feddema J (2010) Effects of white roofs on urban temperature in a global climate model. *Geophys Res Lett* **37** doi:10.1029/2009GL042194

Ortiz LE, Gonzalez JE, Wu W, Schoonen M, Tongue J, Bornstein R (2018) New York City impacts on a regional heat wave. *J Appl Meteorol Climatol* **57**:837-851 doi:10.1175/JAMC-D-17-0125.1

Parker TJ, Berry GJ, Reeder MJ (2013) The influence of tropical cyclones on heat waves in Southeastern Australia. *Geophys Res Lett* **40**:6264-6270 doi:10.1002/2013gl058257

Perkins SE, Alexander LV (2013) On the measurement of heat waves. *J Clim* **26**:4500-4517 doi:10.1175/jcli-d-12-00383.1

Perkins SE, Alexander LV, Nairn JR (2012) Increasing frequency, intensity and duration of observed global heatwaves and warm spells. *Geophys Res Lett* **39** doi:10.1029/2012gl053361

Pezza AB, van Rensch P, Cai W (2012) Severe heat waves in Southern Australia: Synoptic climatology and large scale connections. *Climate Dynamics* **38**:209-224 doi:10.1007/s00382-011-1016-2

Purich A et al. (2014) Atmospheric and oceanic conditions associated with Southern Australian heat waves: A CMIP5 analysis. *J Clim* **27**:7807-7829 doi:10.1175/JCLI-D-14-00098.1

Queensland University of Technology (2010) Impacts and adaptation response of infrastructure and communities to heatwaves: the southern Australian experience of 2009. National Climate Change Adaptation Research Facility, Gold Coast, Australia

Quinting JF, Reeder MJ (2017) Southeastern Australian heat waves from a trajectory viewpoint. *Mon Weather Rev* **145**:4109-4125 doi:10.1175/MWR-D-17-0165.1

Ramamurthy P, Bou-Zeid E (2017) Heatwaves and urban heat islands: A comparative analysis of multiple cities. *Journal of Geophysical Research* **122**:168-178 doi:10.1002/2016JD025357

Rasul A, Balzter H, Smith C (2015) Spatial variation of the daytime Surface Urban Cool Island during the dry season in Erbil, Iraqi Kurdistan, from Landsat 8. *Urban Climate* **14**:176-186 doi:10.1016/j.uclim.2015.09.001

Reichstein M et al. (2013) Climate extremes and the carbon cycle. *Nature* **500**:287-295 doi:10.1038/nature12350

Roberge F, Sushama L (2018) Urban heat island in current and future climates for the island of Montreal. *Sustainable Cities Soc* **40**:501-512 doi:10.1016/j.scs.2018.04.033

Runnalls KE, Oke TR (2000) Dynamics and controls of the near-surface heat island of Vancouver, British Columbia. *Phys Geogr* **21**:283-304 doi:10.1080/02723646.2000.10642711

Sachindra DA, Ng AWM, Muthukumaran S, Perera BJC (2016) Impact of climate change on urban heat island effect and extreme temperatures: A case-study. *Q J R Meteorol Soc* **142**:172-186 doi:10.1002/qj.2642

Scott AA, Waugh DW, Zaitchik BF (2018) Reduced Urban Heat Island intensity under warmer conditions. *EnvironResLett* **13**:064003 doi:10.1088/1748-9326/aabd6c

Smithers RJ et al. (2018) Comparing the relative abilities of tree species to cool the urban environment. *Urban Ecosyst* **21**:851-862 doi:10.1007/s11252-018-0761-y

Soltani A, Sharifi E (2017) Daily variation of urban heat island effect and its correlations to urban greenery: A case study of Adelaide. *Front Archit Res* **6**:529-538 doi:10.1016/j.foar.2017.08.001

Sun T, Kotthaus S, Li D, Ward HC, Gao Z, Ni GH, Grimmond CSB (2017) Attribution and mitigation of heat wave-induced urban heat storage change. *EnvironResLett* **12** doi:10.1088/1748-9326/aa922a

Targino AC, Krecl P, Coraiola GC (2014) Effects of the large-scale atmospheric circulation on the onset and strength of urban heat islands: A case study. *Theor Appl Climatol* **117**:73-87 doi:10.1007/s00704-013-0989-7

Tong H, Walton A, Sang J, Chan JCL (2005) Numerical simulation of the urban boundary layer over the complex terrain of Hong Kong. *Atmos Environ* **39**:3549-3563 doi:10.1016/j.atmosenv.2005.02.045

Torok SJ, Morris CJG, Skinner C, Plummer N (2001) Urban heat island features of southeast Australian towns. *Aust Meteorol Mag* **50**:1-13

Trewin B (2013) A daily homogenized temperature data set for Australia. *Int J Climatol* **33**:1510-1529 doi:10.1002/joc.3530

Tryhorn L, Risbey J (2006) On the distribution of heat waves over the Australian region. *Aust Meteorol Mag* **55**:169-182

Unger J (1996) Heat island intensity with different meteorological conditions in a medium-sized town: Szeged, Hungary. *Theor Appl Climatol* **54**:147-151 doi:10.1007/BF00865157

United Nations (2018) World Urbanization Prospects: The 2018 Revision - Key Facts.

Unwin DJ (1980) The Synoptic Climatology of Birmingham's Urban Heat Island, 1965–74. *Weather* **35**:43-50 doi:10.1002/j.1477-8696.1980.tb03484.x

van Vuuren DP et al. (2011) The representative concentration pathways: An overview. *Clim Change* **109**:5-31 doi:10.1007/s10584-011-0148-z

Verdon-Kidd DC, Kiem AS (2009) On the relationship between large-scale climate modes and regional synoptic patterns that drive Victorian rainfall. *Hydrol Earth Syst Sci* **13**:467-479 doi:10.5194/hess-13-467-2009

Whetton P et al. (2015) CSIRO and Bureau of Meteorology 2015, Climate Change in Australia Information for Australia's Natural Resource Management Regions: Technical Report, CSIRO and Bureau of Meteorology, Australia. 222 pages. http://www.climatechangeinaustralia.gov.au/en/publications-library/technical-report.

Wilby RL (2003) Past and projected trends in London's Urban heat island. *Weather* **58**:251-260 doi:10.1256/wea.183.02

Williams S et al. (2012a) Heat and health in Adelaide, South Australia: Assessment of heat thresholds and temperature relationships. *Sci Total Environ* **414**:126-133 doi:10.1016/j.scitotenv.2011.11.038

Williams S, Nitschke M, Weinstein P, Pisaniello DL, Parton KA, Bi P (2012b) The impact of summer temperatures and heatwaves on mortality and morbidity in Perth, Australia 1994-2008. *Environ Int* **40**:33-38 doi:10.1016/j.envint.2011.11.011

Yagüe C, Zurita E, Martinez A (1991) Statistical analysis of the Madrid urban heat island. *Atmos Environ Part B Urban Atmos* **25**:327-332 doi:10.1016/0957-1272(91)90004-X

Yukimoto S et al. (2012) A new global climate model of the Meteorological Research Institute: MRI-CGCM3: -Model description and basic performance. *J Meteorol Soc Jpn* **90**:23-64 doi:10.2151/jmsj.2012-A02

Zhang B, Xie GD, Gao JX, Yang Y (2014a) The cooling effect of urban green spaces as a contribution to energy-saving and emission-reduction: A case study in Beijing, China. *Building and Environment* **76**:37-43 doi:10.1016/j.buildenv.2014.03.003

Zhang F, Cai X, Thornes JE (2014b) Birmingham's air and surface urban heat islands associated with lamb weather types and cloudless anticyclonic conditions. *Prog Phys Geogr* **38**:431-447 doi:10.1177/0309133314538725

Zhang Y, Ayyub BM (2018) Urban Heat Projections in a Changing Climate: Washington, DC, Case Study. *ASCE-ASME J Risk Uncertain Eng Syst Part A Civ Eng* **4** doi:10.1061/AJRUA6.0000985

Zhao L et al. (2018) Interactions between urban heat islands and heat waves. *EnvironResLett* **13** doi:10.1088/1748-9326/aa9f73

Zhou Y, Shepherd JM (2010) Atlanta's urban heat island under extreme heat conditions and potential mitigation strategies. *Natural Hazards* **52**:639-668 doi:10.1007/s11069-009-9406-z

Zittis G, Hadjinicolaou P, Fnais M, Lelieveld J (2016) Projected changes in heat wave characteristics in the eastern Mediterranean and the Middle East. *Reg Environ Change* **16**:1863-1876 doi:10.1007/s10113-014-0753-2

# Appendix A

| City | Station | Lag 0 | | | Lag 3 | | | Lag 6 | | |
|---|---|---|---|---|---|---|---|---|---|---|
| | | *n* | *r* | *p* | *n* | *r* | *p* | *n* | *r* | *p* |
| Melbourne | 87113 | 121 | 0.03 | 0.72 | 39 | 0.14 | 0.41 | 41 | 0.13 | 0.43 |
| | 86383 | 120 | 0.02 | 0.84 | 40 | 0.11 | 0.51 | 41 | -0.22 | 0.18 |
| | 86282 | 122 | 0.13 | 0.14 | 41 | 0.02 | 0.92 | 40 | -0.16 | 0.33 |
| | 86071 | 50 | -0.01 | 0.93 | 17 | -0.05 | 0.86 | 16 | -0.26 | 0.33 |
| | 86077 | 122 | -0.01 | 0.94 | 39 | -0.00 | 0.98 | 40 | -0.22 | 0.17 |
| | 86104 | 115 | 0.14 | 0.14 | 38 | 0.05 | 0.75 | 40 | -0.19 | 0.24 |
| | 87168 | 101 | 0.09 | 0.39 | 34 | -0.28 | 0.11 | 34 | 0.18 | 0.30 |
| Adelaide | 23090 | 221 | 0.05 | 0.45 | 74 | 0.23 | 0.04 | 75 | -0.07 | 0.53 |
| | 23034 | 223 | 0.15 | 0.02 | 75 | 0.26 | 0.02 | 75 | 0.11 | 0.37 |
| | 23083 | 215 | 0.07 | 0.27 | 74 | -0.12 | 0.31 | 73 | -0.20 | 0.09 |
| | 23013 | 223 | 0.04 | 0.51 | 75 | 0.14 | 0.25 | 75 | -0.18 | 0.13 |
| | 23122 | 90 | -0.06 | 0.60 | 30 | 0.15 | 0.43 | 30 | -0.12 | 0.52 |
| | 24580 | 51 | 0.04 | 0.79 | 16 | 0.56 | 0.02 | 17 | 0.59 | 0.01 |
| Perth | 9178 | 146 | -0.15 | 0.07 | 49 | -0.29 | 0.04 | 48 | -0.15 | 0.32 |
| | 9204 | 157 | -0.16 | 0.04 | 55 | 0.06 | 0.65 | 54 | -0.22 | 0.11 |
| | 9172 | 165 | -0.12 | 0.12 | 55 | -0.32 | 0.02 | 54 | -0.20 | 0.16 |
| | 9053 | 141 | -0.10 | 0.23 | 49 | -0.12 | 0.39 | 50 | -0.25 | 0.08 |
| | 9021 | 151 | -0.08 | 0.30 | 51 | 0.01 | 0.95 | 52 | -0.10 | 0.49 |
| | 9225 | 164 | -0.00 | 0.97 | 55 | -0.27 | 0.04 | 54 | -0.20 | 0.14 |

Table A1: Sample sizes (*n*), Pearson correlation coefficients (*r*), and *p*-values for the relationships between wind speed and citywide UHI strength for each station in Melbourne, Adelaide, and Perth. Table shows results for lag 0, lag 3, and lag 6 winds. See Section 4.3.3 for the definition of wind categories.

| City | Station | Lag 0 | | | Lag 3 | | | Lag 6 | | |
|---|---|---|---|---|---|---|---|---|---|---|
| | | *n* | median UHI (˚C) | *p* | *n* | median UHI (˚C) | *p* | *n* | median UHI (˚C) | *p* |
| Melbourne | 87113 | 46 | 0.65 | 0.79 | 8 | -0.46 | 0.02 | 8 | -0.22 | 0.29 |
| | 86383 | 68 | 0.71 | 0.59 | 17 | -0.36 | 0.24 | 26 | 0.27 | 0.78 |
| | 86282 | 92 | 0.70 | 0.29 | 21 | 0.17 | 0.91 | 24 | 0.27 | 0.63 |
| | 86071 | 11 | 0.66 | 1.00 | 5 | -0.24 | 0.51 | 3 | -0.01 | 0.89 |
| | 86077 | 68 | 0.62 | 0.87 | 13 | -0.45 | 0.12 | 16 | 0.27 | 0.85 |
| | 86104 | 98 | 0.68 | 0.43 | 18 | -0.19 | 0.25 | 21 | 0.19 | 0.37 |
| | 87168 | 78 | 0.71 | 0.39 | 8 | -0.46 | 0.02 | 15 | -0.04 | 0.54 |
| Adelaide | 23090 | 67 | 0.71 | 0.79 | 4 | -0.57 | 0.38 | 5 | -0.90 | 0.02 |
| | 23034 | 65 | 1.17 | 0.11 | 5 | 0.14 | 0.77 | 7 | -0.55 | 0.35 |
| | 23083 | 54 | 1.47 | 0.10 | 4 | 0.46 | 0.77 | 3 | -1.20 | 0.18 |
| | 23013 | 54 | 1.05 | 0.38 | 5 | 0.14 | 0.71 | 2 | -0.73 | 0.77 |
| | 23122 | 15 | 0.13 | 0.73 | 1 | -0.09 | 0.48 | 5 | -0.82 | 0.00 |
| | 24580 | 26 | 0.66 | 0.91 | 1 | 0.14 | 0.68 | 4 | -0.10 | 0.76 |
| Perth | 9178 | 15 | -0.68 | 0.21 | 3 | 0.19 | 0.75 | 4 | 0.61 | 0.05 |
| | 9204 | 5 | -0.12 | 0.51 | 0 | n/a | n/a | 8 | 1.19 | 0.00 |
| | 9172 | 12 | -1.00 | 0.73 | 0 | n/a | n/a | 2 | 1.08 | 0.26 |
| | 9053 | 21 | -0.97 | 0.87 | 0 | n/a | n/a | 4 | 0.61 | 0.04 |
| | 9021 | 18 | -1.12 | 0.42 | 0 | n/a | n/a | 2 | 1.44 | 0.22 |
| | 9225 | 28 | -0.91 | 0.72 | 2 | 2.73 | 0.04 | 4 | 1.40 | 0.03 |

Table A2: Sample sizes (*n*), median UHI strengths (˚C), and *p*-values for the relationships between the citywide UHI distribution when winds are northerly vs. the citywide UHI distribution for winds from all other directions at each station in Melbourne, Adelaide, and Perth. Table shows results for lag 0, lag 3, and lag 6 winds. See Section 4.3.3 for the definition of wind categories. Median UHI varies from station to station because UHI data corresponding to dates where wind data are missing are excluded.

| City | Station | Lag 0 | | | Lag 3 | | | Lag 6 | | |
|---|---|---|---|---|---|---|---|---|---|---|
| | | *n* | median UHI (˚C) | *p* | *n* | median UHI (˚C) | *p* | *n* | median UHI (˚C) | *p* |
| Melbourne | 87113 | 29 | 0.50 | 0.27 | 12 | 0.27 | 0.03 | 20 | 0.52 | 0.24 |
| | 86383 | 15 | 0.60 | 0.85 | 9 | 1.03 | 0.06 | 6 | -0.26 | 0.57 |
| | 86282 | 12 | 0.77 | 0.47 | 2 | 0.56 | 0.73 | 4 | 0.24 | 0.89 |
| | 86071 | 33 | 0.67 | 0.79 | 7 | 0.18 | 0.67 | 7 | 0.52 | 0.89 |
| | 86077 | 35 | 0.96 | 0.62 | 6 | 0.96 | 0.15 | 0 | n/a | n/a |
| | 86104 | 10 | 0.80 | 0.90 | 9 | 0.62 | 0.04 | 3 | -0.32 | 0.11 |
| | 87168 | 14 | 1.80 | 0.01 | 16 | 0.32 | 0.06 | 5 | 0.21 | 0.96 |
| Adelaide | 23090 | 121 | 0.95 | 0.79 | 9 | 1.86 | 0.03 | 4 | 0.27 | 0.06 |
| | 23034 | 109 | 0.62 | 0.03 | 8 | 2.03 | 0.01 | 1 | 4.72 | 0.10 |
| | 23083 | 106 | 0.74 | 0.26 | 9 | 0.45 | 0.18 | 3 | 0.26 | 0.14 |
| | 23013 | 126 | 0.70 | 0.30 | 9 | 1.31 | 0.03 | 4 | -0.27 | 0.80 |
| | 23122 | 65 | 0.63 | 0.97 | 3 | 0.14 | 0.42 | 1 | 0.26 | 0.62 |
| | 24580 | 0 | n/a | n/a | 0 | n/a | n/a | 1 | -0.10 | 0.39 |
| Perth | 9178 | 74 | -1.24 | 0.03 | 12 | 0.04 | 0.68 | 19 | 0.31 | 0.39 |
| | 9204 | 123 | -0.97 | 0.01 | 22 | -0.13 | 0.54 | 24 | 0.35 | 0.93 |
| | 9172 | 97 | -1.03 | 0.09 | 8 | -0.35 | 0.92 | 17 | 0.81 | 0.03 |
| | 9053 | 81 | -1.04 | 0.01 | 15 | 0.10 | 0.62 | 25 | 0.42 | 0.12 |
| | 9021 | 83 | -1.03 | 0.01 | 16 | 0.15 | 0.16 | 22 | 0.78 | 0.06 |
| | 9225 | 82 | -1.14 | 0.01 | 8 | -0.07 | 0.33 | 17 | 0.81 | 0.05 |

Table A3: Same as for Table A2 but for easterly winds.

| City | Station | Lag 0 | | | Lag 3 | | | Lag 6 | | |
|---|---|---|---|---|---|---|---|---|---|---|
| | | *n* | median UHI (˚C) | *p* | *n* | median UHI (˚C) | *p* | *n* | median UHI (˚C) | *p* |
| Melbourne | 87113 | 21 | 0.33 | 0.49 | 19 | 0.35 | 0.20 | 9 | 0.52 | 0.80 |
| | 86383 | 33 | 0.46 | 0.68 | 12 | 0.00 | 0.18 | 5 | 0.21 | 0.26 |
| | 86282 | 8 | 0.13 | 0.09 | 17 | 0.23 | 0.78 | 10 | 0.17 | 0.59 |
| | 86071 | 2 | 0.97 | 0.97 | 1 | -0.45 | 0.62 | 2 | 1.10 | 0.61 |
| | 86077 | 12 | 0.70 | 0.93 | 19 | 0.30 | 0.73 | 18 | -0.03 | 0.47 |
| | 86104 | 6 | -0.09 | 0.01 | 11 | -0.29 | 0.54 | 11 | 0.53 | 0.58 |
| | 87168 | 6 | -0.17 | 0.06 | 7 | -0.63 | 0.20 | 5 | -0.19 | 0.59 |
| Adelaide | 23090 | 26 | 0.68 | 0.90 | 40 | 0.37 | 0.05 | 11 | -0.03 | 0.87 |
| | 23034 | 33 | 0.66 | 0.65 | 55 | 0.21 | 0.08 | 27 | -0.20 | 0.88 |
| | 23083 | 41 | 0.61 | 0.71 | 50 | 0.23 | 0.53 | 21 | -0.20 | 0.64 |
| | 23013 | 26 | 0.61 | 0.77 | 44 | 0.23 | 0.13 | 20 | -0.24 | 0.97 |
| | 23122 | 7 | -0.10 | 0.86 | 24 | 0.26 | 0.97 | 12 | -0.04 | 0.98 |
| | 24580 | 5 | 1.79 | 0.41 | 14 | 0.34 | 0.61 | 7 | -0.58 | 0.87 |
| Perth | 9178 | 46 | -0.75 | 0.26 | 24 | -0.40 | 0.53 | 13 | 0.18 | 0.93 |
| | 9204 | 27 | -0.25 | 0.08 | 24 | -0.05 | 0.89 | 6 | 0.20 | 0.59 |
| | 9172 | 47 | -0.72 | 0.13 | 32 | -0.05 | 0.98 | 6 | -0.05 | 0.29 |
| | 9053 | 31 | -0.02 | 0.00 | 26 | -0.21 | 0.70 | 10 | -0.44 | 0.12 |
| | 9021 | 42 | -0.17 | 0.00 | 22 | -0.18 | 0.38 | 12 | 0.29 | 0.81 |
| | 9225 | 47 | -0.25 | 0.00 | 38 | -0.10 | 0.10 | 18 | 0.20 | 0.27 |

Table A4: Same as for Table A2 but for southerly winds.

| City | Station | Lag 0 | | | Lag 3 | | | Lag 6 | | |
|---|---|---|---|---|---|---|---|---|---|---|
| | | *n* | median UHI (˚C) | *p* | *n* | median UHI (˚C) | *p* | *n* | median UHI (˚C) | *p* |
| Melbourne | 87113 | 25 | 1.15 | 0.07 | 0 | n/a | n/a | 4 | -1.00 | 0.06 |
| | 86383 | 4 | 1.06 | 0.65 | 2 | -0.24 | 0.56 | 4 | 0.99 | 0.17 |
| | 86282 | 10 | 0.47 | 0.93 | 1 | 0.62 | 0.42 | 2 | 1.76 | 0.04 |
| | 86071 | 4 | 1.16 | 0.66 | 4 | 0.23 | 0.87 | 4 | 0.26 | 1.00 |
| | 86077 | 7 | 0.29 | 0.84 | 1 | -0.63 | 0.31 | 6 | 0.75 | 0.18 |
| | 86104 | 1 | 0.80 | 0.73 | 0 | n/a | n/a | 5 | 0.57 | 0.58 |
| | 87168 | 3 | -0.38 | 0.13 | 3 | 0.89 | 0.53 | 9 | 0.31 | 0.17 |
| Adelaide | 23090 | 7 | 2.14 | 0.21 | 21 | -0.09 | 0.02 | 55 | -0.25 | 0.64 |
| | 23034 | 16 | 1.82 | 0.13 | 7 | -0.05 | 0.83 | 40 | -0.24 | 0.99 |
| | 23083 | 14 | 1.12 | 0.45 | 11 | -0.15 | 0.16 | 46 | -0.26 | 0.63 |
| | 23013 | 17 | 2.02 | 0.06 | 17 | -0.09 | 0.32 | 49 | -0.20 | 1.00 |
| | 23122 | 3 | 1.68 | 0.32 | 2 | -0.64 | 0.57 | 12 | 0.30 | 0.04 |
| | 24580 | 20 | 0.81 | 0.90 | 1 | 4.17 | 0.11 | 5 | -0.45 | 0.84 |
| Perth | 9178 | 11 | -0.78 | 0.90 | 10 | 0.01 | 0.59 | 12 | -0.17 | 0.15 |
| | 9204 | 2 | 0.46 | 0.08 | 9 | -0.09 | 0.63 | 16 | -0.25 | 0.03 |
| | 9172 | 9 | -0.02 | 0.29 | 15 | -0.02 | 0.95 | 29 | 0.22 | 0.10 |
| | 9053 | 8 | -0.83 | 0.82 | 8 | 0.01 | 0.26 | 11 | 0.19 | 0.25 |
| | 9021 | 8 | -0.83 | 0.87 | 13 | -0.09 | 0.07 | 16 | -0.05 | 0.03 |
| | 9225 | 7 | -0.02 | 0.46 | 7 | -0.02 | 0.68 | 15 | 0.04 | 0.07 |

Table A5: Same as for Table A2 but for westerly winds.

| City | Station | Lag 0 | | Lag 3 | | Lag 6 | |
|---|---|---|---|---|---|---|---|
| | | *n* | median UHI (˚C) | *n* | median UHI (˚C) | *n* | median UHI (˚C) |
| Melbourne | 87113 | 121 | 0.65 | 39 | 0.18 | 41 | 0.21 |
| | 86383 | 120 | 0.66 | 40 | 0.19 | 41 | 0.21 |
| | 86282 | 122 | 0.65 | 41 | 0.18 | 40 | 0.26 |
| | 86071 | 50 | 0.66 | 17 | -0.02 | 16 | 0.35 |
| | 86077 | 122 | 0.65 | 39 | 0.20 | 40 | 0.26 |
| | 86104 | 115 | 0.65 | 38 | 0.22 | 40 | 0.26 |
| | 87168 | 101 | 0.67 | 34 | 0.07 | 34 | -0.03 |
| Adelaide | 23090 | 221 | 0.89 | 74 | 0.17 | 75 | -0.22 |
| | 23034 | 223 | 0.90 | 75 | 0.21 | 75 | -0.22 |
| | 23083 | 215 | 0.90 | 74 | 0.17 | 73 | -0.22 |
| | 23013 | 223 | 0.89 | 75 | 0.21 | 75 | -0.22 |
| | 23122 | 90 | 0.60 | 30 | 0.17 | 30 | 0.03 |
| | 24580 | 51 | 0.84 | 16 | 0.34 | 17 | -0.45 |
| Perth | 9178 | 146 | -0.94 | 49 | -0.03 | 48 | 0.24 |
| | 9204 | 157 | -0.88 | 55 | -0.07 | 54 | 0.24 |
| | 9172 | 165 | -0.93 | 55 | -0.07 | 54 | 0.24 |
| | 9053 | 141 | -0.83 | 49 | -0.02 | 50 | 0.22 |
| | 9021 | 151 | -0.88 | 51 | -0.03 | 52 | 0.24 |
| | 9225 | 164 | -0.93 | 55 | -0.07 | 54 | 0.24 |

Table A6: Sample size (*n*), and citywide median UHI strength (˚C) for winds from all directions at each station in Melbourne, Adelaide, and Perth. Table shows results for lag 0, lag 3, and lag 6 winds. See Section 4.3.3 for the definition of wind categories. Median UHI varies from station to station because UHI data corresponding to dates where wind data are missing are excluded.